



**HAL**  
open science

**Role of ponds in mitigating of the contaminants  
(nitrogen and metals) in an agricultural critical zone  
(Vallée de la Save, Gascogne, France)**

Xinda Wu

► **To cite this version:**

Xinda Wu. Role of ponds in mitigating of the contaminants (nitrogen and metals) in an agricultural critical zone (Vallée de la Save, Gascogne, France). Hydrology. Université Paul Sabatier - Toulouse III, 2021. English. NNT : 2021TOU30120 . tel-03595198

**HAL Id: tel-03595198**

**<https://theses.hal.science/tel-03595198v1>**

Submitted on 3 Mar 2022

**HAL** is a multi-disciplinary open access archive for the deposit and dissemination of scientific research documents, whether they are published or not. The documents may come from teaching and research institutions in France or abroad, or from public or private research centers.

L'archive ouverte pluridisciplinaire **HAL**, est destinée au dépôt et à la diffusion de documents scientifiques de niveau recherche, publiés ou non, émanant des établissements d'enseignement et de recherche français ou étrangers, des laboratoires publics ou privés.



# THÈSE

**En vue de l'obtention du  
DOCTORAT DE L'UNIVERSITÉ DE TOULOUSE  
Délivré par l'Université Toulouse 3 - Paul Sabatier**

---

**Présentée et soutenue par  
Xinda WU**

Le 25 mars 2021

**Rôle des étangs dans l'atténuation des contaminants (azote et métaux) dans une zone critique agricole  
(Vallée de la Save, Gascogne, France)**

---

Ecole doctorale : **SDU2E - Sciences de l'Univers, de l'Environnement et de l'Espace**

Spécialité : **Surfaces et interfaces continentales, Hydrologie**

Unité de recherche :  
**Laboratoire écologie fonctionnelle et environnement**

Thèse dirigée par  
**Anne PROBST**

Jury

**Mme Josette GARNIER**, Rapporteur  
**Mme Cecile GROSBOIS**, Rapporteur  
**M. Gwenaël IMFELD**, Examineur  
**M. Jérôme VIERS**, Examineur  
**Mme Anne PROBST**, Directrice de thèse

*For my parents and my wife*

## Acknowledgement

I would like to give the sincere thanks to the director of thesis, Dr. Anne PROBST, not only for her high-level scientific directions, but also for her supports in my daily life. It is her unlimited supports that encourage me to reach the top of the mountain, especially when I feel greatly lonely and frustrated. It is her luminous light that scatters the darkness around me. My very gratitude to my dear supervisor.

I would like to give my warm thanks to the members of the defense jury (Mme. Josette GARNIER, M. Gwenaël IMFELD, Mme. Cécile GROSBOIS, and M. Jérôme VIERS). Thanks for their generous help to evaluate the “cliche” thesis, which is always time and energy consuming. Their inspiring questions and recommendations give me a great help to improve this thesis. I am very obliged to these kindly members.

My thanks also go to my Ph.D. colleagues (M. Youen GRUSSON, M. Léonard BERNARD-JANNIN, M. Amine ZETTAN, M. Amine BENABDELKADER, M. Vivien PONNOU-DELAFFON, M. Francesco ULLOA-CEDAMANOS, and Mme. Chuxian LI). I am grateful for their kindly helps for my thesis work, particularly in its beginning, which let me more easily get access to the new research field. Meanwhile, I enjoy very much the off-duty time with my colleagues.

The thesis work cannot be finished without the physical and mental helps from members of BIZ team, EcoLab. Gratitude goes to Mme. Virginie PAYRE-SUC, M. Thierry CAMBOULIVE, M. Franck GRANOUILLAC, M. Jean-Luc PROBST, Huguette AVOUMADI, M. Théo BADASSAN for their great assistances in the sampling campaigns. Many thanks to Mme. Marie-Jo TAVELLA, M. Frédéric Julien, M. Didier LAMBRIGOT, M. Gaël LE ROUX for the analyses of samples and data sets. Special thanks to Mme. Maïalen BARRET for her guidance about the qPCR analysis and the help to improve the writing about the molecular analysis.

It has been a long journey since the time when my first landing in France. I can never forget the interesting and strange feeling due to immediately switching from the Eastern to the Western atmosphere. I want to thank M. Simon RIZZETTO for picking me up at the airport and helping me get familiar with the new environments of both Toulouse and EcoLab. Best wishes go to M. Pierre RAFFAELE and his wife for their kindly help to my first-year personal life in Toulouse.

I am also glad to thank my friends, Qiuming MA, Chen ZHANG, Jianzhong LU. I will remember the wonderful time we enjoy together.

Finally, my family gives me numerous strong supports. It is always the sweet home where I can harbor.

**Abstract**

As in many critical zones (CZ) with traditional agriculture, southwestern France is confronted with some agro-environmental risks due to the contamination by nitrogen and potential toxic elements (PTE) (metals) from anthropogenic inputs. For decades, numerous ponds have been constructed in this area for irrigation and/or landscaping. Few studies have focused on the distribution of the two types of contaminants at the catchment scale of an agricultural CZ. The role of ponds on the distribution and transfer of these two types of contaminants has also been rarely studied. To fill this knowledge gap, we studied nitrogen and PTE behavior in the water and sediments of streams and ponds of three adjacent catchments of the Save basin (southwestern France), particularly for their spatial distributions and the main controlling factors, while addressing the consequences in terms of pond management.

Potential denitrification rate (PDR) in sediments varied spatially due to the heterogeneity of geo-physico-chemical properties even at a small scale. Although PDR in stream was more active than in pond due to the greater nutrient availability, larger ponds have showed high  $\text{NO}_3^-$  removal efficiency. Long hydraulic retention time (HRT) could increase the reaction time and mitigate  $\text{NO}_3^-$  further. A chain of multiple constructed ponds along the stream provided a better ability to mitigate  $\text{NO}_3^-$  compared to a single pond. Denitrification was higher in ponds located upstream of a catchment, but the incomplete denitrification process in these ponds can lead to the release of  $\text{N}_2\text{O}$  contributing to the greenhouse gas emission and negative consequences for the environment, which requires further investigations.

Application of fertilizers and pesticides to cultivated soils has contributed to PTE accumulation in stream and pond sediments, especially for Cu, Ni, and Cd in upstream sediments attributing to high soil erosion and low discharge dilution. PTE distribution has also been affected by pond management. High temperature, high pH, and long HRT in a large pond created a favorable environment for PTE sedimentation via adsorption to fine particles and co-precipitation with carbonates from this agricultural CZ. Although the sediments accumulated in ponds can store PTEs, the sediments drained by streams left the pond as a secondary source of PTEs through resuspension and turbulence of the running water, especially for small, non-dredged ponds.

PTE accumulation did not affect PDR since the PTE contamination was not very severe in this agricultural CZ. However, sediment clay content can affect denitrification rate and PTE accumulation simultaneously. Pond management must therefore consider both denitrification and PTE accumulation. A chain of several constructed ponds can be able to store PTEs and mitigate excessive nitrate simultaneously, especially with some large ponds located in upstream. The dredging activity for pond sediments should also be managed carefully.

**Keywords:** nitrate, denitrification, metal, agricultural catchment, critical zone, pond, sediment, nutrient, environmental factors, multivariate analysis

**Résumé**

Comme dans de nombreuses zones critiques (ZC) à agriculture traditionnelle, le sud-ouest de la France est confronté à certains risques agro-environnementaux dus à la contamination par l'azote et les Eléments Potentiellement Toxiques (EPT) (métaux) issus des intrants anthropiques. Depuis des décennies, de nombreux étangs ont été construits dans cette zone pour l'irrigation et / ou l'aménagement paysager. Peu d'études ont abordé la distribution des deux types de contaminants à l'échelle du bassin versant d'une ZC agricole. Le rôle des étangs sur la distribution et le transfert de ces deux types de contaminants a été également rarement étudié. Pour combler ce manque de connaissance, nous avons étudié le comportement de l'azote et des EPT dans l'eau et les sédiments de fond des cours d'eau et des étangs de trois bassins versants adjacents du bassin de la Save (sud-ouest de la France), à travers notamment leurs distributions spatiales et les principaux facteurs de contrôle, tout en abordant les conséquences en termes de gestion.

Le taux de dénitrification potentiel (TDP) dans les sédiments varie spatialement en raison de l'hétérogénéité des propriétés géo-physico-chimiques, même à petite échelle. Bien que le TDP dans les ruisseaux soit plus important que dans les étangs à cause d'une plus grande disponibilité des éléments nutritifs, les plus grands étangs ont montré une efficacité élevée d'élimination des nitrates. Un long temps de résidence hydraulique (TRH) pourrait augmenter les temps de réaction et atténuer davantage les nitrates. Une chaîne de plusieurs étangs consécutifs le long du cours d'eau permet une meilleure atténuation des nitrates par rapport à la présence d'un seul étang. La dénitrification est plus élevée dans les étangs localisés en amont du bassin versant, mais le processus de dénitrification incomplet dans ces étangs peut entraîner un dégazage de  $\text{N}_2\text{O}$  contribuant à la production des émissions de gaz à effet de serre et des conséquences négatives pour l'environnement, qui nécessitent des études plus approfondies.

L'application d'engrais et de pesticides sur les sols cultivés a contribué à l'accumulation de EPT, en particulier pour Cu, Ni et Cd, dans les sédiments des ruisseaux et des étangs, notamment en amont des bassins versants, en raison d'une forte érosion du sol et d'une plus faible dilution. La distribution des EPT a également été affectée par la gestion des étangs. Une température élevée, un pH élevé et un TRH long dans un grand étang créent un environnement favorable à la sédimentation des EPT par adsorption sur des particules fines et la co-précipitation avec les carbonates de cette zone critique agricole. Bien que les sédiments accumulés dans les étangs puissent stocker des EPT, les sédiments drainés par les ruisseaux en sortie d'étang sont une source secondaire de EPT par la remise en suspension et la turbulence des eaux courantes, en particulier pour les petits étangs non dragués.

L'accumulation de EPT n'a pas affecté le TDP car la contamination par les EPT n'était pas très conséquente dans cette zone critique agricole. Toutefois, la teneur en argiles des sédiments affecte simultanément le taux de dénitrification et l'accumulation des EPT. La gestion des étangs doit ainsi prendre en compte à la fois la dénitrification et l'accumulation de EPT. Une chaîne de plusieurs étangs peut permettre de stocker les EPT et atténuer les excès de nitrate simultanément, en particulier en positionnant de grands étangs en amont des bassins versants. L'activité de dragage des sédiments des étangs doit également être gérée avec précaution.

**Mots clés :** nitrate, dénitrification, métal, bassin versant agricole, zone critique, étang, sédiment, nutriment, facteurs environnementaux, analyse multivariée

## Table of contents

Table of contents.....	I
List of figures .....	IX
List of tables .....	XIII
List of abbreviations .....	XII
Scientific production.....	XIV
General Introduction.....	2
Chapter I State of the art.....	13
1. Overview of the Critical Zone (CZ).....	13
1.1 Current state of CZ.....	13
1.1.1 Definition.....	13
1.1.2 Compartments and interacts within the CZ.....	15
1.1.3 Interactions within CZ .....	15
1.1.4 Influence of CZ on the environment .....	16
1.1.5 Critical Zone Observatories (CZO).....	16
1.2 Agriculture in the CZ .....	17
1.2.1 Share of land use and cover .....	17
1.2.2 Land occupation types in France .....	19
1.2.3 Fertilizer input.....	20
1.2.4 Pesticide input.....	23
1.2.5 Consequences of intensively agricultural activities .....	25
1.3 Constructed wetlands and ponds in agricultural catchments .....	28
1.3.1 Definition of catchments, constructed wetlands, constructed ponds, and sediments ..	28
1.3.2 History and types of CWs .....	31
1.3.3 Effects of CWs on contaminants.....	31
2. Nitrogen in aquatic ecosystem .....	33
2.1 Nitrogen in biogeochemical cycle.....	33
2.1.1 Fixation .....	34
2.1.2 Volatilization .....	34
2.1.3 Ammonification .....	34
2.1.4 Nitrification.....	35
2.1.5 Nitrate reduction .....	36
2.1.6 Assimilation and plant uptake.....	36
2.1.7 Ammonia adsorption.....	37
2.1.8 Organic nitrogen burial and accretion.....	38
2.1.9 Anaerobic ammonium oxidation.....	38
2.2 Nitrate transfer, transformation, and controlling factors .....	38
2.2.1 Anthropogenic sources of nitrogen .....	39
2.2.2 Nitrate transfer from soil to water .....	39
2.2.3 Nitrate removal pathways in aquatic system.....	40
3. Potential toxic metals (PTE) in sediments .....	44
3.1 Brief of sediments .....	44
3.2 Characteristics and toxicity of PTEs .....	44

3.3	Sources of PTEs in agricultural soils and sediments .....	47
3.3.1	Natural source .....	47
3.3.2	Anthropogenic source .....	49
3.4	Anthropogenic PTE transportation and distribution in sediments .....	50
3.4.1	From soil to sediment.....	50
3.4.2	Major pathways and controlling factors.....	51
Chapter II Materials and methods.....		54
Introduction.....		54
1.	Sampling site.....	56
1.1	Pond selection .....	56
1.2	Catchment and pond descriptions.....	67
1.2.1	Catchment characteristics .....	67
1.2.2	Pond characteristics .....	72
2.	Sampling strategies .....	73
2.1	Water .....	74
2.2	Sediment.....	75
3.	Physicochemical and biological analyses .....	78
3.1	Water .....	78
3.1.1	Basic physicochemical analyses .....	78
3.1.2	Stable isotopes .....	78
3.2	Sediment.....	79
3.2.1	Physicochemical analyses .....	79
3.2.2	Denitrification analyses .....	79
3.2.3	Total digestion.....	81
3.2.4	single EDTA extraction.....	81
3.2.5	Metal analyses.....	81
3.2.6	Molecular analysis .....	82
4.	Data analyses .....	84
Chapter III Role of constructed ponds in denitrification and nitrate behavior: key controlling factors in streams and ponds at a catchment scale .....		86
Introduction.....		86
Materials and methods .....		90
Part I. Denitrification and its controlling factors .....		91
1.	Results.....	92
1.1	Water characteristics.....	92
1.2	Sediment characteristics.....	93
1.2.1	Physicochemical characteristics.....	93
1.2.2	Potential denitrification rate (PDR) .....	95
1.3	Relationships between variables.....	96
1.3.1	Principal component analysis (PCA) .....	101
1.3.2	Relationship between PDR and N <sub>2</sub> O emission rate.....	104
1.4	qPCR assay for denitrification genes in pond sediments.....	105
1.5	Multilinear regression model for PDR .....	107
2.	Discussion.....	110

2.1	PDR magnitude and spatial variation .....	110
2.2	Controlling factors of PDR.....	111
2.3	Predictive models and interest from a management perspective .....	114
Part II. Nitrate behavior and the role of ponds .....		116
1.	Results.....	117
1.1	NO <sub>3</sub> <sup>-</sup> concentration, discharge, and NO <sub>3</sub> <sup>-</sup> flux patterns.....	117
1.2	Stable isotopes.....	118
1.3	Multilinear regression model for NO <sub>3</sub> <sup>-</sup> removal efficiency .....	120
2.	Discussion.....	124
Summary .....		128
Chapter IV Influence of ponds on hazardous metal distribution in sediments at a catchment scale (agricultural critical zone, S-W France).....		131
Introduction.....		131
1.	Materials and methods .....	134
1.1	Geoaccumulation index (I <sub>geo</sub> ).....	134
1.2	Enrichment factor (EF).....	134
1.3	Anthropogenic contribution (AC, %).....	137
1.4	Statistical analysis .....	138
2.	Results.....	138
2.1	Concentrations of major elements and eight potential toxic elements (PTE) in sediments 138	
2.2	Sediment texture.....	141
2.3	Contamination indices.....	142
2.3.1	Geoaccumulation index (I <sub>geo</sub> ).....	142
2.3.2	Enrichment factor (EF) .....	143
2.4	Principal component analysis (PCA) and correlation matrix (CM) .....	145
2.4.1	All sediments .....	148
2.4.2	Stream sediments .....	148
2.4.3	Pond sediments .....	149
2.5	EDTA extraction.....	150
3.	Discussion.....	152
3.1	Natural vs. anthropogenic origins of PTEs in sediments, and their distributions .....	152
3.2	Distribution of PTE concentration and its controlling factors .....	155
3.3	Availability of PTE in sediments.....	156
3.4	Effect of ponds on PTE transfer in catchments .....	157
Summary .....		160
Chapter V Role of ponds in mitigating contaminants (nitrate and trace metals): a synthetical study in agricultural critical zone (southwestern France).....		163
Introduction.....		163
1.	Materials and methods .....	165
1.1	Multi-element contamination indices .....	165
1.1.1	Contamination degree (CD).....	166
1.1.2	Modified contamination degree (mCD).....	167
1.1.3	Pollution load index (PLI).....	167



1.1.4	Nemerow’s pollution index (PI).....	167
1.1.5	Modified pollution index (mPI).....	168
1.1.6	Potential ecological risk index (PERI).....	168
1.2	Sediment quality guidelines (SQGs).....	168
1.3	Statistical analysis.....	169
2.	Results and discussion.....	170
2.1	Overall metal contamination in sediments.....	170
2.1.1	Integrated contamination magnitude.....	170
2.1.2	Potential ecological risk in sediments and the effect of metal contamination on denitrification.....	174
2.2	Role of ponds in types of contaminants simultaneously.....	177
2.2.1	All sediments.....	177
2.2.2	Stream and pond sediments.....	181
	Summary.....	186
	Conclusions and perspectives.....	188
	References.....	205

## List of figures

Fig. I-1. Schematic diagram of the Critical Zone (CZ), after NRC, 2001 .....	14
Fig. I-2. Schematic diagram of pedosphere (adapted from Schaetzl and Thompson, 2015).....	15
Fig. I-3. Interactions between different spheres in the critical zone (adapted from Schaetzl and Thompson, 2015).....	16
Fig. I-4. Regional shares of land use and cover at the worldwide scale in 2010 (source: FAO).....	18
Fig. I-5. Share of agricultural lands in the world in 2016 (Antarctica excluded) .....	18
Fig. I-6. Land occupation by different usages at the global and the western Europe scale in 2010, respectively (source: FAO, <a href="http://www.fao.org/faostat/en/#data/LC">http://www.fao.org/faostat/en/#data/LC</a> ).....	19
Fig. I-7. Share of agricultural lands in European continent in 2016 (source: The World Bank).....	20
Fig. I-8. Total N nutrients used by agriculture by regions and nations in 2018 (source: FAO) .....	21
Fig. I-9. Total N nutrients used by agriculture in the European continent in 2018 (source: FAO) .....	22
Fig. I-10. Total N fertilizer used by the first seven countries in Europe from 2000 to 2018. DEU = German, FRA = France, ITA = Italy, TUR = Turkey, ESP = Spain, GBR = Great Britain, POL = Poland. ....	22
Fig. I-11. Amount of used pesticides: (A) in worldwide, (B) in the United States, (C) in France from 2000 to 2018 (data source: FAO).....	24
Fig. I-12. Use of pesticides per area of cropland in 2018 (Source: FAO).....	24
Fig. I-13. Use of pesticides per area of cropland in Europe in 2018 (source: FAO).....	25
Fig. I-14. Soil erosion by water in agricultural areas in France, 2016 (Source: EuroStat) .....	28
Fig. I-15. Illustration of a catchment (e.g., the Montoussé catchment, a CZO of OZCAR).....	29
Fig. I-16. Photos of different types of wetlands: (A1) a shallow marsh in Guilin, China; (A2) a lake in Guilin, China; (B1) a constructed pond in Marestaing, France; (B2) a constructed pond in Montoussé, France. (Photographer: G. WU and X. WU).....	30
Fig. I-17. Schematic diagram of N-cycling in an aquatic system .....	33
Fig. I-18. Three modes of ammonia adsorption rate: (a) increase to stable; (b) increase to decrease to increase; (c) increase to decrease to stable. (Note: the curves are only schematic and do not reveal the real adsorption rates).....	37
Fig. I-19. Schematic diagram of transfer of potentially toxic elements (PTE) in water and sediment. ....	50
Fig. II-1. (A) Location of the Gers department in France; (B) Types of main land cover in the Gers department in 2013. ....	56
Fig. II-2. Constructed ponds located in the Gers department and its Save basin (source: DDT32).....	57
Fig. II-3. Water basins in the Gers department. The Save basin is highlighted by the red oval (source: DDT32/SER). ....	58
Fig. II-4. Types of land use in the Save basin (CEMAGREF, 2010) .....	59
Fig. II-5. Flow chart of pond selection procedure.....	60
Fig. II-6. Cumulative histograms of pond surface areas (m <sup>2</sup> ): (A) from 0 to 23000000 m <sup>2</sup> ; (B) from 0 to 100000 m <sup>2</sup> . The number above each bar indicates the proportion of total pond numbers. ....	62
Fig. II-7. Cumulative histograms of volumes (m <sup>3</sup> ): (A) volumes from 0 to 2.4×10 <sup>7</sup> m <sup>3</sup> ; (B) volumes from 0 to 1×10 <sup>6</sup> m <sup>3</sup> . The number above each bar indicates the proportion of total pond numbers. ....	63
Fig. II-8. Cumulative histogram of depth (m). The depth (x-axis) covers the depth range from 0 to 30 m. The number above each bar indicates the proportion of total pond numbers.....	64
Fig. II-9. Example of a connected pond and a disconnected (isolated) pond (adapted from the Google Maps)	

.....	65
Fig. II-10. Schematic diagram of a chain of ponds and a single pond along the stream channel .....	65
Fig. II-11. Cumulative histogram of the year of pond construction. The number above each bar indicates the proportion of pond number over the total numbers of ponds.....	66
Fig. II-12. Regional map of suitable ponds in the Save basin. Selected ponds after the field surveys are labeled in red. Note: some small ponds are not visible at the given scale in this map.....	67
Fig. II-13. Location of the studied ponds and of the three relative catchments (Montoussé (MON), Mican (MIC), Nuguet (NUG)) within the Save basin, southwestern France.....	68
Fig. II-14. Hydrograph in the Montoussé stream at the outlet in Auradé, during the two years (2015/12 to 2018/04). The sampling periods of our investigations on the Montoussé upper sub-catchment, the Mican and the Nuguet (March 2016 and March 2018) are indicated by focus to evaluate the local hydrological conditions of sampling. The sampling occurred during a recession period of the late winter water flow conditions.....	71
Fig. II-15. Photos of sampling ponds.....	73
Fig. II-16. Schematic diagram of the sampling strategy (MIC1 as example) .....	74
Fig. II-17. Preprocesses and preservation for water samples before analysis.....	75
Fig. II-18. (A) Schema of the straight core sampler used in the sampling campaign; (B) pond sediments collected by the core sampler.....	76
Fig. II-19. Processes for further analyses for sediment samples.....	77
Fig. II-20. Schematic diagram of the acetylene (C <sub>2</sub> H <sub>2</sub> ) inhibition technique (AIT). The addition of C <sub>2</sub> H <sub>2</sub> can inhibit the function of N <sub>2</sub> O reductase and lead to the N <sub>2</sub> O accumulation.....	80
Fig. III-1. Piper plot for major ion compositions (%) in water samples of the two sampling campaigns (2016 and 2018) .....	93
Fig. III-2. Potential denitrification rates (PDR) in stream and pond sediments from the three catchments: (A) PDR values (i) in all stream and pond sediments for each catchment, (ii) separately in stream and pond sediments of each catchment, (iii) in two different depths of pond sediment cores. (B) and (C) indicate individual PDR values in each sampling site in the three catchments: (B) Montoussé [two ponds MON1 (dashed line) and MON2], (C) Nuguet (NUG) and Mican (MIC): vertically from upstream (No. 1) to downstream (No. 4). IN: stream pond inlet, UP: upper part of a pond, CP: pond center part, LP: lower part of a pond, OUT: stream pond outlet. ....	96
Fig. III-3. Principal component analysis (PCA) combining the first two principal components (PC1 and PC2; variable loadings (left) and individual scores (right)). (A) All sediments; (B) Stream sediments; (C) Pond sediments. For variable names, refer to the legend in Table 3 and for sites refer to Section 2.2. For the individual scores (right column), the color palette distinguishes the catchments, and the sediment types are highlighted by shapes. ....	100
Fig. III-4. Relationship between N <sub>2</sub> O emission rate and <i>log10</i> potential denitrification rate (PDR) in stream and pond sediments from the three catchments. (1) the dotted line: the general pattern without the nine labelled outliers ( $N_2O = (\log_{10} PDR + 1.98) / 482$ , $R^2 = 0.64$ , $p < 0.0001$ , $n = 36$ ); (2) the dashed line: NUG sediments ( $N_2O = (\log_{10} PDR + 1.42) / 303.3$ , $R^2 = 0.53$ , $p < 0.001$ , $n = 16$ ); (3) the solid line: MON + MIC ( $N_2O = -0.0954(3.14 - \log_{10} PDR) / 2.41$ , $R^2 = 0.71$ , $p < 0.0001$ , $n = 29$ ). ....	104
Fig. III-5. Gene abundances (A) and differences between genes (B) and different sediment layers (C)...	106
Fig. III-6. Relationships among gene properties, denitrification rates, and water/sediment characteristics. Red block indicates a significant positive relationship while green block indicates a significant negative	

one ( $p < 0.05$ ).....	106
Fig. III-7. All subsets regression for (A) stream sediments; (B) pond sediments. The grey-scaled color indicates the level of adjusted $R^2$ with different combinations of various variables.....	109
Fig. III-8. Measured vs. predicted PDR values according to the multiple linear regression model. A: stream sediments; B1 and B2: pond sediments. ....	110
Fig. III-9. $\text{NO}_3^-$ concentration (A), discharge (B), and $\text{NO}_3^-$ flux (C) along the stream from the inlet of the first pond to the outlet of the last pond in each catchment for the two sampling campaigns (2016 in black solid line and 2018 in red dashed line). IN: inlet of pond; CP: center of pond; OUT: outlet of pond; WWTP: wastewater treatment plant. The blue dot-dashed line indicates the $\text{NO}_3^-$ concentration in MON1 in 2016, in 2018 the pond was dry.....	117
Fig. III-10. $^2\text{H}$ versus $^{18}\text{O}$ (A) in water samples of two sampling campaigns, (B) in water samples of 2016 sampling campaign, (C) in water samples of 2018 sampling campaign. Local meteoric water line (red line, data source: Ponnou-Delaffon, Thesis,2020) and global meteoric water line (black line) are indicated.....	119
Fig. III-11. $\delta^{15}\text{N}-\text{NO}_3^-$ versus $1/\text{NO}_3^-$ of water samples collected in 2016. The $\delta^{15}\text{N}$ signatures in fertilizers and denitrification were highlighted (data source: Paul et al., 2015).....	120
Fig. III-12. All subsets regression of removal efficiency for (A) $\text{NO}_3^-$ concentration; (B) $\text{NO}_3^-$ flux. The grey-scaled color indicates the level of adjusted $R^2$ with different combinations of various variables. ....	123
Fig. III-13. Measured vs. predicted PDR values according to the multiple linear regression model for removal efficiency of (A) $\text{NO}_3^-$ concentration and of (B) $\text{NO}_3^-$ flux. ....	124
Fig. III-14. Graphical summary of the Chapter III.....	129
Fig. IV-1. Enrichment factor (EF) using different background materials. The color indicated different background materials: the local molasse bedrock (in light red) and the upper continent crust (UCC, in indigo-blue).....	135
Fig. IV-2. Concentration of candidate reference elements (Al, Fe, Cs, and Sc) vs. the clay content. The linear regression line is shown with its confidence interval in grey.....	136
Fig. IV-3. Enrichment factor (EF) based on 4 different reference elements (Al, Cs, Fe, and Sc). The dashed line indicated the EF value of 1.5. ....	137
Fig. IV-4. Ternary diagrams for (A) major elements composition, and (B) sediment texture. Stream and pond sediments are indicated by round and square points, respectively. The red, blue, and yellow colors correspond to the Montoussé (MON), Mican (MIC), and Nuguet (NUG) catchments, respectively. ....	140
Fig. IV-5. Mean concentrations and standard variation of eight potential toxic elements (PTE): (A) all sediments; (B) by different catchments (Montoussé/Mican/Nuguet); (C) by different sediment types (stream/pond sediments); (D) by different layers of pond sediments (surface/deeper layers). “M” indicates the concentration of a given element in the background molasse (data from N’guessan et al., 2009).....	141
Fig. IV-6. Granulometry of particle size distribution of sediments. The colors of lines indicated the stream sediments (in red) and the pond sediments (in blue), respectively.....	142
Fig. IV-7. Enrichment factors (EF) of trace elements: (A) all samples; (B) by different catchments (Montoussé/Mican/Nuguet); (C) by different sediment types (stream/pond sediments); (D) by different layers of pond sediments (surface/deeper layers). ....	144
Fig. IV-8. First two dimensions (also known as ‘axes’ or ‘components’) of principal component analysis (PCA) for: (A) all sediments; (B) stream sediments; (C) pond sediments. The left column represents the	

variable loadings of PCA, while the right shows the individual scores. The PCA was calculated based on the concentrations of major and trace elements. Other physicochemical variables were abbreviated as follows: Corg = organic carbon content, Q = discharge, HRT = hydraulic retention time, and UC.Area = upstream sub-catchment area. Catchments were differentiated by colors (MON = Montoussé, MIC = Mican, NUG = Nuguet in the legend). Sediments were classified into different symbols (IN = Inlet (stream sediment), S = Surface layer (pond sediment), D = Deeper layer (pond sediment), OUT = Outlet (stream sediment) in the legend).....	147
Fig. IV-9. Available fractions (%) of eight potential toxic elements (PTE) extracted by EDTA: (A) all samples; (B) by different catchments (Montoussé/Mican/Nuguet); (C) by different sediment types (stream/pond sediments); (D) by different layers of pond sediments (surface/deeper layers).....	151
Fig. IV-10. Enrichment factor (EF) using Fe as the reference element. Different colors indicated the stream sediments (in white) and the pond sediments (in grey), respectively.....	154
Fig. IV-11. Correlation matrix of concentrations, available fractions (%), and sediment properties in all sediments. The color bar indicated the r value from -1 (blue) to 1 (red). The significance level ( $p < 0.01$ ) was highlighted by colored blocks in the figures.....	157
Fig. IV-12. Graphical summary of the Chapter IV.....	161
Fig. V-1. Various indices for sediments regarding different types of sediments. Red italic texts indicate the range of contamination levels highlighted by dashed lines. ....	172
Fig. V-2. (A) The potential ecological risk (Er) of each element for all sediments; (B) Er for Cd in detail. The dashed lines indicate the levels of the potential ecological risk highlighted by the red italic texts. ...	175
Fig. V-3. $\log_{10}$ (potential denitrification rate) vs. the sediment clay content in pond sediments. Colors indicated the different catchment (MON = the Montoussé catchment; MIC = the Mican catchment; NUG = the Nuguet catchment), and symbols highlighted the sediment type (stream sediment: IN = inlet   OUT = outlet; pond sediment: S = surface layer   D = deeper layer).....	176
Fig. V-4. Probable effect quotient (PEQ, %) for the concerned metals according to the consensus-based sediment quality guidelines (SQGs). The dashed line indicates below above which the adverse effect on sediment-living organisms. ....	176
Fig. V-5. Principal component analysis (PCA) for (A) all sediments, (B) stream sediments, and (C) pond sediments. The variable loadings were presented in the left column, while the individual scores for sediments were shown in the right column. Colors indicated the different catchment (MON = the Montoussé catchment; MIC = the Mican catchment; NUG = the Nuguet catchment), and symbols highlighted the sediment type (stream sediment: IN = inlet   OUT = outlet; pond sediment: S = surface layer   D = deeper layer). $\log_{10}$ PDR = $\log_{10}$ (potential denitrification rate); PERI = potential ecological risk index; PLI = pollution load index; Clay = sediment clay content; Fe = sediment Fe concentration; EDTA% = the sum of concentration ratios of EDTA-extractable for 8 concerned metals; Corg = sediment organic content; Q = stream discharge; HRT = hydraulic retention time. ....	180
Fig. V-6. $\log_{10}$ (potential denitrification rate) vs. the sediment clay content in pond sediments. Colors indicated the different catchment (MON = the Montoussé catchment; MIC = the Mican catchment; NUG = the Nuguet catchment), and symbols highlighted the layer of pond sediments (S = surface layer   D = deeper layer).....	185
Fig. V-7. Schematic diagrams that depicted the geophysicochemical controlling factors for the denitrification and the metal contamination simultaneously regarding different categories of sediments: (A) all sediments, (B) stream sediments, and (C) pond sediments.....	185

## List of tables

Table I-1. Concentrations of elements in various types of bedrocks .....	48
Table II-1. Distribution of the different types of land surfaces in the Gascogne region, 2013 (Source: Occupation du sol à grande échelle (OCS GE)).....	55
Table II-2. Descriptive statistics of pond sizes (surface area, volume, and pond depth) based on more than 3000 ponds in the Gers department recorded by DDT .....	61
Table II-3. Characteristics of sampling sites (catchments and ponds). YC = year of construction, YD = year of last dredging; <i>HRT</i> (Hydraulic Retention time) = $(Pond\ volume)/(Q_{outlet}-Q_{inlet})$ where <i>Q</i> is the discharge. Note that the inside of NUG4 pond was not collected (see Section 1.2.2 of this chapter). .....	69
Table II-4. List of primers, and thermocycling programs used for each gene. ....	83
Table III-1. Physicochemical characteristics of waters (streams and ponds) for the 2016 and the 2018 sampling campaign in Mican, Nuguet, and Montoussé catchments. N is the number of samples. NA: data not available (since the pond was dry).....	92
Table III-2. Physicochemical characteristics of sediments from ponds and streams taken together or separately, taken by catchment and by depth (surface and deep layers) of the sediment cores of the ponds. The asterisk (*) highlights the significant difference between different kinds of sediments ( $p < 0.05$ ). n is the number of samples; ORP: Oxidation - Reduction Potential; DBD: Dry Bulk Density; WC: Water content; Norg: Organic nitrogen content; Corg: Carbon Organic content. ....	94
Table III-3. Pearson correlation matrix (R) concerning main physicochemical parameters from all (a), stream (b) and pond (c) sediments in the three catchments considered together. Note that more parameters were considered for ponds sediments. Values in bold red and black bold italic mean $p$ -value $< 0.05$ and $< 0.1$ , respectively. PDR: Potential Denitrification Rate; ORP: Oxidation- Reduction Potential; WC: Water Content in sediment; pH_s: pH in sediment; pH_w: pH in water; NO <sub>3</sub> _w: nitrate concentration in waters; T_w: water temperature; LW_ratio: pond length over width; Q: discharge; Slope: pond slope; HRT: Hydraulic Retention Time. (a) All sediments (n = 31); (b) Stream sediments (n = 16); (c) Pond sediments (n = 14). ....	98
Table III-4. Eigenvalues and explained variances by the first ten components of PCA: (A) all sediments, (B) stream sediments, and (C) pond sediments.....	102
Table III-5. Loadings and contributions of variables to the first four components of PCA: (A) all sediments (n = 31), (B) stream sediments (n = 16), and (C) pond sediments (n = 14). R is the loading of a given variable, while % represents its contribution to the components. PDR: potential denitrification rate; N <sub>2</sub> O: N <sub>2</sub> O emission rate; pH_s: pH in sediment; ORP: oxidation-reduction potential; WC: water content in sediments; C <sub>org</sub> : organic carbon content in sediment; N <sub>org</sub> : organic nitrogen content in sediment; T_w: water temperature; pH_w: pH in water; DOC: dissolved organic carbon; NO <sub>3</sub> _w: nitrate concentration in water; Q: discharge; Slope: pond slope; L/W: pond length over width; HRT: hydraulic retention time; Depth: depth of pond. ....	102
Table III-6. Gene abundances and their percentages in the selected ponds. Values from 12 samples and the descriptive statistics are listed.....	105
Table III-7. Multiple linear regression results for PDR. “Preliminary” indicates the consideration of all	

variables and “Updated” indicates the variables selected by the all-subsets regression method; ORP: Oxidation-Reduction Potential; Depth: Depth of the pond; Tw: Temperature of the water; DOC: Dissolved Organic Carbon; HRT: Hydraulic Retention Time (days); Dist: Distance to stream source; with * $p < 0.1$ ; ** $p < 0.05$ ; *** $p < 0.01$ .....	108
Table III-8. $\text{NO}_3^-$ removal efficiency (RE, %) in pond (2016 and 2018).....	121
Table III-9. Correlation of removal efficiencies with environmental factors in ponds. The italic font indicates $p < 0.1$ .....	122
Table III-10. Multiple linear regression results for $\text{NO}_3^-$ removal efficiency. “Preliminary” indicates the consideration of all variables and “Updated” the selected variables by all subsets regression method. HRT: Hydraulic Retention Time (days). * $p < 0.1$ ; ** $p < 0.05$ ; *** $p < 0.01$ .....	123
Table IV-1. Concentration of major elements and eight potential toxic elements (PTE) in sediments and other materials.....	139
Table IV-2. Geoaccumulation index ( $I_{\text{geo}}$ ) of eight potential toxic elements (PTE) in all sediments.....	143
Table IV-3. Eigenvalues and variances of components for (A) all sediments, (B) stream sediments, and (C) pond sediments. The first six components were listed.....	146
Table IV-4. Relationships and contributions of variables to principal components of principal component analyses for (A) all sediments; (B) stream sediments; and (C) pond sediments. The % symbol stands for the contribution (%) of a given variable to a dimension. Bold fonts indicate significant factors in the component. Corg = organic carbon content, Q = discharge, HRT = hydraulic retention time, and UC.Area = upstream sub-catchment area. ....	146
Table IV-5. Concentration ( $\mu\text{g g}^{-1}$ ) of metal in the available fraction and its proportion (%) of the total concentration in all sediments using EDTA extraction. ....	151
Table V-1. Classes of contamination intensities defined by the integrated multi-element indices, including concentration-based indices (PLI, CD, mCD, PI, and mPI) and ecological indices ( $\text{Er}^i$ and PERI). PLI = pollution load index, CD = contamination degree, mCD = modified contamination degree, PI = Nemerow’s pollution index, mPI = modified Nemerow’s pollution index, $\text{Er}^i$ = potential ecological risk of a single element, PERI = potential ecological risk of all calculated metals (sum of $\text{Er}^i$ ). ....	166
Table V-2. Consensus-based sediments quality guidelines (SQGs) for freshwater sediments (MacDonald et al., 2000). TEC: threshold effect concentration; PEC: probable effect concentration, unit = $\text{mg kg}^{-1}$ dry weight of sediment.....	169
Table V-3. Values and scores calculated by integrated multi-element indices and the ecological index. CD = contamination degree, mCD = modified contamination degree, PLI = pollution load index, PI = Nemerow’s pollution index, mPI = modified Nemerow’s pollution index, PERI = potential ecological risk index, Sum.1 = sum of scores for indices except PERI, Sum.2 = sum of scores for all studied indices. The level of scores for each index is listed in Table V-1.....	171
Table V-4. Correlation matrix for metal concentrations and various indices. Bold: $p < 0.01$ , Italic: $0.01 < p < 0.05$ . ....	173
Table V-5. Relationship of the denitrification process to metal concentrations and their indices. $\log\text{N}_2\text{O}$ = $\log_{10}(\text{N}_2\text{O emission rate})$ , $\log\text{PDR}$ = $\log_{10}(\text{potential denitrification rate})$ .....	175
Table V-6. Eigenvalues and variance (%) explained by the principal component analysis (PCA): (A) all sediments, (B) stream sediments, and (C) pond sediments.....	179
Table V-7. Loadings and contributions (%) of variables to the first 3 principal components (PC) in PCA for	

(A) all sediments, (B) stream sediments, and (C) pond sediments. The significant variables to a given PC were highlighted by bold texts. logPDR = log10(potential denitrification rate); PERI = potential ecological risk index; PLI = pollution load index; Clay = sediment clay content; Fe = sediment Fe concentration; EDTA% = the sum of concentration ratios of EDTA-extractable for 8 concerned metals; Corg = sediment organic content; Q = stream discharge; HRT = hydraulic retention time. ....179

Table V-8. Correlation matrix between the denitrification process, contamination intensity, sediment physicochemical characteristics, and environmental factors for (A) all sediments, (B) stream sediments, and (C) pond sediments. Bold:  $p < 0.01$ , Italic:  $0.01 < p < 0.05$ . logPDR = log10(potential denitrification rate); PERI = potential ecological risk index; PLI = pollution load index; Clay = sediment clay content; Fe = sediment Fe concentration; EDTA% = the sum of concentration ratios of EDTA-extractable for 8 concerned metals; Corg = sediment organic content; Q = stream discharge; HRT = hydraulic retention time. ....184



## List of abbreviations

Abbreviation	Description
AC	Anthropogenic contribution
ANAMMOX	Anaerobic ammonium oxidation
ANOVA	Analysis of variance
CD	Contamination degree
CEC	Cation exchange capacity
CEMAGREF	Centre national du machinisme agricole, du génie rural et des eaux et forêts
Corg	organic carbon
CPond	Constructed pond
CW	Constructed wetland
CZ	Critical zone
CZO	Critical zone observatory
DBD	Dry bulk density
DEM	Digital elevation model
DO	Dissolved oxygen
DOC	Dissolved organic carbon
EF	Enrichment factor
EPA	Environmental Protection Agency, US
EuroStat	Statistical office of the European Union
FAO	Food and agricultural Organization, UN
FSW	Free surface wetland
GISCO	Geographic Information System of the Commission, EU
HDPE	High-density polyethylene
HRT	Hydraulic retention time
$I_{geo}$	Geoaccumulation index
IPCC	Intergovernmental Panel on Climate Change
mCD	modified contamination degree
MIC	Mican
MON	Montoussé
mPI	modified pollution index
Norg	Organic nitrogen
NUG	Nuguet
NUTS	Nomenclature of territorial units for statistics
OMP	Observatoire Midi-Pyrénées
ORP	Oxidation-reduction potential
OZCAR	French network of Critical Zone Observatories
PAAS	Post Archean Australian Shales
PAPC	Plateforme d'Analyses Physico-Chimiques
PDR	Potential denitrification rate
PERI	Potential ecological risk index
PI	Pollution index
PLI	Pollution load index

---

POC	Particulate organic carbon
PTE	Potential hazardous element
Q	Stream discharge
qPCR	quantitative Polymerase Chain Reaction
REE	Rare earth element
SQGs	Sediment quality guidelines
SWAT	Soil & Water Assessment Tool
TOC	Total organic carbon
TSM	Total suspended matter
UAA	Utilized agricultural area
WD	World bank
WDI	World development indicators
WWTP	Wastewater treatment plant
YC	Year of construction
YD	Year of dredging

---

## Scientific production

This thesis has been partly published in peer-reviewed scientific journals. Some key fruits have been presented in several international conferences.

### Publications

X. WU, A. PROBST, 2021. Influence of ponds on hazardous metal distribution in sediments at a catchment scale (agricultural critical zone, S-W France). *Journal of Hazardous Materials*. 411, 125077. DOI: 10.1016/j.jhazmat.2021.125077

X. WU, A. PROBST, M. BARRET, V. PAYRE-SUC, T. CAMBOULIVE, F. GRANOUILAC, 2021. Spatial variation of denitrification and key controlling factors in streams and ponds sediments from a critical zone (southwestern France). *Applied Geochemistry*. 131, 105009. DOI: 10.1016/j.apgeochem.2021.105009

### International conferences

X. WU, V. PAYRE-SUC, T. CAMBOULIVE, A. PROBST, 2017. Role of very common artificial ponds on nitrogen behavior in the critical zone of agricultural areas (South-West of France). *Goldschmidt*, Paris, France, 13 – 18 August. (poster)

X. WU, V. PAYRE-SUC, T. CAMBOULIVE, A. PROBST, 2017. Role of very common artificial ponds on nitrogen behavior in the critical zone of agricultural areas (South-West of France). *Functional Ecology and Environmental Conference*, Toulouse, France, 11 – 12 July. (poster)

# **General Introduction**

## General Introduction

Intensively agricultural activities provide food and other nutritious supplies with the increasing world population (FAO, 2020), however this kind of anthropogenic activities can lead to severe environmental issues, such as river eutrophication caused by excessive nitrogen input due to the fertilizer spreading (Harper, 1992; Yang et al., 2008), accumulation of potentially toxic elements in sediments (Bur et al., 2009; N'guessan et al., 2009; Benabdelkader et al., 2018), emission of greenhouse gases (IPCC, 2006, 2019; Butterbach-Bahl and Dannenmann, 2011), etc. These agro-environmental problems can pose a great threaten to food security and human health. Excessive nitrate in drinking water and high level of toxic elements accumulated in food, soil, and sediment become two major environmental concerns (Kapoor et al., 1997; Ali et al., 2019; FAO, 2020).

According to Ministère de l'Agriculture et de l'Alimentation, France is the fifth largest wheat-planting country, after China, India, Russia, and the United States in 2018 (<https://infographies.agriculture.gouv.fr>). Meanwhile, share of agricultural lands in France reaches 52.4% of the total land area in 2016 (World Bank, <https://databank.worldbank.org/>). The total use of N fertilizers in France ranks the first in the European mainland in 2018 (FAO, <http://www.fao.org/faostat>). Therefore, considering agriculture is an important economic structure in France, the environmental problems due to agriculture draw researchers' attention to develop investigations with the aim to build a better and sustainable environment.

Southwestern France is a traditional agricultural area for centuries. Taking the Gascogne region as an example, the agricultural land accounts for 77% of the total surface area. Many constructed ponds have been established since the 1960s for water storage and agricultural irrigation in this region. In such a condition, the thesis focuses on two types of key contaminants (nitrate and potential toxic elements) in southwestern France to investigate their behaviors and main controlling factors in the agricultural critical zones, especially in water and sediment. The role of ponds in their distributions and behaviors is also concerned.

Constructed ponds are biogeochemical reactors, which can affect nitrate ( $\text{NO}_3^-$ ) behavior as they have been found to be effective to mitigate  $\text{NO}_3^-$  in the stream waters draining agricultural catchments (Vymazal, 2007; Tournebize et al., 2017). The denitrification process,

a microbial process which reduces  $\text{NO}_3^-$  to molecular nitrogen gas ( $\text{N}_2$ ) in four steps ( $\text{NO}_3^- \rightarrow \text{NO}_2^- \rightarrow \text{NO} \rightarrow \text{N}_2\text{O} \rightarrow \text{N}_2$ ) (Tiedje, 1994), is the main occurring process. It may lead ecosystem to be N-limiting when N is not in excess, but in agricultural context with important  $\text{NO}_3^-$  load due to fertilizer input, it can remove excessive  $\text{NO}_3^-$  and participate to  $\text{NO}_3^-$  mitigation in stream (Fisher and Acreman, 2004). Nevertheless, this process may not be complete and may lead to  $\text{N}_2\text{O}$  production, which is a harmful intermediate greenhouse gas that can burden the global warm phenomenon (Garnier et al., 2010). The factors influencing the denitrification process have been investigated by many studies. Nitrate in overlying water columns and organic carbon can influence the denitrification rate as they are two key reactants in the process (Groffman et al., 2006; Arango et al., 2007; Saeed and Sun, 2012; Saggari et al., 2013). Meanwhile, the abundance of denitrifiers and other water/sediment characteristics (pH, water content, redox potential, etc.) may also play an important role (Oehler et al., 2007; Attard et al., 2011; Luo et al., 2012; Iribar et al., 2015). Combining geochemical investigation on denitrification process with looking to in situ denitrifier at the ecosystem scale, is not so often found in the literature (Valero et al., 2010; Błaszczak et al., 2018). The denitrification rate has been shown to be related to specific gene abundance (Braker et al., 2000), meanwhile some studies showed that the presence of a given gene did not influence the denitrification process very much compared to other sediment physicochemical characteristics, especially at a small scale (Shrewsbury et al., 2016).

Potential hazardous elements (PTE) in agricultural areas have drawn much attention because of their potential risks to the ecosystem, food security, and human health (Senesil et al., 1999). The anthropogenic sources of PTEs in these areas are mainly commercial inorganic fertilizers (N'guessan et al., 2009), manures (Leclerc and Laurent, 2017), pesticides (Gimeno-García et al., 1996) and wastewater effluent and irrigation (Xu et al., 2010). For instance, commercial mineral fertilizers are responsible for up to 85% of anthropogenic Cd in French cultivated soils (Sterckeman et al., 2018). Spreading Cu-fungicides (e.g., Bordeaux mixtures) contributed to the enrichment of Cu and Zn in the soils of French vineyards (Duplay et al., 2014). Physical erosion leads to the removal of soil particles, which are then transported downstream as suspended matter. PTEs are mainly adsorbed onto those particles in carbonated systems with high pH conditions (N'guessan et al., 2009; Roussiez et al., 2013). Stream and

river waters contribute to most of their transfer downstream from soils to oceans. Generally, intensively cultivated catchments undergoing traditional practices such as tillage are affected by a high soil erosion rate due to their frequent exposure to various erosive powers (such as runoff), particularly when slopes are significant (Oost et al., 2009). In addition to physical erosion, fertilizers can increase soil chemical weathering due to excessive protons produced during the nitrification process under intensive N-P-K fertilizer spreading (Perrin et al., 2008) and consequently lead to an increasing release of base cations (Gandois et al., 2011). All the above processes enhance the transfer and deposition of suspended particulate matter along the main water channels and constitute the bottom sediments. The transfer of such sediments may be delayed by other anthropogenic objects such as reservoirs and dams, which are known to be important traps for both particles and PTEs in large basins (Audry et al., 2004; Benabdelkader et al., 2018). Such transfer of sediments and their anthropogenic content from upstream to downstream in the presence of ponds has rarely been evaluated in agricultural areas.

Bottom sediments are usually recognized as a sink for most PTEs (Çevik et al., 2009; P. Singh, 2009; Duan et al., 2010), and thus can be a reservoir for both anthropogenic and geogenic PTEs (Jiao et al., 2015). The accumulation of PTEs in sediments is controlled by several processes depending on the properties of both the sediments and the PTEs themselves: adsorption, absorption, and/or complexation to fine particles containing clay minerals, iron and/or manganese oxides, organic matter, and co-precipitation with other elements (Ghrefat and Yusuf, 2006; Çevik et al., 2009). Sediment physicochemical properties, including pH, carbonate and organic matter contents, and redox condition, and so on, can affect these processes (Du Laing et al., 2007). The different combining processes and the sources mean that PTEs in sediments are associated with residual and/or labile phases. Anthropogenic PTEs are normally prone to bond to non-residual rather than to residual phases (Leleyter et al., 2012), which makes them more or less easily released from the sediments by water disturbance and changes in water/sediment physicochemical conditions (Duan et al., 2010). Sediments can then be a secondary source of the downstream contamination (Jiao et al., 2015). Meanwhile, metal distribution between sediments and plants may be a concern in places where vegetation is abundant, as some plants can absorb the metals through the rhizosphere (Nagajyoti et al., 2010). Evaluating the available fraction of PTEs in sediment is thus a necessary step in investigating

their potential risks to the environment, and especially to living organisms.

The constructed ponds can store water and sediments transported by surface runoff and stormwaters and provide a favorable environment for sedimentation (Casey et al., 2007; Frost et al., 2015) and the unintentional storage of PTEs. Few studies have examined the different distributions of PTEs in stream and pond sediments from upstream agricultural catchments, as these kinds of sediments and catchments can have different physicochemical characteristics. The position and the characteristics of the ponds that contribute to the PTE transfer downstream remain poorly understood, particularly in channels with a chain of multiple connected ponds. Such ponds can be alternatively dredged by the owners, which question the effect of the pond management on the transfer. Meanwhile, although a great number of studies have shown the relationship between denitrification and some water/sediment properties, the power of environmental factors (the distance to stream source, stream hydrology, pond size, etc.) upon denitrification, was not well identified in the literature. Moreover, few studies have focused on the two different kinds of contaminant ( $\text{NO}_3^-$  and PTEs) simultaneously. The role of ponds in these contaminants is still not well clarified, especially at a small catchment scale (Fisher and Acreman, 2004).

To fill the gap of the knowledge about the role of ponds in the two types of the contaminants ( $\text{NO}_3^-$  and PTEs) in the agricultural critical zone, the main objectives of the thesis are to:

- (1) Investigate  $\text{NO}_3^-$  behavior from upstream to downstream the catchments and sediment denitrification rate in both streams and ponds; find out controlling factors that regulate the denitrification process and  $\text{NO}_3^-$  distribution; set up predictive empirical models for denitrification and for  $\text{NO}_3^-$  removal (Chapter III);
- (2) Investigate various sources of PTEs and assess the contamination magnitude; identify key physico-chemical and environmental factors that regulate the contribution and distribution of PTEs in stream and pond sediments, respectively; assess the availability of PTEs in the different kinds of sediments (Chapter IV);
- (3) Study the potential links between the denitrification process and PTE distribution (Chapter V); investigate the role of ponds in denitrification process individually



(Chapter III), in PTE individually (Chapter IV), and in both denitrification and PTE simultaneously (Chapter V).

The main hypotheses of the thesis are that:

- (1) Denitrification rate and PTE distribution varies in streams and ponds in a given agricultural area.
- (2) Denitrification rate and PTE can be controlled by both sediment/water characteristics and environmental factors (*e.g.*, catchment properties and pond management).
- (3) Denitrification rate and PTE may be linked together.
- (4) Pond can affect the behaviors of both denitrification rate and PTEs.

After this general introduction, other chapters are relative to the state of the art based on a literature review (Chapter I), and the description of methods and materials (Chapter II) used in this thesis. General conclusions and perspectives end the manuscript.

## Introduction Générale

Les activités agricoles intensives fournissent la ressource alimentaire à une population mondiale croissante (FAO, 2020), mais ce type d'activités anthropiques peut entraîner de graves problèmes environnementaux, tels que l'eutrophisation des rivières causée par un apport excessif d'azote dû à l'épandage d'engrais (Harper, 1992; Yang et al., 2008), une accumulation d'éléments potentiellement toxiques dans les sédiments (Bur et al., 2009; N'guessan et al., 2009; Benabdelkader et al., 2018), des émissions de gaz à effet de serre (GIEC, 2006) ; Butterbach-Bahl and Dannenmann, 2011; GIEC, 2019), etc. Ces perturbations agro-environnementales peuvent constituer une menace importante pour la sécurité alimentaire et la santé humaine. L'excès de nitrate dans l'eau potable et le niveau élevé d'éléments toxiques accumulés dans les cultures, les sols et les sédiments deviennent deux préoccupations environnementales majeures (Kapoor et al., 1997 ; Ali et al., 2019 ; FAO, 2020).

Selon le ministère de l'Agriculture et de l'Alimentation, la France est le cinquième pays producteur de blé, après la Chine, l'Inde, la Russie et les États-Unis en 2018 (<https://infographies.agriculture.gouv.fr>). Parallèlement, la part des terres agricoles en France atteint 52,4% de la superficie totale des terres en 2016 (World Bank, <https://databank.worldbank.org/>). L'utilisation totale d'engrais azotés en France est la première en Europe continentale en 2018 (FAO, <http://www.fao.org/faostat>). Par conséquent, étant donné que l'agriculture est une structure économique importante en France, les problèmes environnementaux dus à l'agriculture constituent des préoccupations de recherches des chercheurs afin de construire un environnement meilleur et durable.

Le sud-ouest de la France est une zone agricole traditionnelle depuis des siècles. En Gascogne, les terres agricoles représentent 77% de la surface totale. De nombreux étangs ont été construits pour le stockage de l'eau et l'irrigation agricole dans cette région. Dans ce contexte, la thèse se concentre sur deux types de contaminants clés (nitrates et éléments toxiques potentiels) pour étudier leurs comportements et les principaux facteurs de contrôle dans l'eau et les sédiments d'une zone critique agricole de cette région, en se focalisant notamment sur le rôle des étangs dans la distribution et le comportement de ces contaminants.

Les étangs construits sont des réacteurs biogéochimiques, qui peuvent affecter le

comportement du  $\text{NO}_3^-$ , car ils se sont avérés efficaces pour atténuer le  $\text{NO}_3^-$  dans les eaux des cours d'eau drainant les bassins versants agricoles (Vymazal, 2007 ; Tournebize et al., 2017). La dénitrification, processus microbien qui réduit le  $\text{NO}_3^-$  en azote moléculaire ( $\text{N}_2$ ) en quatre étapes ( $\text{NO}_3^- \rightarrow \text{NO}_2^- \rightarrow \text{NO} \rightarrow \text{N}_2\text{O} \rightarrow \text{N}_2$ ) (Tiedje, 1994), constitue un processus majeur. Il peut constituer un facteur limitant pour la disponibilité de l'azote s'il n'est pas en excès, mais dans un contexte agricole avec une charge importante de  $\text{NO}_3^-$  due à l'apport de fertilisants azotés, il peut éliminer le  $\text{NO}_3^-$  et participer à l'atténuation du  $\text{NO}_3^-$  dans les cours d'eau (Fisher et Acreman, 2004). Néanmoins, ce processus peut ne pas être complet et conduire à la production de  $\text{N}_2\text{O}$ , qui est un gaz à effet de serre intermédiaire qui peut contribuer à accroître le phénomène de réchauffement planétaire (Garnier et al., 2010). Les facteurs influençant le processus de dénitrification ont été étudiés dans de nombreux travaux. Le nitrate dans les colonnes d'eau sus-jacentes et le carbone organique peuvent influencer le taux de dénitrification car ils représentent deux réactifs clés dans le processus (Groffman et al., 2006 ; Arango et al., 2007 ; Saeed et Sun, 2012 ; Saggar et al., 2013). Parallèlement, l'abondance des dénitrifiants et d'autres caractéristiques physico-chimiques eau / sédiments (pH, teneur en eau, potentiel redox, etc.) peuvent également jouer un rôle important (Oehler et al., 2007 ; Attard et al., 2011 ; Luo et al., 2012 ; Iribar et al., 2015). La combinaison d'investigation géochimiques sur le processus de dénitrification et la recherche de dénitrifiants *in situ* à l'échelle de l'écosystème, n'est pas très courant dans la littérature (Valero et al., 2010 ; Blaszcak et al., 2018). Il a été démontré que le taux de dénitrification était lié à l'abondance de gènes spécifiques (Braker et al., 2000). Toutefois, certaines études ont montré que la présence d'un gène donné n'influçait pas beaucoup le processus de dénitrification par rapport à d'autres caractéristiques physico-chimiques des sédiments, en particulier à petite échelle (Shrewsbury et al., 2016).

Les éléments potentiellement dangereux (PTE) dans les zones agricoles ont beaucoup attiré l'attention en raison de leurs risques potentiels pour l'écosystème, la sécurité alimentaire et la santé humaine (Senesil et al., 1999). Les sources anthropiques de PTE dans les zones agricoles sont principalement les engrais inorganiques commerciaux (N'guessan et al., 2009), les fumures organiques (Leclerc et Laurent, 2017), les pesticides (Gimeno -García et al., 1996), les effluents d'eaux usées et l'irrigation (Xu et al., 2010) et. Par exemple, les engrais minéraux commerciaux sont responsables jusqu'à 85% du Cd anthropique présent dans les sols cultivés

en France (Sterckeman et al., 2018). L'épandage de fongicides à base de cuivre (ex : bouillie bordelaise) a contribué à l'enrichissement en Cu et Zn dans les sols des vignobles français (Duplay et al., 2014). L'érosion physique conduit à l'arrachement de particules du sol, qui sont ensuite transportées en aval sous forme de matières en suspension. Les PTE sont principalement adsorbés sur ces particules dans des systèmes carbonatés à pH élevé (N'guessan et al., 2009 ; Roussiez et al., 2013) et les eaux des cours d'eau et des rivières contribuent à l'essentiel de leur transfert en aval des sols vers les océans. En général, les bassins versants cultivés de manière intensive soumis à des pratiques traditionnelles telles que le travail du sol, sont affectés par un taux élevé d'érosion du sol en raison de leur exposition fréquente à divers processus érosifs (comme le ruissellement), en particulier lorsque les pentes sont importantes (Oost et al., 2009). En plus de l'érosion physique, les engrais peuvent augmenter l'altération chimique du sol en raison de la production excessive de protons pendant le processus de nitrification lors de l'épandage intensif d'engrais N-P-K (Perrin et al., 2008), et par conséquent accroître la libération de cations basiques (Gandois et al., 2011). Tous les processus ci-dessus participent au transfert et au dépôt des particules en suspension le long des principaux cours d'eau et constituent les sédiments de fond. Le transfert de ces sédiments peut être retardé par d'autres ouvrages anthropiques tels que les réservoirs et les barrages, qui sont connus pour être des pièges importants pour les particules et les PTE dans les grands bassins (Audry et al., 2004 ; Benabdelkader et al., 2018). Un tel transfert de sédiments et de leur contenu anthropique de l'amont vers l'aval en présence d'étangs a rarement été évalué dans les zones agricoles.

Les sédiments de fond sont généralement reconnus comme un puits pour la plupart des PTE (Çevik et al., 2009 ; Singh, 2009 ; Duan et al., 2010), et peuvent donc être un réservoir pour les PTE anthropiques et géogéniques (Jiao et al., 2015). L'accumulation de PTE dans les sédiments est contrôlée par plusieurs processus en fonction des propriétés à la fois des sédiments et des PTE eux-mêmes : adsorption, absorption et / ou complexation sur de fines particules contenant des minéraux argileux, des oxydes de fer et / ou de manganèse, de la matière organique et coprécipitation avec d'autres éléments (Ghrefat et Yusuf, 2006 ; Çevik et al., 2009). Les propriétés physicochimiques des sédiments, y compris le pH, la teneur en carbonate et en matière organique, les conditions redox, etc., peuvent affecter ces processus (Du Laing et al., 2007). L'analyse des différents processus pris en combinaison et des sources

de PTE révèlent que dans les sédiments ils sont associés à des phases résiduelles et / ou labiles. Les PTE anthropiques sont susceptibles de se lier à des phases non résiduelles des sédiments (Leleyter et al., 2012), ce qui les rend plus ou moins facilement mobilisables suite à des changements de conditions physico-chimiques de l'eau / sédiment (Duan et al., 2010). Les sédiments peuvent alors être une source secondaire de contamination vers l'aval (Jiao et al., 2015). En outre, la partition des métaux entre les sédiments et les plantes peut être importante à considérer dans les endroits où la végétation est abondante, car certaines plantes peuvent absorber les métaux via la rhizosphère (Nagajyoti et al., 2010). L'évaluation de la fraction disponible de PTE dans les sédiments est donc une étape nécessaire pour étudier leurs risques potentiels pour l'environnement, et en particulier pour les organismes vivants.

Les étangs peuvent stocker l'eau et les sédiments transportés par le ruissellement de surface et les eaux pluviales et fournir un environnement favorable à la sédimentation (Casey et al., 2007 ; Frost et al., 2015) et au stockage non intentionnel des PTE. Peu d'études ont considéré les différentes distributions des PTE dans les sédiments des cours d'eau et des étangs des bassins versants agricoles en amont, car ces types de sédiments et de bassins versants peuvent avoir des caractéristiques physico-chimiques différentes. L'influence de la position et des caractéristiques des étangs qui contribuent au transfert de PTE en aval restent mal connus, en particulier dans les cours d'eau avec une chaîne de plusieurs étangs connectés au cours d'eau. Au cours du temps, ces étangs peuvent également être curés par les propriétaires, ce qui interroge sur l'effet de la gestion de ces étangs sur le transfert des PTE. Bien qu'un grand nombre d'études aient montré une relation entre la dénitrification et certaines propriétés de l'eau / des sédiments, le rôle des facteurs environnementaux (distance à la source du cours d'eau, hydrologie du cours d'eau, taille de l'étang, etc.) sur la dénitrification, n'a pas été documentée dans la littérature. De plus, peu d'études se sont intéressées sur les deux types de contaminants ( $\text{NO}_3^-$  et PTE) considérés simultanément. Le rôle des étangs vis-à-vis de ces contaminants n'est pas encore bien connu, en particulier à l'échelle de petits bassins versants dans leur ensemble (Fisher et Acreman, 2004).

Pour combler le manque de connaissances sur le rôle des étangs sur les deux types de contaminants ( $\text{NO}_3^-$  et PTE) dans une zone critique agricole, les principaux objectifs de cette thèse sont de :

(1) étudier l'évolution du  $\text{NO}_3^-$  de l'amont à l'aval des bassins versants, et le taux de dénitrification des sédiments dans les cours d'eau et les étangs ; déterminer les facteurs de contrôle qui régulent le processus de dénitrification et la distribution de  $\text{NO}_3^-$  ; développer des modèles empiriques prédictifs de dénitrification et de réduction du  $\text{NO}_3^-$  (chapitre III) ;

(2) rechercher les différentes sources de PTE et évaluer les intensités de contamination ; identifier les principaux facteurs physico-chimiques et environnementaux qui régulent la contribution et la distribution des PTE dans les sédiments des cours d'eau et des étangs ; évaluer la disponibilité des PTE dans les différents types de sédiments (chapitre IV) ;

(3) identifier les liens potentiels entre le processus de dénitrification et la distribution de PTE (chapitre V) ; étudier le rôle des étangs dans le processus de dénitrification (chapitre III), dans les PTE (chapitre IV), ainsi que dans les deux volets considérés simultanément (chapitre V).

Les hypothèses principales de cette thèse sont que :

(1) le taux de dénitrification et la distribution des PTE est variable dans les étangs et les cours d'eau d'une zone agricole donnée.

(2) le taux de dénitrification et les PTE peuvent être contrôlés à la fois par les caractéristiques des sédiments / eau et des facteurs environnementaux (par exemple, les propriétés du bassin versant et la conception des étangs).

(3) le taux de dénitrification et les PTE peuvent être liés.

(4) l'étang peut affecter les comportements du taux de dénitrification et des PTE.

Après une introduction générale, les autres chapitres concernent l'état de l'art (chapitre I), la description du matériel et des méthodes considérés dans cette thèse (chapitre II). Les conclusions générales et des perspectives terminent le manuscrit.

# **Chapter I**

## **State of the Art**

# Chapter I

## State of the art

### 1. Overview of the Critical Zone (CZ)

#### 1.1 Current state of CZ

##### 1.1.1 Definition

D. E. Tsikalotos (a German chemist) first proposed the term of “Critical Zone (CZ)” in 1909 to describe the zone of a binary mixture of two fluids (cited from Lin, 2010; “Earth’s Critical Zone,” 2019). In geology, this term has also been long used by some geologists to describe the complex geology of the Eastern Bushveld Complex (Cameron, 1980). It was then adopted by G. Ashley to first refer to the thin surface zone of the Earth (Ashley, 1998). Later, in 2001, the National Research Council (NRC) suggested the need for comprehensive study on the CZ and defined CZ as “*the heterogeneous, near-surface environment in which complex interactions involving rock, soil, water, and living organisms regulate the natural habitat and determine the availability of life-sustaining resources*” (NRC, 2001). The CZ was regarded as “*one of the most compelling research areas in Earth sciences in the twenty-first century*” by this Council (NRC, 2001).

The CZ was “*perhaps the most heterogeneous and complex region of the Earth*” by NRC (2001) due to its large and wide extent (Fig. I-1). It includes the outermost layers of the continental crust, ranging from the upper limit of vegetation canopy down to the bottom of freely circulating fresh groundwater (Brantley et al., 2007; White, 2012), which is a result of evolving refinement to the original rough definition. However, this refined definition of the CZ is still not so clear for the researchers so that some of them may think the CZ includes all the surface areas of the Earth. This is not the case. With the development of the study on the CZ over the past two decades, the definition of the CZ has been more clarified as it additionally comprises “*the Polar/Arctic, alpine, and dessert realms where no trees may exist, and excludes deep connate brines and confined aquifers that clearly are not part of the CZ but are part of*



*the groundwater system*” (White, 2012). Some other disputes on the definition of the CZ were pointed out as well by Lin (2010). For instance, some researchers may think that the CZ is identical to soils. Indeed, the CZ is much wider than the pedosphere (Fig. I-1), although the pedosphere is the only entire sphere that is encompassed by the CZ. Secondly, the CZ has been used as a synonym with “*regolith*”, which is defined as “*the layer or mantel of fragmental and unconsolidated rock material, whether residual or transported and of highly varied character, that nearly everywhere forms are surface of the land and overlies or covers the bedrock. It includes rock debris of all kinds, volcanic ash, glacial drift, alluvium, loess and aeolian deposits, vegetal accumulations, and soil*” (Bates and Jackson, 1987). This misunderstanding is similar to the first one. They narrow the wide extent of the CZ, and does not take into consideration the above vegetation, the bedrocks/sediments beneath the regolith, and the groundwater which interact with the CZ.

The detailed compartments of the CZ will be described in the next section (1.1.2).

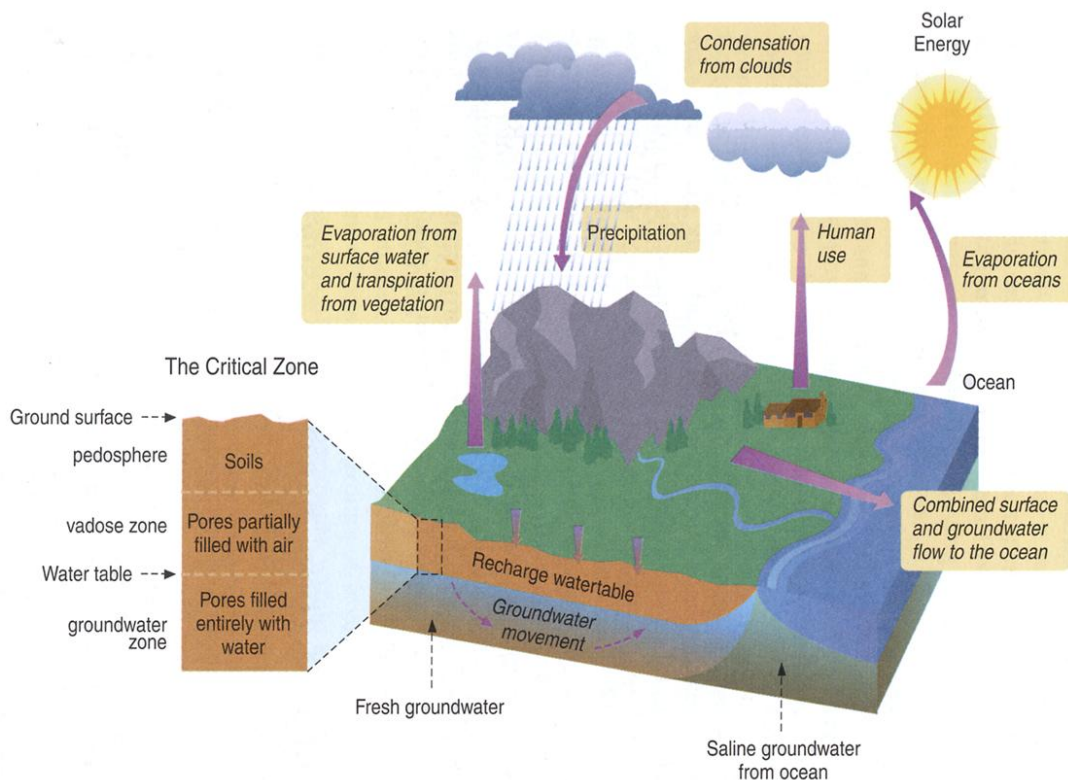


Fig. I-1. Schematic diagram of the Critical Zone (CZ), after NRC, 2001

### 1.1.2 Compartments and interacts within the CZ

What needs to be noticed is that the CZ is not merely a single object, but a mixture of various spheres comprised by the near-surface and surface zones of the Earth, including the near-surface atmosphere and biosphere, the total pedosphere, and the near-surface and surface part of the lithosphere and the hydrosphere (Guo and Lin, 2016).

As Fig. I-1 illustrates, the CZ encompasses the entire pedosphere, which is generally defined as the outermost soil mantle of the Earth as a consequence of interactions of soil-forming factors, such as parent material, climate, topography, and time, *etc.* (Targulian et al., 2019). Generally, the pedosphere can be regarded as the sum of regolith and the consolidated bedrock (Fig. I-2).

The pedosphere is considered as an important part in the CZ due to its extensive position in the near-surface and surface of the Earth. Therefore, soil is, no doubt, the junction of the CZ and plays a key role within. Meanwhile, water is a key driver responsible for the exchanges and transports of energies and matters in the CZ.

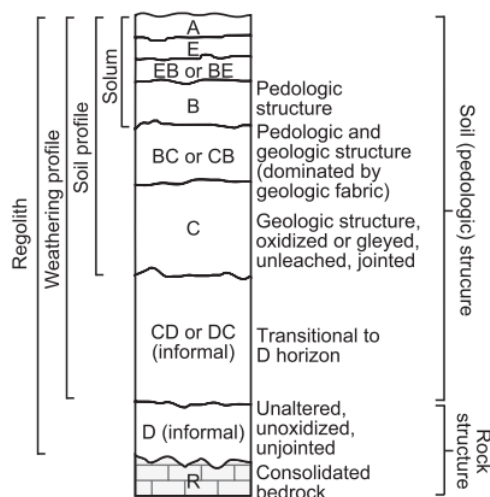


Fig. I-2. Schematic diagram of pedosphere (adapted from Schaetzl and Thompson, 2015)

### 1.1.3 Interactions within CZ

Since almost all terrestrial life are sustained by the CZ (its surface and near-surface environment) (NRC, 2001), the CZ is of great importance to be well studied in order to understand the complex processes within it (Fig. I-3).

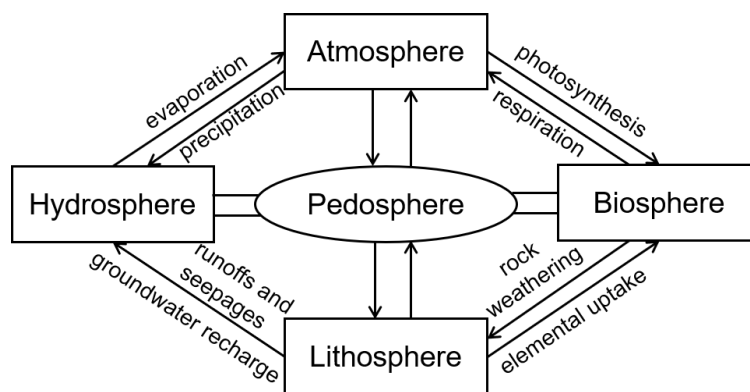


Fig. I-3. Interactions between different spheres in the critical zone (adapted from Schaetzl and Thompson, 2015)

Generally, researchers consider that the CZ contains two central cycles that are different at temporal and spatial scales. One is the geological cycle, and the other one is the biological cycle (Guo and Lin, 2016). The geological cycle includes the weathering process of the rocks, the erosion, transport, and deposition of the weathered products, which finally become sediments. Sediments can be lithified and/or uplifted back to the land by tectonic or hydrological activities. The geological cycle, then, is involved in the pedosphere, the lithosphere, and the hydrosphere. The biological cycle refers to the events of the production and consumption of food and energy in the CZ, as well as organic matters in soils and other living things. This cycle can occur in the atmosphere, the biosphere, and the hydrosphere.

Transport by water flow has been observed in both the geological and biological cycles. Therefore, water is the key medium for mass and energy transfer in the CZ (Lin, 2010).

#### 1.1.4 Influence of CZ on the environment

As CZO (U.S.) states, the CZ is where soil meets life. The CZ is a major place that can support the growth of human beings and other lives. Nowadays, the agricultural activities occur in the CZ is indispensable to the food supply (see Section 1.2).

#### 1.1.5 Critical Zone Observatories (CZO)

Annex I presents a table for the existing CZOs in the world. Since the studies on the CZ have gained an increasing attention during the first twenty years in the new millennium, the CZOs have been established by various countries and organizations at the regional, national,

and global scales. These CZOs aim to aim to investigate the complex interactions in the CZ, to study the anthropogenic impacts on the CZ, and to finally better protect the CZ (Chorover et al., 2011). In France, the OZCAR Research Infrastructure (see Annex I) is a multidisciplinary organization established since 2016, which consists of 9 types of CZs with different geomorphological, biological, and geophysicochemical characteristics (Gaillardet et al., 2018). In southwestern France, the Montoussé catchment at Auradé is an observatory member of RI-OZCAR.

## **1.2 Agriculture in the CZ**

With the increasing world population and the demand of food supply, the agriculture and its related topics have gained more and more attentions over the last few decades (FAO, 2020).

The agricultural-related data used in this section have been collected from several official organizations (e.g., The World Bank and FAO). The code for collecting these data can be found in Annex II.

### **1.2.1 Share of land use and cover**

Nearly 50% of the habitable land is occupied for agriculture according to FAO (<http://www.fao.org/faostat/en/#data/LC>, Fig. I-4, Fig. I-5). In 2010, the cultivated land and the grassland accounted for 47% of the total land use at the global scale, while this value reached up to 64% in the western Europe (Fig. I-6).

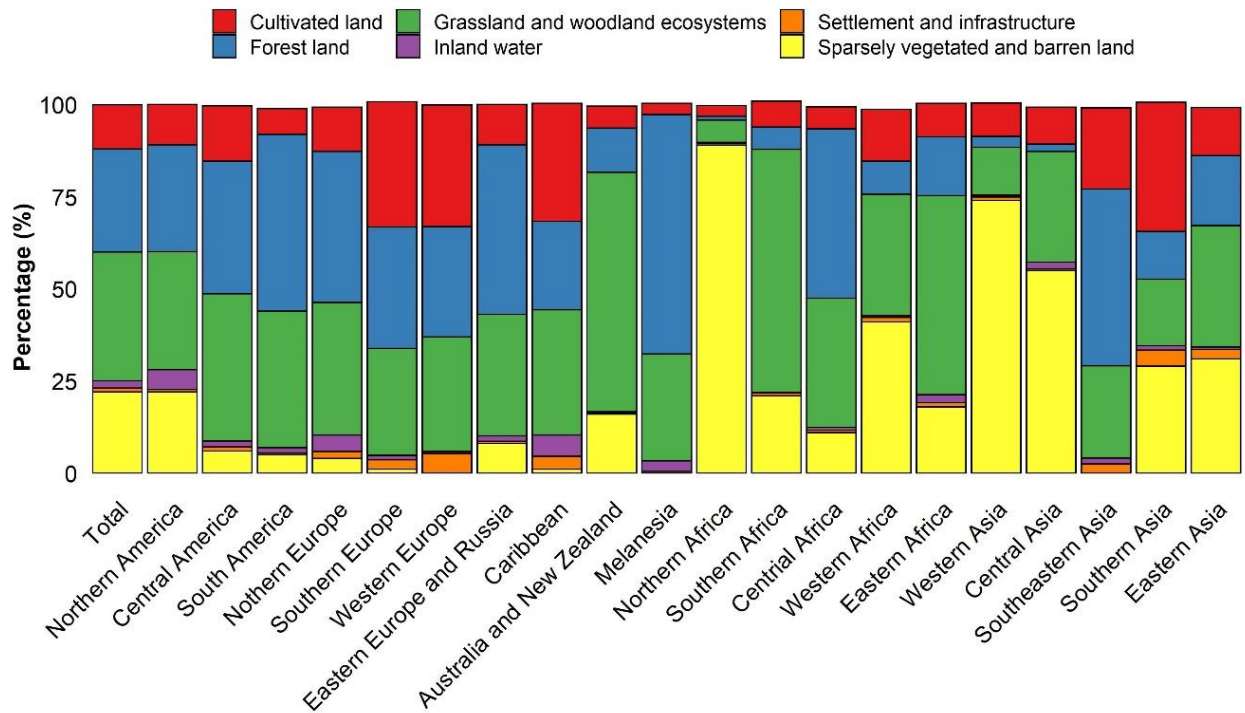


Fig. I-4. Regional shares of land use and cover at the worldwide scale in 2010 (source: FAO)

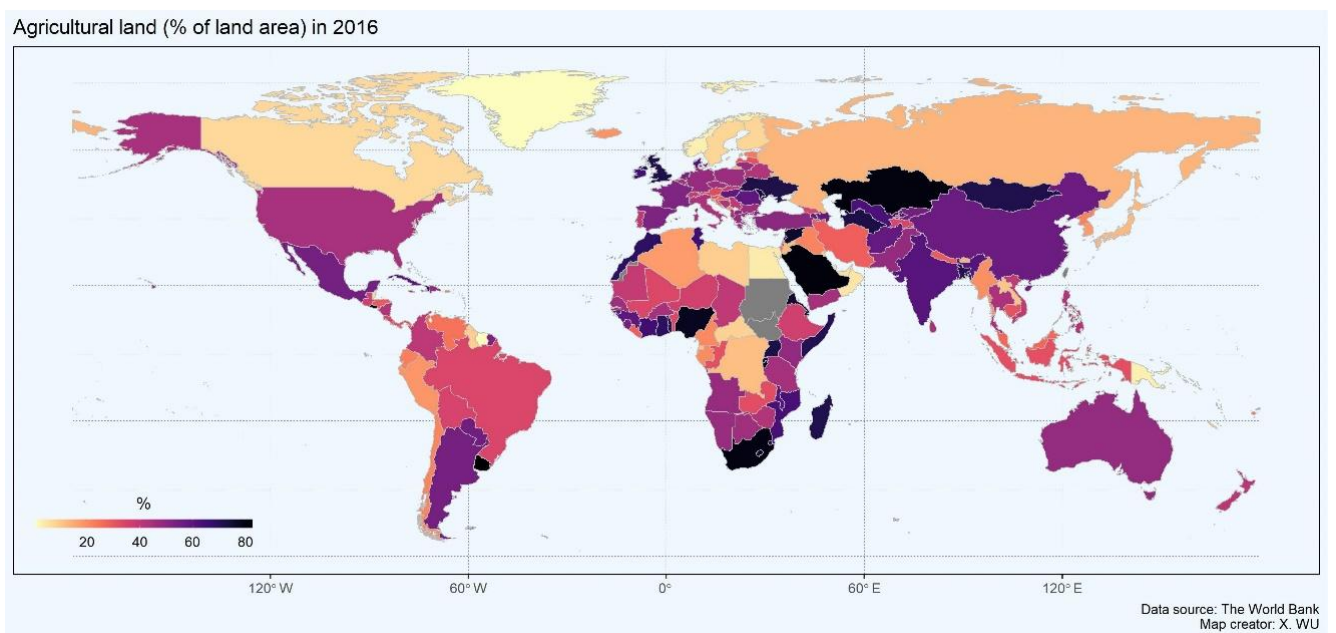


Fig. I-5. Share of agricultural lands in the world in 2016 (Antarctica excluded)

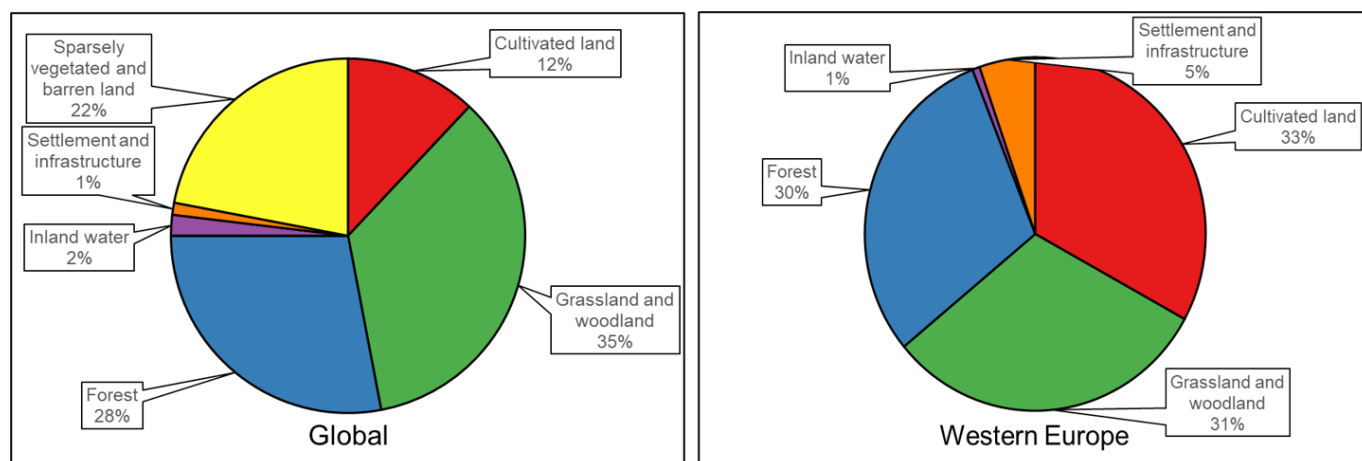


Fig. I-6. Land occupation by different usages at the global and the western Europe scale in 2010, respectively (source: FAO, <http://www.fao.org/faostat/en/#data/LC>).

Unfortunately, the arable land use has been challenged by the extensive urbanization and the explosion of the global population in the world. Studies have shown that the change of land use exhibits strong regional dominance, which are mainly deforestation, temperate reforestation/afforestation, and urbanization (Song et al., 2018). As a consequence, the global arable land has declined around 30% during the last 40 years (Wu et al., 2018) due to soil erosion, physicochemical deterioration, desertion, and human inhabitation (Weinzettel et al., 2013). Many policies have been set up to preserve and protect the arable land, including the *Common Agricultural Policy* in EU (Ackrill, 2000), *the Agricultural Section of the Fourteenth Five-Year Plan of China* ([http://www.gov.cn/zhengce/2020-11/03/content\\_5556991.htm](http://www.gov.cn/zhengce/2020-11/03/content_5556991.htm)), and *the Soil and Water Resources Conservation Act in the United States*, etc.

### 1.2.2 Land occupation types in France

The share of agricultural lands in France accounts for 52.4% of the total land area in 2016 (Fig. I-7), which is a top-rank number in European countries. Numerous types of crops have been cultivated in these agricultural areas. According to Ministère de l'Agriculture et de l'Alimentation, France is the fifth largest wheat-planting country, after China, India, Russia, and the United States. Meanwhile, France is the No.1 European country, which accounts for 18% of the European agricultural products before Italy and Spain (<https://infographies.agriculture.gouv.fr/>).

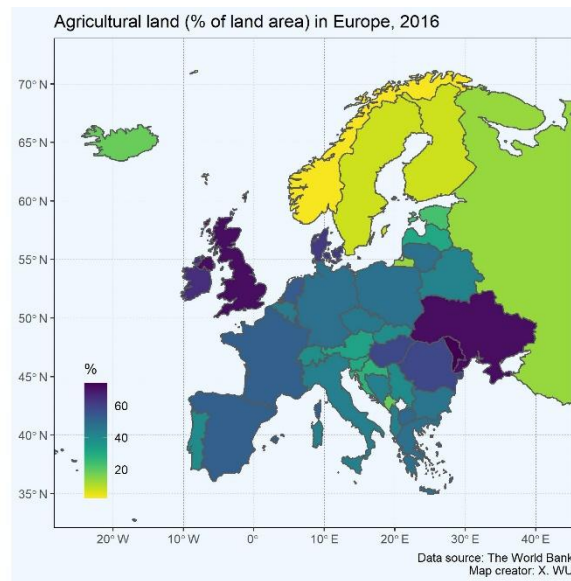


Fig. I-7. Share of agricultural lands in European continent in 2016 (source: The World Bank)

### 1.2.3 Fertilizer input

In general, modern agriculture mainly relies on two materials: fertilizers and pesticides. These two have been extensively used in agricultural areas for more than half a century to (1) increase the soil fertility and the food yield, and to (2) protect crops from diseases and hazards from fungi, weeds, and/or harmful pests and/or other animals.

#### 1.2.3.1 Definition, types, and markets

The healthy growth of the plants needs the adequate supply of nutrients, which the plants absorb from the soil via the root system. Sixteen elements, also known as nutrients, have been identified to be indispensable for the growth of the plants, which are carbon (C), hydrogen (H) and oxygen (O) (from atmosphere, soil, and water), and nitrogen (N), phosphorous (P), potassium (K), calcium (Ca), magnesium (Mg), sulphur (S), iron (Fe), zinc (Zn), manganese (Mn), copper (Cu), boron (B), molybdenum (Mo), and chlorine (Cl), which can be supplied from the reservoirs in the soil or via application of manures and fertilizers. Studies have shown that crops mainly use six of the nutrients in relatively large amounts, which are N, P, K, S, Ca, and Mg (Frink et al., 1999). Since the balance of the nutrients is negative in nearly all agricultural areas due to the removal of the harvested crops, additionally adequate nutrients must be added to the soil by different kinds of fertilizers in order to maintain the normal soil

fertility and to ensure the plant productivity (FAO, 2014). Fertilizer is defined as “*a substance (such as manure or a chemical mixture) used to make soil more fertile.*” (Merriam-Webster dictionary).

In general, fertilizer can be organic or inorganic. Though organic fertilizers (i.e., manures) provide both essential nutrients and organic matters, the nutritious content in manures is relatively low and hard to control the release of nutrient. The proportion of manure application is low compared to inorganic fertilizers. International Standard ISO-7851 has classified several categories of inorganic fertilizers, including (1) straight fertilizers, (2) compound fertilizers, (3) Ca, Mg, Na, S fertilizers, (4) trace element fertilizers, and (5) inorganic soil conditioners (or amendments).

### 1.2.3.2 Amounts used by agriculture

Extensive application of inorganic fertilizers can be found almost everywhere in the world. China, India, and the U.S. are top three countries that uses the largest amount of total N nutrients in the world (Fig. I-8). While in the European continent, France ranks the No.1 from 2000 to 2018 (Fig. I-9, Fig. I-10). Fortunately, under the control of fertilizer application by French government, the total amount of applied N fertilizers decreased from above 2500 kilo tons per year to around 2100 kilo tons per year (Fig. I-10).

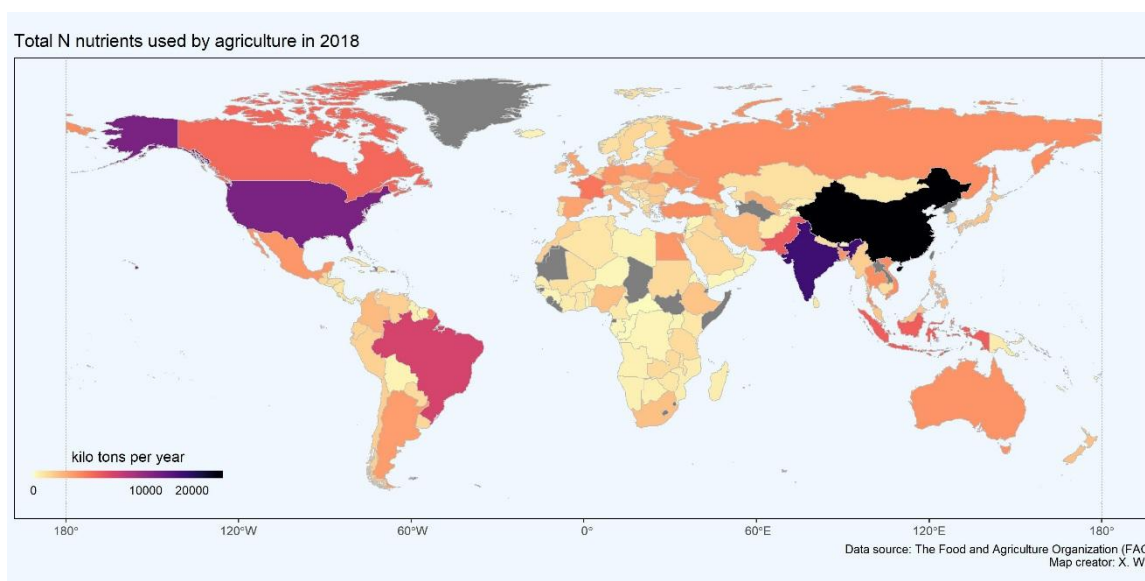


Fig. I-8. Total N nutrients used by agriculture by regions and nations in 2018 (source: FAO)



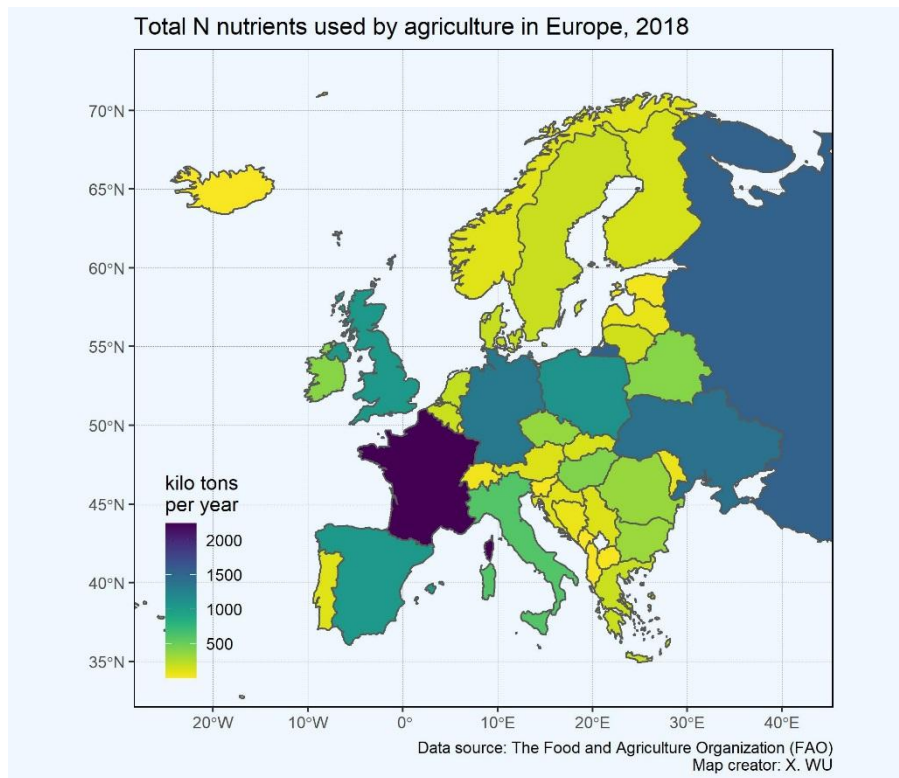


Fig. I-9. Total N nutrients used by agriculture in the European continent in 2018 (source: FAO)

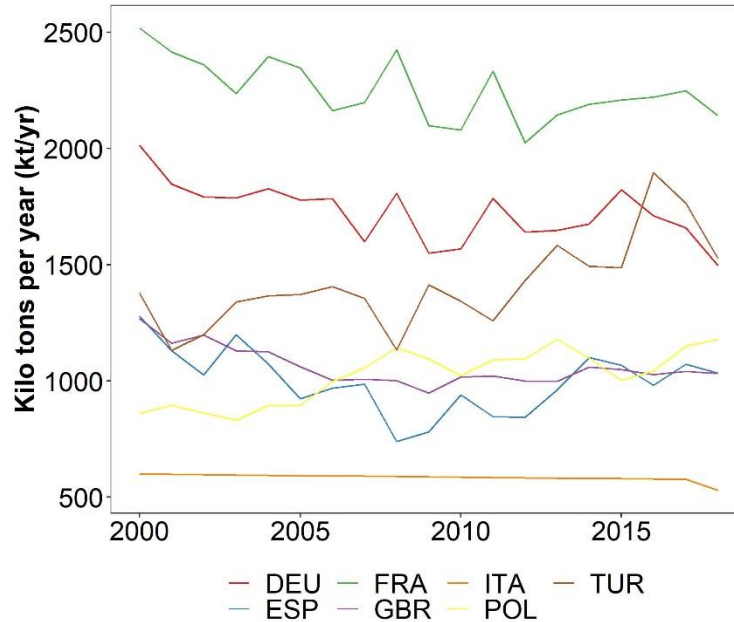


Fig. I-10. Total N fertilizer used by the first seven countries in Europe from 2000 to 2018. DEU = German, FRA = France, ITA = Italy, TUR = Turkey, ESP = Spain, GBR = Great Britain, POL = Poland.

## **1.2.4 Pesticide input**

### **1.2.4.1 Definition and types**

Pesticides are matters that are used in agricultural activities to protect the crops and plants from fungi, weeds, and/or harmful insects, which represents a large family, including insecticides, herbicides, nematicides, molluscicide, piscicides, rodenticides, avicides, bactericides, insect repellents, animal repellents, antimicrobials, fungicides, and virucides, etc. (Thostenson, 2014; FAO, 2020). More detailed information can be found at FAO.

Since the beginning of the 21<sup>st</sup> century, the use of pesticides in agriculture shows an increasing trend in general, from 3100 to 4100 kilo tons (Fig. I-11A, FAO). Herbicides constitutes the largest parts of total pesticides consumed by agriculture in the world. It should be noticed that, so far, the amount of consumed pesticides reaches a plateau around 4100 kilo tons since 2010, which can be a good signal to reflex the effectiveness of pesticide control by many organizations and nations. The structure of different types of pesticides used in agriculture is varying between countries. For instance, in U.S., herbicides accounts for the most of total pesticides (Fig. I-11B), while in France, the uses of fungicides and herbicides are almost equal after 2010 (Fig. I-11C). Meanwhile, the total amount of pesticides used in French agriculture exhibits a decreasing tendency, especially for the fungicides and bactericides (Fig. I-11C).

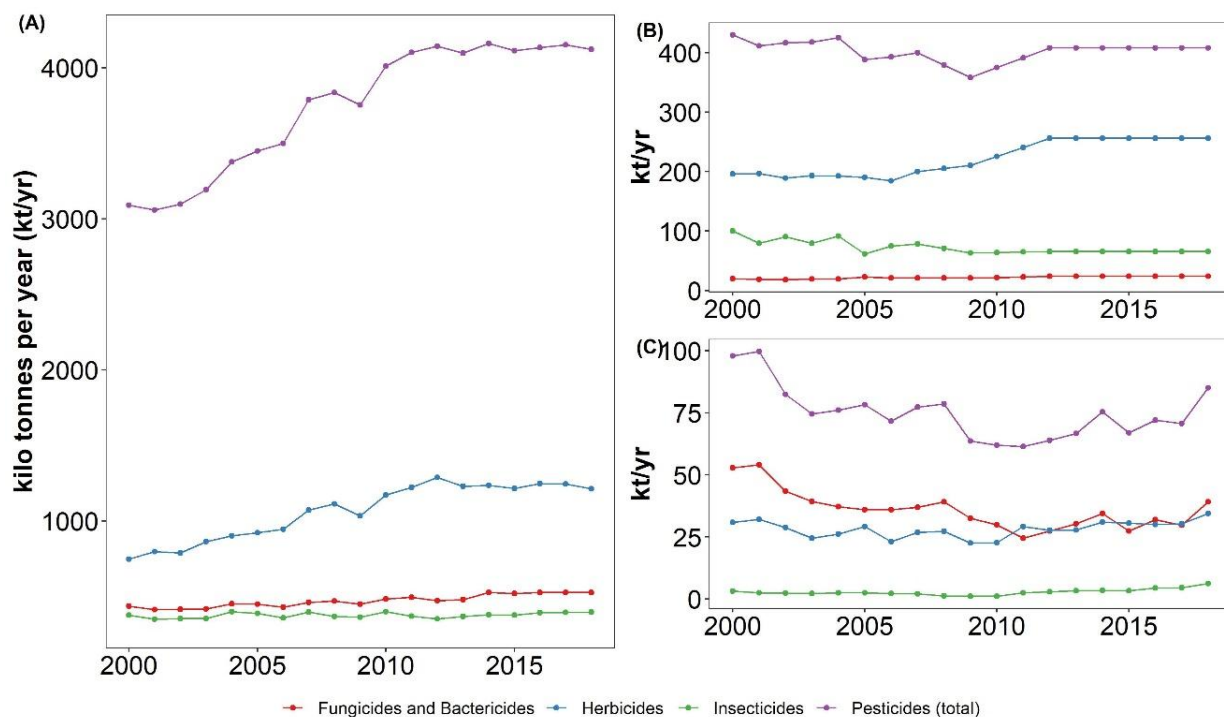


Fig. I-11. Amount of used pesticides: (A) in worldwide, (B) in the United States, (C) in France from 2000 to 2018 (data source: FAO)

The use of pesticides per area of cropland is also an important indicator to reveal the intensity of used pesticides in agricultural areas (Fig. I-12, Fig. I-13, data source: FAO, 2020).

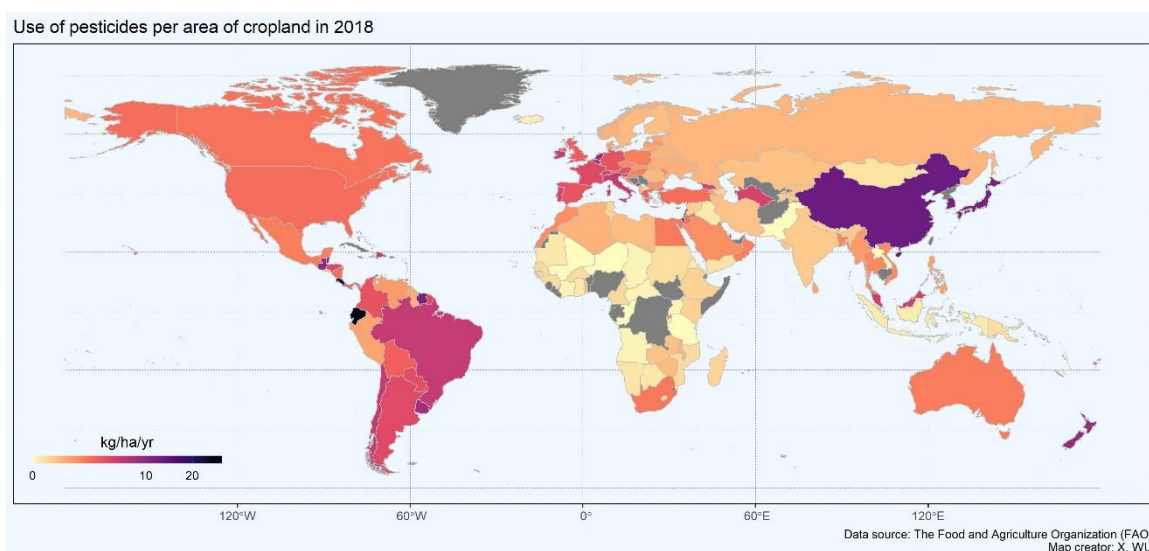


Fig. I-12. Use of pesticides per area of cropland in 2018 (Source: FAO)

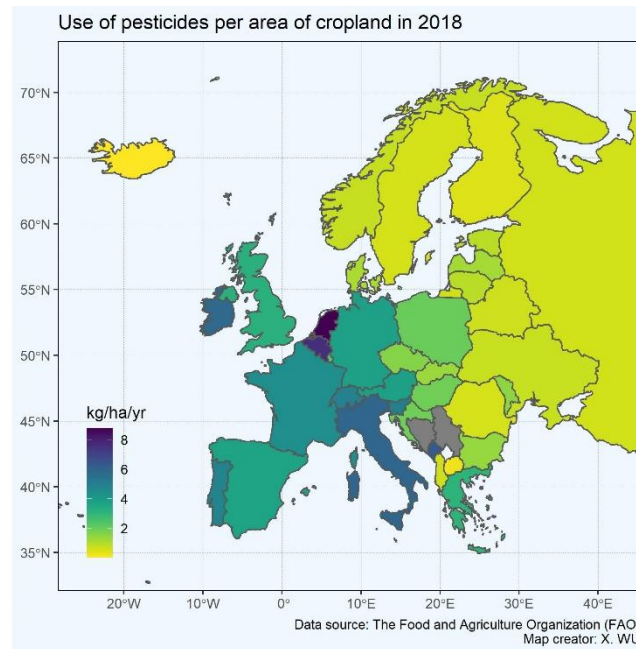


Fig. I-13. Use of pesticides per area of cropland in Europe in 2018 (source: FAO)

## 1.2.5 Consequences of intensively agricultural activities

Though the intensively agricultural activities provide the food supply, a variety of environmental issues have emerged, which result in many adverse effects on the humans and other life-forms.

### 1.2.5.1 River eutrophication by fertilizers

Eutrophication in the aquatic system is a biological consequence resulting from the enrichments of nutrient (nitrogen and phosphorous) in water, which have drawn wide attention since the middle of the 20<sup>th</sup> century due to the increasing use of inorganic, synthetic fertilizers in agricultural areas (Schindler, 2006). The common sign of eutrophication in water is the algae blooming (Sinha et al., 2017). The unlimited growth of algae and other macrophytes after the large input of nutrients in water will cause serious environmental problems, such as (1) the depletion of dissolved oxygen in water, (2) the periodic fish kills, (3) the degradation of the local ecosystem, and so on (Schindler, 2006). Needless to say, the eutrophication is hazardous to a healthy aquatic ecosystem. A typical case of the eutrophication is the Taihu Lake in China, which is plagued by algae bloom and hypoxia (Xu et al., 2010).

### **1.2.5.2 Trace metals hazards**

Sediments have a favorable affinity to PTEs. The concentrations of PTEs in sediments are normally far greater than in waters from the agricultural areas. Especially in a calcareous system, the concentration ratio between waters and sediments is even below 1% (Wu and Probst, 2021). The PTEs in sediments are thus a major concern as regard the environment. Although PTEs are complexed with minerals and Fe/Mn oxides, they can be released again to the environment by turbulences, such as sediment dredging activities and storm flood events. It is important to keep the dwelling sediments from becoming a secondary source of hazardous metals.

### **1.2.5.3 Emission of greenhouse gases**

The term of greenhouse gas (GHG) is defined as “*those gaseous constituents of the atmosphere, both natural and anthropogenic, that absorb and re-emit infrared radiation*” (UNFCCC, 1992), mainly including carbon dioxide (CO<sub>2</sub>), methane (CH<sub>4</sub>), nitrous oxide (N<sub>2</sub>O), hydrofluorocarbons (HFCs), perfluorocarbons (PFCs), sulphur hexafluoride (SF<sub>6</sub>), nitrogen trifluoride (NF<sub>3</sub>), trifluoromethyl sulphur pentafluoride (SF<sub>5</sub>CF<sub>3</sub>), halogenated ethers (e.g., C<sub>4</sub>F<sub>9</sub>OC<sub>2</sub>H<sub>5</sub>), and other halocarbons not covered by the Montreal Protocol including CF<sub>3</sub>I, CH<sub>2</sub>Br<sub>2</sub>, CHCl<sub>3</sub>, CH<sub>3</sub>Cl, CH<sub>2</sub>Cl<sub>2</sub> (IPCC, 2006, 2019). In the agricultural areas, the main emitted GHGs are CO<sub>2</sub>, CH<sub>4</sub>, and N<sub>2</sub>O.

The balance of CO<sub>2</sub> between the atmosphere and the agricultural ecosystem is affected by the uptake by plant photosynthesis and the release of respiration, the decomposition of organic matters. Although the flux of CO<sub>2</sub> accounts for the largest proportion of the GHG in agricultural areas, the emission of CH<sub>4</sub> and N<sub>2</sub>O cannot be neglected. N<sub>2</sub>O is mainly released from soil and sediment as an intermediate product of nitrification and denitrification, especially in agricultural catchments. Studies have shown that N<sub>2</sub>O emission is significant in agricultural areas with high nitrate concentrations in the aquatic system since high nitrate concentration can result in an incomplete denitrification (Hefting et al., 2003; Saggar et al., 2013).

### **1.2.5.4 Pesticide hazards to living organisms**

Compared to the very long history of pesticide application, the adverse effects of

pesticides on the environment were not drew much attention until the publication of the famous book *Silent Spring* by Rachel Carson. It reported the devastating aftermath brought by the unlimited use of dichlorodiphenyltrichloroethane (DDT), not only for the environment, but also for the humans. Meanwhile, some pesticides contain toxic metals. For example, the Bordeaux mixture is a fungicide vastly used in vineyards to protect the wine grapes. It consists of copper sulphate ( $\text{CuSO}_4$ ) and hydrated lime ( $\text{Ca(OH)}_2$ ). The application of Cu-fungicides over the years increases the Cu content in many vineyard soils from 100 to 1500  $\text{mg kg}^{-1}$  (Duplay et al., 2014). Copper concentration higher than 100  $\text{mg kg}^{-1}$  can cause adverse effects on soil functioning and growth of plants (Kabata-Pendias, 2010).

#### **1.2.5.5 Soil erosion**

Soil erosion is an acute problem that threaten the agriculture. It is a kind of soil degradation, which displaces the upper layer of soil. In addition to the natural weathering processes, soil erosion is more increased by anthropogenic activities, including deforestation, overgrazing, and the excessively use of agrochemicals (Shi and Shao, 2000). The huge amount of soil erosion and soil loss has contributed to harsh agricultural issues.

Studies have shown that high rainfall intensity, the steep slopes, poor soil nutrients, and low organic matter can contribute to the soil erosion (Novara et al., 2011). Besides, soil erosion can also be triggered by chemical factors due to the soil dissolution by the proton release because of the excessive nitrate in soils (Gandois et al., 2011). Both mechanical and chemical factors contribute to the high soil erosion intensity in southwestern France, which is a traditional agricultural region (Fig. I-14).

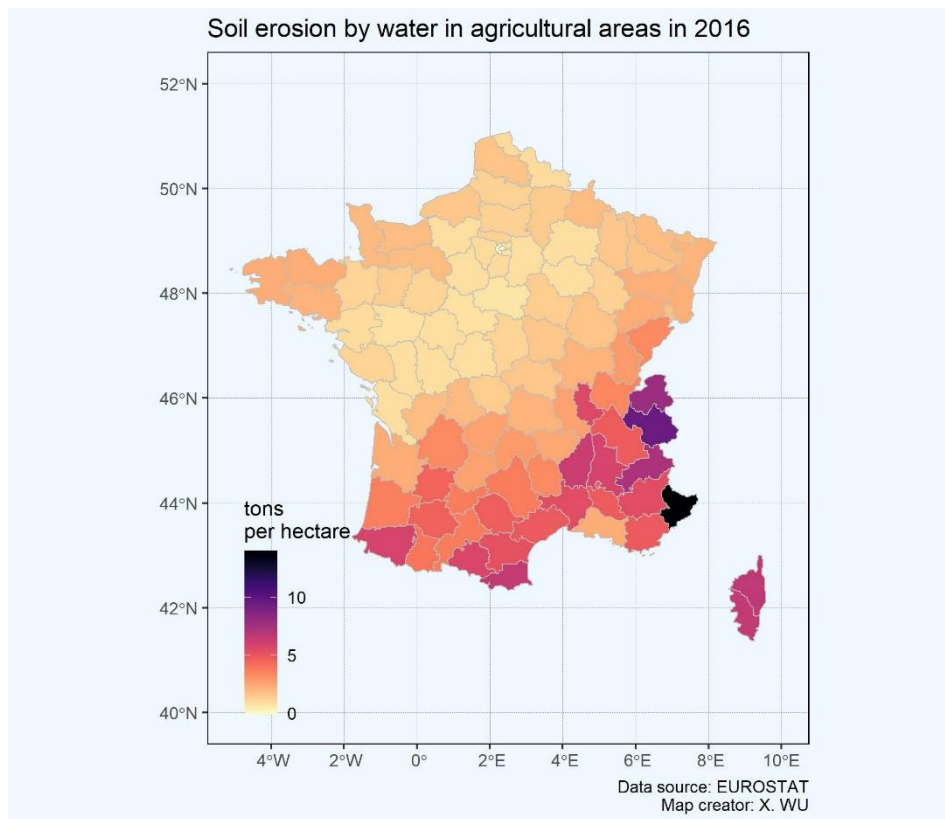


Fig. I-14. Soil erosion by water in agricultural areas in France, 2016 (Source: EuroStat)

Of course, the effects of intensive agriculture on the environment are not only the above consequences. Due to the increasing global population and the vast demand of food, more and more studies on the agro-environmental questions are emerging. Countries and governments are also in action to solve the environmental problems related to agriculture. Various techniques have been developed in order to mitigate the different contaminants released to the ecosystem surrounding the cultivated land. The constructed wetland has been proved to be effective among these novel techniques (Vymazal, 2007).

### 1.3 Constructed wetlands and ponds in agricultural catchments

#### 1.3.1 Definition of catchments, constructed wetlands, constructed ponds, and sediments

The term of “catchment” has been used by various scientific communities with different specific meanings. In geology, hydrology and environmental science, the “catchment” is a

drainage area that contributes water to a particular point along a channel network or a depression based on its surface topography (Fig. I-15) (Wagener et al., 2007).

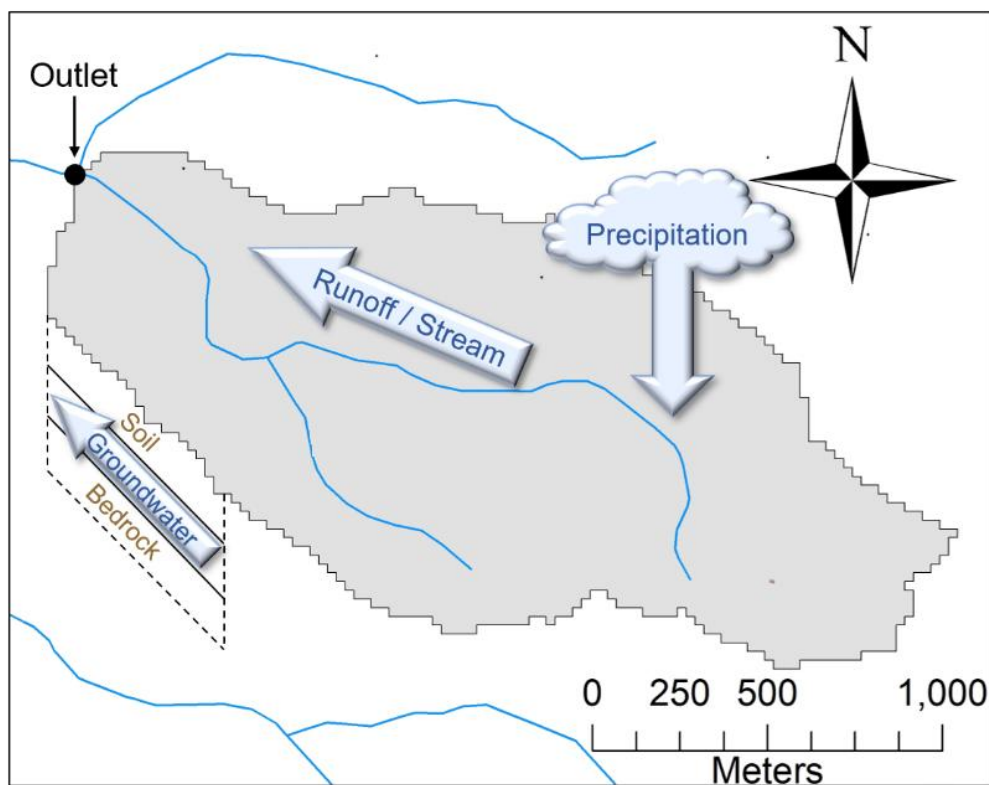


Fig. I-15. Illustration of a catchment (e.g., the Montoussé catchment, a CZO of OZCAR)

The wetlands are “*areas of marsh, fen, peatland or water, whether natural or artificial, permanent or temporary, with water that is static or flowing, fresh, brackish or salt, including areas of marine water the depth of which at low tides does not exceed six meters*” (Ramsar Convention, 2016). According to this definition, various types of inland habitats can be regarded as the wetlands (Fig. I-16 A1 and A2), including “*marshes, peatlands, floodplains, rivers and lakes, and coastal areas such as saltmarshes, mangroves, intertidal mudflats and seagrass beds, and also coral reefs and other marine areas no deeper than six meters at low tide, as well as human-made wetlands such as dams, reservoirs, rice paddies and wastewater treatment ponds and lagoons*” (Ramsar Convention, 2016).

The constructed wetland is an artificial wetland, which is engineered for a wide range of specific purposes by humans, such as water storage, agricultural irrigation, flood prevention, and landscape, etc. (Hammer, 2020). The constructed pond (Fig. I-16 B1 and B2) is a branch



of the constructed wetland (Ramsar Convention, 2016, 2018). It is normally smaller than the generic constructed wetland in size.

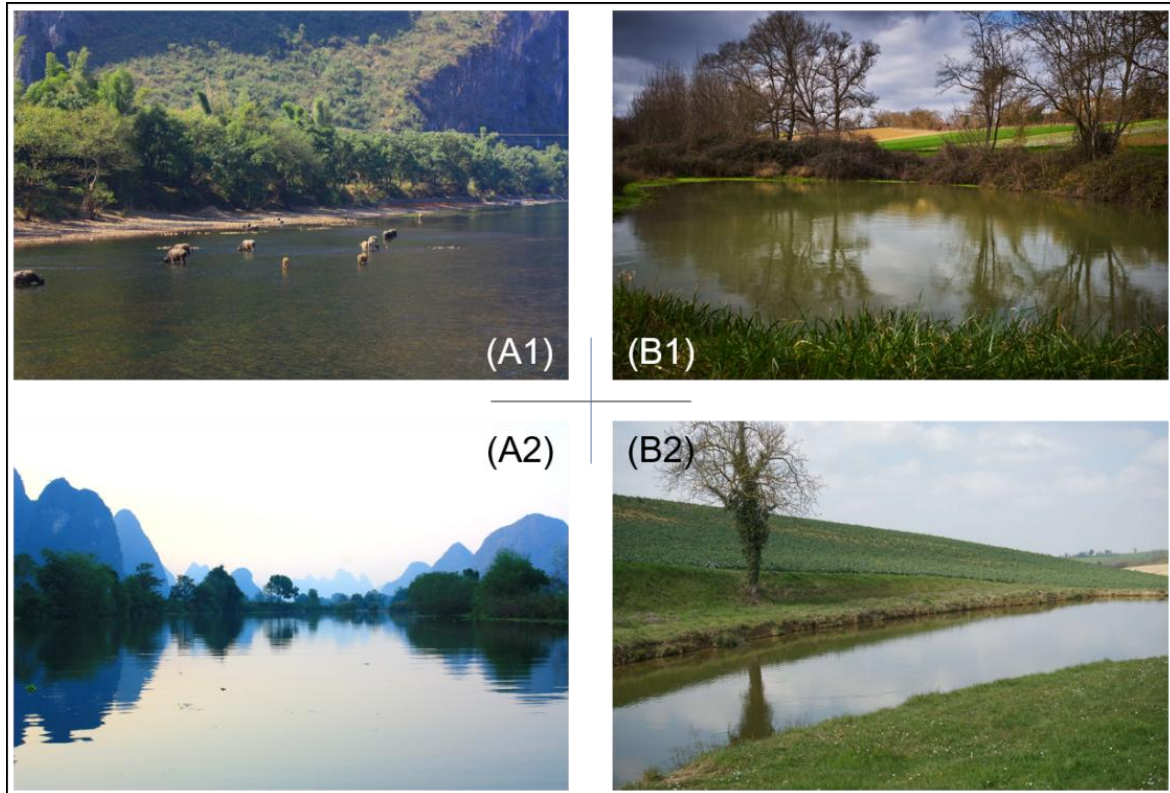


Fig. I-16. Photos of different types of wetlands: (A1) a shallow marsh in Guilin, China; (A2) a lake in Guilin, China; (B1) a constructed pond in Marestaing, France; (B2) a constructed pond in Montoussé, France. (Photographer: G. WU and X. WU)

Whatever natural or constructed, the wetlands mostly have these key components (Hammer, 2020):

- Hydraulically conductible substrate
- Water flowing in/above the substrate
- Aerobic and anaerobic environments supporting the growth of microbiomes
- (In)vertebrates
- Hydrophytes

Sediment plays an important role in these wetlands and ponds, which cannot be ignored. Sediment is a naturally occurring material that is broken down by processes of weathering and erosion of rocks or soils, and is subsequently transported by the action of wind, water, or ice or

by the force of gravity acting on the particles (Boggs, 2014).

### **1.3.2 History and types of CWs**

Before the appearance of constructed wetlands, natural wetlands have been applied for wastewater treatment for many centuries. However, these natural sites have been used as “disposal” instead of real treatment since these natural wetlands are just near the water way of the target wastewater. Meanwhile, these natural wetlands were not specifically engineered, and they were usually deteriorated by uncontrolled wastewater discharge (Vymazal, 2011). In such a condition, the concept of the constructed wetland (CW) was proposed by the middle of the 20<sup>th</sup> century. The first application of the CW can be traced back to the 1950s by Dr. Käthe Seidel in Germany (Vymazal, 2011). Due to a better treatment efficiency compared to the natural wetlands, CWs have been preferred worldwide.

In general, CWs are specifically designed ecosystems, which aim to treat single or multiple contaminants in wastewater by a number of natural processes. Three major types of CWs have been categorized due to various design parameters: (1) surface flow constructed wetlands, (2) subsurface flow constructed wetlands, and (3) hybrid constructed wetlands.

### **1.3.3 Effects of CWs on contaminants**

In agricultural areas, non-point sources of contaminants pose a great threat to the local aquatic system, especially for nitrogen and potentially toxic elements (PTE), which mainly originate from the spreading of inorganic fertilizers and some pesticides containing metals. Rather than other specified techniques, the constructed wetland have been proved to be suitable for mitigating multiple types of contaminants, including nitrate and PTEs (Vymazal, 2007).

The next two sections will introduce the nitrogen and several PTEs in agricultural catchments since this thesis focus on these two different types of contaminants.

Since 1700, up to 87% of the worldwide wetlands has been lost due to the stressed anthropogenic activities (Ramsar Convention, 2018). Meanwhile, the diverse species dwelling in the wetland show a sharp decline since 1970, which affects 81% of inland wetland species and 36% of coastal and marine species (Ramsar Convention, 2018). In such a condition, it is of great importance to protect the wetlands and surrounding environments. The wetlands and

the water resources are also great legacies to our next generations.

## 2. Nitrogen in aquatic ecosystem

### 2.1 Nitrogen in biogeochemical cycle

The term of “nitrogen” here does not only refer to the single chemical element N. It encompasses a variety of organic and inorganic nitrogen compounds, from molecules to ions, including dinitrogen ( $N_2$ ), nitrous oxide ( $N_2O$ ), ammonia ( $NH_3$ ), organic nitrogen ( $N_{org}$ ), ammonium ( $NH_4^+$ ), nitrate ( $NO_3^-$ ), and nitrite ( $NO_2^-$ ), which are common and important in the wetland system (Fig. I-17).

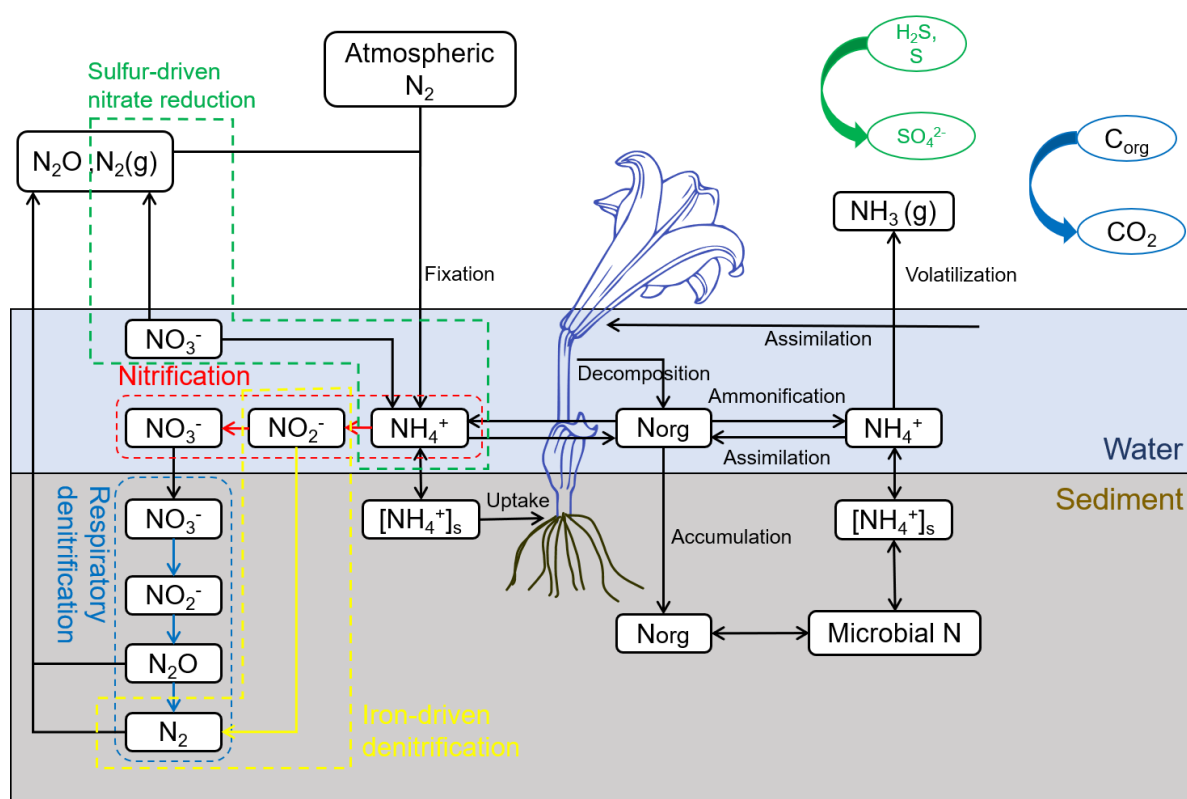


Fig. I-17. Schematic diagram of N-cycling in an aquatic system

Nitrogen exhibits an intricate biogeochemical cycle, which couples with various abiotic and biotic transfer and transformations (Fig. I-17). The transfer and transformations, from inorganic nitrogen to organic nitrogen and *vice versa*, can be classified into various categories according to the types of reactions. It should be also noticed that the Haber-Bosch process, which is applied to produce synthetic fertilizers, is one of the largest sources to reactive nitrogen in the biosphere (Erisman et al., 2008). This process can cause an anthropogenic

disruption to the nitrogen cycle.

### 2.1.1 Fixation

Atmospheric dinitrogen (N<sub>2</sub>) can be fixed to ammonia by nitrogenase (Raymond et al., 2004). This kind of fixation has been observed in the flood water, in anaerobic flooded soils, in the rhizosphere of macrophytes (Vymazal, 2007). Studies have shown that nitrogen fixation in the flooded soils is more significant under reduced than under oxidized conditions (Peoples et al., 1995). However, nitrogen fixation needs a significant amount of cellular energy which seems wasted in a nitrogen-rich environment (Kadlec and Wallace, 2008). In such a condition, the fixation rate in agricultural wetlands can be probably much lower or negligible compared to other nitrogen transformations since the agricultural wetlands receives a large load of nitrogen input.

### 2.1.2 Volatilization

Volatilization is a physicochemical process that converts NH<sub>4</sub><sup>+</sup> to gaseous NH<sub>3</sub> released to the atmosphere (Eq. I-1). The ammonia volatilization depends on the water pH value. Alkaline water is more likely to increase the ammonia volatilization when pH value exceeds 9.3 (Saeed and Sun, 2012). The nitrogen loss via volatilization is normally unnoticeable compared to biological nitrate reductions in agricultural wetlands since most stream waters in agricultural areas are not highly alkaline (Białowiec et al., 2011; Saeed and Sun, 2012). A recent study shows that ammonia volatilization is only responsible for less than 5% of the total removal of NH<sub>4</sub><sup>+</sup>-N in an intensified constructed wetland (Lyu et al., 2018).



### 2.1.3 Ammonification

Ammonification biologically converts the organic nitrogen to its inorganic form (NH<sub>4</sub><sup>+</sup>-N) mainly by microorganisms and plankton, which is a complex, multi-step, mineralizing biochemical process (Eq. I-2 to Eq. I-4) (Vymazal, 2007; Kadlec and Wallace, 2008).

*Amino acids* → *Imino acids* → *Keto acids* →  $NH_3$  (*oxidative deamination*) (Eq. I-2)

*Amino acids* → *Saturated acids* →  $NH_3$  (*reductive deamination*) (Eq. I-3)

$NH_3 + H_2O \rightleftharpoons NH_4^+ + OH^-$  (Eq. I-4)

Ammonification can both occur in the oxidized soil (Eq. I-2) and in the reduced soil (Eq. I-3). Ammonification is observed to be faster in the upper layer of a wetland with an aerobic condition, while it is slower in the deeper anaerobic layer (Vymazal, 2007; Reddy et al., 2009). Ammonification rate is affected by temperature, pH, concentration of available nutrients, and the characteristics of medium where ammonification occurs (Vymazal, 2007). Vymazal (1995) concludes several optimal parameters for ammonification, such as the temperature between 40 – 60 °C and the pH value of 6.5 to 8.5.

Considering that ammonification is faster than nitrification (see section 2.1.4) in terms of the kinetics of these two reactions, ammonification can be the first step of nitrogen transformation in a wetland ecosystem, particularly when organic nitrogen is abundant in inlet water (Kadlec and Knight, 1996; Saeed and Sun, 2012). In addition, photo-ammonification has been observed by Bushaw et al (1996), which converts organic nitrogen into smaller nitrogenous substances (e.g.,  $NH_4^+$ ). This photo-chemical process has been proved to play an important role in biomass production and eutrophication (Yang et al., 2020).

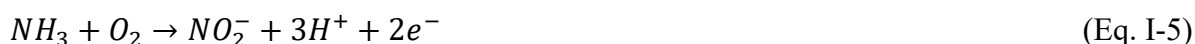
Although ammonification turns organic nitrogen to another form, the net amount of nitrogen in a given aquatic ecosystem does not change.

#### 2.1.4 Nitrification

Nitrification plays a key role in the nitrogen cycle in a wetland ecosystem as it builds a link between the mineralization of organic nitrogen and the removal pathway of nitrate. Nitrification can occur in three parts of a constructed wetland, (1) water column, (2) water-sediment interface, and (3) plant root-sediment interface (Reddy et al., 1989). Both autotrophic and heterotrophic nitrifications have been observed (Park et al., 2015), although the  $^{15}N$ -labeling technique identifies that autotrophic nitrification is more common than heterotrophic nitrification in an agricultural system (Barraclough and Puri, 1995; Islam et al., 2007).

A classic autotrophic nitrification contains two steps. Ammonia-oxidizing microbes (e.g.,

*Nitrosomonas*) transform ammonia to nitrite in the first step (Eq. I-5). The second step is to oxidize nitrite to nitrate by nitrite-oxidizing microbes, e.g., *Nitrobacter* (Eq. I-6). Heterotrophic nitrification is initiated by heterotrophic nitrifiers, directly oxidizing organic nitrogen to nitrite and/or nitrate (EPA, 2002). However, heterotrophic nitrification rate is much slower than autotrophic nitrification rate, and the contribution of heterotrophic nitrification is greatly less than autotrophic nitrification (EPA, 2002; Subbarao et al., 2006; Sahrawat, 2008).



Autotrophic nitrification rate depends on a variety of parameters, including temperature, pH, inorganic carbon availability, microbial abundance and population, and concentrations of ammonium-N and dissolved oxygen (Vymazal, 2007; Sahrawat, 2008).

### 2.1.5 Nitrate reduction

A chapter in this thesis mainly focuses on the nitrate reduction (particularly for denitrification). See Section 2.2.3 for detailed information about the classical and newly discovered removal pathways for nitrate in the ecosystem of a constructed wetland.

### 2.1.6 Assimilation and plant uptake

Nitrogen assimilation refers to the biological processes, which transform inorganic nitrogen compounds to organic nitrogen forms (Vymazal, 2011). Studies have shown that the most commonly used nitrogenous forms in assimilation are ammonia and nitrate (Kadlec and Knight, 1996). Ammonia is a preferable substance for assimilation due to its more reduced valence of N compared to nitrate (Vymazal, 2007). Assimilation of ammonia can account for 67.4 - 76.5% of the total amount of ammonia in a constructed wetland, even under saline conditions (Klomjek and Nitisoravut, 2005). In agricultural areas, nitrate is the most abundant nitrogen in water. However, the proportion of assimilated nitrate by macrophytes remains very low compared to the total N loads in agricultural water (Lu et al., 2009; Tournebize et al., 2017), which only accounts for 7 – 14% of total nitrate concentration.

A variety of macrophytes are commonly found in a constructed wetland. They are essential to support the ecosystem service of the wetland. Macrophytes can be considered as an indispensable constituent to improve the efficiency of nitrogen removal in a constructed wetland due to their ability.

### 2.1.7 Ammonia adsorption

Ammonia adsorption is a physical adsorption and/or ion exchange process, which can occur in some specific media, such as biochar and zeolite (Saeed and Sun, 2012; Yong et al., 2016). A variety of specific media have been deployed in constructed wetlands to optimize the nitrogen retention ability (Yong et al., 2016; Kizito et al., 2017). Three modes of ammonia adsorption rate in a number of different media have been discovered (Yong et al., 2016). The different trends of ammonia adsorption depend on the adsorption mechanism of a given substrate (Fig. I-18). Therefore, the desorption of adsorbed ammonia should be considered in order to promote the efficiency of ammonia retention in specific media. Studies have shown that volcanic rock, porcelain ceramist, zeolite, and biochar are good media to optimize ammonia adsorption in agricultural constructed wetlands due to their high ion exchange capacity and relatively small desorption rate (Lu et al., 2009; Yong et al., 2016; Kizito et al., 2017).

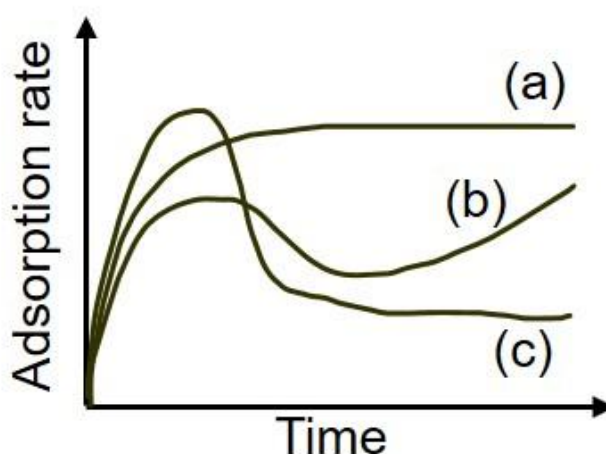


Fig. I-18. Three modes of ammonia adsorption rate: (a) increase to stable; (b) increase to decrease to increase; (c) increase to decrease to stable. (Note: the curves are only schematic and do not reveal the real adsorption rates)



### **2.1.8 Organic nitrogen burial and accretion**

In some cases, some part of the organic nitrogen combined with detritus could become an unavailable phase, which can no longer participate in the nitrogen cycling, as a consequence of sediment formation and burial. Nevertheless, the data on the nitrogen burial in the constructed wetland is very limited. A study shows that the contribution of nitrogen burial to the total N removal in a constructed wetland is very variable, ranging from 1 to 46% (Chen et al., 2014).

### **2.1.9 Anaerobic ammonium oxidation**

Anaerobic ammonium oxidation (ANAMMOX) converts  $\text{NO}_2^-$  and  $\text{NH}_4^+$  to  $\text{N}_2$  (Mulder et al., 1995). During ANAMMOX, nitrite/nitrate acts as the electron acceptor.

ANAMMOX is a promising technology to treat nitrogen in wastewater. However, to date, the study of ANAMMOX in constructed wetlands is still not abundant compared to the studies on other nitrogen removal reactions, such as nitrification and denitrification.

In general, the nitrogen cycle infiltrates vast spheres in a constructed wetland in CZ, which is from the near-surface layer of atmosphere (volatilization and fixation) to the bottom sediment (assimilation, denitrification, burial, etc.).

## **2.2 Nitrate transfer, transformation, and controlling factors**

Although nitrogen exists in various forms as stated above, nitrate is generally the most abundant N substance in agricultural aquatic environment. The knowledge of nitrate has accumulated through the worldwide studies over past 100 years. However, the pathways of nitrate removal in agricultural waters and streams are still not totally clarified since novel mechanisms of nitrate removal have been discovered in recent years with the development of new methods and analytical techniques. Meanwhile, although nitrate is indispensable, it also exerts burdens on the environment and brings adverse effects on the living organisms. In such a condition, many organizations and countries have set several upper limits on the concentration of nitrate in drinking water, which is based on the consideration of human health (Powlson et al., 2008). The European Union (EU), for example, regulates an upper limit of 50 mg of nitrate  $\text{L}^{-1}$  and 44 mg  $\text{L}^{-1}$  in the United States. Considering nitrate as a double-edged

sword, it is of great importance to know where nitrate comes from and its main removal pathways in the agricultural aquatic system.

### **2.2.1 Anthropogenic sources of nitrogen**

Galloway et al (2004) reported that the nitrogen availability has been greatly increased by human activities at most regional scales. Though the increased use of inorganic fertilizers supports the augmented crop yields, a large fraction of N applied to crops finally enters the freshwater system and cause several environmental issues. A recent global study has revealed that around 75% of N loads derived from agricultural diffuse sources (Mekonnen and Hoekstra, 2015). Meanwhile, the cereals showed the largest contribution to the N-related contaminated freshwater (Mekonnen and Hoekstra, 2015). To prevent the N-related contamination in freshwater in France is then much important since she is the 5<sup>th</sup> largest wheat producer. In fact, the excessive nitrate concentration ( $> 50 \text{ mg L}^{-1}$ ) has been already observed in some French agricultural catchments due to the intensive fertilizer application (Paul et al., 2015).

### **2.2.2 Nitrate transfer from soil to water**

Nitrate is highly soluble in water, which contributes to its considerable mobility from one compartment to another. The agricultural activities, especially the fertilizer spreading, have been regarded as the major source of nitrate in agricultural water channels (Bur et al., 2009; N'guessan et al., 2009; Guo et al., 2010). Meanwhile, other fertilizers (e.g., manure, home-made fertilizers, etc.) also introduce some non-nitrate nitrogen compounds into the water. For instance,  $\text{NH}_4^+\text{-N}$  can be released after the application of manure in croplands. It can be transported to the downstream water channels due to the runoff and subsequent soil erosion. Once entered the water,  $\text{NH}_4^+\text{-N}$  is transformed to nitrite and/or nitrate by the microbiological nitrification (see Section 2.1.4).

Soil erosion and leaching are responsible first for nitrate transfer from soil to the aquatic system. Leached nitrate passes a variety of compartments and landscapes prior to discharge of the aquatic system. Two kinds of landscape components have been identified by Haag and Kaupenjohann (2001): retention compartments and corridors. Corridors, including macropores, preferential paths, drainage tiles and streams, direct nitrate to the aquatic systems very fast,

while retention compartments can delay the movement of leach nitrate to the aquatic system or even remove nitrate during the retention by various nitrate removal pathways. The retention compartments are capillary tubes, saturated zones, and macrophytes, etc.

Meanwhile, Paul et al (2015) revealed a lag phenomenon of nitrate increase in stream water during the storm flood event. The stream nitrate concentration did not increase in the first stage of the flood due to the dilution of rainfalls and surface water. When the subsurface water and soil solution reached the stream in the second stage of the flood event, the stream nitrate began to increase.

### **2.2.3 Nitrate removal pathways in aquatic system**

The biogeochemical cycle of nitrogen has been presented in Section 2.1. In consideration of the high abundance of nitrate in the agricultural aquatic system, to investigate the nitrate pathways is critical to remove excessive nitrate and then maintain the sustainable development of an ecosystem, as well as to ensure a healthy environment for the living organisms. These removal pathways include various processes.

#### **2.2.3.1 Pathways for nitrate removal**

Current studies agree that the removal of heavy nitrate loads in the aquatic system is largely due to several biological transformations, including assimilation into biomass, or to respiratory denitrification by bacteria (Burgin and Hamilton, 2007). However, according to the direct assays for denitrification, in some cases, the denitrification process only accounted for less than half of the total nitrate removal (Seitzinger et al., 1993; Burgin and Hamilton, 2007), which indicated that part of the nitrate removal could be a result of other processes except assimilation or respiratory denitrification. Indeed, some novel pathways of nitrate have been discovered, such as dissimilatory nitrate reduction to ammonium (DNRA) (Friedl et al., 2018), anaerobic ammonium oxidation (ANAMMOX) (Dong et al., 2009; Humbert et al., 2012), nitrate reduction coupled to iron oxidation (Davidson et al., 2003; Smith et al., 2017), denitrification coupled to sulfide oxidation (Brunet and Garcia-Gil, 1996), etc. However, in agricultural constructed wetlands, the denitrification still accounts for the most proportion of the total nitrate removal since other processes mentioned above normally require strict

conditions, such as high sulfidic or ferrous environments (Vymazal, 2007; Saeed and Sun, 2012).

### 2.2.3.2 Controlling factors of denitrification

Denitrification is a chain of several microbial processes that convert nitrate to nitrogen gases using nitrogen oxides as electron acceptors (Eq. I-7 to Eq. I-10, Saggar et al., 2013).



These intermediate processes are catalyzed by different enzymes in each phase, also known as “denitrifiers”, including nitrate reductase (*nar*), nitrite reductase (*nir*), nitric-oxide reductase (*nor*), and nitrous oxide reductase (*nos*) (Tiedje, 1994).

A variety of factors can affect the denitrification process, including direct factors (nitrate, organic carbon, oxygen, etc.) and indirect ones (temperature, pH, hydrology, etc.)

- Temperature

The gene expressions and activities of denitrifiers are sensitive to temperature (Saleh-Lakha et al., 2009). Although Knowles (1982) proposed that denitrification was still observed between 0 and 75 °C, a moderate temperature can contribute to a considerable denitrification rate. Meanwhile, the nitrate removal efficiency decreased from 94 to 57% due to temperature decrease from 30 to 13 °C (Shen et al., 2020).

- pH

Sediment pH is another key factor that affects denitrification as indicated by Eq. I-7 to Eq. I-10. Both theories and experiments show that denitrification is slower in a very acid environment (Baeseman et al., 2006; Saeed and Sun, 2012). In an acid mine drainage area, the denitrification rate was much lower than in many mountain

catchments (Baeseman et al., 2006). However, many studies also observed that denitrification can still occur under an acid pH value and also account for a significant nitrate removal (Liu et al., 2010; Jung et al., 2019). The debate on the optimum pH for denitrification is still undergoing (Šimek and Cooper, 2002) since the mechanism of pH control on denitrification is not fully clarified yet (Saggar et al., 2013).

It is noticed that sediment pH can also affect the  $N_2O:N_2$  product ratio during the denitrification process. The  $N_2O:N_2$  ratio can be increased at lower soil pH (Liu et al., 2010). Hence, the emission of  $N_2O$  should be taken into consideration since it is a greenhouse gas in drainage areas with low water/sediment pH values. Liu et al (2010) also proposed that  $N_2O$  emission can be relieved by increasing pH above 6.

- Oxygen

Typically, denitrification is an anaerobic process. The presence of  $O_2$  normally suppresses this process in sediment (Knowles, 1982; Saeed and Sun, 2012; Saggar et al., 2013). However, an increasing number of studies also found that denitrification can occur in oxic environment (Gao et al., 2010; Liu et al., 2013). Gao et al (2010) hypothesized that the high denitrification rates in the presence of oxygen may be due to the adaption of the denitrifiers to the environment.

- Nitrate concentration

Nitrate is the prerequisite for denitrification; therefore, the availability of nitrate is one of the most important factors regulating denitrification. Field studies have evidenced that the denitrification rate is higher with greater nitrate availability, especially in sediments from agricultural drainage areas (García-ruiz et al., 1998; Pattinson et al., 1998; Royer et al., 2004; Inwood et al., 2007). Meanwhile, the  $N_2O:N_2$  production ratio can be also affected by nitrate concentration. Higher nitrate concentration can cause a higher  $N_2O:N_2$  since a high-level nitrate concentration leads to incomplete denitrification (Blackmer and Bremner, 1977; Weier et al., 1993).

- Organic carbon

In agricultural catchments, nitrate is generally not the limiting factor for denitrification. When nitrate concentrate is high, labile organic carbon can play a key role in accelerating the denitrification rate. Studies have observed the similar stimulating function of labile carbon for denitrification (Bijay-singh et al., 1988; Arango et al., 2007; Pérez et al., 2010).

### **3. Potential toxic metals (PTE) in sediments**

In contrary to industrial regions or mining sites, PTEs in agricultural areas may not trigger acute toxic responses to living organisms, and their concentrations are normally much lower than heavily metal-contaminated regions. However, the long-term accumulation of PTEs in sediments from cultivated catchments can result in the potentially environmental risks to surrounding ecosystem and various life forms (see Section 1.2.5 for the potential risks and tragic consequences). The transfer and distribution of PTEs thus cannot be neglected.

#### **3.1 Brief of sediments**

In agricultural areas, sediment is a solid material, which is broken down from local upstream soil by the weathering process and is then transported and deposited in river by the fluvial process. Agricultural practices particularly lead to unsustainable soil losses due to the erosion rate greater than the soil production rate (Montgomery, 2007). In such a condition, agricultural soil has been considered as an irreversible resource.

Studies have found that the anthropogenic activities can largely affect the sediment yield and transportation into the river or coastal systems (Syvitski et al., 2005; Wang et al., 2016). Anthropogenic activities have increased the sediment yield through soil erosion by  $2.3 \pm 0.6$  billion metric tons per year. However, constructed reservoirs (from small ponds to large dams) have sequestered  $1.4 \pm 0.3$  billion metric tons per year of sediment flux (Syvitski et al., 2005).

#### **3.2 Characteristics and toxicity of PTEs**

Potential toxic elements (PTE) are those metal(loid)s which can cause adverse effects to the living organisms. The nomenclature of these metals is not unified since some researchers call them “potentially hazardous metals” or “toxic metals”. In this study, eight PTEs have been analyzed, e.g., arsenic (As), copper (Cu), lead (Pb), cobalt (Co), zinc (Zn), chromium (Cr), nickel (Ni), and cadmium (Cd) according to their toxicities and the presence in agricultural areas.

- **Arsenic (As)**

When it comes to arsenic (As), people often imagine many scenarios of conspiracies and murders since this element has already caused a variety of casualties. For French people, the most familiar thing about this poisonous metalloid can be the unsettled suspicion that Napoleon Bonaparte may be murdered via the chronic arsenic poisoning (Lewin et al., 1982; Marchetti et al., 2020).

Arsenic is a steel grey, crystalline metalloid with two major valences: As (III) and As (V). Metallic As can be easily oxidized to arsenous oxide ( $\text{As}_2\text{O}_3$ ) through heating in air. However, arsenic is not harmful conditionally when the concentration is in an acceptable level to the living organisms. Some arsenic-related applications have been developed even to cure the cancer (Waxman and Anderson, 2001).

- **Copper (Cu)**

Copper (Cu) is a soft and ductile metal with one major valence (II). It is quite common in nature. Since it is a natural metal that can be directly exploited from Cu-rich mines, the extensive use of Cu starts the Bronze Age. Nowadays, Cu is an important industrial metal, which have been utilized in a large number of industries. In France, the farmers in vineyards spread a large amount of Bordeaux mixtures ( $\text{CuSO}_4 + \text{Ca}(\text{OH})_2$ ) to protect the wine grapes from fungi.

Copper is an essential element for the growth of living organisms (Mertz, 1981). It is incorporated into many enzymes and is indispensable for their functions. Yet, the exposure to high concentration of Cu can also cause some severe diseases, such as diarrhea and liver damage.

- **Lead (Pb)**

Lead (Pb) is a soft and moldable metal with two major valences (II and IV). The usage of Pb-related productions can be traced back to prehistory. Contemporarily, lead plays an important role in many fields, such as alloy making, batteries, power cables, etc. Though the use of Pb in some developed countries has been regulated to a given extent, it is still used tremendously in the developing countries. The vast use of Pb and its persistent



characteristics in the environment pose a great threat on humans. The lead poisoning can damage central nervous system, which is an irreversible process. Meanwhile, high blood Pb level is also hazardous to the growth of children (Wani et al., 2015).

- **Cobalt (Co)**

Cobalt (Co) is a metallic element that is found in the Earth's crust only in chemically combined form. It is well known for its use in pigments and coloring for "cobalt blue". Cobalt is also an essential element for humans due to its central action in vitamin B12 function. Excess cobalt can lead to polycythemia, bone marrow hyperplasia, etc. It can even interfere with the Fe absorption (Mertz, 1981).

- **Zinc (Zn)**

Zinc (Zn) plays a key role in growth, appetite, mental activities, and so on. It is indispensable for humans. It is also a cofactor with many enzymes to support their proper functioning. Toxicity from Zn can cause flu-like symptoms, fever, fatigue, epigastric pain, vomiting, anemia, dehydration, depressed immune function, etc. Excessive Zn interferes with the function of Cu and Fe (Mertz, 1981).

- **Chromium (Cr)**

Chromium (Cr) is a steel-grey, hard, and brittle transition metal with two major valences, Cr (III) and Cr (VI). Chromium compounds have been widely used in dyes, leathering tanning, and paints for aerospace and automobile refinishing applications. The excessive Cr in human body can result in liver and kidney failure.

- **Nickel (Ni)**

Nickle (Ni) is a silvery-white, hard, and ductile metal with four common valences (I, II, III, and IV). Stainless steel is the major application of Ni. Nickel compounds have been identified as human carcinogens based on increased respiratory cancer risks.

- **Cadmium (Cd)**

Cadmium (Cd) is a soft, silver-white metal with one common valence (II). It has wide applications, including batteries, electroplating, televisions, etc. Cadmium is an environmental hazard. Human exposure is mainly from fuel combustion, phosphate fertilizers, iron and steel production, cement production, etc. The excessive exposure to Cd can cause kidney disease, hypertension, and cardiovascular diseases. It has been banned by the EU's Restriction of Hazardous Substances directive.

### **3.3 Sources of PTEs in agricultural soils and sediments**

In contrary to the industrial, urbanized, or mining regions, the degree of contamination of PTEs is normally lower in agricultural areas. However, this does not mean that the concentrations of metals do not need the monitoring due to the accumulation of PTEs in sediments, especially in the long-term stressed agricultural catchments. The high level of PTE accumulated in sediments, if exists, would be hazardous to the surrounding ecosystem and threaten the living organisms downstream. In addition to the monitoring, knowing the potential sources of these PTEs is a key point to well control the metallic contamination in sediments for a sustainable service of the ecosystem.

#### **3.3.1 Natural source**

The natural source of PTEs in soil and sediment is mainly the weathering process in bedrocks in intensively agricultural areas (Bur et al., 2009; N'guessan et al., 2009; Benabdelkader et al., 2018).

Table I-1. Concentrations of elements in various types of bedrocks

	Molasse (a)	UCC (b)	PAAS (c)
Major element (mg g <sup>-1</sup> )			
<b>Al</b>	46.53	77.44	189
<b>Ca</b>	48.85	29.45	13
<b>Mg</b>	3.6	13.5	22
<b>Fe</b>	28.43	30.89	72
<b>Mn</b>	0.55	0.53	1.1
Potentially toxic element (PTE) (µg g <sup>-1</sup> )			
<b>As</b>	17.19	2	NA
<b>Pb</b>	21.45	17	20
<b>Co</b>	12.19	11.6	23
<b>Cr</b>	57.56	35	110
<b>Zn</b>	80.96	52	85
<b>Cu</b>	18.04	14.3	50
<b>Ni</b>	26.73	18.6	55
<b>Cd</b>	0.2	0.1	NA
<b>Cs</b>	5.5	5.8	15
<b>Sc</b>	14.48	7	16

(a): Molasse is the local background bedrock of Gascogne (N'guessan et al., 2009)

(b): Upper Continental Crust (Wedepohl, 1995)

(c): Post Archean Australia Shale (McLennan, 2001). NA: data not available

Although the concentrations of PTEs in a given bedrock represent the natural PTE levels, heterogeneity can also be found in different regions at a large scale (Table I-1). One big discrepancy is observed for arsenic. In molasse of the Gascogne region (southwestern France), the natural level of As reaches 17.19 µg g<sup>-1</sup>, almost 8 times higher than that in the upper continental crust (UCC). It is thus important to investigate the local natural levels of PTEs before assessing the degree of PTE contamination in soil and/or sediment if conditions permit.

Using a universal background value arbitrarily may lead to misinterpret the local level of contamination (Roussiez et al., 2005; N'guessan et al., 2009).

### **3.3.2 Anthropogenic source**

The major anthropogenic sources of PTEs in agricultural areas include (1) inorganic fertilizers (N'guessan et al., 2009; Jiao et al., 2012), (2) wastewater effluent and irrigation (Xu et al., 2010), (3) manures (Leclerc and Laurent, 2017), and (4) pesticides (Gimeno-García et al., 1996). For instance, inorganic fertilizers are responsible for up to 85% of anthropogenic Cd in French cultivated soils (Sterckeman et al., 2018). Spreading of Bordeaux mixtures contributed to the enrichment of Cu and Zn in the soils of French vineyards (Duplay et al., 2014).

Inorganic N-P-K fertilizers have been identified as the top anthropogenic contributor for the enrichment of PTEs in long-term agricultural soils and sediments in some southwestern French catchments, though these substances were not heavily contaminated by PTEs (N'guessan et al., 2009).

### 3.4 Anthropogenic PTE transportation and distribution in sediments

#### 3.4.1 From soil to sediment

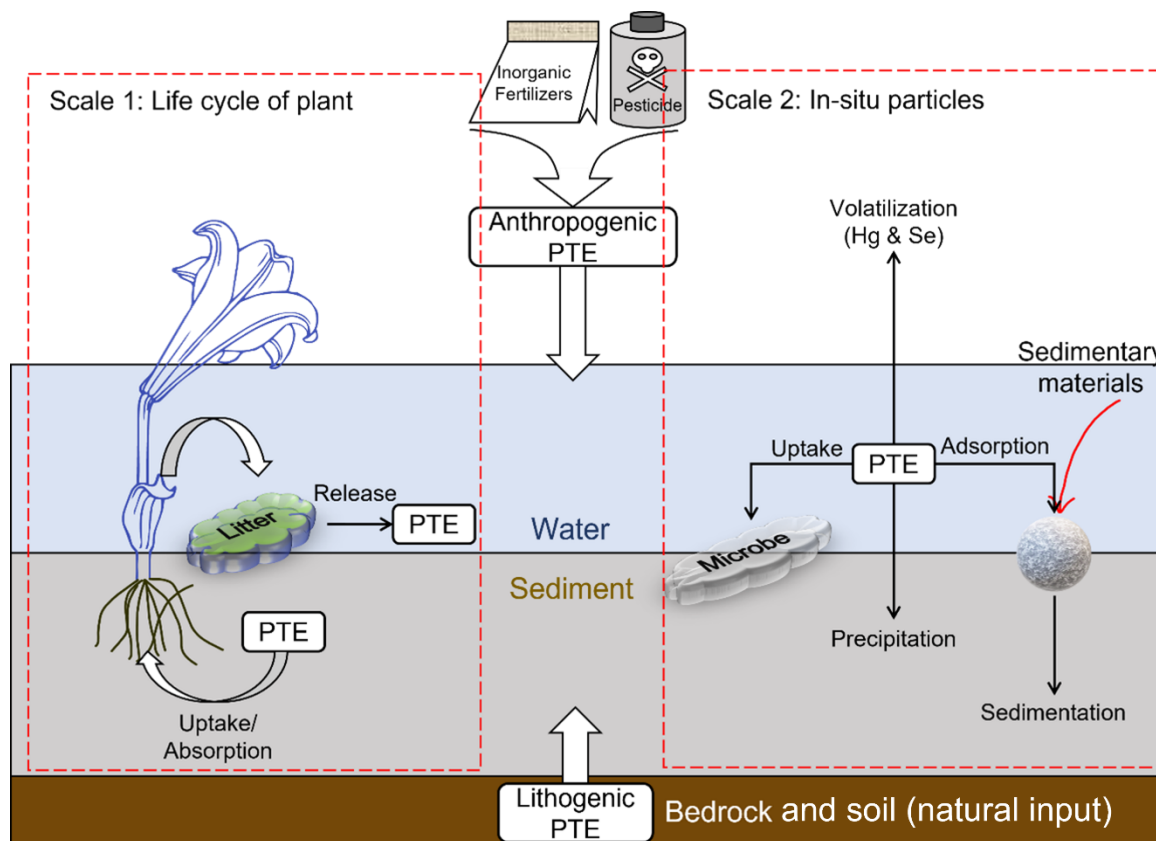


Fig. I-19. Schematic diagram of transfer of potentially toxic elements (PTE) in water and sediment.

Physical erosion leads to the movement of soil particles, which are then transported downstream as suspended matter by the fluvial process. Intensively cultivated catchments undergoing traditional practices such as tillage show a high soil erosion rate due to their frequent exposure to various erosive powers (such as runoff and ploughing), especially when slopes are significant (Oost et al., 2009). In addition to physical erosion, inorganic fertilizers are capable of increasing soil chemical weathering by increasing the release of base cations due to excessive protons produced during the nitrification process in soil under intensive fertilizer spreading (Perrin et al., 2008; Gandois et al., 2011). Bottom sediments are usually considered as a sink for most PTEs (Singh et al., 2002; Çevik et al., 2009; Duan et al., 2010), and thus can be a reservoir for both anthropogenic and lithogenic PTEs (Fig. I-19) (Jiao et al.,

2015).

### **3.4.2 Major pathways and controlling factors**

The spatial distribution of PTEs in sediments is associated with the transportation and deposition processes. The transportation and fate of PTEs can be affected by the physical, chemical, and biological processes once entered the aquatic systems with the eroded soils (Fig. I-19) (Duan et al., 2010). A number of factors can affect the transfer and distribution of PTEs in sediment, including characteristics of PTEs themselves, physicochemical properties of sediment, environmental features of constructed ponds and wetlands.

#### **3.4.2.1 Adsorption and desorption**

Positively charged elements can be attached to the negatively charged surfaces of organic matter, clay minerals, and Fe/Al/Mn oxides (Du Laing et al., 2007). The cation exchange capacity (CEC) shows the ability for such a process (Lin and Chen, 1998). A high CEC can reduce metal mobility and increase metal retention in the surface of particles. Meanwhile, the physical characteristics of sediments (i.e., particle size and sediment composition) can also affect the physical accumulation in sediments due to the larger specific surface areas of fine particles compared to coarse particles. Studies have shown that the PTE concentration in fine particles are higher than in coarse particles (N'guessan et al., 2009; Duan et al., 2010; Benabdelkader et al., 2018). Due to the high affinity between PTEs and fine particles, the fine particles can be a major carrier for transferring PTEs from upstream to downstream if the particle does not deposit in the bottom. Hydraulic condition and deposition conditions are thus the driving power influencing the PTEs in benthic sediments. Long hydraulic retention time can favor the sedimentation. Studies have shown that sediments from large ponds normally contain higher PTEs than those from very small and shallow ponds (Casey et al., 2007; Frost et al., 2015). Same observation was also reported in the Bohai Bay. High PTEs and fine particles were found where the hydrodynamic force was weak (Duan et al., 2010).

However, adsorbed metals can be released again because of the change of ambient physicochemical environment. The turbulence of upstream incoming water can wash sediments and break the adsorption balance. Hence, some sediments may become the secondary source

of contaminants.

### **3.4.2.2 Precipitation and dissolution**

The low pH can prevent the transfer of most PTEs from the water phase to the sediment phase. It can also trigger the desorption from the sediment (Du Laing et al., 2007; Duan et al., 2010). However, carbonates in calcareous sediments can be a buffer to the pH decrease. Meanwhile, carbonate can also co-precipitate with some metals, such as Cd (N'guessan et al., 2009).

# **Chapter II**

## **Materials and methods**



## Chapter II

### Materials and methods

#### Introduction

Intensively agricultural activities provide food and other nutritious supplies with the increasing world population (FAO, 2020), however this kind of anthropogenic activities can lead to severe environmental issues, such as river eutrophication caused by excessive nitrogen input due to the fertilizer spreading (Harper, 1992; Yang et al., 2008), accumulation of potentially toxic elements in sediments (Bur et al., 2009; N'guessan et al., 2009; Benabdelkader et al., 2018), emission of greenhouse gases (IPCC, 2006; Butterbach-Bahl and Dannenmann, 2011; IPCC, 2019), etc. These agro-environmental problems can pose a great threaten to food security and human health. Excessive nitrate in drinking water and high level of toxic elements accumulated in food, soil, and sediment become two major environmental concerns (Kapoor et al., 1997; Ali et al., 2019; FAO, 2020).

According to the Ministère de l'Agriculture et de l'Alimentation, France is the fifth largest wheat-planting country, after China, India, Russia, and the United States in 2018 (<https://infographies.agriculture.gouv.fr>). Meanwhile, share of agricultural lands in France reaches 52.4% of the total land area in 2016 (World Bank, <https://databank.worldbank.org/>). The total use of N fertilizers in France ranks the first in the European mainland in 2018 (FAO, <http://www.fao.org/faostat>). Therefore, considering agriculture is an important economic structure in France, the environmental problems due to agriculture should draw researchers' attention to build a better and sustainable environment.

Southwestern France is a traditional agricultural area for centuries. Taking the Gascogne region as an example, the agricultural land accounts for 77% of the total surface area (Table II-1). For decades, many constructed ponds have been established for water storage and agricultural irrigation in this region. In such a condition, the thesis focuses on two types of key contaminants (nitrate and potentially toxic elements) in agricultural critical zone of the southwestern France to investigate their behaviors and main controlling factors, especially in water and sediment.

Table II-1. Distribution of the different types of land surfaces in the Gascogne region, 2013  
(Source: Occupation du sol à grande échelle (OCS GE))

Type	Percent (%)
Water surface	1
Artificialized surface	7
Natural surface	15
Agricultural surface	77

The “Materials and Methods” chapter includes 4 aspects:

- (1) Sampling site investigation, including the selection procedure for appropriate ponds and catchments, and sampling sites description.
- (2) Sampling strategies for water and sediment samples (i.e., collection, preservation, and pretreatment for further analyses).
- (3) Physicochemical and biological analyses for water and sediment samples.
- (4) Tools and methods for data analyses.

## 1. Sampling site

### 1.1 Pond selection

At the beginning of the main body of the thesis, it is critical to find a proper sampling area to perform the investigation. The basic guideline is to select the most representative ponds in a certain agricultural area. Based on this, the focus moves to the Gers department in the southwestern France (Fig. II-1A) since the Gers department is a traditional agricultural area for decades. According to Corine Land Cover, nearly 90% of the total land cover was dominated by the agricultural activities in the Gers department in 2013 (Fig. II-1B, source: <https://www.annuaire-mairie.fr/occupation-des-sols-departement-gers.html>). The detailed land cover can be found in Annex III and Annex IV.

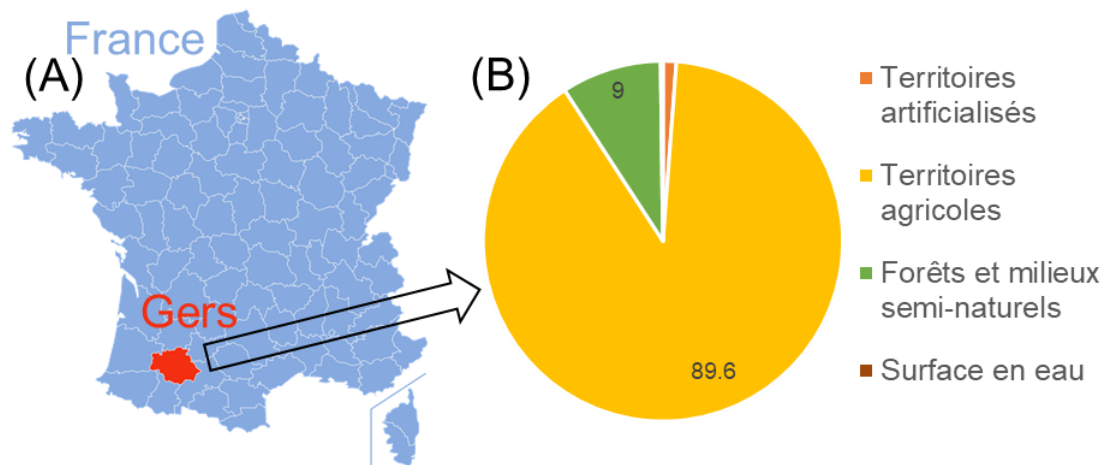


Fig. II-1. (A) Location of the Gers department in France; (B) Types of main land cover in the Gers department in 2013.

Moreover, a large number of constructed ponds (more than 3000!) are located in Gers (Fig. II-2). Considering the traditional agriculture and the huge pond number, the Gers department can be an appreciated inventory to select the proper ponds for the thesis.

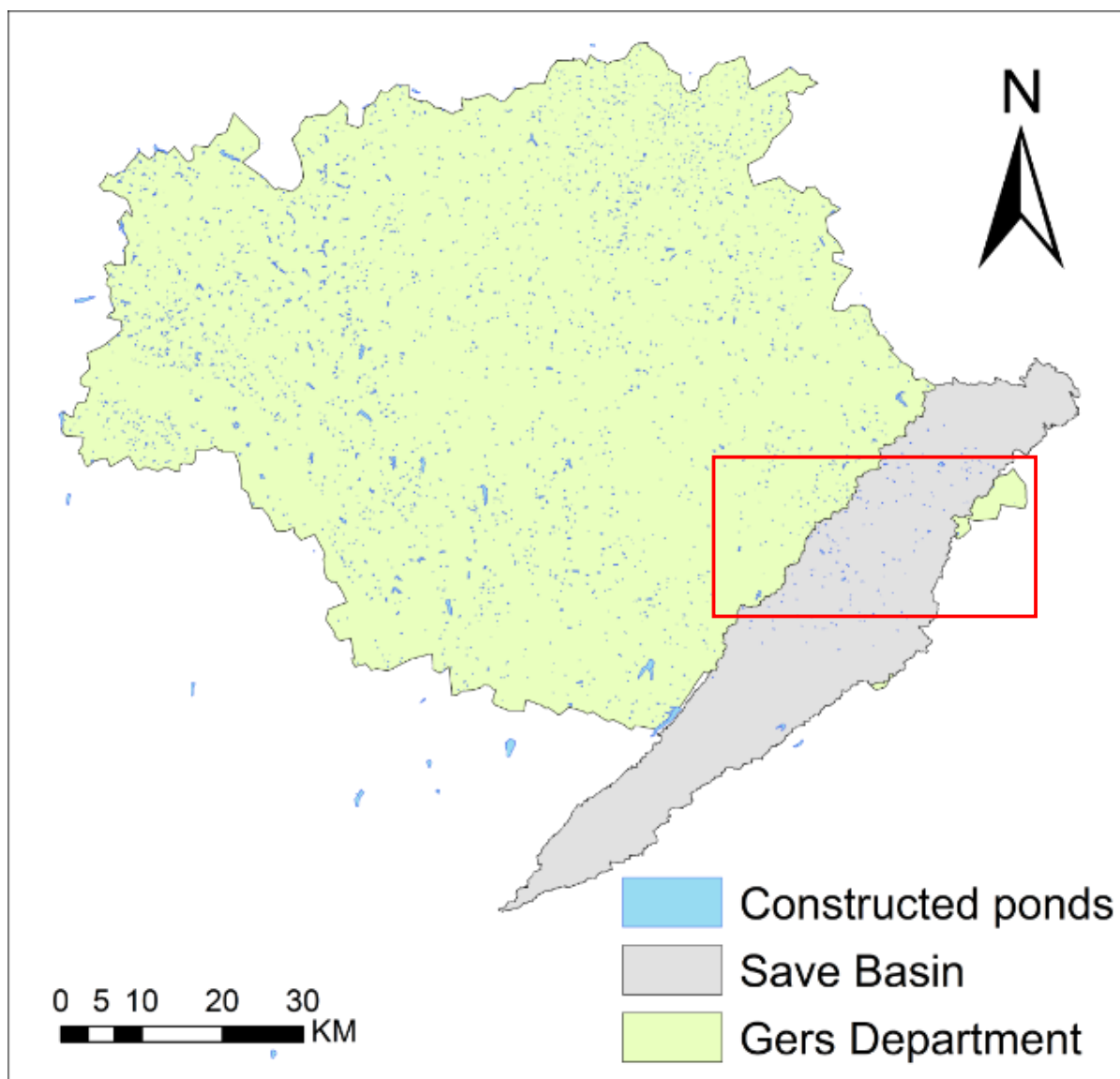


Fig. II-2. Constructed ponds located in the Gers department and its Save basin (source: DDT32)

The Gers department contains several main river basins. The Save basin is also an important tributary of the Garonne river (Annex V) among them. The land use and the geomorphological characteristics of the Save basin are representative of Gers and southwestern France, particularly of the Côteaux de Gascogne area. Another key point to choose the Save basin as the target of the thesis is that the EcoLab (the host of the thesis) has performed various studies in the Save basin in past 10 years, including:

- nitrate behavior (Perrin et al., 2008; Ferrant et al., 2011; Gandois et al., 2011),
- suspended matter, metal, and pesticide transfer (Taghavi et al., 2010, 2011; Roussiez et al., 2013; El Azzi et al., 2018; Ponnou-Delaffon et al., 2020),

- sediment contamination (Bur et al., 2009; N'guessan et al., 2009),
- ecotoxicological studies (Bur et al., 2010),
- modelling predictions (Boithias et al., 2011; Ferrant et al., 2011; Casal et al., 2019),
- and risk assessment (Macary et al., 2013, 2014), etc.

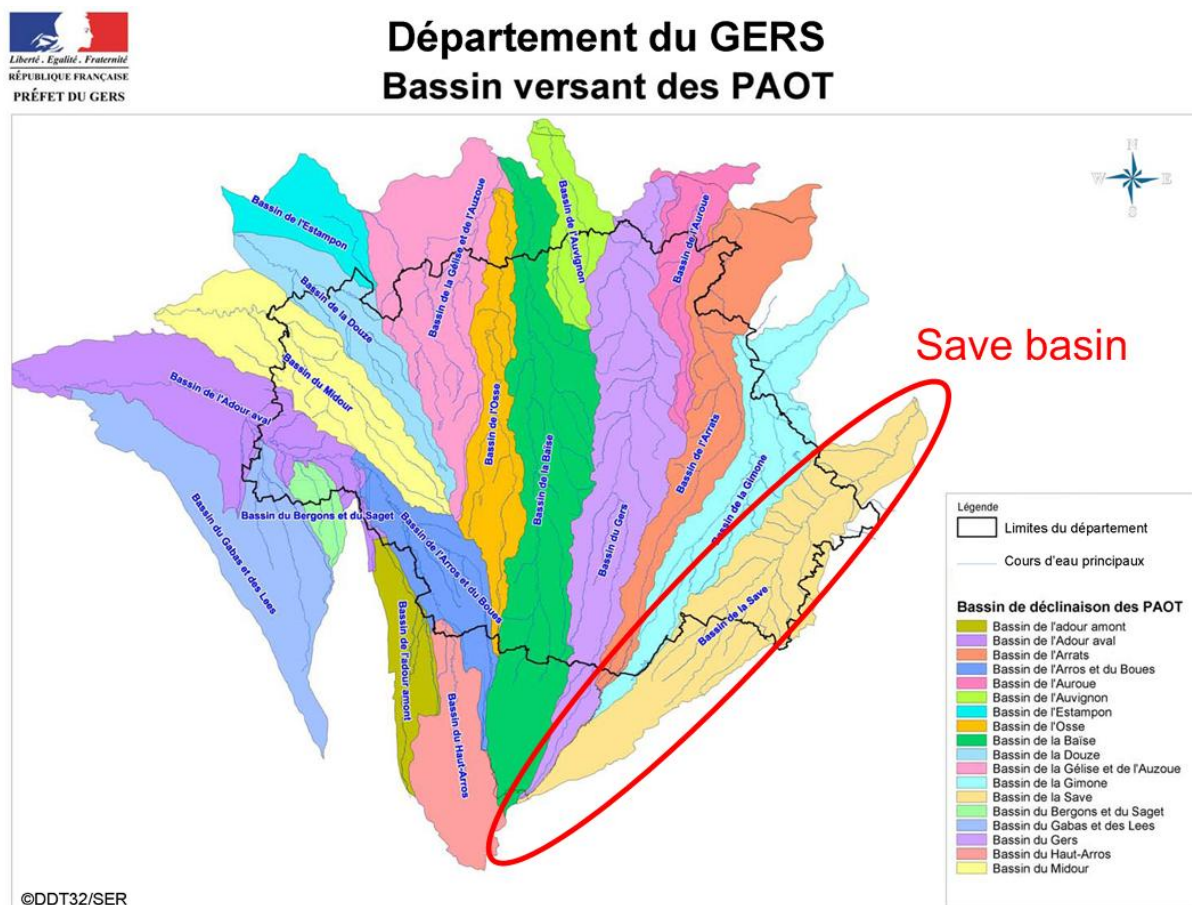


Fig. II-3. Water basins in the Gers department. The Save basin is highlighted by the red oval (source: DDT32/SER).

Fig. II-4 illustrated various types of land use in the Save basin in 2009 (CEMAGREF, 2010). Forest and meadow dominated in the upstream, whilst in the middle and downstream part of the Save basin, the soils were occupied by a great variety of different agricultural crops (Fig. II-4). Wheat and sunflower were two most common cultivated crops (highlighted by the red square in Fig. II-4), particularly on the hillslopes where the soils are shallow and irrigation not possible. The preferable pond should be located in the cultivated land since the thesis focuses on the role of constructed ponds in mitigation of contaminants (nitrate and potentially

toxic elements) in the agricultural areas. Therefore, the constructed ponds from the middle and downstream part of the Save basin meets the interests of the thesis.

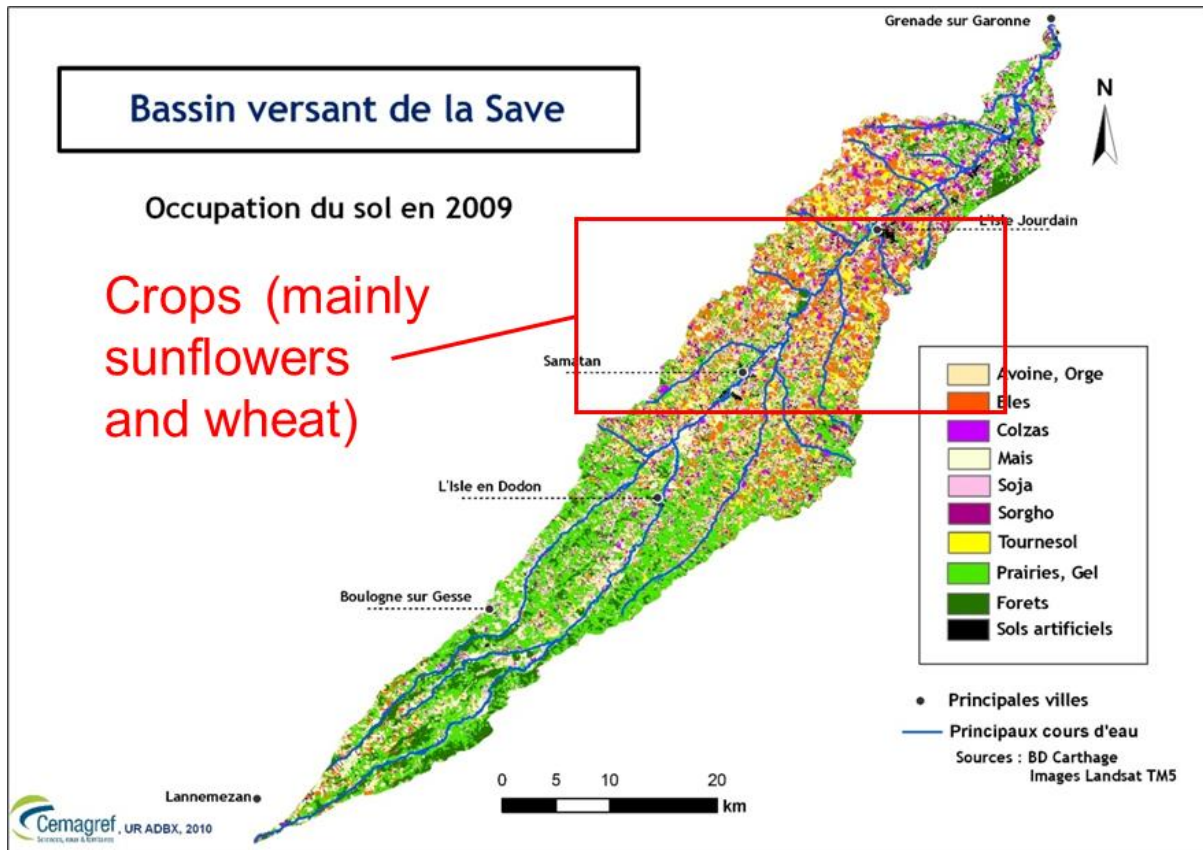


Fig. II-4. Types of land use in the Save basin (CEMAGREF, 2010)

Following the above steps, several key datasets were collected from multiple sources for the pond selection procedure:

- ArcGIS Shapefiles describing the geographic information of the recorded ponds located in Gers, provided by the organization DDT (Direction Départementale des Territoires).
- ArcGIS shapefiles of the water courses and river nodes in the Gers department (Grusson, 2016).
- The DEM (digital elevation model) data depicting the Gers elevation (Grusson, 2016).
- Map of land use of the Save basin in 2009 (CEMAGREF, 2010).

The flow chart of the pond selection procedure is shown in Fig. II-5.

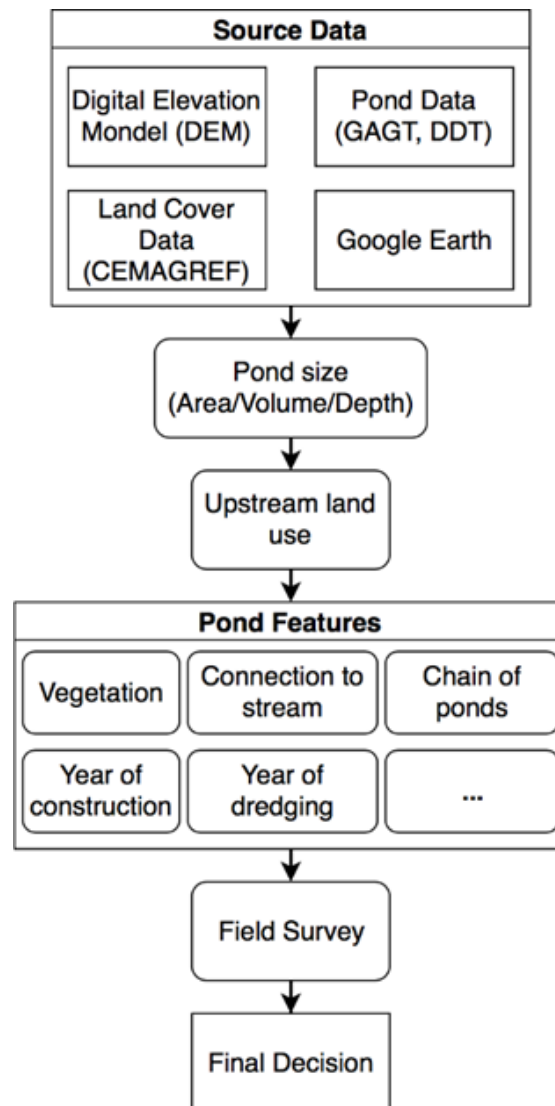


Fig. II-5. Flow chart of pond selection procedure

The determination of the representative size of these ponds is the first step for the selection. Table II-2 showed the descriptive statistics of pond sizes (surface, volume, and depth) recorded in the shapefiles provided by DDT.

Table II-2. Descriptive statistics of pond sizes (surface area, volume, and pond depth) based on more than 3000 ponds in the Gers department recorded by DDT

	Surface (m <sup>2</sup> )	Volume (m <sup>3</sup> )	Depth (m)
Min	1.25	50	0.5
Max	2247659	24000000	29
Median	6091	18000	5.50
Mean	14200	53533	5.70
Standard deviation	65080	506587	2.50
Variation coefficient (CV%)	5	9	0.44

The surface area of ponds ranged from 1.25 to 2247659 m<sup>2</sup> with an average of 14200 m<sup>2</sup> (Table II-2). Almost 98.6% of surface areas were less than 100000 m<sup>2</sup> (Fig. II-6A). Therefore, a second histogram was created based on the <100000 m<sup>2</sup> ponds, which showed that the ponds (<20000 m<sup>2</sup>) accounted for 90.6% of ponds (<100000 m<sup>2</sup>) (Fig. II-6B). Considering both the representativeness and the feasibility of sampling, the threshold of surface area (20000 m<sup>2</sup>) was adopted. Meanwhile, the ponds (<10000 m<sup>2</sup>) were preferable compared to the ponds (10000 ~ 20000 m<sup>2</sup>) due to the surface area distribution.



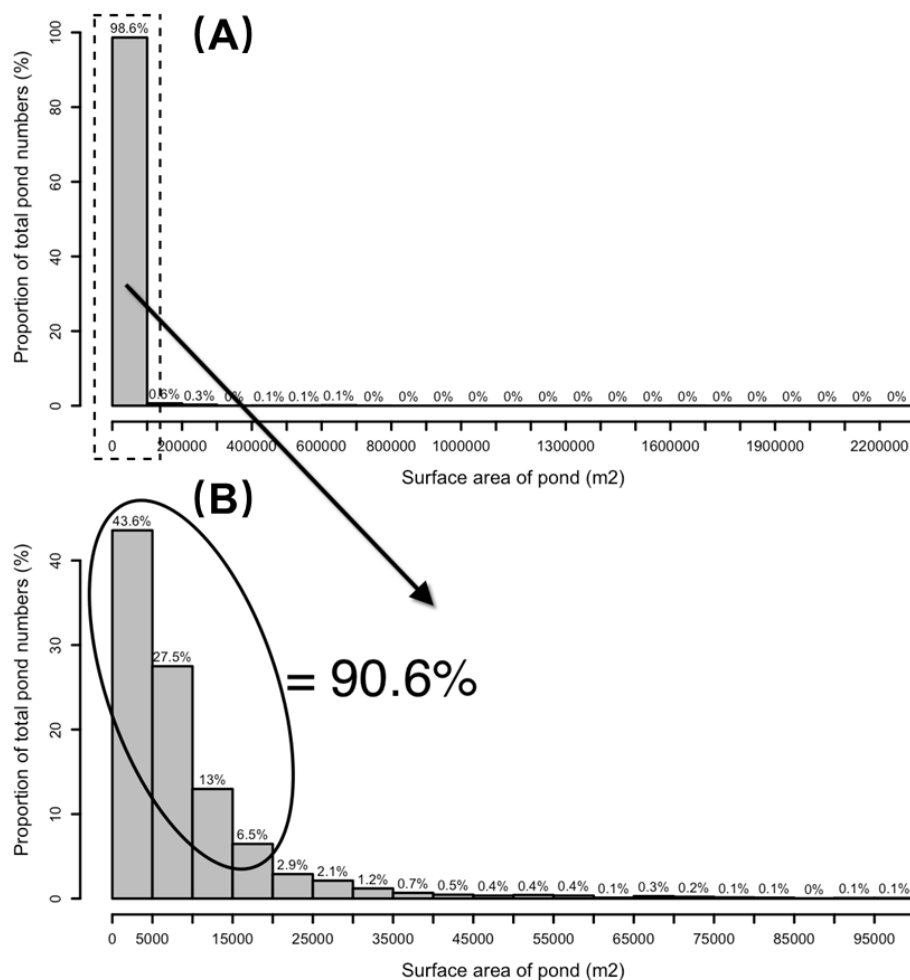


Fig. II-6. Cumulative histograms of pond surface areas (m<sup>2</sup>): (A) from 0 to 23000000 m<sup>2</sup>; (B) from 0 to 100000 m<sup>2</sup>. The number above each bar indicates the proportion of total pond numbers.

The volume of ponds varied from 50 to 24000000 m<sup>3</sup> with the mean value of 53533 m<sup>3</sup> (Table II-2). There were 99.5% of all the ponds that were less than 1000000 m<sup>3</sup> (Fig. II-7A). Among the ponds (<1000000 m<sup>3</sup>), 95.6% of these ponds were less than 100000 m<sup>3</sup>. Hence, the threshold of 100000 m<sup>3</sup> was accepted and the emphasis would be put on the ponds (<50000 m<sup>3</sup>), which accounted for 87.5% of the ponds (<1000000 m<sup>3</sup>) (Fig. II-7B).

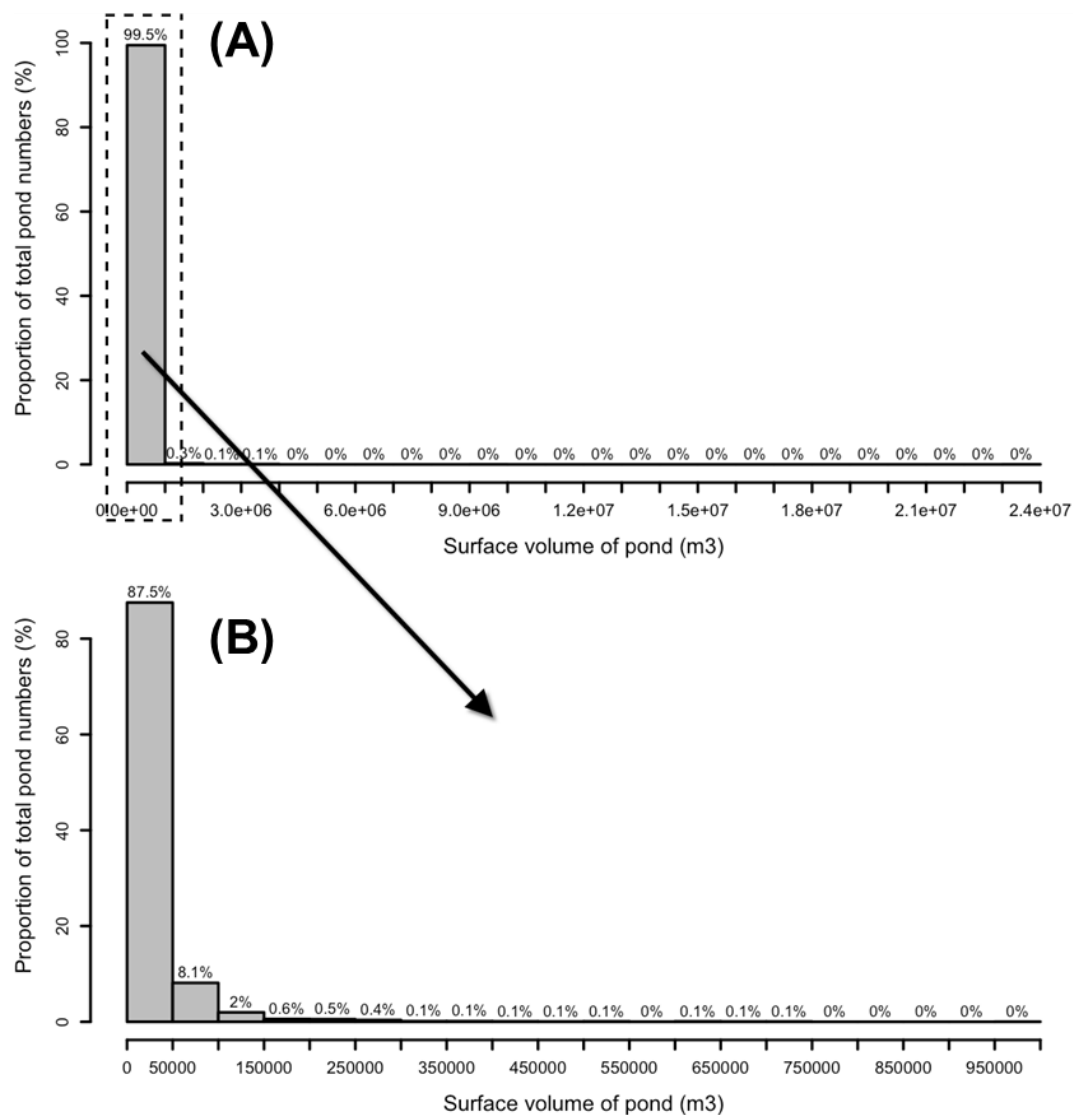


Fig. II-7. Cumulative histograms of volumes (m<sup>3</sup>): (A) volumes from 0 to  $2.4 \times 10^7$  m<sup>3</sup>; (B) volumes from 0 to  $1 \times 10^6$  m<sup>3</sup>. The number above each bar indicates the proportion of total pond numbers.

The depths of ponds were from 0.5 to 29 m with an average of 5.7 m (Table II-2). The depths of 95.9% of all ponds were less than 10 m. Moreover, the ponds (depth <6 m) are the majority (Fig. II-8).

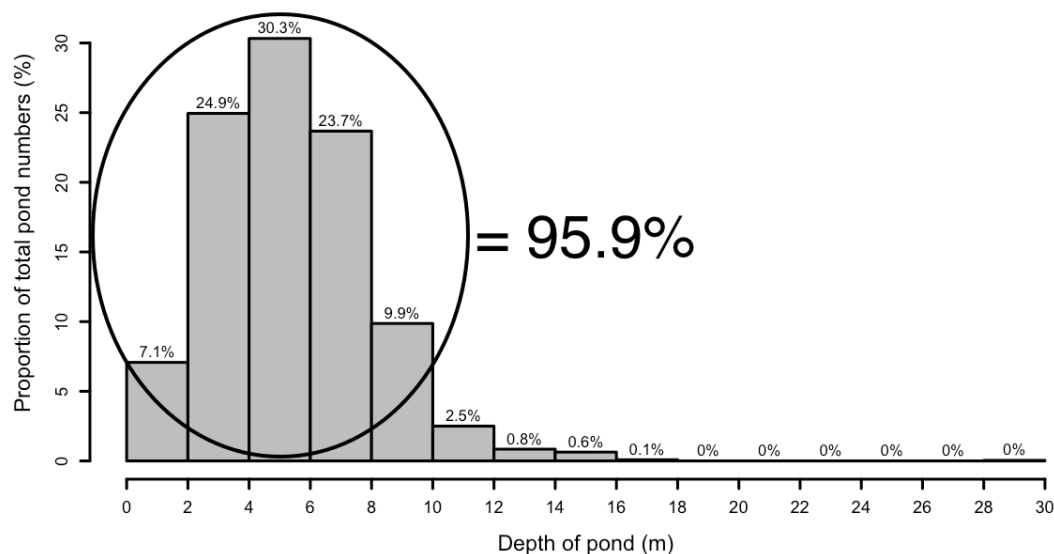


Fig. II-8. Cumulative histogram of depth (m). The depth (x-axis) covers the depth range from 0 to 30 m. The number above each bar indicates the proportion of total pond numbers.

In general, three thresholds were adopted according to the statistical survey based on the pond information collected by DDT: surface area (20000 m<sup>2</sup>), volume (100000 m<sup>3</sup>), and depth (10 m). These thresholds considered not only the representativeness of the ponds, but also the feasibility for the sampling campaign.

After the determination of the pond size, the type of land use was the second selection criteria. As stated before, the middle part of the Save basin shows a main land use of wheat and sunflower in two-year rotation, which is very representative of the sampling region.

Meanwhile, different featured ponds rather than sameness could provide the diversity of samples, thus, the roles of different ponds in the mitigation of contaminations along stream flows could be evaluated. In this thesis, several features were taken into consideration:

- Connection to stream

It is of great interest to estimate the different impact on the mitigation of contaminants between a connected pond and a disconnected (isolated) one (Fig. II-9). It is easy to identify the connection situation by using the function ('Selection by Location') in the ArcGIS, however, some errors are inevitable resulting from information uncertainty and projection errors. For this reason, some field investigations were carried out to

verify the real connection situations in February and March 2016.

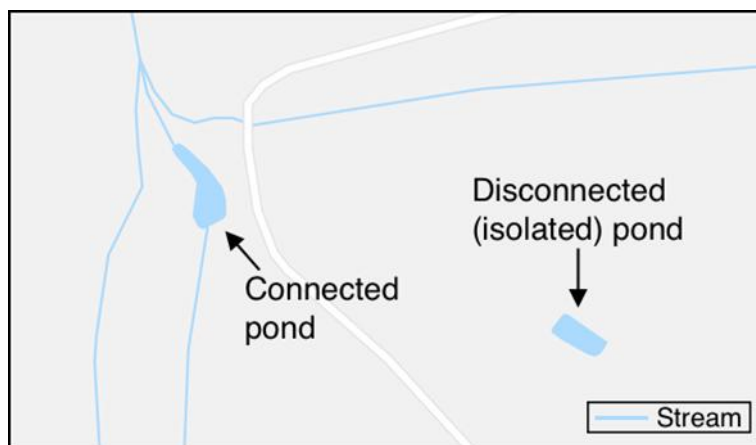


Fig. II-9. Example of a connected pond and a disconnected (isolated) pond (adapted from the Google Maps)

- Chain of ponds

Sometimes, more than one constructed pond may exist along the flow direction of a given stream. These ponds form a chain of ponds (Fig. II-10). Through the chain of ponds, the cumulative impact of ponds on contaminants transfer downstream, could be evaluated. Meanwhile, the different function between a chain of ponds and a single pond could be investigated.

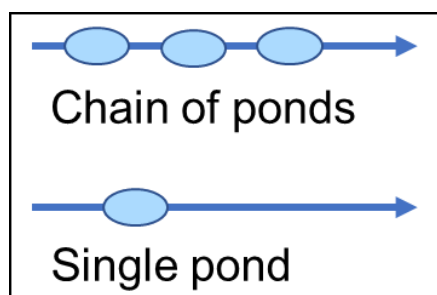


Fig. II-10. Schematic diagram of a chain of ponds and a single pond along the stream channel

- Year of pond construction and sediment dredging

The year of construction of ponds in the Save basin was recorded by DDT. Fig II-10 showed the descriptive statistics of these years. It found out that most ponds were constructed from 1970 to 1995, which accounts for 86% of all ponds in the Save basin

(Fig. II-11). The sediment dredging action was operated by the pond owners. However, this action is random and depends on the willing of owners, so that the database did not record the information about the dredging year. Hence, the year of dredging action were inquired from the owner once the pond is selected.

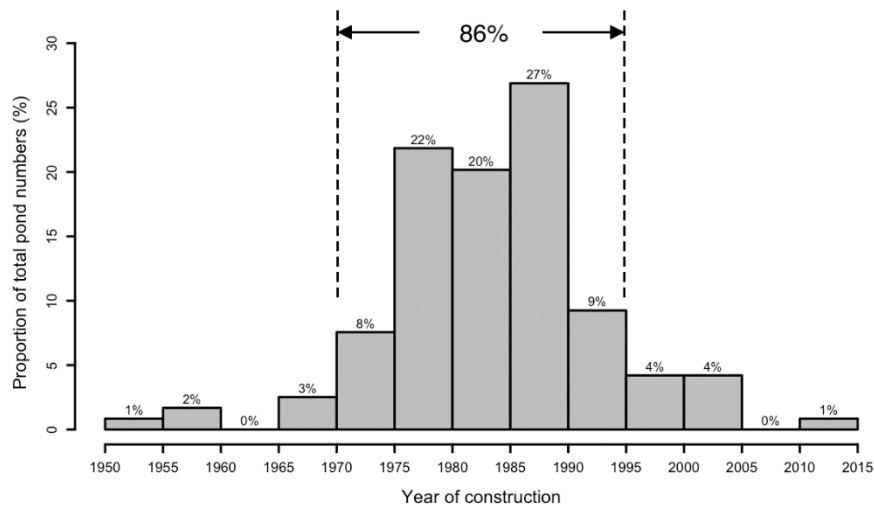


Fig. II-11. Cumulative histogram of the year of pond construction. The number above each bar indicates the proportion of pond number over the total numbers of ponds.

After the completion of the selection according to the above criteria, a field investigation was carried out in order to make a final decision for the most fitted ponds to the thesis purposes (about 20 ponds located in Auradé, Montoussé, Marestaing, Castillon, Moufielle, and L'isle Jourdain) (Fig. II-12). Finally, ten ponds from three adjacent catchments were selected: two ponds in the Montoussé catchment (MON), four ponds in the Mican catchment (MIC), and four ponds in the Nuguet catchment (NUG), which are drained by sub-tributaries of the Save river. Their characteristics will be described in Section 1.2.

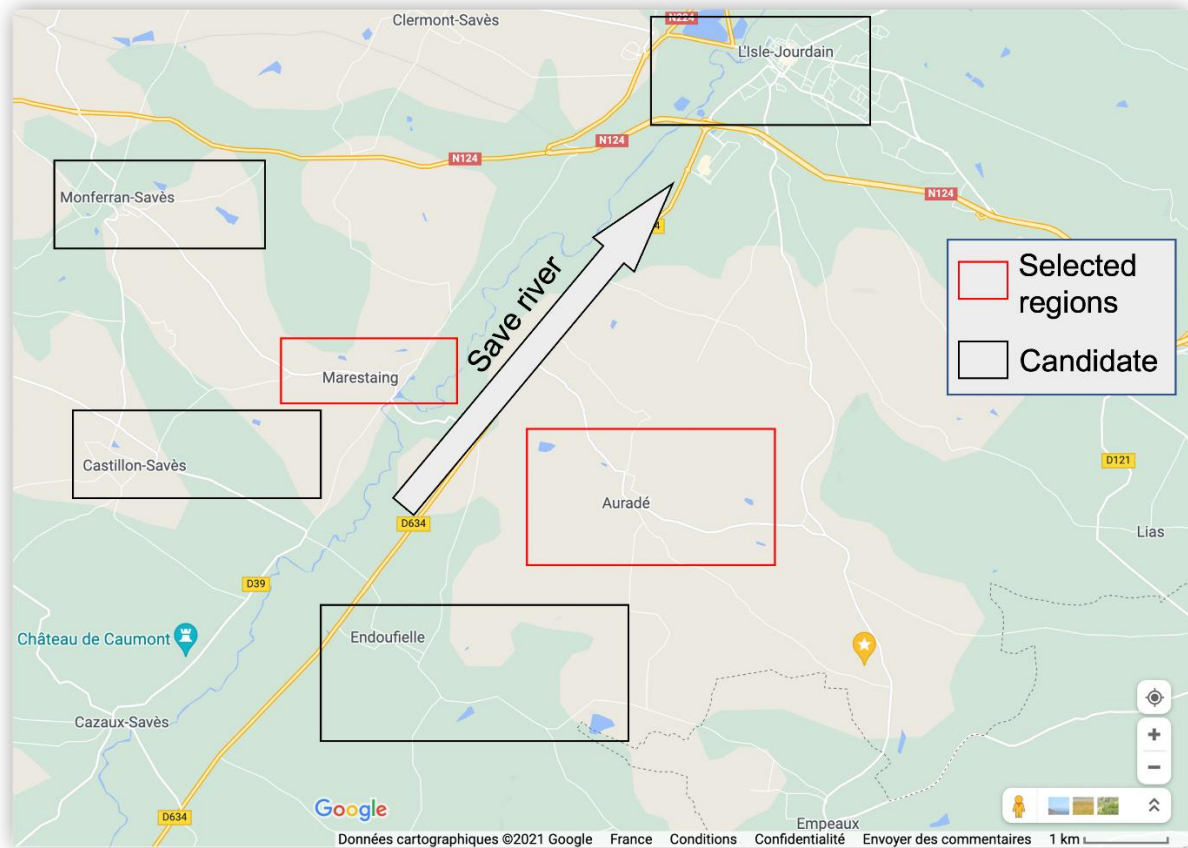


Fig. II-12. Regional map of suitable ponds in the Save basin. Selected ponds after the field surveys are labeled in red. Note: some small ponds are not visible at the given scale in this map.

## 1.2 Catchment and pond descriptions

### 1.2.1 Catchment characteristics

The sampling site lies in the Save basin (1100 km<sup>2</sup>), which is drained by the Save river, a left tributary of the Garonne river in southwestern France (Fig. II-13). As an agricultural basin, the Save basin is dominated by meadows and forests in the upstream part, whilst various cultivated land uses were dominant in the middle and downstream part of the basin (wheat/sunflower rotation in the hilly slope in the middle part, and corn in the lower part) (Fig. II-4) (Taghavi et al., 2011). In the Save basin, with hot summer climatic conditions, a large number of ponds were constructed during the last century for traditional agriculture, and more recently for some crops water supply.

The selected ten representative ponds (in terms of size and volume, but with different position in the catchment, shapes, and management) located in three adjacent catchments in the Save basin. The three catchments are located closely on the right (Montoussé, MON; Mican, MIC) and the left bank (Nuguet, NUG) of the middle Save river on the same latitude segment (Fig. II-13 and Table II-3).

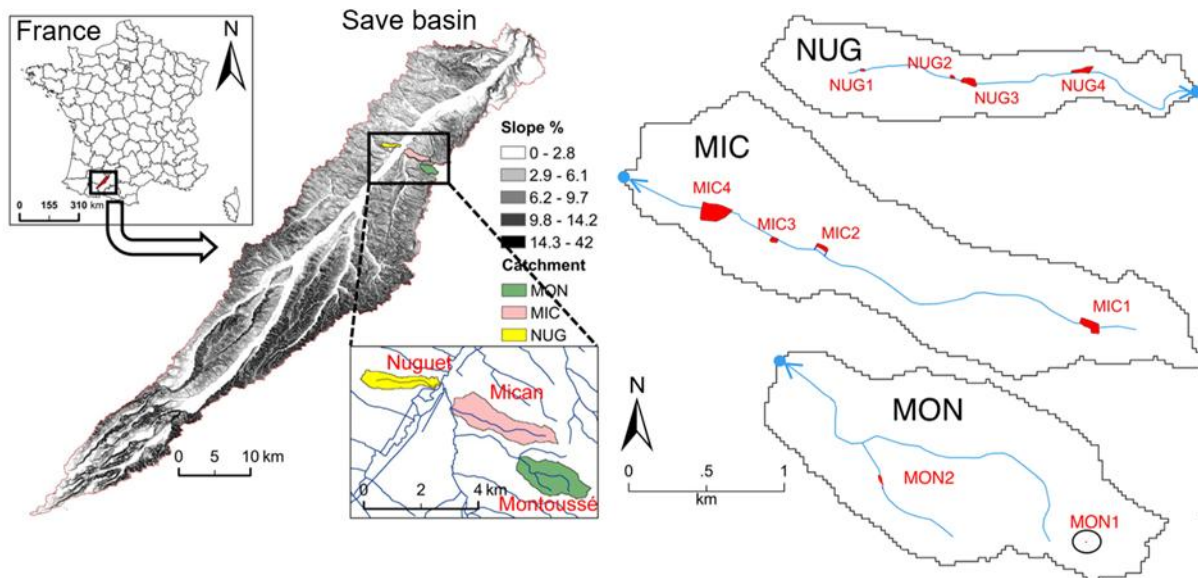


Fig. II-13. Location of the studied ponds and of the three relative catchments (Montoussé (MON), Mican (MIC), Nuguet (NUG)) within the Save basin, southwestern France.

Table II-3. Characteristics of sampling sites (catchments and ponds). YC = year of construction, YD = year of last dredging;  $HRT$  (Hydraulic Retention time) =  $(Pond\ volume)/(Q_{outlet}-Q_{inlet})$  where  $Q$  is the discharge. Note that the inside of NUG4 pond was not collected (see Section 1.2.2 of this chapter).

Catchment	Montoussé (MON)		Mican (MIC)				Nuguet (NUG)			
Area (ha)	325		277				116			
Slope (%)	6.59 ± 3.10		4.44 ± 2.49				4.01 ± 2.56			
Stream length (m)	900		3595				2550			
Stream elevation (m)	226.4 ~ 192.7		220.6 ~ 149.0				190.4 ~ 146.0			
Pond	MON1	MON2	MIC1	MIC2	MIC3	MIC4	NUG1	NUG2	NUG3	NUG4
Longitude	1.0936	1.0773	1.0762	1.0547	1.0509	1.0460	1.0073	1.0145	1.0157	1.0246
Latitude	43.5480	43.5513	43.5656	43.5696	43.5699	43.5715	43.5815	43.5813	43.5810	43.5818
Distance	NA	0.644	0.068	0.598	0.691	0.789	0.075	0.306	0.329	0.627
Slope (%)	2.72	4.49	1.81	3.94	1.03	1.46	1.46	1.62	3.15	1.63
Area (m <sup>2</sup> )	80	1050	4200	2500	1566	18000	480	550	3800	3641
Depth (m)	0.526	1.602	1.570	1.228	0.844	3.567	0.478	0.657	2.863	2.934
Volume (m <sup>3</sup> )	23.0	1520.7	8515.7	2183.7	1123.3	62213.3	169.3	293.3	10144.7	5481.3
Shape (L/W)	1.525	1.697	1.201	1.293	1.584	1.657	1.831	1.213	1.772	3.183
HRT (day, 2016)	NA	41.8	1202.0	186.8	13.5	1956.7	26.8	41.4	1151.1	379.9
YC	1970	1970	1977	1960s	late 1970s	1965	before 1970s	1970s early	1980s	1995
YD	Never	2015	Never	1999	Never	1985	1980s	1990s	(c)	Never
Connection	Isolated	Connected	Connected	(a) Connected	(b)	Connected	Connected	Connected	Connected	Connected

(a): This pond is disconnected during high floods periods with large loads of suspended matters and connected the rest of the time. It was connected to the Mican stream while sampling;

(b): It was disconnected unless the owner opens its valve linked to the channel very scarcely, not in flood conditions. It was disconnected while sampling.

(c): Only the border was dredged a little.

The catchment areas are of the same order of magnitude (hundred ha) in the decreasing order (MON (325 ha) > MIC (277 ha) > NUG (116 ha)). The catchment slopes fall in the range of 4 to 10%, which is about 80% of the situations usually observed in the Save basin (Perrin et al., 2008), although slopes in MON and MIC are steeper than in NUG (Table II-3). The Montoussé sub-stream (900 m) is the shortest stream. The Mican stream (3595 m) crosses the small village of Auradé and converges into the Boulouze stream, while the Nuguet stream (2550 m) crosses the village of Marestaing in its middle course. Then these streams flow into the Save river (Fig. II-13).

The regional climate is oceanic (Köppen Climate Classification) with an average annual precipitation and air temperature of 620 mm and 13.9 °C over the last 32 years, respectively (Ponnou-Delaffon et al., 2020). The dry and wet periods extend normally from June to August and from October to May, respectively, with some intense rainfalls generating significant flood events, particularly as flash floods in Spring. The stream discharge is mainly controlled by the surface and subsurface runoff since the underground flow is very limited (Perrin et al., 2008;



Ponnou-Delaffon et al., 2020).

The three catchments are mainly cultivated by wheat and sunflower in a two-year rotation strategy. In this traditional wheat/sunflower rotation agricultural area, farmers applied chemical fertilizers on soils, mainly as synthetic fertilizers of the N-P-K type (N, P<sub>2</sub>O<sub>5</sub>, and K<sub>2</sub>O), and direct fertilizers containing ammonium nitrate (NH<sub>4</sub>NO<sub>3</sub>). Limited quantities of urea and ammonium sulphate ((NH<sub>4</sub>)<sub>2</sub>SO<sub>4</sub>) was locally introduced (Perrin et al., 2008). During both sampling periods, wheat was the dominating crop in the area. The fertilization activity for wheat usually occurs between middle of January and March, with an optional application in April (Paul et al., 2015). In this area, the amount of spread fertilizers was close to the crop needs. According to the previous study in this region (Perrin et al., 2008), typical fertilizer rate applied by local farmers for different representative crops are listed below:

- Wheat: 670 kg ha<sup>-1</sup> yr<sup>-1</sup> (30%, 5%, and 2% for N, P<sub>2</sub>O<sub>5</sub>, and K<sub>2</sub>O, respectively)
- Sunflower: 400 kg ha<sup>-1</sup> yr<sup>-1</sup> (22%, 4%, and 5% for N, P<sub>2</sub>O<sub>5</sub>, and K<sub>2</sub>O, respectively)
- Corn: 660 kg ha<sup>-1</sup> yr<sup>-1</sup> (21%, 14%, and 13% for N, P<sub>2</sub>O<sub>5</sub>, and K<sub>2</sub>O, respectively)
- Soybean: 400 kg ha<sup>-1</sup> yr<sup>-1</sup> (0%, 16%, and 26% for N, P<sub>2</sub>O<sub>5</sub>, and K<sub>2</sub>O, respectively)

In the recent years, an increase of the use of urea as a fertilizer (up to 31.7%) was observed (Ponnou-Delaffon, 2020).

Along the streams, buffer strips were set up in the early nineties to decrease nitrate leaching from the surrounding lands into streams.

At the outlet of the Montoussé catchment at Auradé, the water level data and corresponding discharge as well as nitrates were long-term monitored since 1985, and major elements and physicochemical parameters since 2004 (Ponnou-Delaffon et al., 2020). The Montoussé catchment at Auradé was firstly part of the SOERE RBV (French Network of observatories: <http://portailrbv.sedoo.fr/>), today included in the IR OZCAR (Research Infrastructure; <http://www.ozcar-ri.org/>) and, as such, is subjected to a long term and high frequency hydrogeochemical monitoring.

The sampling periods in March 2016 and March 2018 were indicated on the water level and discharge patterns of the Montoussé stream at the catchment outlet, in order to put into perspective the discharge conditions of the samplings of our concerned catchments (Fig. II-14).

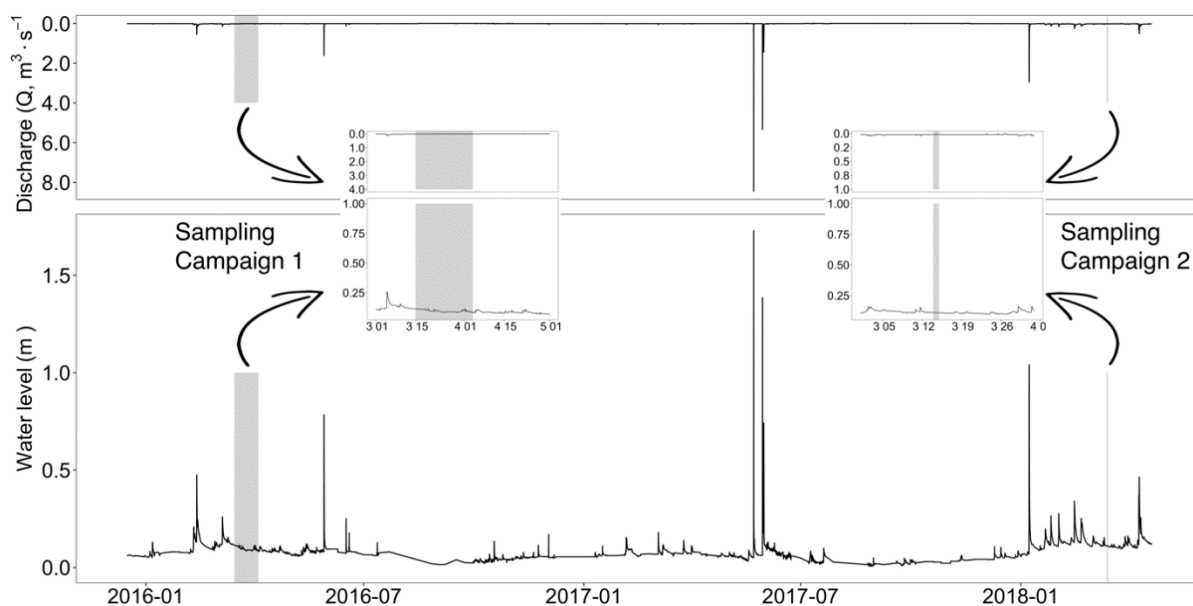


Fig. II-14. Hydrograph in the Montoussé stream at the outlet in Auradé, during the two years (2015/12 to 2018/04). The sampling periods of our investigations on the Montoussé upper sub-catchment, the Mican and the Nuguet (March 2016 and March 2018) are indicated by focus to evaluate the local hydrological conditions of sampling. The sampling occurred during a recession period of the late winter water flow conditions.

The substratum of the sampling sites is a Miocene molassic deposit, defined as “molasse” by Cayeux (1935), originating from the erosion of the Pyrenees Mountains and the subsequent sediment deposition at the end of the Tertiary Period. It consists of clays, sandstones, limestones, and calcareous sediments (Revel and Guisresse, 1995; Perrin et al., 2008). The carbonate content in molasse varies between 60-90% (Perrin et al., 2008). Calcic soils dominate more than 90% of the Save basin with a clay content ranging from 40 to 50%, and non-calcic soils only account for less than 10% (Perrin et al., 2008; Taghavi et al., 2011). The pH values are 7.7 - 8.8 and 5.9 - 6.9 in calcic soils and non-calcic soils, respectively. The organic content in the soils ranges from 1.0 to 2.5% (Perrin et al., 2008). As it is a traditional agricultural area, mechanical erosion due to farming and ploughing have a great impact on downward soil displacement, along with the water erosion (Revel and Guisresse, 1995).

For MON and MIC, the top of the hills is covered by calcareous cambisols or rendzic leptosols (FAO, 2014), while on the long hillsides with moderate slopes, deeper clayey calcareous cambisols or hypereutric cambisols have been developed (Revel and Guisresse, 1995; Perrin et al., 2008; Ponnou-Delaffon et al., 2020). Evidence of clay illuviation was observed sometimes.

On the alluvial plains along the main channels, deep clayey calcareous cambisols with color mosaics or gleyic properties from colluvial and fluvial deposits were mainly occupied (Perrin et al., 2008; Ponnou-Delaffon et al., 2020). The major minerals of the soils are quartz, with a small proportion of feldspar (plagioclase and albite), calcite, zircon, and less commonly monazite, chlorite, epidote, ilmenite, mica (muscovite), apatite, and tourmaline (Perrin et al., 2008). While in NUG, the soils are mainly luvisols and colluviosols.

### 1.2.2 Pond characteristics

Ten ponds were finally selected in this thesis, two ponds in Montoussé (MON), four ponds in Mican (MIC), and four ponds in Nuguet (NUG) catchments (Table II-3; Fig. II-13; Fig. II-15; NUG4 was not sampled inside the pond, see description below). Water and sediment samples were collected from nine ponds, and, if they were connected to the stream, their up and down drainage streams.

MON1 is a very small, isolated pond in the very upstream part of Montoussé catchment surrounded by an area of buffer strip (approximate 1.7 ha), whereas MON2 is surrounded by wheat and some rapeseed, and its pond sediments have been dredged in 2015. In MIC and MON, the first three ponds (MIC1 to MIC3 and NUG1 to NUG3, respectively) were connected to the stream during the sampling campaign, whereas MIC4 was disconnected in the first sampling campaign and connected in the second sampling event. NUG4 is located downstream in the Nuguet stream and was not sampled because of the effect on the quality of waters and sediments from the exudate of the Marestaing village residential wastewater treatment plant (WWTP) upstream of the pond. This would compromise detection of the effect of agricultural activity. MIC1, MIC4, and NUG3 are recognized as large ponds in size, and consistently have the longest hydraulic retention time (HRT, Table II-3)<sup>1</sup>. MIC3 is a shallow pond due to significant sediment accumulation as it has never been dredged since its establishment in the 1960s (Table II-3). There is almost no vegetation in these ponds. Some *Typha latifolia L.* grows at the very upstream source of NUG. A cover of seasonal floating plants was observed in the

---

<sup>1</sup> In this thesis, the hydraulic retention time (HRT) is related to the day of the sampling, which is an instant value. Please see Table II-3 for its calculation.

borders of NUG2, but this cover was very limited relative to its large surface area. Organic debris, mainly decayed fallen leaves from the trees in the surrounding, covered the upper part of pond bed in NUG3. NUG2 and NUG3 are also closely linked (Fig. II-13), and thus the stream outlet of NUG2 was identified as the stream inlet of NUG3.

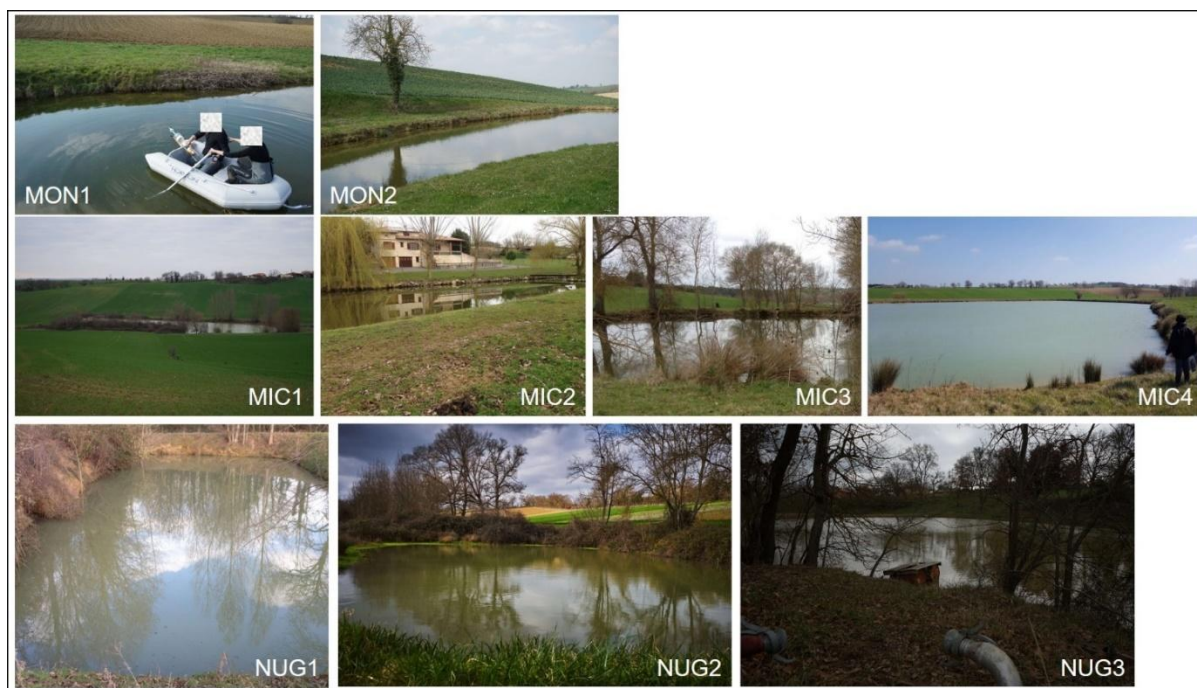


Fig. II-15. Photos of sampling ponds.

## 2. Sampling strategies

Two sampling campaigns were performed. The first sampling campaign was on 15<sup>th</sup> March (MON1 and MON2), 18<sup>th</sup> March (MIC1 and MIC2), 23<sup>rd</sup> March (MIC3 and MIC4), and 4<sup>th</sup> April (four ponds in NUG: NUG1 to NUG4) in 2016, during the spring season of the Save basin. The second sampling campaign was carried out in March 2018. Water and sediment samples were collected in the first sampling campaign, while only water samples were collected in the second sampling campaign. Water and sediment samples inside NUG4 pond were not collected because of the influence of the residential wastes from the village wastewater treatment plant, which was not in the scope of the study.

As shown by the discharge survey of the Montoussé stream, no significant flood events occurred neither before nor during the sampling activities (Fig. II-14), thus the water discharge

during the time corresponded to a recession flow period in both cases, that usually occurred at that time (Perrin et al., 2008; Ponnou-Delaffon et al., 2020). Indeed, the sampling period was also determined according to the fertilizer spreading (January-March). Therefore, the study can investigate the impact of the agricultural activities on streams and ponds. Meanwhile, the temperature during the sampling period was close to the annually mean temperature (Paul et al., 2015; Ponnou-Delaffon et al., 2020).

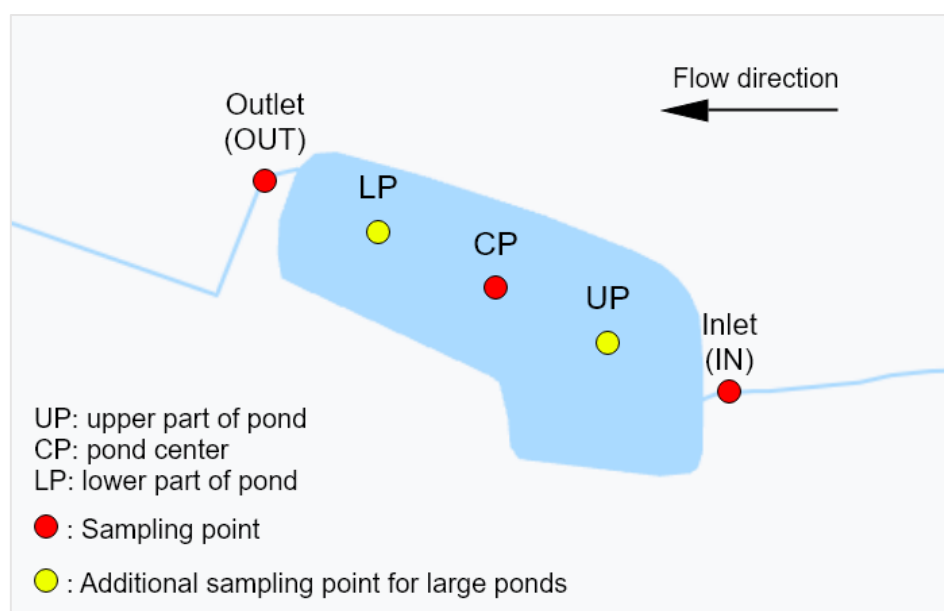


Fig. II-16. Schematic diagram of the sampling strategy (MIC1 as example)

## 2.1 Water

Water samples concerned the stream water and the pond water. Stream water samples were collected from the stream at the inlet (IN) and outlet (OUT) of each pond. They were collected from open-channel surface water (<5 cm) with great attention paid to avoid both the stagnant water zone and the contact with the stream sediment or floating debris. Pond water was sampled using a boat (Fig. II-15) in the center of each pond (CP) within the first 30 cm of surface water. Indeed, it is supposed to represent the main composition of the pond water since several ponds are very shallow and the water depth is less than 1 m (Holland et al., 2004). Temperature ( $T$ , °C), pH, dissolved oxygen (DO,  $\text{mg L}^{-1}$ ), and conductivity (EC,  $\mu\text{S cm}^{-1}$ ) were measured at each sampling point using a WTW Multi 3420 multi-parameter portable meter, which was calibrated in the laboratory before measurement. The discharge of the stream at the inlet and outlet ( $Q$ , L

s<sup>-1</sup>) was measured using a simple bucket method (mean of 5 values) in 2016 and using a flow meter in 2018, whose data were also controlled and validated by using bucket method. Additionally, two 10 mL glass bottles were used to collect water samples for the stable isotopic analysis (<sup>13</sup>C, <sup>2</sup>H, <sup>18</sup>O). The glass bottles were heated in muffle furnace to remove the potential organic matters. Water samples were collected in HDPE bottles, stored and transported on ice in a cooler to the laboratory. Once arriving in the laboratory, 1L water samples were filtered through 0.22µm cellulose acetate membranes (Sartorius, Germany). All the filtered and unfiltered samples were stored in a cool room at 4 °C until analyses (except isotope samples at -20°C). Fig. II-17 illustrated the processes of filtration and preservation for the water samples.

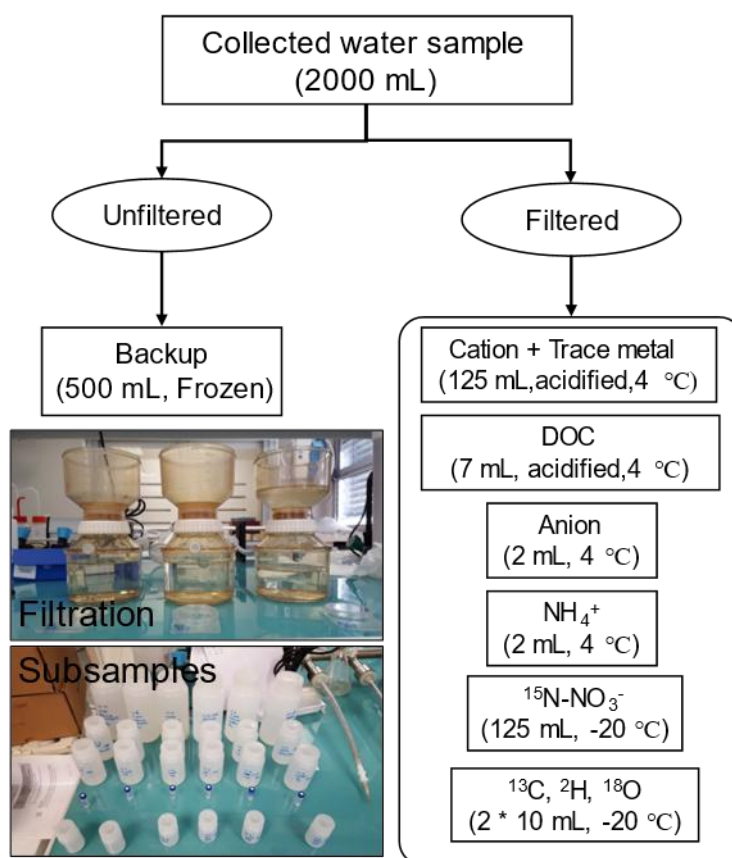


Fig. II-17. Preprocesses and preservation for water samples before analysis

## 2.2 Sediment

Sediment samples were collected from streams and ponds (Fig. II-16). Stream sediments at the inlet/outlet of the ponds were collected by hands in sterilized non-powder gloves from the surface layers of stream sediments (<4 cm, beneath the water- sediment interface). Pond

sediments were collected using a straight core sampler (Fig. II-18A). The sampler was inserted vertically into the benthic sediment and sealed by a rubber stopper at the tail end to obtain a core of sediment. Firstly, the surface layer (S) of the sediment (0 – 4 cm) was extracted from each core. Secondly, the rest of sediment was sliced into one or two layers (called deeper (D) and bottom (B) layers) depending on the sedimentation and change of sediment colors, supposed to represent different oxic and organic conditions (Fig. II-18B). The number of sediment sampling points in each pond was determined by its surface area. For typical sized ponds, sediments were taken from the central part of a pond (CP), and for the largest ones, samples were collected from the upper part (UP), central part (CP), and lower part (LP) inside these ponds (Fig. II-13). The sediment samples were put in plastic containers and kept in coolers during transportation to the laboratory.

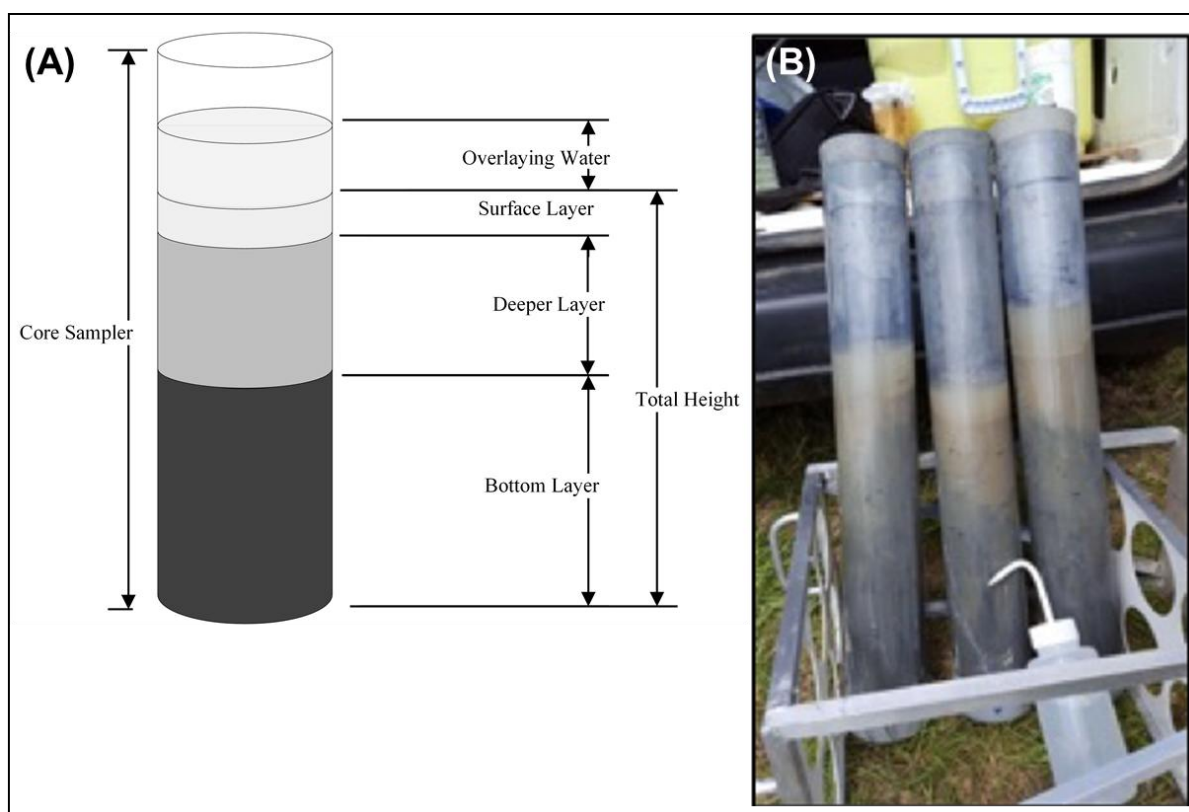


Fig. II-18. (A) Schema of the straight core sampler used in the sampling campaign; (B) pond sediments collected by the core sampler.

A portion of sediment samples were then dried in an oven at 40 °C. The dry sediments were gently homogenized in an agate mortar, and then they were sieved into three fractions, a

fine fraction ( $<63 \mu\text{m}$ ), a coarse fraction ( $63 \mu\text{m} - 2 \text{ mm}$ ), and the coarser fraction ( $>2 \text{ mm}$ ), following very well-established protocols (Benabdelkader et al., 2018; N'guessan et al., 2009). Each fraction was weighed and conserved in a dry place for further analyses. Other sediment subsamples were preserved at  $4^\circ\text{C}$  for denitrification assay experiments, which were performed immediately after arriving in the laboratory, taking into consideration the degradation of nitrogenous ions in sediments caused by bacterial activities. Finally, the other wet sediment subsamples were frozen  $-20^\circ\text{C}$  for further microbiological analysis. The pretreatment for sediment samples was illustrated by Fig. II-19.

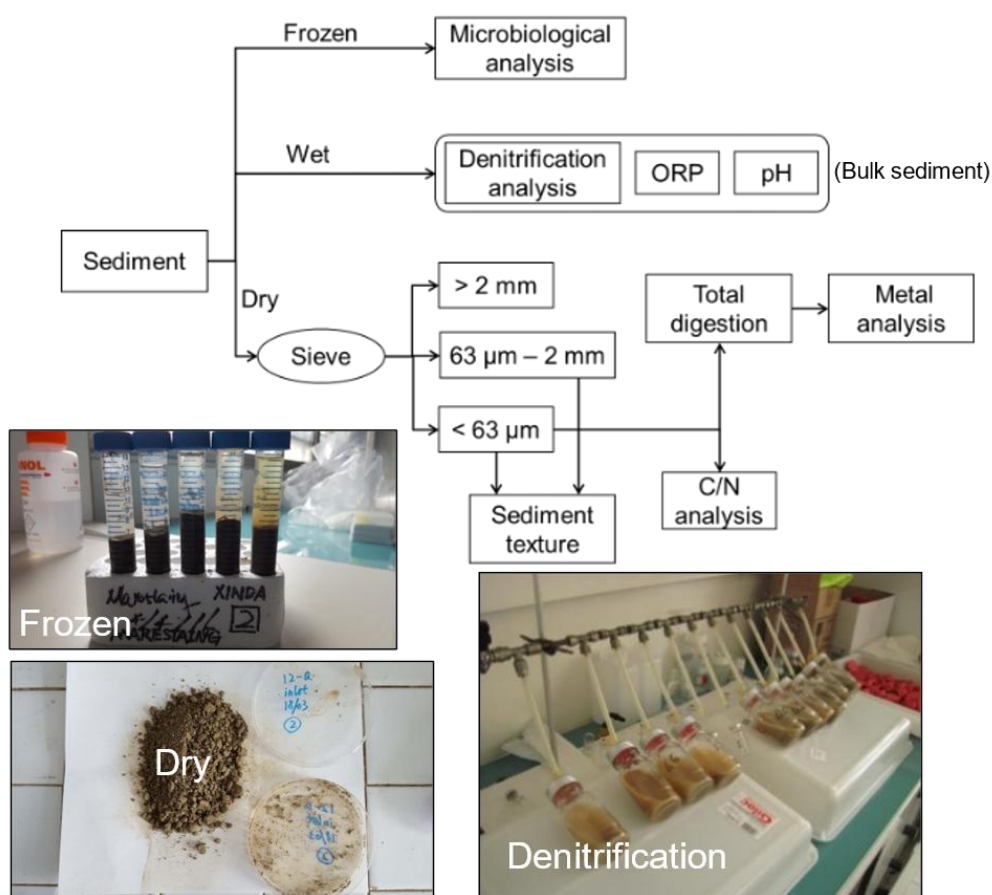


Fig. II-19. Processes for further analyses for sediment samples.



### 3. Physicochemical and biological analyses

#### 3.1 Water

##### 3.1.1 Basic physicochemical analyses

Bicarbonate alkalinity ( $\text{mg L}^{-1}$ ) was analyzed by an acid titration method (ISO 11732: 2005). Nitrate concentration ( $\text{NO}_3^-$ ,  $\text{mg L}^{-1}$ ) and other major anions ( $\text{Cl}^-$  and  $\text{SO}_4^{2-}$ ) were determined with an ion chromatography (Dionex ICS-5000). A Shimadzu TOC-5000 analyzer was utilized to measure dissolved organic carbon (DOC,  $\text{mg L}^{-1}$ ).

##### 3.1.2 Stable isotopes

Three stable isotopes ( $^{13}\text{C}$ ,  $^2\text{H}$ ,  $^{18}\text{O}$ ) were analyzed in all water samples collected in the organic carbon free glass bottles. The  $^{15}\text{N}$  in nitrate ( $^{15}\text{N}\text{-NO}_3^-$ ) was analyzed for 10 water samples in four ponds (MON1, MON2, MIC1, MIC2). In advance of the  $^{15}\text{N}\text{-NO}_3^-$  measurement, nitrate in water samples should be extracted from the dissolved organic nitrogen (DON) in order to obtain a precise value of  $^{15}\text{N}\text{-NO}_3^-$  without the interference cause by isotopic fractionation. A simple and original method has already been developed to separate the organic matter from the solution phase based on the solubility difference between inorganic salts and a mixture of water, acetone, and NaOH solution (Huber et al., 2012). This method was approved to be effective in a previous study in the Montoussé catchment (Paul et al., 2015). A 100 mL frozen filtered water was lyophilized. Then the lyophilized residue was mixed with 350  $\mu\text{L}$  of 1  $\text{mol L}^{-1}$  NaOH solution and 20 mL of pure acetone for 5 minutes. Two phases of different solubility were generated after of several minutes. The supernatant contained the nitrate dissolved in the acetone, while the precipitated phase contained the organic matter and other salts derived from NaOH. Then, the supernatant was separated into other containers and evaporated at 90 °C in a water-bath device. The yield of nitrate extracted from the water sample was up to 80% and no additional fractionation was observed (Huber et al., 2012). The powder generated after the evaporation was sealed in tin capsules and analyzed using EA-IRMS (IsoPrime 100) mass spectrometer at EcoLab's SHIVA platform. The analytical precision was

0.2‰ using the  $\text{KNO}_3$  (IAEA) and  $\text{NH}_4\text{NO}_3$  (Merck).

## **3.2 Sediment**

### **3.2.1 Physicochemical analyses**

Sediment texture was analyzed by a laser diffraction particle distribution analyzer (LA-960, HORIBA) at la Plateforme d'Analyses Physico-Chimiques (PAPC). Two fractions were used in the texture analysis, the fine fraction ( $<63 \mu\text{m}$ ) and the coarse fraction ( $63 \mu\text{m} - 2 \text{mm}$ ). The sediment remaining in the serum bottle after the denitrification assay was dried at  $105 \text{ }^\circ\text{C}$  to a constant weight. The dried material was used to measure the sediment dry bulk density (DBD,  $\text{g cm}^{-3}$ ) and water content (WC, %). Wet sediment subsamples were used to determine oxidation-reduction potential (ORP, mV) by an ORP probe coupled with the WTW Multi 3420 multi-parameter portable meter. Sediment organic carbon (Corg, %) and organic nitrogen (Norg, %) were determined using an element analyzer (Flash 2000, ThermoFisher) after decarbonation with  $1 \text{ mol L}^{-1}$  HCl on a heat block ( $40 \text{ }^\circ\text{C}$ ) until the complete disappearance of effervescence. The concentration of added HCl has been proved to be reliable for obtaining accurate organic carbon in calcareous sediments (Van Iperen and Helder, 1985; Komada et al., 2008), which is a common sediment type in the study area (Bur et al., 2009; N'guessan et al., 2009).

### **3.2.2 Denitrification analyses**

This thesis applied the commonly used acetylene ( $\text{C}_2\text{H}_2$ ) inhibition technique (AIT) (Hynes and Knowles, 1978), as described in Iribar et al (2015). It can measure the intermediate  $\text{N}_2\text{O}$  emission rate (without  $\text{C}_2\text{H}_2$ ) and the potential denitrification rate (with  $\text{C}_2\text{H}_2$ ) (Fig. II-20).

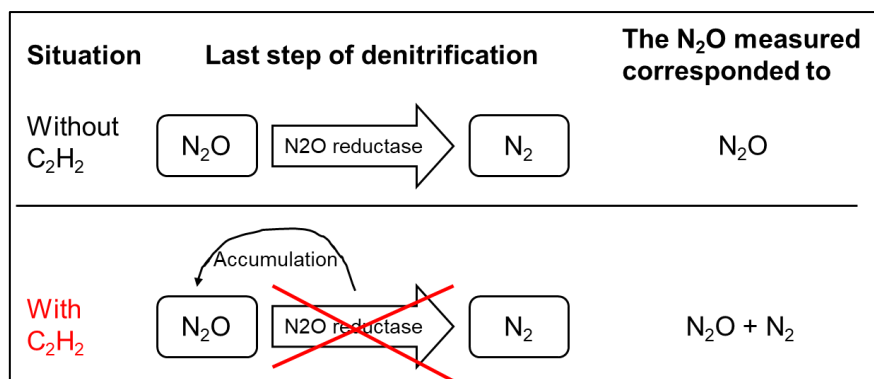


Fig. II-20. Schematic diagram of the acetylene (C<sub>2</sub>H<sub>2</sub>) inhibition technique (AIT). The addition of C<sub>2</sub>H<sub>2</sub> can inhibit the function of N<sub>2</sub>O reductase and lead to the N<sub>2</sub>O accumulation.

### 3.2.2.1 Intermediate N<sub>2</sub>O emission rate

First, 20 ml of sediment was put into a 125 ml serum bottle, and then the incubation solutions (100 mg N L<sup>-1</sup> of KNO<sub>3</sub> and 50 mg C L<sup>-1</sup> of CH<sub>3</sub>COONa) were added into the bottle. After sealing with a septum cap, the headspace of the bottle was purged using nitrogen gas at a speed of 4 L min<sup>-1</sup> in 15 minutes. The serum bottle was then stored in a thermostatic incubator at 13 °C (value representing the average annual air temperature in the field, Ponnou-Delaffon et al., 2020) for 3 hours. Meanwhile, it was shaken every hour, firstly to make the reaction homogenous and secondly to guarantee gas-liquid equilibrium. After 3 hours, 0.2 mL of gas was extracted from the headspace of the serum bottle and then transferred into a gas chromatograph (GC) equipped with an electron capture detector for the determination of N<sub>2</sub>O.

### 3.2.2.2 Potential denitrification rate (PDR)

After the injection into the GC, a further 7 mL of gas was extracted from the headspace of the serum bottle and 15 mL of C<sub>2</sub>H<sub>2</sub> was injected into the bottle. The purpose of the extraction of 7 mL gas was to keep the balance of atmosphere in the bottle. The bottle was stored in a thermostat incubator at the same temperature for 3 hours. After the incubation period, 0.1 or 0.2 mL of gas from the headspace, depending on the concentration of N<sub>2</sub>O, was injected into the GC. Before injection of the gas into the GC, the serum bottle was vigorously shaken for two minutes to ensure the equilibrium of the gas and water phases. The N<sub>2</sub>O emission rate and PDR were expressed as the same unit, microgram of N by gram of dry sediment by hour.

### 3.2.3 Total digestion

The total digestion was performed on the 63 µm fraction owing to its dominance and the affinity for metals (Probst et al., 1999). Sediments were totally digested with a mixture of HF/HNO<sub>3</sub>/H<sub>2</sub>O<sub>2</sub> under a well-validated multiple step procedure in the laboratory clean room. This process has been successfully applied in many studies, particularly for studies in similar carbonated context (Bur et al., 2009; N'guessan et al., 2009; Benabdelkader et al., 2018). Blanks and standard sediments (SUD-1, WQB-1, and STSD-3) were treated using the same digestion procedure. The sediment (100 mg) was digested in a Savillex digestion vessel with 0.6 ml HNO<sub>3</sub> (supra pure, Fisher Scientific) and 0.5 ml HF (supra pure, Fisher Scientific) at 90 °C for 17 hours, followed by an addition of 0.6 ml HNO<sub>3</sub>. The solution was left overnight at 90 °C and then was evaporated. In the second step, H<sub>2</sub>O<sub>2</sub> (0.5 ml) was added three times to remove the organic matter with the help of an ultrasonic device (Branson 1510) until the effervescence disappeared. Then the solution was evaporated again. The residue was recovered using 2 ml HNO<sub>3</sub> (2%).

### 3.2.4 single EDTA extraction

A single EDTA extraction procedure was applied to sediments for the measurement of the available fraction of trace elements. A solution of 1 g sediment and 10 ml of EDTA-2Na (0.05 mol l<sup>-1</sup>, ethylenediaminetetraacetic acid disodium salt dihydrate) was gently mixed for 1 hour at the ambient temperature (20 °C). The extracted solution was then filtered through a 0.22 µm filter membrane. Two blanks were treated by the same process. The 0.05 mol l<sup>-1</sup> EDTA has been widely adopted by previous studies on calcareous soil/sediments (Quevauviller et al., 1996; Leleyter et al., 2012; Benabdelkader et al., 2018), and was proved to be an effective reactant for the single extraction due to the high recovery rate (Sahuquillo et al., 2003; Ghestem and Bermond, 2010).

### 3.2.5 Metal analyses

The major elements (Ca, Al, Fe, Mg, Mn) were analyzed with an inductively coupled plasma optical emission spectrometer (ICP-OES, Thermo IRIS Interpid II XDL) at the Laboratoire écologie fonctionnelle et environnement (Toulouse, France). The trace elements

(Zn, Cr, Ni, Cu, Pb, As, Co, Sc, Cs, Pb) were measured using an inductively coupled plasma-mass spectrometer (ICP-MS, Perkin-Elmer ELAN 6000) at the laboratory GET-OMP (Geoscience Environment Toulouse-Observatory Midi-Pyrénées) analytical platform. Recovery for the standard sediments ranged from 85% and 110%, and the blanks were below the detection limits. The detection limits of ICP-OES for major elements are  $0.5 \mu\text{g L}^{-1}$ . The detection limits of ICP-MS for trace elements are between  $10^{-3}$  and  $10^{-2} \mu\text{g L}^{-1}$ .

### 3.2.6 Molecular analysis

In order to identify a potential link between the presence of genes and the denitrification rate, twelve sediments from five ponds (MON2, MIC1, NUG1, NUG2, and NUG3) were selected to perform qPCR assay. Eleven samples were from surface layers, and one (NUG3-CP-D) from the deeper layer. The selection was proceeded after the denitrification rate measures and considered a large range condition of PDR conditions (low and high values from upstream ponds, MON2, MIC1, respectively) and the potential influence of the succession of ponds from upstream to downstream (NUG1 to NUG3, respectively).

According to the method set up by several authors (see references listed in Table II-4), duplicate DNA samples of each sediment were extracted from approximate 0.5 g aliquot of sediment using NucleoSpin® Soil kit (MACHEREY-NAGEL GmbH & Co. KG), according to the manufacturer's instructions. A final elution volume of 60  $\mu\text{L}$  was used. The quantity and quality of DNA isolated was determined using the NanoDrop spectrophotometer (ThermoFisher SCIENTIFIC). The abundance of total and denitrifier communities was expressed by the gene copies per gram of sediments for 16S rRNA, and *nirS*, *nirK*, and *nosZ* denitrification genes, respectively.

During the denitrification process, the nitrate is firstly reduced to nitrite ( $\text{NO}_2^-$ ), and then the reduction of nitrite to nitric oxide (NO) is catalyzed by two distinguishing nitrite reductases, a cytochrome cd1 encoded by *nirS* or a Cu-containing enzyme encoded by *nirK* (Braker et al., 2000). The last step ( $\text{N}_2\text{O}$  to  $\text{N}_2$ ) is catalyzed by nitrous oxide reductase encoded by *nosZ* (Iribar et al., 2015).

Table II-4 provides the list of primers, and thermocycling programs used for each gene. In a preliminary test, DNA dilution series of 10 were made to detect inhibitory effects and find

optimum concentration for analysis by qPCR. For each gene studied, a standard was used as reference. The standard is a manufactured product (obtained from Eurofins) produced by ligation of a specific version of the gene of concern into the synthetic plasmid pEX-A128 (2450 base pairs, Eurofins). The reaction mixture (10 $\mu$ L) consisted of 5 $\mu$ L of SsoAdvanced Universal SYBR Green Supermix (BioRad, containing the DNA polymerase, appropriate buffer, dNTPs and the SybrGreen chemical which stains double-stranded DNA), the appropriate primers and DNA templates (sample or standard). Each reaction was run in triplicate in 96-wells plates using a CFX96 Touch™ Real-Time PCR Detection System (BioRad). Gene quantification was based on SybrGreen fluorescence emitted when associated with double stranded DNA. After the qPCR run for all gene analyses, the efficiency of the amplification was assessed using the standard curve slope, and the specificity of amplification was assessed through the melting curve.

Table II-4. List of primers, and thermocycling programs used for each gene.

Gene	Primers (0.05 $\mu$ l <sup>-1</sup> )	Sequence	Accession (gene sequence)	Additive	Thermocycler	References
<b>16S rDNA</b>	341F	CCTACGGGAGGCAGCAG	X80731.1, Escherichia coli		95°C, 3 min (D); 35 cycles (95°C for 5 s, 60°C for 30 s)	López- Gutiérrez et al., 2004
	534R	ATTACCGCGCTGCTGGCA				
<b>nirK</b>	876F	ATYGGCGVCAYGCGA	AY536011.1, Sinorhizobium meliloti strain JJ1C10		95°C, 3 min (D); 35 cycles (95°C 5 s, 63°C*, 30 s), touchdown (63°C to 58°C at -1.0 °C per cycle)	Henry et al., 2004; Baudoin et al., 2009
	nirK1040R	GCCTCGATCAGRTRTGGTT				
<b>nirS</b>	nirS4QF	G TSAACGYSAAGGARACSGG	AE004091.2, Pseudomonas aeruginosa PAO1	T4gp32 (0.05 $\mu$ l <sup>-1</sup> )	95°C, 3 min (D); 35 (95°C 5 s, 63°C*, 30 s; 72°C, 30 s), touchdown (63°C to 58°C at -1.0 °C per cycle)	Throback et al., 2004; Gao et al., 2016
	nirS6QR	GASTTCGGRTGSGTCTTSAYGAA				
<b>nosZ</b>	nosZ1840F	CGCRACGGCAASAAGGTSMSST	AE006469.1, Sinorhizobium meliloti		95°C, 3 min (D); 35 cycles (95°C, 15 s; 60°C, 30 s; 72°C, 30 s)	Henry et al., 2006; Hu et al., 2014
	nosZ2090R	CAKRTGCAKSGCRTGGCAGAA				

Note. A = amplification; M = melt.

\*Modification of qPCR using an annealing temperature higher than the projected melting temperatures for primers, gradually reducing the temperature until an optimum annealing temperature is reached,

increasing specificity and sensitivity (Korbie and Mattick, 2008).

#### **4. Data analyses**

The statistical analysis was conducted in R (version 3.4) (R Core Team, 2017). The processes of data analyses will be exhibited specifically in each following chapter since different methods were applied to analyze the results of nitrates and trace elements, respectively.

## **Chapter III**

# **Role of constructed ponds in denitrification and nitrate behavior: key controlling factors in streams and ponds at a catchment scale<sup>1</sup>**

---

<sup>1</sup> The major content of this chapter has been accepted by *Applied Geochemistry*: X. WU, A. PROBST, M. BARRET, V. PAYRE-SUC, T. CAMBOULIVE, F. GRANOUILLAC, 2021. Spatial variation of denitrification and key controlling factors in streams and ponds sediments from a critical zone (southwestern France). *Applied Geochemistry*. 131, 105009. DOI: 10.1016/j.apgeochem.2021.105009



## Chapter III

# Role of constructed ponds in denitrification and nitrate behavior: key controlling factors in streams and ponds at a catchment scale

### Introduction

Nitrate ( $\text{NO}_3^-$ ) contamination in surface waters and groundwaters is a serious global environmental problem, especially in areas of intensive agriculture (Verhoeven et al., 2006). The extensive application of synthetic fertilizer contributes to high  $\text{NO}_3^-$  loadings into agricultural surface waters because of soil leaching, soil erosion, and surface runoff (Verhoeven et al., 2006; Zak et al., 2018). A high  $\text{NO}_3^-$  level can induce water eutrophication and health problems in human beings (Kapoor et al., 1998). In agricultural areas like southwestern France, the  $\text{NO}_3^-$  concentration in many streams and rivers was close to or exceeded the potability threshold ( $50 \text{ mg L}^{-1}$  of  $\text{NO}_3^-$ ) for European rivers set by the European Water Framework Directive in order to control and regulate the  $\text{NO}_3^-$  level in water bodies (Ferrant et al., 2011; Boithias et al., 2014).

As stated in Chapter I and II, constructed ponds are very common in southwestern France (an agricultural region for decades) and there can be several in a chain in a given agricultural catchment. They were mainly set up historically by local farmers for the purpose of water storage for cattle farming and crop irrigation (Carluer et al., 2017). Nowadays, they are used for water irrigation or for private landscaping. Although the quality of stream and river water has been surveyed, the role of such ponds in the quality of downstream water and sediments has rarely been investigated.

Such ponds are biogeochemical reactors, which may influence nitrogen (N) behavior as they were found to be effective in mitigating  $\text{NO}_3^-$  in the stream waters draining agricultural catchments (Vymazal, 2007; Tournebize et al., 2017). The denitrification process, a microbial process which reduces  $\text{NO}_3^-$  to molecular nitrogen gas ( $\text{N}_2$ ) in four steps ( $\text{NO}_3^- \rightarrow \text{NO}_2^- \rightarrow \text{NO} \rightarrow \text{N}_2\text{O} \rightarrow \text{N}_2$ ) (Tiedje, 1994), is one of the main processes contributing to the removal of  $\text{NO}_3^-$  from the aquatic system (Burgin and Hamilton, 2007). It may cause the ecosystem to be

N-limiting when N is not in excess, but in an agricultural context with significant  $\text{NO}_3^-$  loading due to fertilizer inputs, it can remove excessive  $\text{NO}_3^-$  and participate in  $\text{NO}_3^-$  mitigation in streams (Fisher and Acreman, 2004). Nevertheless, the reaction of this process may not be complete and may lead to the production of  $\text{N}_2\text{O}$ , a harmful intermediate greenhouse gas that can contribute to the global warming phenomenon (Garnier et al., 2010). Studies have shown that the magnitude of  $\text{N}_2\text{O}$  production via incomplete denitrification is in response to changes in Dissolved Oxygen (DO), ammonium, and nitrite concentrations (Rassamee et al., 2011).

As mentioned by several authors, it is important to investigate both assessment of the denitrification process (Piña-Ochoa and Álvarez-Cobelas, 2006) and the development of modelling of nitrogen catchment export at the regional scale (Álvarez-Cobelas et al., 2008). Although the spatial variability of the denitrification process at catchment scale has been investigated, it has been less well studied in ponds (Scaroni et al., 2010; Song et al., 2012; Bernard-Jannin et al., 2017). Indeed, with increasing climate change pressure, particularly where water resources are limited, the use of ponds as tools of water storage will probably be extended in many cultivated places around the world. Investigations of nitrogen behavior and particularly the spatial variability of the denitrification process according to environmental conditions are thus a major issue to be evaluated at regional scale, especially where a number of constructed ponds exist.

The factors influencing the denitrification process have been investigated by a large number of studies. Nitrate and organic carbon can influence the denitrification rate as they are two key reactants in the process (Groffman et al., 2006; Arango et al., 2007; Saeed and Sun, 2012; Saggari et al., 2013). Meanwhile, the abundance of denitrifiers and other water and sediment characteristics (pH, water content, redox potential, *etc.*), namely distal and proximal controllers (Wallenstein et al., 2006), may also play an important role (Oehler et al., 2007; Attard et al., 2011; Luo et al., 2012; Iribar et al., 2015).

Works combining geochemical investigation of the denitrification process with examination of the *in situ* microbial genus at ecosystem scale are not often found in the literature (Valero et al., 2010; Blaszczyk et al., 2018). The denitrification rate has been shown to be related to specific gene abundance (Braker et al., 2000), while some studies have found some physicochemical parameters of sediments (e.g.  $\text{NO}_3^-$  concentration, organic carbon

content, and/or sediment texture) to be better explanatory variables of denitrification rates than the abundance of denitrifiers at a small regional scale (Attard et al., 2011, with a similar sampling date to this study); Shrewsbury et al., 2016).

Although a great number of studies have shown the relationship between denitrification and some water and sediment properties, the power of environmental factors (*i.e.*, distance to stream source, stream hydrology, pond size, *etc.*) to influence denitrification has not been well identified in the literature. Moreover, Fisher and Acreman (2004) pointed out that effective attributes of wetlands are important to reduce nitrogen and phosphorous loadings efficiently. Developing simple empirical models based on pond and sediment physicochemical characteristics represents an interesting challenge for a regional-scale approach but requires thorough field data to be robust. This may also help identify the most appropriate pond characteristics for policy makers in charge of water quality management.

Considering the current situation mentioned above, the main objectives of this study were: (1) to investigate the spatial variability of denitrification rates in sediments from several streams and ponds considering their locations and characteristics; (2) to study the main controlling factors that regulate the denitrification process; (3) to draw some lessons and deduce recommendations about pond management to control the impact of  $\text{NO}_3^-$  in such agricultural environments.

The main hypotheses are that (1) the potential denitrification rate exhibits spatial variability in stream and pond sediments even in small agricultural catchments; (2) the magnitude of denitrification is strongly associated with sediment and water characteristics and/or the abundances of denitrifiers.

Therefore, in this study, we measured the physicochemical characteristics of water and sediment samples from various streams and ponds collected at the same time in three small agricultural catchments located in a traditionally agricultural region (the Save basin, southwestern France). In addition, denitrification genes were investigated for some sediments showing relatively low and high denitrification rates. Empirical models using some easily measured characteristics ( $\text{NO}_3^-$  concentration, temperature, pH, *etc.*) were attempted, and environmental catchments and pond characteristics were considered to facilitate better pond management for  $\text{NO}_3^-$  removal.

This chapter has been divided into two parts.

The first part is relative to the denitrification process in the stream and pond sediments with its controlling factors. The role of ponds in the denitrification process in sediments at the catchment scale, is also discussed. The second part introduces the  $\text{NO}_3^-$  behavior in streams and ponds. The  $\text{NO}_3^-$  removal efficiency in the ponds is investigated. This part also discusses the role of ponds in  $\text{NO}_3^-$  removal efficiency inside the ponds. The interactive function of ponds to  $\text{NO}_3^-$  removal and the denitrification rate is also discussed as a synthesis of this chapter.

## Materials and methods

The main materials and methods used in this chapter have been introduced in Chapter II. The statistical analyses in this study are stated in this section.

The statistical analysis was conducted in R (version 3.4) for the Kruskal-Wallis test and the post hoc Dunn's test for multiple-variable analysis and difference comparisons between various samples. Pearson correlation coefficients were used to evaluate the correlations between measured parameters, which included denaturation enzyme activity.

Principle component analysis (PCA) was carried out based on z-scored data to investigate the relationships between denitrification rate and other physicochemical and environmental variables for the datasets taken together and for ponds and streams separately. Multiple linear regressions were performed to identify the main variables that could explain PDR in stream and pond sediments, respectively. To reach the normal distribution of PDR, a log-transformation was applied. Other variables were not transformed since they met the normality. Independencies (sediment, water, and environmental variables) were initially selected to avoid overfitting and multicollinearity based on the correlation matrix and the all-subsets regression method (Miller, 1984). This method performs an exhaustive search for the best subsets of the various variables for predicting the target dependent variable through an efficient branch-and-bound algorithm. The algorithm returns a best model of each size; thus, the results avoid a penalty model considering the model size. Finally, the analyzer can select the proper set of variables with the best fitness according to a number of returned models of each size and the specialistic knowledge. The all-subsets regression was conducted by the function of "regsubsets" from the "leaps" package in R.

The statistical figures proposed in this article were mainly generated via the ggplot2 package in R.

## **Part I. Denitrification and its controlling factors**

## 1. Results

### 1.1 Water characteristics

Analysis indicated rather consistent chemical characteristics for the waters between MIC and NUG in each sampling campaign, sharing similar cation and anion compositions (Table III-1) and relative distribution according to the Piper diagram (Fig. III-1) (Piper, 1944). Generally, the waters are neutral as indicated by the pH values and dominated by  $\text{Ca}^{2+}$  and  $\text{HCO}_3^-$  since the waters are draining carbonate molassic bedrock in this region (Perrin et al., 2008). Regarding the two dominant ions ( $\text{Ca}^{2+}$  and  $\text{HCO}_3^-$ ), no significant difference was observed between the two sampling campaigns for each catchment and between MIC and NUG for the two sampling campaigns (Kruskal-Wallis test,  $\text{Ca}^{2+}$ :  $p = 0.063$ ,  $\text{HCO}_3^-$ :  $p = 0.640$ ).

Table III-1. Physicochemical characteristics of waters (streams and ponds) for the 2016 and the 2018 sampling campaign in Mican, Nuguet, and Montoussé catchments. N is the number of samples. NA: data not available (since the pond was dry)

	2016 Sampling Campaign							
	Mican (n=12)		Nuguet (n=11)		Montoussé (n = 4)			
	Range	Mean	Range	Mean	MON1 (n=1)	MON2 (n=3)		
	Range	Mean	Range	Mean	Range	Mean		
T °C	8.7~12	10.63±0.98	12.5~15.2	13.43±0.86	9.70	10.3~12.3	11.53±1.08	
pH	7.76~8.29	8.06±0.16	7.65~8.17	7.89±0.15	8.07	7.88~8.2	8.08±0.18	
DO, mg L <sup>-1</sup>	8.83~16.14	11.1±1.87	5.09~12.75	9.39±2.68	13.87	9.88~13.8	11.66±1.99	
Cond, µS cm <sup>-1</sup>	507~858	766.42±97.13	701~879	800.73±59.55	452	586~632	604±24.58	
DOC, mg L <sup>-1</sup>	2.16~4.32	2.71±0.72	1.65~5.97	3.13±1.37	5.60	1.69~3.77	2.86±1.06	
NO <sub>3</sub> <sup>-</sup> , mg L <sup>-1</sup>	3.07~44.92	29.39±13.96	11.4~60.56	34.02±16.13	22.87	59.84~61.46	60.63±0.81	
K <sup>+</sup> , meq L <sup>-1</sup>	0.01~0.07	0.05±0.02	0.01~0.12	0.04±0.04	0.01	0.01~0.02	0.02±0.01	
Ca <sup>2+</sup> , meq L <sup>-1</sup>	2.59~7.21	5.35±1.13	4.32~6.31	5.51±0.59	4.62	4.18~6.48	5.44±1.17	
Na <sup>+</sup> , meq L <sup>-1</sup>	0.58~0.77	0.73±0.07	0.62~1.1	0.8±0.15	0.70	0.44~0.47	0.45±0.02	
Mg <sup>2+</sup> , meq L <sup>-1</sup>	1.5~1.9	1.72±0.09	1.28~1.86	1.59±0.2	0.93	1.64~1.77	1.7±0.07	
HCO <sub>3</sub> <sup>-</sup> , meq L <sup>-1</sup>	3.31~7.41	5.85±1.08	4.91~6.82	5.98±0.61	5.00	5.33~5.67	5.48±0.17	
Cl <sup>-</sup> , meq L <sup>-1</sup>	1.22~1.77	1.39±0.18	0.87~1.14	1±0.1	0.82	0.86~0.89	0.87±0.02	
SO <sub>4</sub> <sup>2-</sup> , meq L <sup>-1</sup>	0.9~1.25	0.97±0.09	1~1.38	1.16±0.14	0.74	0.7~0.73	0.71±0.02	
NO <sub>3</sub> <sup>-</sup> , meq L <sup>-1</sup>	0.05~0.73	0.47±0.23	0.18~0.98	0.55±0.26	0.37	0.97~0.99	0.98±0.01	
	2018 Sampling Campaign							
	Mican (n=13)		Nuguet (n=12)		Montoussé (n = 4)			
	Range	Mean	Range	Mean	MON1 (n = 1)	MON2 (n = 3)		
	Range	Mean	Range	Mean	Range	Mean		
T °C	10.2~12.4	11±0.64	10.7~14.3	12.28±1.04	NA	10.70~13.30	12.17±1.33	
pH	7.63~8.4	8.1±0.27	7.73~8.68	8.16±0.22	NA	7.63~8.58	8.07±0.48	
DO, mg L <sup>-1</sup>	6.26~16.01	10.27±2.63	4.46~19.44	11.14±3.71	NA	10.00~11.70	10.59±0.96	
Cond, µS cm <sup>-1</sup>	617~1029	832.08±121.13	698~875	774.25±55.68	NA	755~897	847±80	
DOC, mg L <sup>-1</sup>	2.68~5.51	3.63±0.74	2.21~7.84	3.79±1.54	NA	2.67~3.45	3.12±0.41	
NO <sub>3</sub> <sup>-</sup> , mg L <sup>-1</sup>	5.75~60.97	36.57±17.32	17.49~60.93	36.04±15.49	NA	41.70~44.70	43.25±1.35	
K <sup>+</sup> , meq L <sup>-1</sup>	0.01~0.09	0.06±0.03	0.02~0.16	0.05±0.05	NA	0.02~0.03	0.03±0.01	
Ca <sup>2+</sup> , meq L <sup>-1</sup>	4.29~7.88	6.18±1.08	4.6~6.44	5.71±0.53	NA	4.55~6.04	5.06±0.85	
Na <sup>+</sup> , meq L <sup>-1</sup>	0.63~0.86	0.81±0.07	0.66~1.1	0.82±0.14	NA	0.56~0.57	0.56±0.01	
Mg <sup>2+</sup> , meq L <sup>-1</sup>	1.65~2.04	1.84±0.11	1.25~1.75	1.56±0.18	NA	2.11~2.31	2.18±0.11	
HCO <sub>3</sub> <sup>-</sup> , meq L <sup>-1</sup>	3.91~7.45	5.79±1.05	4.92~6.45	5.69±0.51	NA	5.41~7.37	6.29±1.00	
Cl <sup>-</sup> , meq L <sup>-1</sup>	1.22~1.86	1.42±0.18	0.87~1.12	1±0.08	NA	0.85~0.86	0.85±0.01	
SO <sub>4</sub> <sup>2-</sup> , meq L <sup>-1</sup>	0.91~1.51	1.12±0.18	1.04~1.31	1.13±0.1	NA	0.65~0.66	0.65±0.01	
NO <sub>3</sub> <sup>-</sup> , meq L <sup>-1</sup>	0.09~0.98	0.59±0.28	0.28~0.98	0.58±0.25	NA	0.67~0.71	0.70±0.02	

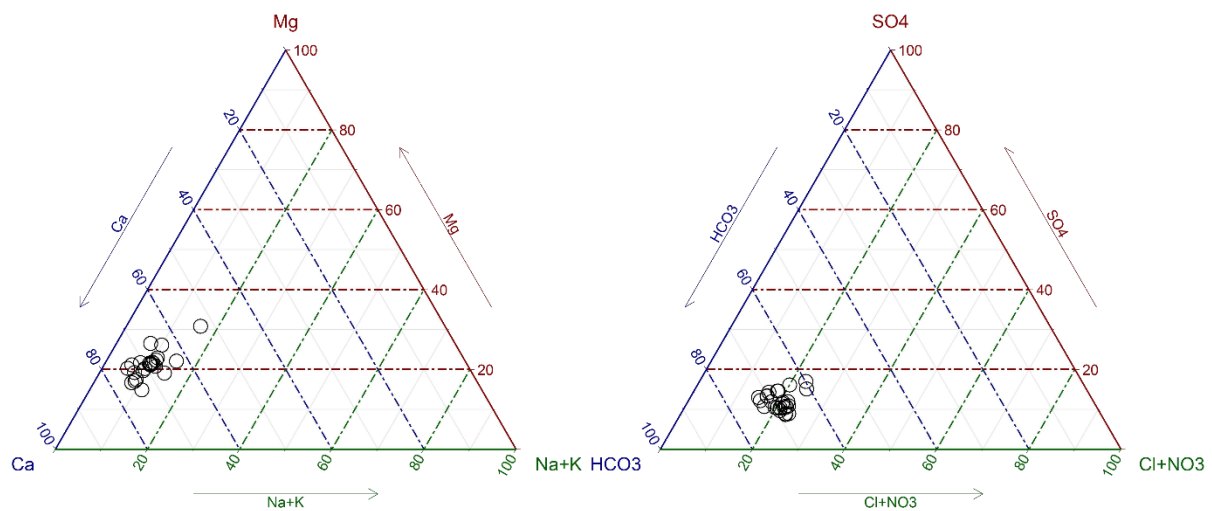


Fig. III-1. Piper plot for major ion compositions (%) in water samples of the two sampling campaigns (2016 and 2018)

In general, the water temperature fluctuated around the annual mean temperature of the sampling area (13.9 °C, Ponnou-Delaffon et al., 2020). The mean temperature in NUG ( $13.43 \pm 0.86$  in 2016 and  $12.28 \pm 1.04$  in 2018) was higher than in MIC ( $10.63 \pm 0.98$  in 2016 and  $11 \pm 0.64$  in 2018), because of the slightly later sampling date and of the lower stream discharge. DOC was also consistent with values already registered in the area (Paul et al., 2015). The average  $\text{NO}_3^-$  concentration in waters from two catchments (MIC and NUG) was close ( $0.47 \pm 0.23$  meq  $\text{L}^{-1}$  *i.e.*,  $34.6 \pm 16.4$  mg  $\text{L}^{-1}$  and  $0.55 \pm 0.26$  meq  $\text{L}^{-1}$  *i.e.*,  $34.2 \pm 16.8$  mg  $\text{L}^{-1}$ ) for the first and second sampling campaigns ( $p = 0.429$ ), respectively. MON1 and MON2 were considered apart since they concern only one upstream pond. Indeed, MON1 has a rather low value compared to the other upstream ponds, and particularly regarding MON2.

## 1.2 Sediment characteristics

### 1.2.1 Physicochemical characteristics

Sediment physicochemical characteristics are summarized in Table III-2. On average, sediment was anoxic, unlike waters, but with a large ORP range (minimum value in NUG1-IN to maximum value in MIC4-OUT), while DBD was variable with an average of  $0.67 \pm 0.19$  g  $\text{cm}^{-3}$ . No difference was observed between catchments for both parameters but ORP was



significantly higher in ponds than in streams ( $p < 0.05$ ) and higher in surface layers than in deep layers ( $p < 0.01$ ), and the reverse was true for DBD. Pond sediments contained more water in surface layers than in deeper ones and more than stream sediments ( $p < 0.01$ ).  $C_{org}$  and  $N_{org}$  were in the range of what was found in sediments and soils from the same region (Bur et al., 2009). A detectable difference between pond sediment depths (deeper > surface,  $p < 0.05$ ) was observed only for  $N_{org}$ , while  $C_{org}$  only differed significantly between sediment types (streams > ponds,  $p < 0.01$ ). Finally, the silty-clayey texture of the sediments did not differ between catchments or between pond layers (Table III-2). Clay and sand contents were significantly higher and lower in pond and stream sediments ( $p < 0.01$ ), respectively, while silt did not differ.

Table III-2. Physicochemical characteristics of sediments from ponds and streams taken together or separately, taken by catchment and by depth (surface and deep layers) of the sediment cores of the ponds. The asterisk (\*) highlights the significant difference between different kinds of sediments ( $p < 0.05$ ). n is the number of samples; ORP: Oxidation - Reduction Potential; DBD: Dry Bulk Density; WC: Water content; Norg: Organic nitrogen content; Corg: Carbon Organic content.

	All sediments (n=49)				Catchment								
	units	min	max	mean	Montoussé (n=9)			Mican (n=22)			Nuguet (n=18)		
					min	max	mean	min	max	mean	min	max	mean
ORP	mV	-228.6	123.1	-71.2±82.0	-175.5	75.7	-47.3±75.2	-191.9	123.1	-67.2±76.5	-228.6	94.7	-87.9±89.4
DBD	g cm <sup>-3</sup>	0.36	1.32	0.67±0.19	0.36	1.32	0.68±0.26	0.39	0.98	0.65±0.17	0.43	1.06	0.70±0.16
WC	%	38.6	221	112.9±39.1	38.6	221	122.0±49.9	56	206.7	115.8±37.8	51.7	181.6	104.6±32.8
Norg	%	0.11	0.36	0.19±0.05	0.13	0.36	0.22±0.06	0.11	0.31	0.18±0.05	0.14	0.33	0.18±0.05
Corg	%	1.02	4.21	1.71±0.74	1.19	3.6	1.86±0.67	1.02	3.92	1.58±0.67	1.08	4.21	1.81±0.83
Clay	%	11.03	51.06	32.2±11.38	22.47	39.52	31.35±5.14	17.88	50.13	34.64±10.61	11.03	51.06	29.51±13.95
Silt	%	37.6	73.51	55.58±6.65	55.95	69.44	60.05±4.52	44.99	73.51	55.64±6.78	37.6	67.02	53.13±6.27
Sand	%	0	51.37	12.22±13.37	3.93	17	8.60±4.26	0.57	35.76	9.72±12.63	0	51.37	17.36±15.87

	units	Type						Layer					
		Pond (n=31)			Stream (n=18)			Surface (n=15)			Deeper (n=14)		
		min	max	mean	min	max	mean	min	max	mean	min	max	mean
ORP	mV	-103.3	94.7	-46.1±54.2*	-228.6	123.1	-114.41±102.06*	-103.3	94.7	-13.13±57.89*	-102.6	-20.4	-74.76±25.35*
DBD	g cm <sup>-3</sup>	0.39	0.94	0.62±0.12*	0.36	1.32	0.77±0.23*	0.39	0.9	0.56±0.11*	0.53	0.94	0.67±0.11*
WC	%	63.9	206.7	122.11±32.43*	38.6	221	96.71±44.48*	66.2	206.7	140.32±31.34*	63.9	135.6	104.93±21.37*
Norg	%	0.14	0.23	0.18±0.03	0.11	0.36	0.21±0.08	0.15	0.23	0.19±0.03*	0.14	0.21	0.17±0.03*
Corg	%	1.02	2.09	1.41±0.26*	1.18	4.21	2.27±0.97*	1.2	2.09	1.51±0.25	1.03	1.82	1.34±0.24
Clay	%	15.19	51.06	38.64±8.28*	11.03	30.28	20.47±5.17*	17.36	48.15	37.61±7.37	15.19	51.06	39.21±9.5
Silt	%	48.94	67.02	56.89±4.6	37.6	73.51	53.18±8.86	51.03	67.02	57.64±4.38	48.94	64.45	56.16±4.94
Sand	%	0	21.98	4.47±4.98*	5.35	51.37	26.35±12.24*	0.82	15.61	4.75±4.02	0	21.98	4.63±6.05

### 1.2.2 Potential denitrification rate (PDR)

PDR was always detected in all sediments from the three catchments (Fig. III-2) in the order  $MON > NUG > MIC$ , with an average of  $0.218 \pm 0.328 \mu\text{g N g}^{-1} \text{ dry sediment h}^{-1}$ . It also showed a great heterogeneity extending from 0.00126 (MIC2-IN) to 2.19 (MON2-OUT) (Fig. III-2), with the highest PDR values in upper catchment ponds (MON2, especially at the stream outlet, Fig. III-2B and NUG1, stream inlet and outlet), with the exception of the stream outlet of NUG4. In general, sediments from MIC exhibited a poor PDR performance (significantly different from the other catchments; Kruskal-Wallis test with post hoc Dunn's test,  $p < 0.0001$ ), with the highest values in MIC1 and MIC3 ponds. Even PDR in MON1 (the isolated impluvium) exceeded these values.

The mean and the standard deviation of PDR in sediments from streams were higher than in ponds (except for MIC3 and MIC1,  $p = 0.427$ , Fig. III-2Aii and NUG1, Fig. III-2C). In the ponds, PDR in surface layers ( $0.305 \pm 0.337$ ) was greater ( $p < 0.001$ ) than in deeper sediments ( $0.118 \pm 0.063$ ) (Fig. III-2Aiii). It should be noticed that as NUG2 and NUG3 were very closely connected, the PDR value in NUG3-IN was considered the same as in NUG2-OUT (Fig. III-2C). Moreover, due to the analytical limitation regarding the coarse nature of the sediment, PDR could not be analyzed in NUG3-OUT. As already stated, only input and output stream sediments were sampled in NUG4.

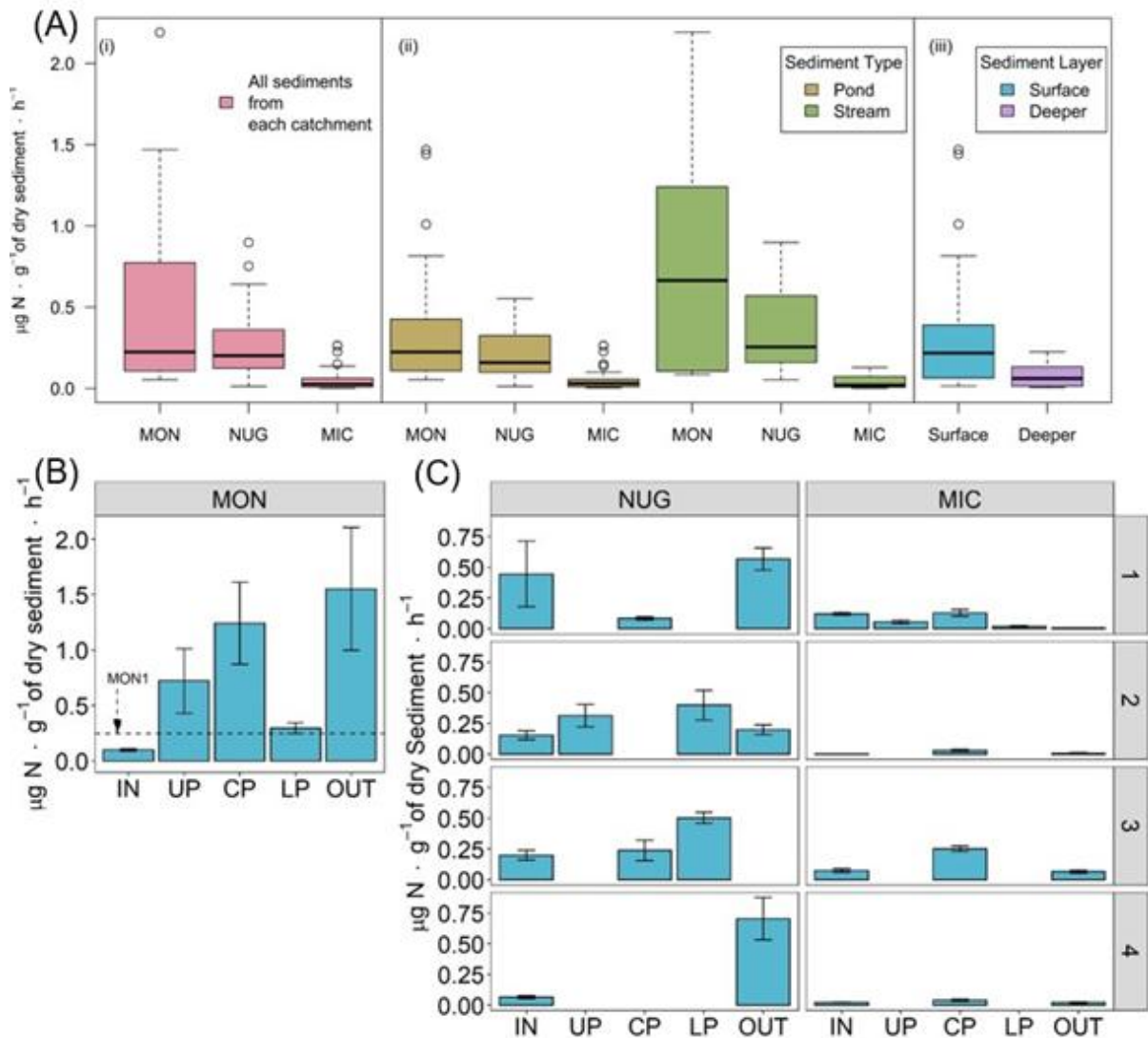


Fig. III-2. Potential denitrification rates (PDR) in stream and pond sediments from the three catchments: (A) PDR values (i) in all stream and pond sediments for each catchment, (ii) separately in stream and pond sediments of each catchment, (iii) in two different depths of pond sediment cores. (B) and (C) indicate individual PDR values in each sampling site in the three catchments: (B) Montoussé [two ponds MON1 (dashed line) and MON2], (C) Nuguet (NUG) and Mican (MIC): vertically from upstream (No. 1) to downstream (No. 4). IN: stream pond inlet, UP: upper part of a pond, CP: pond center part, LP: lower part of a pond, OUT: stream pond outlet.

### 1.3 Relationships between variables

As a synthesis of investigations done using the Pearson correlation matrix (Table III-3), three PCAs were performed on water and sediment parameters considering all samples ( $n = 31$ ), streams ( $n = 16$ ), and ponds ( $n = 14$ , MON1 was not included since it is an isolated impluvium) considered separately (Fig. III-3A, B, C, respectively). The input variables in the

PCA included (1) PDR and  $N_2O$  as the denitrification rates; (2) pH, ORP, water content, organic carbon, organic nitrogen, clay, and silt content as the sediment physicochemical characteristics; (3) water temperature, pH, DOC, and nitrate concentration as water properties. Additionally, stream discharge was introduced to the PCA for stream sediments. Pond slope, hydraulic retention time, pond length/width ratio, and pond depth were taken into consideration for PCA based on pond sediments. Both Bartlett's test of sphericity and the determinant test showed that the datasets were suitable statistically to perform the further PCAs.

Table III-3. Pearson correlation matrix (R) concerning main physicochemical parameters from all (a), stream (b) and pond (c) sediments in the three catchments considered together. Note that more parameters were considered for ponds sediments. Values in bold red and black bold italic mean p-value < 0.05 and < 0.1, respectively. PDR: Potential Denitrification Rate; ORP: Oxidation- Reduction Potential; WC: Water Content in sediment; pH\_s: pH in sediment; pH\_w: pH in water; NO<sub>3</sub>\_w: nitrate concentration in waters; T\_w: water temperature; LW\_ratio: pond length over width; Q: discharge; Slope: pond slope; HRT: Hydraulic Retention Time. (a) All sediments (n = 31); (b) Stream sediments (n = 16); (c) Pond sediments (n = 14).

(a) All sediments (n = 31)

	PDR	N2O	N2O/PDR	pH_s	ORP	Depth	WC	Clay	Silt	Sand	Corg	Norg	C/N	T_w	pH_w	DOC	NO3_w
PDR	1.00																
N2O	<b>0.70</b>	1.00															
N2O/PDR	-0.21	0.10	1.00														
pH_s	0.15	<b>0.39</b>	0.13	1.00													
ORP	-0.20	0.11	0.06	0.21	1.00												
Depth	-0.23	-0.06	<b>0.38</b>	0.23	0.12	1.00											
WC	<b>0.44</b>	0.28	0.04	-0.01	-0.11	0.05	1.00										
Clay	-0.20	0.07	0.20	<b>0.40</b>	<b>0.41</b>	<b>0.53</b>	<b>0.40</b>	1.00									
Silt	0.23	0.29	0.28	0.04	0.30	0.13	0.31	0.19	1.00								
Sand	0.03	-0.21	-0.30	-0.32	<b>-0.47</b>	<b>-0.46</b>	<b>-0.47</b>	<b>-0.85</b>	<b>-0.68</b>	1.00							
Corg	<b>0.45</b>	0.07	-0.03	-0.21	<b>-0.50</b>	-0.34	0.30	<b>-0.42</b>	0.21	0.20	1.00						
Norg	<b>0.55</b>	0.22	0.02	-0.04	<b>-0.38</b>	-0.18	<b>0.58</b>	-0.06	<b>0.36</b>	-0.15	<b>0.89</b>	1.00					
C/N	0.13	-0.17	-0.17	<b>-0.43</b>	<b>-0.46</b>	<b>-0.51</b>	-0.31	<b>-0.85</b>	-0.17	<b>0.72</b>	<b>0.67</b>	0.28	1.00				
T_w	0.27	0.04	<b>-0.43</b>	-0.29	-0.25	-0.15	0.02	<b>-0.44</b>	-0.08	<b>0.37</b>	0.13	-0.02	0.32	1.00			
pH_w	0.06	0.20	0.19	0.10	0.28	0.35	0.29	<b>0.37</b>	0.19	<b>-0.38</b>	-0.30	-0.09	<b>-0.50</b>	-0.06	1.00		
DOC	0.22	0.09	-0.08	0.20	0.06	0.15	0.19	0.05	0.14	-0.11	0.06	0.11	-0.06	0.25	0.35	1.00	
NO3_w	<b>0.36</b>	0.33	-0.18	0.11	-0.07	-0.15	-0.09	-0.12	-0.08	0.13	-0.04	0.02	-0.04	0.11	-0.21	<b>-0.59</b>	1.00

(b) Stream sediments (n = 16)

	PDR	N2O	Ratio	pH_s	ORP	WC	Sand	Clay	Silt	Corg	Norg	C/N	T_w	pH_w	DOC	NO3_w	Q	Flux
PDR																		
N2O	<b>0.92</b>																	
Ratio	-0.29	-0.17																
pH_s	-0.07	-0.05	-0.01															
ORP	-0.33	-0.19	-0.02	0.28														
WC	<b>0.73</b>	<b>0.70</b>	0.04	-0.28	<b>-0.50</b>													
Sand	-0.14	-0.37	-0.14	-0.34	-0.28	-0.27												
Clay	-0.14	0.07	-0.15	0.37	0.41	-0.09	<b>-0.77</b>											
Silt	0.27	0.47	0.27	0.25	0.15	0.41	<b>-0.93</b>	0.48										
Corg	<b>0.51</b>	0.42	0.12	-0.30	-0.43	<b>0.76</b>	-0.27	-0.20	0.47									
Norg	<b>0.60</b>	<b>0.57</b>	0.06	-0.24	-0.44	<b>0.85</b>	-0.38	-0.04	<b>0.54</b>	<b>0.96</b>								
C/N	0.06	-0.12	0.15	<b>-0.52</b>	-0.22	0.25	0.23	<b>-0.56</b>	0.00	<b>0.65</b>	0.43							
T_w	0.40	0.17	-0.42	-0.04	-0.46	0.22	0.43	-0.40	-0.37	0.22	0.19	0.26						
pH_w	0.19	0.30	0.08	-0.14	0.00	0.16	-0.03	0.18	-0.06	-0.01	0.06	-0.10	-0.02					
DOC	0.42	0.27	-0.20	-0.01	-0.26	0.35	0.05	-0.23	0.06	0.33	0.32	0.29	<b>0.56</b>	0.05				
NO3_w	0.33	0.38	-0.25	0.18	0.06	-0.01	0.11	0.08	-0.19	-0.31	-0.16	<b>-0.60</b>	-0.12	0.15	<b>-0.51</b>			
Q	-0.48	-0.38	0.11	-0.34	0.26	-0.27	0.24	0.13	-0.40	-0.38	-0.40	-0.05	-0.25	<b>0.57</b>	-0.30	0.01		
Flux	-0.46	-0.35	0.14	-0.26	0.21	-0.31	0.28	0.11	-0.45	-0.45	-0.44	-0.18	-0.31	<b>0.58</b>	-0.39	0.19	<b>0.97</b>	

(c) Pond sediments (n = 14)

	PDR	N2O	N2O/PDR	Depth	pH_s	ORP	WC	Clay	Silt	Sand	Corg	Norg	C/N	T_w	pH_w	DOC	NO3_w	Slope	LWRatio	Distance	HRT	
<b>PDR</b>	1.00																					
<b>N2O</b>	<b>0.97</b>	1.00																				
<b>N2O/PDR</b>	-0.02	0.15	1.00																			
<b>Depth</b>	-0.34	-0.23	<b>0.51</b>	1.00																		
<b>pH_s</b>	0.43	<b>0.47</b>	0.22	0.24	1.00																	
<b>ORP</b>	0.26	0.12	-0.19	-0.44	-0.02	1.00																
<b>WC</b>	0.18	0.16	-0.26	-0.40	0.21	0.06	1.00															
<b>Clay</b>	-0.23	-0.14	0.21	0.26	0.40	-0.20	<b>0.54</b>	1.00														
<b>Silt</b>	0.36	0.33	0.07	-0.20	-0.43	0.20	-0.35	<b>-0.85</b>	1.00													
<b>Sand</b>	0.09	-0.02	-0.37	-0.25	-0.31	0.16	<b>-0.57</b>	<b>-0.92</b>	0.57	1.00												
<b>Corg</b>	<b>0.45</b>	0.42	0.05	-0.43	-0.07	0.07	0.02	-0.27	0.40	0.12	1.00											
<b>Norg</b>	<b>0.45</b>	<b>0.45</b>	0.13	-0.34	0.36	0.10	0.41	0.35	-0.13	<b>-0.45</b>	<b>0.69</b>	1.00										
<b>C/N</b>	0.05	-0.01	-0.18	-0.21	<b>-0.54</b>	-0.01	<b>-0.50</b>	<b>-0.83</b>	<b>0.67</b>	<b>0.79</b>	0.43	-0.34	1.00									
<b>T_w</b>	0.13	0.03	<b>-0.54</b>	-0.26	-0.38	0.04	-0.30	<b>-0.72</b>	<b>0.49</b>	<b>0.76</b>	0.03	<b>-0.57</b>	<b>0.78</b>	1.00								
<b>pH_w</b>	0.05	0.09	0.07	0.13	0.15	0.12	0.04	-0.18	0.22	0.12	<b>-0.51</b>	-0.31	-0.25	-0.08	1.00							
<b>DOC</b>	0.00	-0.02	-0.02	0.13	0.16	0.25	-0.02	-0.27	0.11	0.34	<b>-0.61</b>	<b>-0.62</b>	0.01	0.21	<b>0.76</b>	1.00						
<b>NO3_w</b>	0.41	0.39	-0.12	-0.19	0.15	-0.18	-0.20	-0.17	0.16	0.14	<b>0.72</b>	<b>0.49</b>	0.32	0.24	<b>-0.63</b>	<b>-0.72</b>	1.00					
<b>Slope</b>	<b>0.46</b>	<b>0.47</b>	-0.08	-0.03	0.42	-0.08	-0.27	-0.37	0.33	0.33	0.17	0.19	0.05	0.17	0.35	0.02	<b>0.46</b>	1.00				
<b>LWRatio</b>	0.22	0.14	-0.39	-0.31	<b>-0.47</b>	-0.05	-0.06	<b>-0.48</b>	0.44	0.41	0.37	-0.19	<b>0.70</b>	<b>0.77</b>	-0.38	-0.22	<b>0.45</b>	-0.07	1.00			
<b>Distance</b>	0.19	0.20	0.16	-0.13	-0.24	0.08	0.08	-0.22	<b>0.47</b>	-0.01	0.21	0.25	-0.05	-0.21	<b>0.49</b>	0.00	-0.11	0.19	0.08	1.00		
<b>HRT</b>	-0.27	-0.27	-0.13	0.12	-0.19	0.12	0.14	-0.10	0.02	0.13	<b>-0.75</b>	<b>-0.74</b>	-0.05	0.21	<b>0.69</b>	<b>0.86</b>	<b>-0.87</b>	-0.27	-0.10	0.05	1.00	

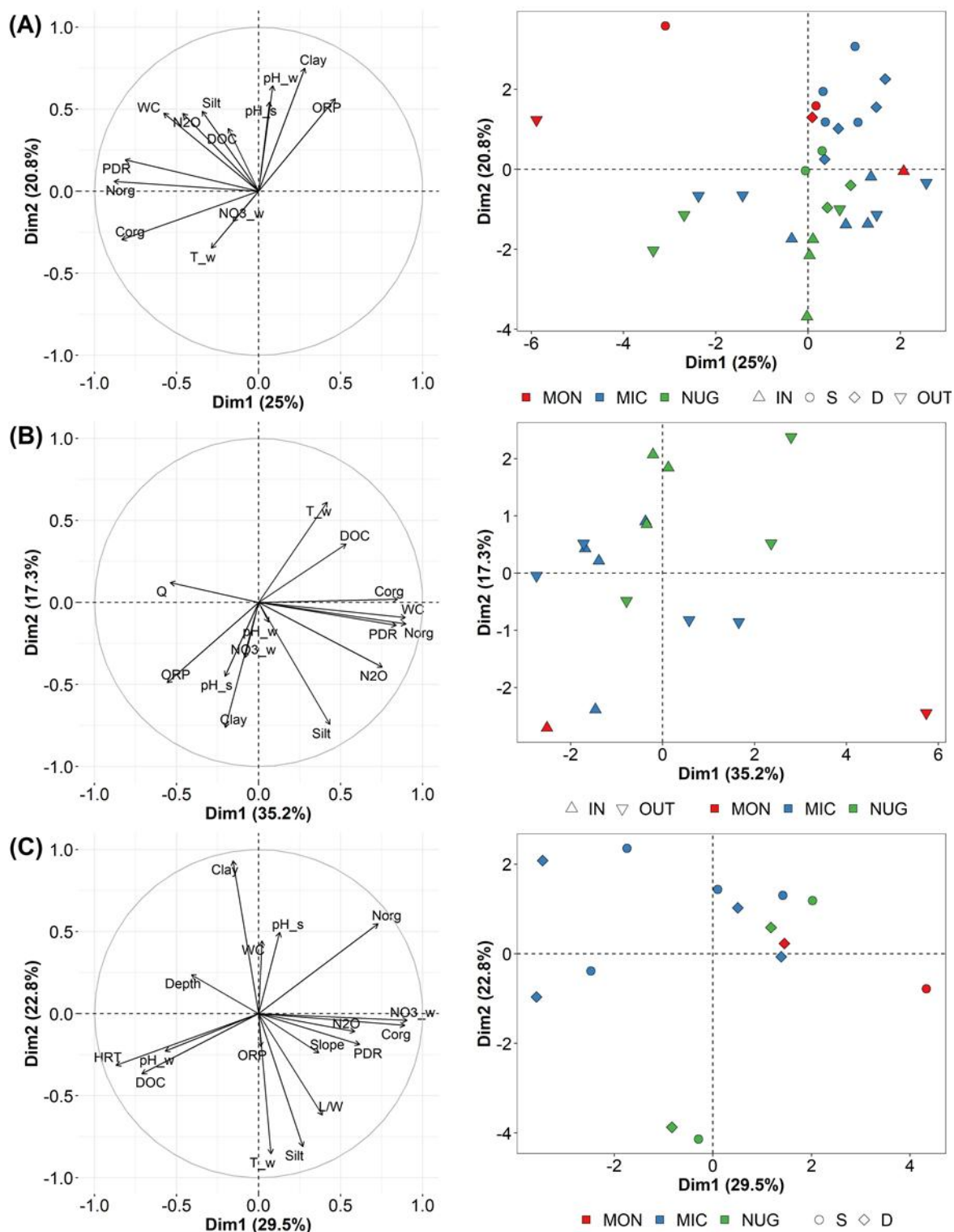


Fig. III-3. Principal component analysis (PCA) combining the first two principal components (PC1 and PC2; variable loadings (left) and individual scores (right)). (A) All sediments; (B) Stream sediments; (C) Pond sediments. For variable names, refer to the legend in Table 3 and for sites refer to Section 2.2. For the individual scores (right column), the color palette distinguishes the catchments, and the sediment types are highlighted by shapes.

### 1.3.1 Principal component analysis (PCA)

#### 1.3.1.1 All sediments

All sediments included both stream and pond sediments considered together. For all sediments, four principal components (PC) explained the majority of the total variance (71.1%). The first two components (PC1 and PC2) were the more explicative ones for the whole data set (25.0% and 20.8% of the total variance, respectively) (Fig. III-3A and Table III-4).

The component 1 was mainly driven by biochemical variables including N<sub>org</sub>, C<sub>org</sub> and PDR (in decreasing order), although to a lesser extent WC also contributed to PC1 (Table III-5). The majority of samples scored positively, while only seven samples scored negatively (the lowest and highest values for MON2-OUT and MIC4-OUT, respectively). The component 2 mostly gathered physicochemical variables such as clay content, water pH, sediment ORP, sediment pH, silt content and WC, in decreasing order. Although N<sub>2</sub>O was associated to this component, the significance of the correlation was much lower compared to the physicochemical variables listed above. Most pond sediments scored positively and stream sediments negatively (except MON2-OUT). MON2-CP-S and NUG1-IN scored the highest and the lowest, respectively. The majority of pond sediments were clustered in Quadrant I, to which water content (-), N<sub>org</sub> (-), and C<sub>org</sub> (-) made the most contribution. In addition, N<sub>2</sub>O was rather strongly associated with PC3 along with NO<sub>3</sub><sup>-</sup> concentration (+) and DOC (-), even if the explained variance (14.1%, Table III-4) for this component was lower than the first two components. MIC1 and MIC4 scored the highest values, while MON2 sediments scored the lowest negative values (see Annex VI). PC4 (11% of the total variance) represented mainly DOC and water temperature.



Table III-4. Eigenvalues and explained variances by the first ten components of PCA: (A) all sediments, (B) stream sediments, and (C) pond sediments.

	(A) All sediments			(B) Stream sediments			(C) Pond sediments		
	Eigenvalue	Variance %	Total Variance%	Eigenvalue	Variance %	Total Variance %	Eigenvalue	Variance %	Total Variance%
Dim.1	3.2	25.0	25.0	4.9	35.2	35.2	5.0	29.5	29.5
Dim.2	2.7	20.8	45.8	2.4	17.3	52.5	3.9	22.8	52.3
Dim.3	1.8	14.1	60.0	1.9	13.5	66.0	2.9	16.9	69.2
Dim.4	1.5	11.2	71.1	1.7	11.9	77.9	1.9	11.4	80.6
Dim.5	1.0	7.9	79.0	1.2	8.7	86.6	1.2	6.8	87.4
Dim.6	0.9	7.2	86.2	0.6	4.6	91.1	0.8	4.6	92.0
Dim.7	0.6	4.4	90.6	0.4	2.9	94.0	0.7	3.9	96.0
Dim.8	0.4	3.1	93.7	0.4	2.7	96.7	0.3	1.6	97.6
Dim.9	0.3	2.6	96.4	0.2	1.5	98.2	0.2	1.3	99.0
Dim.10	0.2	1.6	98.0	0.1	1.0	99.3	0.1	0.6	99.6

Table III-5. Loadings and contributions of variables to the first four components of PCA: (A) all sediments (n = 31), (B) stream sediments (n = 16), and (C) pond sediments (n = 14). R is the loading of a given variable, while % represents its contribution to the components. PDR: potential denitrification rate; N<sub>2</sub>O: N<sub>2</sub>O emission rate; pH<sub>s</sub>: pH in sediment; ORP: oxidation-reduction potential; WC: water content in sediments; C<sub>org</sub>: organic carbon content in sediment; N<sub>org</sub>: organic nitrogen content in sediment; T<sub>w</sub>: water temperature; pH<sub>w</sub>: pH in water; DOC: dissolved organic carbon; NO<sub>3</sub><sub>w</sub>: nitrate concentration in water; Q: discharge; Slope: pond slope; L/W: pond length over width; HRT: hydraulic retention time; Depth: depth of pond.

Variable	(A) All sediments								(B) Stream sediments								(C) Pond sediments							
	PC1		PC2		PC3		PC4		PC1		PC2		PC3		PC4		PC1		PC2		PC3		PC4	
	r	(%)	r	(%)	r	(%)	r	(%)	r	(%)	r	(%)	r	(%)	r	(%)	r	(%)	r	(%)	r	(%)	r	(%)
PDR	<b>-0,8</b>	<b>20,3</b>	0,2	1,4	-0,3	5,4	0,3	6,6	<b>0,8</b>	<b>14,2</b>	-0,1	0,8	0,3	4,1	-0,4	<b>8,3</b>	<b>0,6</b>	<b>7,5</b>	-0,2	0,9	<b>-0,7</b>	<b>15,8</b>	0,1	0,5
N <sub>2</sub> O	-0,5	6,6	0,5	<b>8,3</b>	<b>-0,5</b>	<b>15,0</b>	0,3	6,3	<b>0,8</b>	<b>11,5</b>	-0,4	6,4	0,4	6,6	-0,3	4,2	<b>0,6</b>	6,9	-0,1	0,3	<b>-0,7</b>	<b>16,4</b>	0,0	0,0
pH <sub>s</sub>	0,1	0,1	<b>0,5</b>	<b>11,0</b>	-0,4	7,3	0,1	0,4	-0,2	0,8	-0,4	<b>8,4</b>	-0,4	<b>8,1</b>	<b>-0,5</b>	<b>16,8</b>	0,1	3,3	<b>0,5</b>	<b>6,3</b>	<b>-0,7</b>	<b>15,1</b>	-0,3	<b>26,8</b>
ORP	0,5	6,7	<b>0,6</b>	<b>11,7</b>	-0,1	0,7	0,0	0,1	-0,6	6,3	-0,5	<b>9,9</b>	-0,1	0,4	0,1	0,2	0,0	0,0	-0,2	1,0	-0,3	3,5	<b>0,5</b>	<b>15,2</b>
WC	<b>-0,6</b>	<b>10,3</b>	0,5	<b>8,4</b>	0,2	1,9	-0,2	3,0	<b>0,9</b>	<b>16,2</b>	-0,1	0,3	0,2	1,7	0,2	1,7	0,0	0,0	0,4	5,1	-0,2	2,2	<b>0,7</b>	<b>23,8</b>
Clay	0,3	2,4	<b>0,8</b>	<b>20,8</b>	0,0	0,0	-0,3	<b>8,3</b>	-0,2	0,8	<b>-0,8</b>	<b>24,0</b>	0,0	0,0	0,2	1,5	-0,2	0,5	<b>0,9</b>	<b>22,4</b>	0,0	0,1	0,1	0,6
Silt	-0,3	3,6	0,5	<b>8,8</b>	0,1	0,3	-0,2	2,6	0,4	3,8	<b>-0,7</b>	<b>22,8</b>	-0,4	6,9	0,3	4,0	0,3	1,4	<b>-0,8</b>	<b>16,9</b>	-0,1	0,6	0,0	0,0
Corg	<b>-0,8</b>	<b>21,4</b>	-0,3	3,2	0,2	2,4	-0,3	5,1	<b>0,8</b>	<b>14,5</b>	0,0	0,0	-0,2	1,2	0,4	<b>8,1</b>	<b>0,9</b>	<b>15,8</b>	-0,1	0,1	0,1	0,3	0,1	1,0
Norg	<b>-0,9</b>	<b>23,9</b>	0,1	0,1	0,1	1,1	-0,4	<b>9,7</b>	<b>0,9</b>	<b>16,3</b>	-0,1	0,7	-0,1	0,1	0,3	5,2	<b>0,7</b>	<b>10,6</b>	<b>0,5</b>	<b>7,8</b>	-0,2	1,7	0,2	1,9
T <sub>w</sub>	-0,3	2,6	-0,3	4,4	0,1	0,7	<b>0,7</b>	<b>33,8</b>	0,4	3,5	<b>0,6</b>	<b>15,4</b>	0,0	0,0	-0,4	<b>8,9</b>	0,1	0,1	<b>-0,9</b>	<b>18,8</b>	0,2	1,3	0,0	0,0
pH <sub>w</sub>	0,1	0,2	<b>0,6</b>	<b>15,3</b>	0,2	2,8	0,3	5,1	0,1	0,1	-0,1	0,6	<b>0,8</b>	<b>30,2</b>	0,3	3,9	<b>-0,6</b>	6,5	-0,2	1,3	<b>-0,7</b>	<b>15,6</b>	-0,1	0,3
DOC	-0,2	1,0	0,4	5,4	<b>0,6</b>	<b>20,0</b>	<b>0,5</b>	<b>19,0</b>	<b>0,5</b>	5,8	0,4	5,3	-0,3	3,4	0,0	0,0	<b>-0,7</b>	<b>10,1</b>	-0,4	3,5	<b>-0,5</b>	<b>9,5</b>	0,0	0,1
NO <sub>3</sub> <sub>w</sub>	-0,2	0,8	-0,2	1,3	<b>-0,9</b>	<b>42,2</b>	0,0	0,0	-0,1	0,1	-0,3	4,7	<b>0,6</b>	<b>18,4</b>	<b>-0,6</b>	<b>22,7</b>	<b>0,9</b>	<b>16,3</b>	0,0	0,0	0,2	1,1	-0,3	4,4
Q	(-)	(-)	(-)	(-)	(-)	(-)	(-)	(-)	<b>-0,5</b>	5,9	0,1	0,6	<b>0,6</b>	<b>18,7</b>	0,5	<b>14,5</b>	(-)	(-)	(-)	(-)	(-)	(-)	(-)	(-)
Slope	(-)	(-)	(-)	(-)	(-)	(-)	(-)	(-)	(-)	(-)	(-)	(-)	(-)	(-)	(-)	(-)	0,4	2,7	-0,2	1,5	<b>-0,5</b>	<b>9,8</b>	<b>-0,5</b>	<b>15,3</b>
L/W	(-)	(-)	(-)	(-)	(-)	(-)	(-)	(-)	(-)	(-)	(-)	(-)	(-)	(-)	(-)	(-)	0,4	3,0	<b>-0,6</b>	<b>9,9</b>	0,4	5,1	0,2	2,0
HRT	(-)	(-)	(-)	(-)	(-)	(-)	(-)	(-)	(-)	(-)	(-)	(-)	(-)	(-)	(-)	(-)	<b>-0,9</b>	<b>15,0</b>	-0,3	2,6	-0,2	1,7	0,2	2,8
Depth	(-)	(-)	(-)	(-)	(-)	(-)	(-)	(-)	(-)	(-)	(-)	(-)	(-)	(-)	(-)	(-)	-0,4	0,3	0,2	1,5	0,1	0,3	<b>-0,7</b>	5,2

### 1.3.1.2 Stream sediments

In the PCA for stream sediments (Fig. III-3B), four principal components (PCs) explained the majority of the total variance (77.9%, Table III-4B), with PC1 and PC2 as the most explicative ones (35.2 and 17.3%, respectively, Fig. III-3B). As for all sediments, the same variables including N<sub>2</sub>O mostly contributed positively to PC1 (Fig. III-3A) and to PC2 (except N<sub>2</sub>O, pH and WC). They were negatively related to PC2, while T<sub>w</sub> was positively related (Fig. III-3B and Table III-5). The majority of samples were clustered negatively in PC1 (Fig. III-3B right), whereas four samples were positively scattered (MIC1-OUT, NUG1-OUT, NUG4-OUT, and particularly MON2-OUT). Except for six samples, most individuals were in the positive sector of axis 2, with the highest scores for NUG1-IN, NUG4-IN and particularly NUG4-OUT, and the lowest ones for MON2-IN, MON2-OUT and MIC1-IN. Components 3 and 4 (13.5 and 11.9% of the variance, respectively) were mainly explained by discharge, NO<sub>3</sub><sup>-</sup>, and pH of water and sediment. PDR was partially associated with PC4, in an opposite position to discharge (Table III-4 and Table III-5), and it mainly discriminated the sediments in MIC and NUG (highest value in MIC1-OUT and lowest negative value in NUG1-IN, Annex VI).

### 1.3.1.3 Pond sediments

The first four components reached a higher score of 80.6% of the total variance (Table III-4 and Fig. III-3C). with 29.5 and 22.8% explained by PC1 and PC2, respectively. PC1 was mostly contributed by water NO<sub>3</sub><sup>-</sup>, C<sub>org</sub>, HRT, N<sub>org</sub> and DOC and secondarily by PDR and N<sub>2</sub>O in a decreasing order (Table III-5), with only HRT and DOC negatively related (Table III-5 and Fig. III-3C). PC2 was mainly positively composed of clay content and, negatively related, to water temperature, silt content, and L/W (length/width of a pond) in decreasing order (Table III-5). Sediments from three high-HRT ponds (MIC1, MIC4, and NUG3) scored negatively along PC1, with the highest score for MON2-CP-S. Among them, the highest and the lowest scores were for MIC1 and NUG3 in PC2, respectively. Other sediments were clustered in Quadrant I and close to the center. One can observe that except for MIC4, surface layers of pond sediments were more linked to the axis PC1 or PC2 than to deeper ones. Despite PC3 explained a lower variance score than the two first components (17%), PDR, N<sub>2</sub>O, and pH of sediment and water, as well as the pond slope and to a lesser extent DOC, were well represented

by this axis. Finally, ORP was linked to axis 4 (11% of the variance) with sediment pH, water content, and pond slope.

### 1.3.2 Relationship between PDR and N<sub>2</sub>O emission rate

N<sub>2</sub>O emission rate was positively related to  $\log_{10}$  PDR ( $N_2O = (\log_{10} \text{PDR} + 1.98) / 482$ ,  $R^2 = 0.64$ ,  $p < 0.0001$ ,  $n = 36$ ; Fig. III-4), considering all sediments together if the nine labelled sediments with high N<sub>2</sub>O were not taken into consideration. These nine samples were out of the linear relationship with higher N<sub>2</sub>O emission rate compared to the dotted linear regression line, particularly for MON2. If NUG is separated from MON + MIC (the two closest catchments with the highest slope), the relationships are different: a linear type (dashed line) for the former and an exponential type for the latter group (solid line) (Fig. III-4; see the respective equations in the legend).

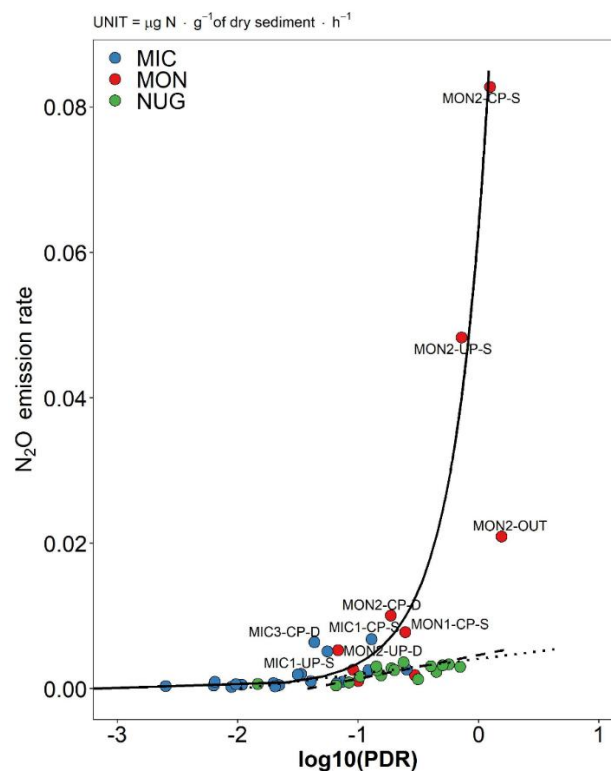


Fig. III-4. Relationship between N<sub>2</sub>O emission rate and  $\log_{10}$  potential denitrification rate (PDR) in stream and pond sediments from the three catchments. (1) the dotted line: the general pattern without the nine labelled outliers ( $N_2O = (\log_{10} \text{PDR} + 1.98) / 482$ ,  $R^2 = 0.64$ ,  $p < 0.0001$ ,  $n = 36$ ); (2) the dashed line: NUG sediments ( $N_2O = (\log_{10} \text{PDR} + 1.42) / 303.3$ ,  $R^2 = 0.53$ ,  $p < 0.001$ ,  $n = 16$ ); (3) the solid line: MON + MIC ( $N_2O = -0.0954 \sqrt{(3.14 - \log_{10} \text{PDR}) / 2.41}$ ,  $R^2 = 0.71$ ,  $p < 0.0001$ ,  $n = 29$ ).

### 1.4 qPCR assay for denitrification genes in pond sediments

Among the 12 sediments selected from the five ponds, the copy numbers of the *16S rRNA* gene had a mean value of  $5.83 \times 10^{10} \pm 2.46 \times 10^{10}$  copies g<sup>-1</sup> dry sediment, from  $2.63 \times 10^{10}$  (MIC1-UP-S) to  $1.14 \times 10^{11}$  (NUG1-CP-S) (Table III-6). Three denitrifier genes (*nirK*, *nirS*, and *nosZ*) were detected in all analyzed samples (Table III-6 and Fig. III-5A), but with significantly different abundances from each other ( $p < 0.01$ , Fig. III-5B). Generally, *nosZ* was the most abundant gene and represented a ratio of *nosZ* to *16S rRNA* of  $21.5 \pm 8.8\%$  followed by *nirS* ( $11.5 \pm 3.4\%$ ) and *nirK* ( $2.4 \pm 0.5\%$ ) (Table III-6). In the deeper layer of NUG3 (the only deeper layer of pond sediment analyzed for genes), the denitrifier abundances were lower in absolute values as well as relative to the whole gene abundances (Fig. III-5C).

Table III-6. Gene abundances and their percentages in the selected ponds. Values from 12 samples and the descriptive statistics are listed.

Sample	Abundance (copy numbers per gram of dry sediment)				Ratio				
	<i>16S rRNA</i>	<i>nirK</i>	<i>nirS</i>	<i>nosZ</i>	<i>nirK/16S rRNA</i>	<i>nirS/16S rRNA</i>	<i>nosZ/16S rRNA</i>	<i>nirK/nirS</i>	
MON2-UP-S	5.11E+10	1.18E+09	5.49E+09	6.16E+09		2.4	10.7	12.0	22.5
MON2-CP-S	4.26E+10	1.01E+09	7.26E+09	5.04E+09		2.4	17.0	11.8	13.9
MON2-LP-S	7.84E+10	1.48E+09	7.58E+09	7.40E+09		1.9	9.8	11.0	18.8
MIC1-UP-S	2.63E+10	9.10E+08	3.58E+09	6.40E+09		3.1	12.2	23.6	25.3
MIC1-CP-S	7.20E+10	2.00E+09	7.12E+09	1.23E+10		2.8	10.2	17.8	28.2
MIC1-LP-S	5.74E+10	1.26E+09	9.19E+09	1.75E+10		2.6	16.6	29.8	13.2
NUG1-CP-S	1.14E+11	1.82E+09	6.63E+09	1.58E+10		1.6	6.0	13.7	26.8
NUG2-UP-S	7.22E+10	1.74E+09	1.04E+10	1.60E+10		2.8	15.4	25.6	17.7
NUG2-LP-S	5.60E+10	1.34E+09	5.53E+09	1.26E+10		2.4	10.1	22.7	24.4
NUG3-CP-S	6.61E+10	1.92E+09	8.56E+09	2.71E+10		3.0	12.4	40.4	24.9
NUG3-CP-D	3.54E+10	7.10E+08	3.02E+09	7.05E+09		2.2	9.5	23.3	23.6
NUG3-LP-S	2.85E+10	5.72E+08	2.34E+09	7.50E+09		2.1	8.0	26.8	22.6
min	2.63E+10	5.72E+08	2.34E+09	5.04E+09		1.6	6.0	11.0	13.2
max	1.14E+11	2.00E+09	1.04E+10	2.71E+10		3.1	17.0	40.4	28.2
mean	5.83E+10	1.33E+09	6.39E+09	1.17E+10		2.4	11.5	21.5	21.8
sd	2.46E+10	4.76E+08	2.50E+09	6.52E+09		0.5	3.4	8.8	4.9

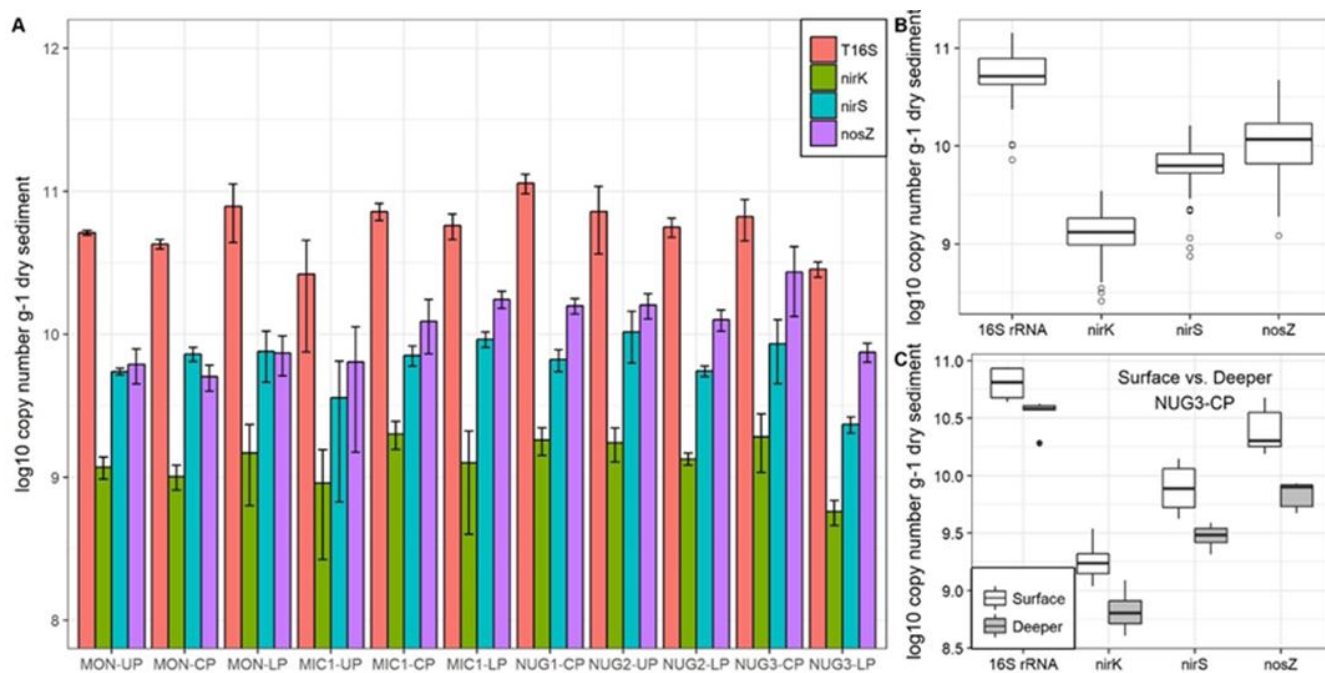


Fig. III-5. Gene abundances (A) and differences between genes (B) and different sediment layers (C).

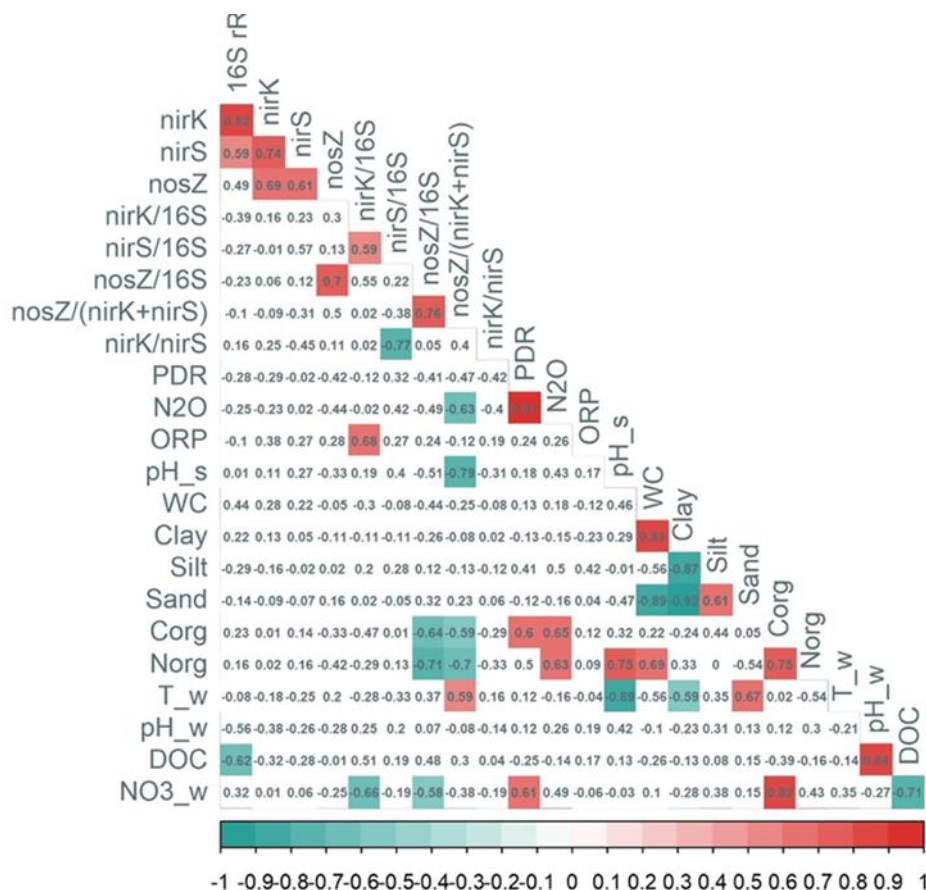


Fig. III-6. Relationships among gene properties, denitrification rates, and water/sediment characteristics. Red block indicates a significant positive relationship while green block indicates a significant negative one ( $p < 0.05$ ).

A two-by-two Pearson's correlation matrix was performed (Fig. III-6) since the limited number of samples investigated for microbiological analysis did not allow a strong multivariate analysis, as done above with PCA. PDR was related to  $N_2O$ ,  $C_{org}$ , and  $NO_3^-$  in waters (Fig. III-6) consistently with the results above, but considering this dataset, no significant relationship with the abundance of each denitrifier (Fig. III-6).

The four gene abundances were positively related to each other with the exception of *nosZ* and *16S rRNA* ( $p < 0.05$ , Fig. III-6). Only 16S rRNA was significantly related to water DOC ( $r = -0.62$ ,  $p < 0.05$ , Fig. III-6). The ratio of *nirK* to *16S rRNA* was positively related to *nirS/16S rRNA* and sediment ORP and was negatively associated with water  $NO_3^-$  concentration ( $p < 0.05$ , Fig. III-6).

### 1.5 Multilinear regression model for PDR

To ensure a potential prediction of the spatial variability of PDR in response to physicochemical and environmental variables, multiple linear regressions (MLRs) were applied to the potential denitrification rate (PDR) as the dependent variable in stream sediments and ponds considered separately. Only physicochemical and environmental variables were considered in the multilinear regressions since water, sediment, and geomorphological characteristics could be better predictors of the denitrification rate than the denitrifier properties (Fig. III-6). Indeed, the smaller number of data for the denitrifiers would weaken the model prediction. We also considered empirical models for easy-to-measure variables that are applicable for pond management and  $NO_3^-$  water quality control by stakeholders or local pond managers. It should be noticed that we used the entire dataset to setup the empirical model instead of using a training dataset (e.g., 70-75% of the dataset) since the dataset was not big enough to support the training/testing strategy. It should be improved the scale of the dataset in the further studies.

Preliminary models including all variables were able to explain 89% of the variance of PDR in stream sediments and 91% of the variance of PDR in pond sediments, respectively (Table III-7). Although these preliminary models could explain a high percentage of variance of PDR, they could not be adopted since a few independent variables were unrelated or weakly

related to  $\log(\text{PDR})$ , and multicollinearity may still exist, which means the information provided by one variable may be explained by other collinear variables that make the model redundant. Hence, the all-subsets regression method was applied to construct the best model with non-redundant variables and a high percentage of the variance of dependent variables. The results of all subset's regressions are shown in Fig. III-7.

Table III-7. Multiple linear regression results for PDR. “Preliminary” indicates the consideration of all variables and “Updated” indicates the variables selected by the all-subsets regression method; ORP: Oxidation-Reduction Potential; Depth: Depth of the pond; Tw: Temperature of the water; DOC: Dissolved Organic Carbon; HRT: Hydraulic Retention Time (days); Dist: Distance to stream source; with \*  $p < 0.1$ ; \*\*  $p < 0.05$ ; \*\*\*  $p < 0.01$ .

Variable	Stream Sediment		Pond Sediment		
	log (PDR)		log (PDR)		
	Preliminary	Updated	Preliminary	Updated 1	Updated 2
pH	-2.28	-2.819**	1.092		
ORP (mV)	0.002		0.003	0.005**	0.007**
Depth (cm)			-0.083**	-0.064**	-0.090***
Water content (%)	-0.001		0.006	0.010*	
Clay content (%)	0.195	0.148**	0.065		0.026
Silt content (%)	-0.065		0.099		
Organic carbon content (%)	0.451		-0.222		
Tw (°C)	0.342	0.487**	0.727**	0.417***	0.210**
DOC (mg L <sup>-1</sup> )	1.161	0.809**	1.816**	1.224***	0.518*
NO <sub>3</sub> <sup>-</sup> (mg L <sup>-1</sup> )	0.06	0.060***	-0.008		0.049***
Discharge (L s <sup>-1</sup> )	0.441				
Slope (%)			-0.219		
HRT (d)			-0.003***	-0.002***	
Dist (m)	-0.002	-0.001***	0.001*		
Constant	4.034	4.887*	-30.291**	-10.637***	-8.373***
Number of observations	16	16	28	28	28
R <sup>2</sup>	0.89	0.86	0.91	0.86	0.79
Adjusted R <sup>2</sup>	0.58	0.76	0.83	0.83	0.73
p value	0.16	0.002		<0.001	<0.001

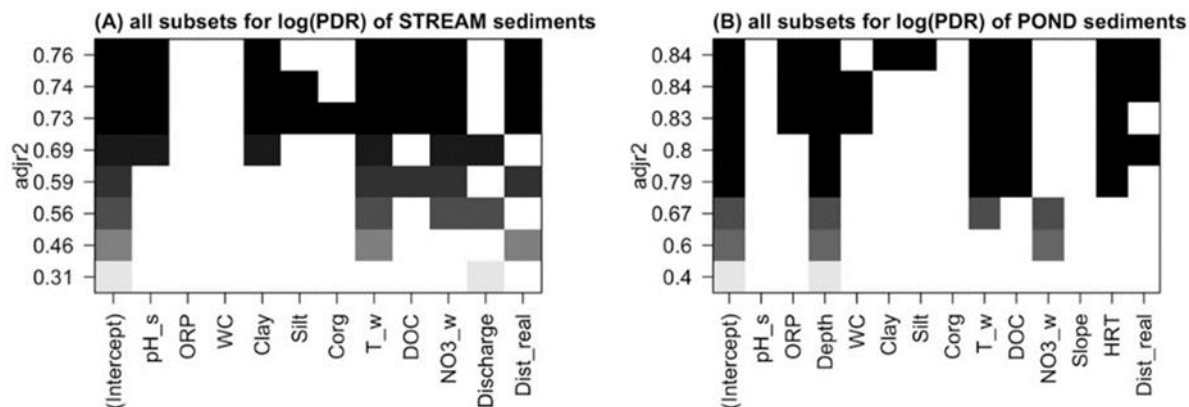


Fig. III-7. All subsets regression for (A) stream sediments; (B) pond sediments. The grey-scaled color indicates the level of adjusted  $R^2$  with different combinations of various variables.

Finally, the predictive models for stream and pond sediments, respectively, were listed below.

- For stream sediments:

$$\log(PDR) = -2.819 \text{ pH}_s + 0.148 \text{ Clay} + 0.487 \text{ Tw} + 0.809 \text{ DOC} + 0.060 \text{ NO}_3\text{-w} - 0.001 \text{ Dist} + 4.887 \quad (\text{Eq. III-1})$$

with  $p = 0.002$ ,  $R^2 = 0.86$ , adjusted  $R^2 = 0.76$ ,  $n=16$  (see Table III-7 for units).

- For pond sediments, two predictive models were proposed:

$$(1) \log(PDR) = 0.005 \text{ ORP} - 0.064 \text{ Depth} + 0.010 \text{ WC} + 0.417 \text{ Tw} + 1.224 \text{ DOC} - 0.002 \text{ HRT} - 10.637 \quad (\text{Eq. III-2})$$

with  $p < 0.001$ ,  $R^2 = 0.86$ , adjusted  $R^2 = 0.83$ ,  $n=28$  (see Table III-7 for units).

$$(2) \log(PDR) = 0.007 \text{ ORP} - 0.090 \text{ Depth} + 0.026 \text{ Clay} + 0.210 \text{ Tw} + 0.518 \text{ DOC} - 0.049 \text{ NO}_3\text{-w} - 8.373 \quad (\text{Eq. III-3})$$

with  $p < 0.01$ ,  $R^2 = 0.79$ , adjusted  $R^2 = 0.73$ ,  $n=28$  (see Table III-7 for units).

The agreement between measured and predicted values shown in Fig. III-8 indicated that the proposed predictive models had the ability to calculate the actual PDR values in sediment using a few sets of physicochemical and environmental variables. For ponds, the first model (Eq. III-2) showed better regression results ( $R^2$  and adjusted  $R^2$ ) than the second one (Eq. III-



3). However, HRT and WC (Eq. III-2) were less accessible data for investigations and applied procedures, and thus the second one (Eq. III-3), involving more commonly measured data, was also proposed.

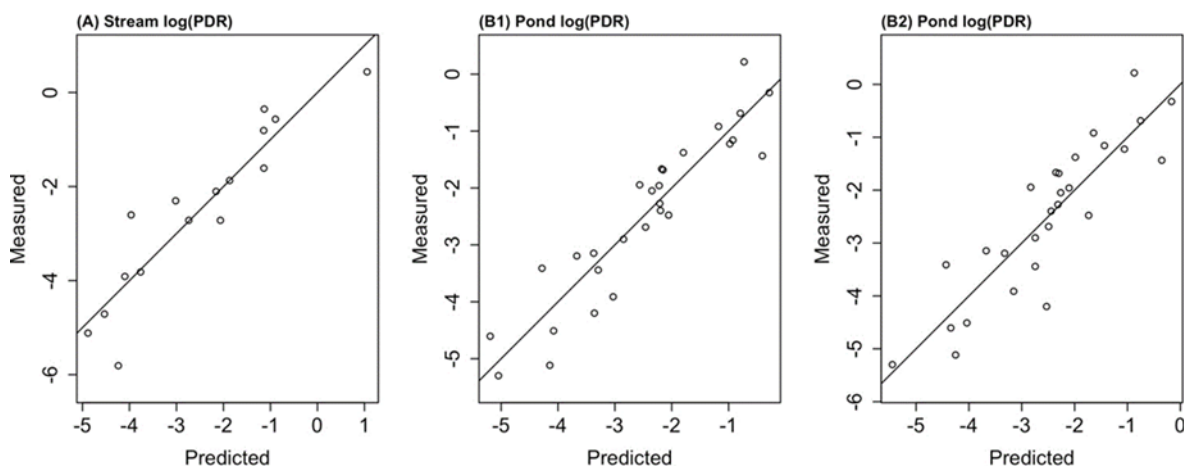


Fig. III-8. Measured vs. predicted PDR values according to the multiple linear regression model. A: stream sediments; B1 and B2: pond sediments.

## 2. Discussion

### 2.1 PDR magnitude and spatial variation

PDR values exhibited a wide range and were one order of magnitude greater than the values of groundwater sediments in the Garonne river, which is the large drainage basin of the area considered (Bernard-Jannin et al., 2017). The observed spatial heterogeneity (Fig. III-2A) between and within the three closely adjacent catchments is consistent with the non-uniformity observed in the groundwater sediment in the Garonne River and stream sediments in the Seine River (Bernard-Jannin et al., 2017; Garnier et al., 2010, respectively). Higher PDR values were observed for upper ponds in two catchments (MON and NUG), which behaved similarly, while PDR was very low in the third one (MIC), the ponds having lower PDR than draining streams and a higher PDR at the pond surface than at depth. This heterogeneity could be attributed to the influence of some key factors related to the physicochemical characteristics of waters and sediments, such as the organic matter content (Greblinas and Perry, 2016) and other

physicochemical factors discussed below (see next Section, Burgin and Hamilton, 2007; Sagggar et al., 2013).

Indeed, this was observed in a period (March) where PDR was supposed to be at lower values compared to the hot season (Birgand et al., 2007) since PDR could vary in time. The results are thus supposed to represent lowered denitrification conditions (Song et al., 2012). One must notice that various methods have been developed to measure the denitrification rate, which may contribute to the difficulty in comparing denitrification rates between different studies (Groffman et al., 2006; Garnier et al., 2010), and currently Almaraz et al. (2020) recommended a standardization of protocols by creating the Global Denitrification Research Network (GDRN). The present study evaluated PDR considering non-limited  $\text{NO}_3^-$  and carbon supply to sediment core samples that could reflect the potential capacity of the denitrification process under optimized conditions (Iribar et al., 2008). However, according to some authors (Seitzinger et al., 1993), the acetylene technique may only measure approximately 50% of the denitrification due to nitrate from the overlying water. Our data could thus be underestimated. However, Well et al. (2003) mentioned that the denitrification rates obtained using  $^{15}\text{N}$  *in situ* and using the  $\text{C}_2\text{H}_2$  technique in the laboratory were in the same range. These authors thus recommended measuring denitrification in the lab for large-scale investigations because of the easier application of the protocol. This gave us confidence in the PDR estimation as a comparative point of view at our studied scale and in its ability to be related to the environmental factors. Nevertheless, we only compared our data with the literature using a similar protocol.

## 2.2 Controlling factors of PDR

Considering all sediments from the three catchments, each factor taken alone was not able to explain PDR with a strong power (as expressed by the Pearson correlation matrix, Table III-3). Nevertheless, some key factors such as the sediment water content (WC), the organic carbon content ( $\text{C}_{\text{org}}$ ), and the  $\text{NO}_3^-$  concentration in overlying water columns were highlighted, as indicated by the positive significant correlation coefficients with PDR (Table III-3). Indeed, sediment  $\text{C}_{\text{org}}$  was considered as the “fuel” for denitrification (Birgand et al., 2007) and was not only the carbon source for denitrifiers (García-ruiz et al., 1998) but also a proxy for

denitrifier biomass (Iribar et al., 2008). Meanwhile, PDR was associated with WC and ORP positively and negatively, respectively, which indicated that high WC could inhibit the O<sub>2</sub> diffusion in sediment particle pores, and thus providing a desirable anaerobic environment for denitrification. The similar observation for WC and PDR has been reported by other studies (García-ruiz et al., 1998; Attard et al., 2011; Saggar et al., 2013). Moreover, hotspots of denitrification were observed in upstream ponds with high water NO<sub>3</sub><sup>-</sup> and sediment C<sub>org</sub> (MON2-OUT and NUG1-OUT; Fig. III-2). This was also consistent with the lower PDR values associated with lower sediment C<sub>org</sub> and NO<sub>3</sub><sup>-</sup> concentration in waters (as observed in the MIC catchment). The weak positive relationship between water NO<sub>3</sub><sup>-</sup> and PDR might indicate that in stream sediments, water NO<sub>3</sub><sup>-</sup> was not a very limiting factor controlling denitrification since NO<sub>3</sub><sup>-</sup> could be supplied continuously by the stream flow (Table III-5) in this agricultural context. This observation was similar to that of Oehler et al. (2007) in an agricultural catchment in Brittany with heavy N loads. Meanwhile, the discharge could also play an important role by controlling the sediment texture and consequently C<sub>org</sub> (Luo et al., 2012). A fast discharge might have washed away fine fractions in sediments, contributing to a decrease of the C<sub>org</sub> content (Fig. III-3B) and leading to a stronger dilution and a reduced PDR (see Mican catchment with higher discharge, PC1, Fig. III-3B and Table III-5B). This was more particularly evidenced in MIC4-OUT, which showed a relatively low clay content and C<sub>org</sub> with the highest discharge. Indeed, the texture in stream sediments was coarser and more heterogeneous than in pond sediments (Table III-2).

A specific discussion is needed for ponds. Similar explanatory variables as for stream sediments were involved in the PDR explanation for PC 1 and 2, but some specific parameters like HRT and pond slope directly influence the PDR of pond sediments. The highest PDR was related with the lowest HRT and the highest pond slope (PC1 and PC3, Fig. III-3 and Table III-5). Indeed, these variables could indirectly affect C<sub>org</sub> and NO<sub>3</sub><sup>-</sup>. A long HRT meant a more stagnant hydrologic condition that could inhibit the supplementation of NO<sub>3</sub><sup>-</sup>. The denitrifiers could only utilize the limited NO<sub>3</sub><sup>-</sup> and C<sub>org</sub> to run the denitrification process, as also indicated by the positive link between DOC and 16 *rRNA* gene. Because the nutrients continued to be consumed, the denitrification process in a long-HRT pond would be less active. Nevertheless, the PDR rate in NUG3 (one of the ponds with the longest HRT) was still higher than in other

long-HRT ponds (MIC1 and MIC4). Contrary to other ponds, the large amount of leaf debris in the bottom of pond NUG3 could act as an additional carbon source for the denitrification process (Hang et al., 2016). The denitrifiers in MIC1-UP and NUG3-LP (two long-HRT ponds) were the least abundant compared to other analyzed short-HRT ponds (Table III-6), which also reflected the importance of HRT in the denitrification process of pond sediments. However, the absence of a significant relationship between the abundance of denitrifiers and PDR did mean that they might be inactive during the rather low-temperature conditions of the study (Shrewsbury et al., 2016). In addition, the sediment dredging managed by the farmers might have influenced the denitrification process. The denitrification rate would be decreased after the dredging activity due to the removal of surface sediments enriched with denitrifiers and organic carbon (Smith and Pappas, 2007). However, MON2, which was dredged recently in 2015, still possessed a high denitrification rate. Its upper position in the catchment, the high erosion rate in the surrounding cultivated parcels, and its small scale and elongated shape along the stream connection have led to a quick sediment accumulation (Wu and Probst, 2021). With the supply of water  $\text{NO}_3^-$  due to close connection to soil water drainage and low HRT, a preferable denitrification environment could thus be generated soon for the growth of denitrifiers. In MIC3, which has not been dredged in the last three decades, the sediment has accumulated, leading to a shallow water depth, low HRT, and a favorable environment for denitrifiers. Therefore, the denitrification rate was the highest in MIC3 in the Mican catchment. As a result, the dredging activity should be well considered in relation to other environmental conditions.

The higher PDR rates observed in surface layers of pond sediments compared to the deeper layers, were in agreement with previous studies (F. Li et al., 2010). Although the deeper layer sediment had a more reduced and anoxic condition than surface layer sediment, which should favor the denitrification process (Burgin et al., 2010), the lower  $\text{C}_{\text{org}}$  and available  $\text{NO}_3^-$  limited the denitrification process in the deeper layers of sediments. The qPCR results (Table III-6) consistently showed that the denitrifier abundances were lower in the deeper layer of NUG3. Although no direct relationships were found between the denitrification rates and the denitrifier abundances, the strong association between water  $\text{NO}_3^-$  concentration and *nirK/16S rRNA* potentially highlighted the function of denitrifiers, especially for *nirK*, in mitigating the

water  $\text{NO}_3^-$  as part of the denitrifying activity.

### 2.3 Predictive models and interest from a management perspective

In such agricultural contexts, the evaluation of key explanatory factors is important to quantify and allow a good prediction of PDR on the basis of accessible parameters.

The empirical models concerning stream (Eq. III-1) and pond (Eq. III-2 and Eq. III-3) sediments have shown the importance of nutrients and some physicochemical characteristics to predict PDR in a convergent way. These parameters (*i.e.*, water  $\text{NO}_3^-$ , water temperature, water DOC, *etc.*) are known in the literature to explain PDR (García-ruiz et al., 1998; Song et al., 2012), but few studies have considered the complexity of streams and ponds taken together (Attard et al., 2011; Tuttle et al., 2014). In flowing water conditions (stream sediments, Eq. III-1), the model highlighted the importance of environmental factors such as the discharge (*i.e.*, regulated by the distance to stream source) as a key parameter influencing sediment pH and the clay component. On the contrary, in pond sediments where water was more stagnant, suitable anaerobic sediment conditions and HRT were prevalent factors (Eq. III-2 and Eq. III-3, Li and Irvin, 2007; Vymazal, 2017). The predictive models could thus identify the denitrification hotspots in both stream and pond sediments.

In a context of climate and land cover changes, the water demand in cultivated areas will probably be more and more important. Stakeholders and farmers had in mind that water storage in ponds in upstream catchments might be an interesting local solution. However, they might have potential negative influences on the water cycle (increased evaporation for example), water transfer downstream, and other ecological impacts. One major environmental issue was related to the greenhouse gas emissions such as  $\text{N}_2\text{O}$  when the denitrification process was not complete (Beaulieu et al., 2011). Indeed, the PDR/ $\text{N}_2\text{O}$  pattern (Fig. III-4) depended on the catchment characteristics (linear or exponential), with some PDR saturation limit (MON) and outlier ponds having high  $\text{N}_2\text{O}$  emission (MON and MIC). The upstream position of ponds with high  $\text{NO}_3^-$  loads might thus contribute to greenhouse gas emissions in some cases.

The interest of our detailed area investigations was that a set of field conditions in the same region was considered at a given time. Even if some previous studies found beneficial to consider only one short-period sampling in an extensive area rather than a small site under

long-term monitoring as well (García-ruiz et al., 1998), one must be cautious of the study limitations.

Moreover, since denitrification might vary temporally (Chen et al., 2014), samples could thus be representative only for lower values in seasonal spring conditions. Additional campaigns in contrasting seasonal conditions would thus be advantageous at least regarding the importance of the N<sub>2</sub>O emissions (which are more erratic to evaluate, Well et al., 2003), which could be constrained using additional *in situ* measurements of atmospheric N<sub>2</sub>O at the pond surface. Finally, these management tools must also be combined with better agricultural practices in the drainage catchments. Among them, the limitation of fertilizer inputs and/or the choice of periods of spreading, the location of strip bands along the streams and a land sharing/landscaping approach were shown to reduce nitrogen inputs and/or improve surface water quality in the area regarding nitrates (Ferrant et al., 2011; Casal et al., 2019; Ponnou-Delaffon et al., 2020).

## **Part II. Nitrate behavior and the role of ponds**

## 1. Results

### 1.1 NO<sub>3</sub><sup>-</sup> concentration, discharge, and NO<sub>3</sub><sup>-</sup> flux patterns

The NO<sub>3</sub><sup>-</sup> concentration patterns differed between MIC and NUG (Fig. III-9). This pattern decreased significantly and regularly from upstream to downstream (60.6 to 11.4 and 60.9 to 19.6 mg L<sup>-1</sup> in 2016 and 2018, respectively), whereas in MIC, though the overall patterns were in two campaigns were alike, NO<sub>3</sub><sup>-</sup> concentrations in upstream and downstream differ and the pattern was not regularly decreasing. In 2016, NO<sub>3</sub><sup>-</sup> concentrations in MIC1 (IN) and MIC4 (OUT) were similar (31.8 and 31.2 mg L<sup>-1</sup>, respectively), while in 2018, NO<sub>3</sub><sup>-</sup> concentration in MIC1 (IN) (52.4) was three times that in MIC4 (OUT) (17.4 mg L<sup>-1</sup>). After MIC1, NO<sub>3</sub><sup>-</sup> strongly decreased. Between MIC1 (OUT) and the Auradé village, NO<sub>3</sub><sup>-</sup> increased again to a highest value. After the village, it decreased regularly to the catchment outlet. Note that in the first campaign the site upstream the village was not sampled and that in NUG the NO<sub>3</sub><sup>-</sup> decrease was lower, particularly at the step of NUG2 and NUG3 than in 2016.

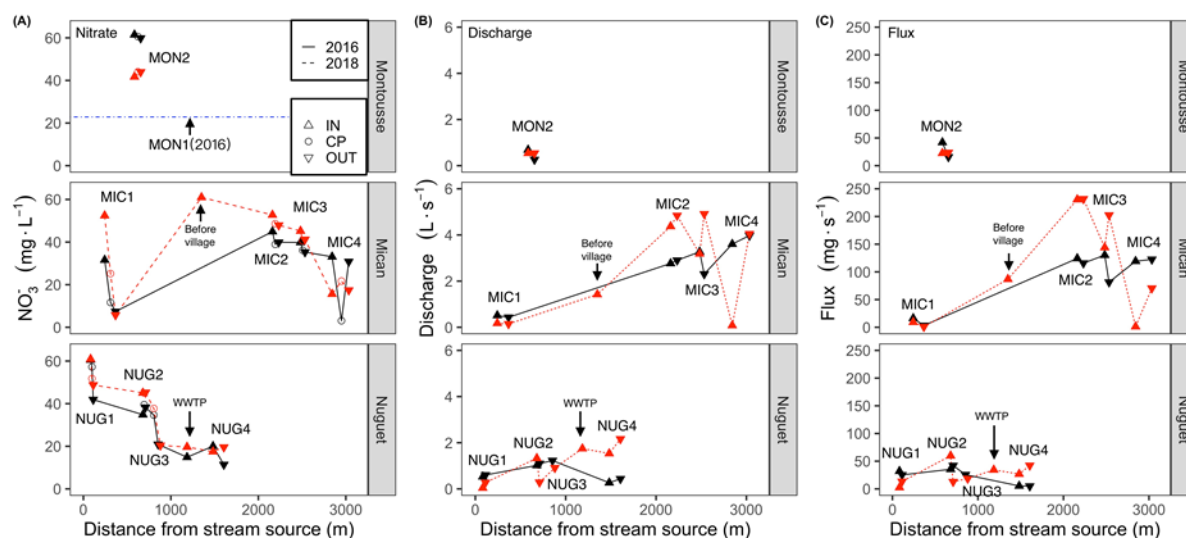


Fig. III-9. NO<sub>3</sub><sup>-</sup> concentration (A), discharge (B), and NO<sub>3</sub><sup>-</sup> flux (C) along the stream from the inlet of the first pond to the outlet of the last pond in each catchment for the two sampling campaigns (2016 in black solid line and 2018 in red dashed line). IN: inlet of pond; CP: center of pond; OUT: outlet of pond; WWTP: wastewater treatment plant. The blue dot-dashed line indicates the NO<sub>3</sub><sup>-</sup> concentration in MON1 in 2016, in 2018 the pond was dry.

In 2016, MIC4 (CP) exhibited the lowest NO<sub>3</sub><sup>-</sup> concentration 3.07 mg L<sup>-1</sup>, whereas the



stream inlet of MON2 (IN) and NUG1 (IN) has the highest values (61.46 and 60.56 mg L<sup>-1</sup>, respectively). The isolated pond in MON catchment (MON1), NO<sub>3</sub><sup>-</sup> was 22.9 mg L<sup>-1</sup>. In 2018 campaign, the highest NO<sub>3</sub><sup>-</sup> concentration was detected before the Mican village (61.0 mg L<sup>-1</sup>). The NO<sub>3</sub><sup>-</sup> concentration in MIC1 (IN) and NUG1 (IN) was 52.4 and 60.9 mg L<sup>-1</sup>, respectively. Regarding inlet and outlet of single ponds, a similar decreasing trend was observed in MIC and NUG for the two campaigns, with exception of MIC4 and NUG4 in 2018, respectively.

Considering the distance from the stream sources, the discharge pattern in MIC and NUG behaved similarly (from 0.51 to 3.97 L s<sup>-1</sup> in 2016 and 0.17 to 4.05 L s<sup>-1</sup> in 2018, and 0.153 to 0.27 L s<sup>-1</sup> in 2016 and 0.04 to 2.184 L s<sup>-1</sup> in 2018, respectively, from inlet to outlet of the catchments, Fig. III-9B). After 1.6 km, the discharge in MIC continue to increase regarding the size of the catchment. In MIC, the discharge pattern was more variable for the 2018 campaign. It varied similarly in MIC before the Auradé village; in 2018, a significant increase was observed in MIC2 and a strong decrease in MIC4, whereas in 2016 only a decrease was observed in MIC3. For NUG, the discharge decreased after MIC3 outlet in 2016, whereas it only dropped at NUG2 outlet, before increasing again. The NO<sub>3</sub><sup>-</sup> flux showed a similar pattern with the discharge in each catchment, respectively (Fig. III-9C).

## 1.2 Stable isotopes

Two stable isotopes (<sup>2</sup>H and <sup>18</sup>O) in water samples of two sampling campaigns were analyzed (Fig. III-10 with the labels of the two large ponds, MIC1 and MIC4). δ<sup>2</sup>H ranged from -46.24 (MIC4-OUT) to -18.34‰ (MIC4-CP) in 2016, and from -42.62 (MIC4-IN) to -15.52‰ (MIC1-OUT) in 2018, respectively. No statistical difference of δ<sup>2</sup>H was observed between the two sampling campaigns. For δ<sup>18</sup>O, it varied from -6.17 (MIC3-OUT) to -1.55‰ (MIC4-CP) in 2016, while it was from -7.08 (MIC4-IN) to -2.88‰ (MIC1-OUT) in 2018. There was significant different of δ<sup>18</sup>O (p < 0.05) between the two sampling campaigns. Meanwhile, outliers were found to be collected from two large ponds (MIC1 and MIC4), especially for those of inside ponds and outlets. MIC4-OUT was somehow different between 2016 and 2018 as it was an outlier in 2018, while in 2016, it was close to the major cluster (Fig. III-10A). In 2016, the values of isotopes were close to the Global Meteoric Water Line (Fig. III-10B). However, in 2018, they were more consistent with the Local Meteoric Water Line (Fig. III-

10C) (Ponnou-Delaffon et al., 2020). The other ponds showed no differences for isotopic values ( $p > 0.05$ ). Similar isotopic values have been observed in the stream outlet of the Montoussé catchment at the same period out of storm events (Ponnou-Delaffon, Thesis, 2020).

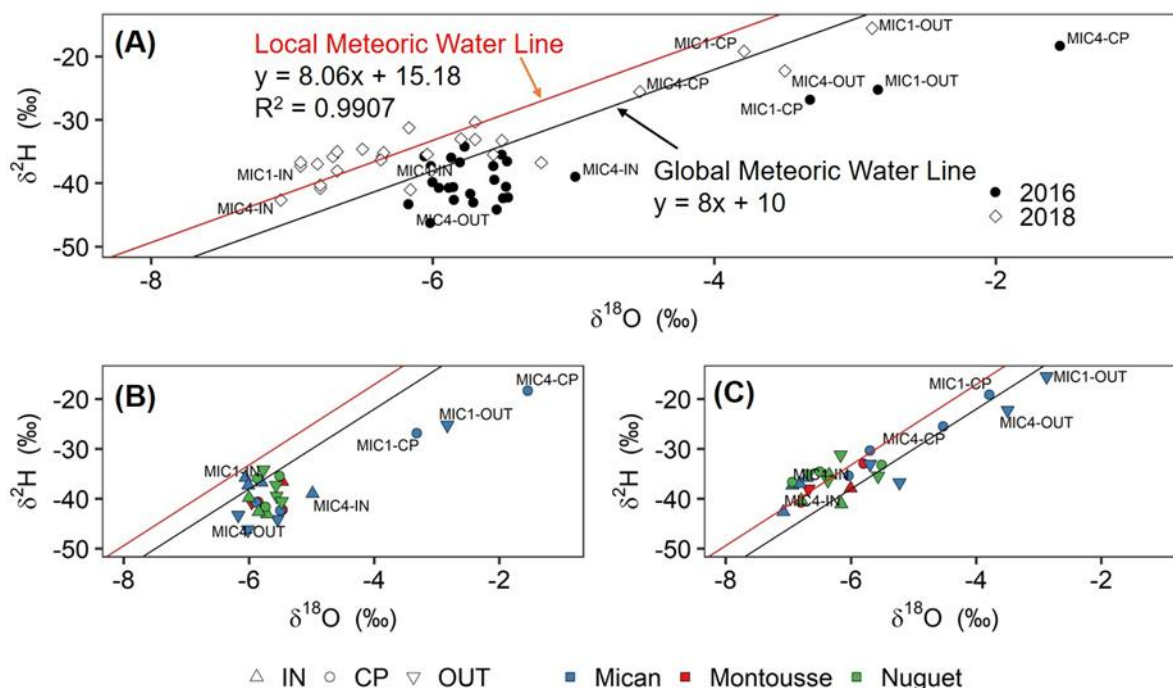


Fig. III-10.  $^2\text{H}$  versus  $^{18}\text{O}$  (A) in water samples of two sampling campaigns, (B) in water samples of 2016 sampling campaign, (C) in water samples of 2018 sampling campaign. Local meteoric water line (red line, data source: Ponnou-Delaffon, Thesis, 2020) and global meteoric water line (black line) are indicated.

Nitrogen isotope in  $\text{NO}_3^-$  ( $\delta^{15}\text{N}-\text{NO}_3^-$ ) was analyzed using the water samples in three ponds (MON2, MIC1, and MIC2) collected in the 2016 sampling campaign. It varied between 2.81 (MIC1-CP) and 11.68‰ (MIC1-IN). Two samples (MIC1-CP and MIC1-OUT) were close to the source of fertilizers and had the lowest  $\text{NO}_3^-$  concentration (Fig. III-11). On the contrary, MIC1-IN showed higher  $\text{NO}_3^-$  concentration and higher  $\delta^{15}\text{N}-\text{NO}_3^-$  signature than MIC1-CP and MIC1-OUT. Other water samples behaved similarly as they formed a cluster shown in Fig. III-11. Ponnou-Delaffon (2020) reported a range of  $\delta^{15}\text{N}-\text{NO}_3^-$  (between 7.9 and 12.7‰) in the Montoussé stream waters. And Paul et al (2015) obtained a range between 5.3 and 11.0‰. The value reported in this thesis were in the range of the above two studies except for two outliers (MIC1-CP and MIC1-OUT).

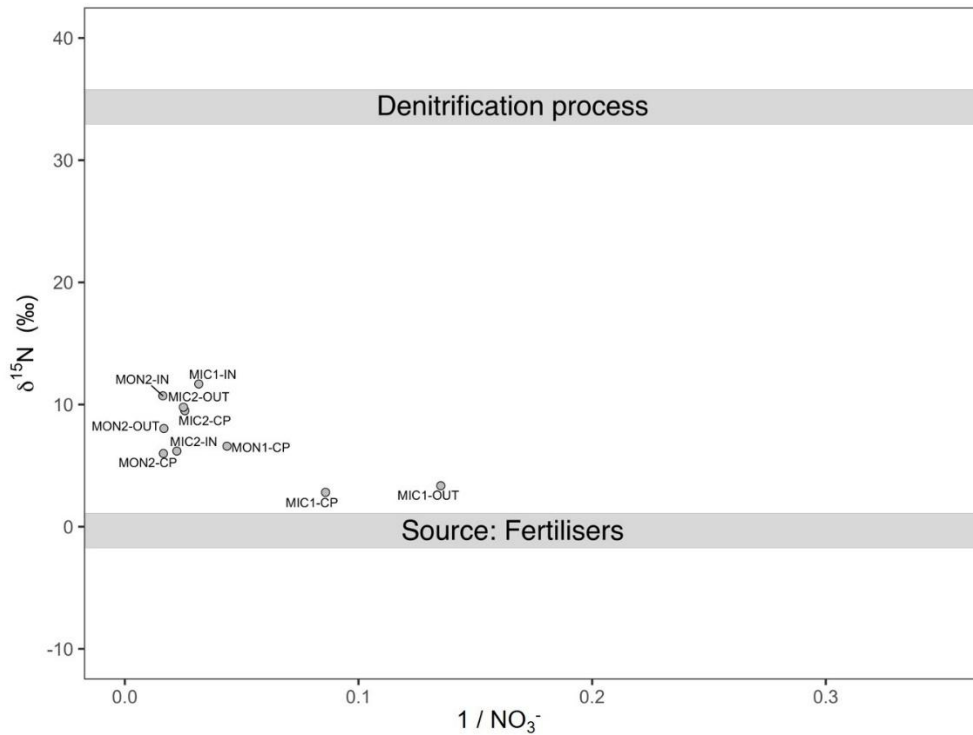


Fig. III-11.  $\delta^{15}\text{N-NO}_3^-$  versus  $1/\text{NO}_3^-$  of water samples collected in 2016. The  $\delta^{15}\text{N}$  signatures in fertilizers and denitrification were highlighted (data source: Paul et al., 2015).

### 1.3 Multilinear regression model for $\text{NO}_3^-$ removal efficiency

The  $\text{NO}_3^-$  removal efficiency varied among ponds, not only for  $\text{NO}_3^-$  concentration but also for  $\text{NO}_3^-$  flux (Table III-8). The removal efficiency (%) can be calculated as follows, respectively:

$$RE_{conc} (\%) = \frac{C_{outlet} - C_{inlet}}{C_{inlet}} \times 100\% \quad (\text{Eq. III-4})$$

$$RE_{flux} (\%) = \frac{F_{outlet} - F_{inlet}}{F_{inlet}} \times 100\% \quad (\text{Eq. III-5})$$

$$F = C \times Q \quad (\text{Eq. III-6})$$

Where,

- $RE_{conc}$ : the removal efficiency of  $\text{NO}_3^-$  concentration (%).
- $C_{inlet}$ ,  $C_{outlet}$ :  $\text{NO}_3^-$  concentration in inlet and outlet, respectively ( $\text{mg L}^{-1}$ ).
- $RE_{flux}$  is the removal efficiency of  $\text{NO}_3^-$  flux (%).
- $F_{inlet}$ ,  $F_{outlet}$ :  $\text{NO}_3^-$  flux in inlet and outlet, respectively ( $\text{mg s}^{-1}$ ).
- $Q$ : Discharge ( $\text{L s}^{-1}$ ).

Table III-8. NO<sub>3</sub><sup>-</sup> removal efficiency (RE, %) in pond (2016 and 2018).

Catchment	Pond	RE (Concentration, %)		RE (Flux, %)	
		2016	2018	2016	2018
Montoussé	MON1	-	-	-	-
	MON2	2.6	5	62.6	57.5
Mican	MIC1	76.6	89.0	80.3	91.0
	MIC2	11.2	9.2	6.9	-0.5
	MIC3	11.4	8.8	37.5	-40.6
	MIC4	6.8	-11.6	-2.7	-5549.4
Nuguet	NUG1	30.8	20.0	21.3	-428.8
	NUG2	-9.8	-0.4	-18.7	78.4
	NUG3	45.4	65.9	40.4	-44.4
	NUG4	43.1	-11.9	7.6	-57.8

The removal efficiency of NO<sub>3</sub><sup>-</sup> concentration (RE<sub>conc</sub>) was positive in most ponds, ranging from 2.6% (MON2, 2016) to 89.0% (MIC1, 2018). MIC4 and NUG4 both showed two reverse RE<sub>conc</sub> (one positive and one negative) in the two sampling campaigns, 6.8% and 43.1%, and -11.6% for and -11.9% in 2016 and 2018, respectively. In NUG2, RE<sub>conc</sub> kept a negative value constantly in 2016 and 2018 sampling campaigns. Meanwhile, in most ponds, RE<sub>conc</sub> performed similarly in the two sampling campaigns. Nevertheless, the removal efficiency of NO<sub>3</sub><sup>-</sup> flux (RE<sub>flux</sub>) varied in each pond and only RE<sub>flux</sub> of MIC1 stayed at the same level.

According to the relationships between removal efficiencies and environmental factors in ponds (Table III-9), RE<sub>conc</sub> was positively related to the ratio of pond area to upper catchment area ( $r = 0.43$ ) and HRT ( $r = 0.60$ ). It was also negatively related to the distance to the stream source ( $r = -0.62$ ). RE<sub>flux</sub> was positively related to HRT ( $r = 0.45$ ) and negatively related to distance to the stream source ( $r = -0.45$ ) and pond Length/Width ratio ( $r = -0.45$ ). Meanwhile, HRT was positively related to pond area ( $r = 0.58$ ) and its volume ( $r = 0.55$ ). The confidence level is 90% ( $p < 0.1$ ).

Table III-9. Correlation of removal efficiencies with environmental factors in ponds. The italic font indicates  $p < 0.1$ .

	RE(Conc.)	RE(Flux)	Inlet Conc.	Inlet Flux	Area (Pond)	Area (Pond/Entire Catchment)	Area (Pond/Upper Catchment)	Volume	HRT	Distance
RE(Conc.)	1.00									
RE(Flux)	<b>0.43</b>	1.00								
Inlet Conc.	0.08	0.35	1.00							
Inlet Flux	<b>-0.40</b>	-0.19	0.23	1.00						
Area (Pond)	0.10	-0.09	-0.31	0.13	1.00					
Area (Pond/Entire Catchment)	0.07	-0.22	-0.41	-0.18	<b>0.84</b>	1.00				
Area (Pond/Upper Catchment)	<b>0.43</b>	-0.18	-0.20	-0.23	<b>0.46</b>	<b>0.65</b>	1.00			
Volume	0.05	-0.08	-0.25	0.11	<b>0.98</b>	<b>0.82</b>	<b>0.47</b>	1.00		
HRT	<b>0.60</b>	<b>0.45</b>	-0.04	-0.23	<b>0.58</b>	0.42	0.29	<b>0.55</b>	1.00	
Distance to source	<b>-0.62</b>	<b>-0.45</b>	-0.21	<b>0.51</b>	0.29	0.37	-0.09	0.27	-0.26	1.00

The procedure to construct the predictive models for  $\text{NO}_3^-$  removal efficiency was the same as for PDR (Fig. III-12). The predictive models are as follows:

- For concentrations:

$$RE_{conc} = 0.996 \text{NO}_3^-_{w,inlet} - 6.613 \text{AreaRatio} + 0.011 \text{Volume} - 8.990 \text{Slope} - 27.395 \quad (\text{Eq. III-7})$$

with  $p < 0.001$ ,  $R^2 = 0.96$ , adjusted  $R^2 = 0.93$ ,  $n = 11$  (see Table III-10).

- For fluxes:

$$\log(100 - RE_{flux}) = 0.004 \text{NO}_3^-_{flux,inlet} + 0.152 \text{AreaRatio} - 0.001 \text{HRT} + 3.886 \quad (\text{Eq. III-8})$$

with  $p = 0.004$ ,  $R^2 = 0.88$ , adjusted  $R^2 = 0.81$ ,  $n = 10$  (see Table III-10).

The agreement between measured and predicted values were shown in as Fig. III-13 well.

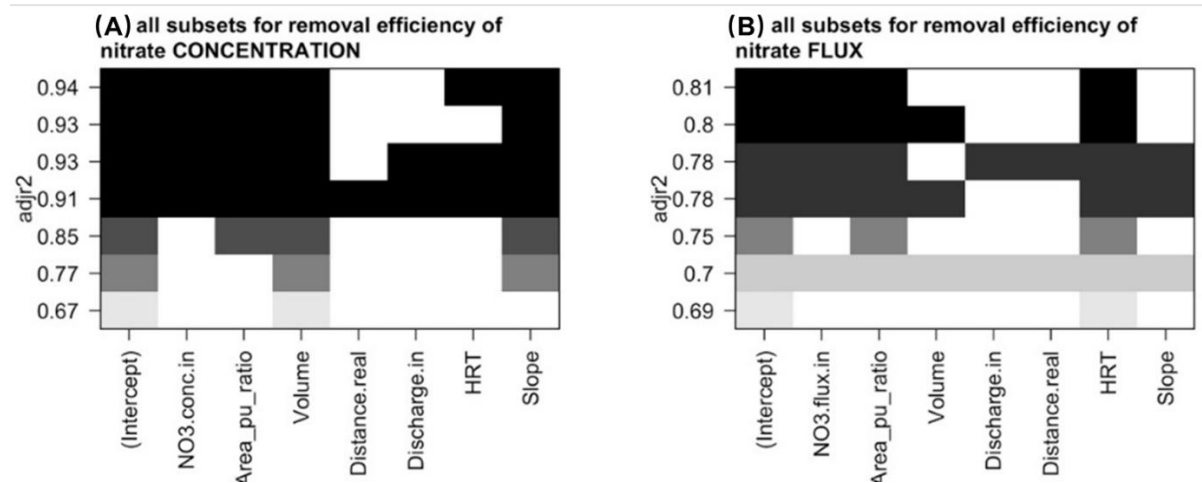


Fig. III-12. All subsets regression of removal efficiency for (A)  $\text{NO}_3^-$  concentration; (B)  $\text{NO}_3^-$  flux. The grey-scaled color indicates the level of adjusted  $R^2$  with different combinations of various variables.

Table III-10. Multiple linear regression results for  $\text{NO}_3^-$  removal efficiency. “Preliminary” indicates the consideration of all variables and “Updated” the selected variables by all subsets regression method. HRT: Hydraulic Retention Time (days). \* $p < 0.1$ ; \*\* $p < 0.05$ ; \*\*\* $p < 0.01$ .

Variable	Removal efficiency of nitrate concentration		Removal efficiency of nitrate flux	
	Preliminary	Updated	Preliminary	Updated
Inlet $\text{NO}_3^-$ concentration ( $\text{mg L}^{-1}$ )	0.969	0.996**		
Inlet $\text{NO}_3^-$ flux ( $\text{mg s}^{-1}$ )			0.025	0.004
AreaRatio (Pond/Upstream Catchment, %)	-8.859	-6.613**	0.241	0.152**
Pond volume ( $\text{m}^3$ )	0.012**	0.011***	-0.0001	
Distance to source (m)	-0.001		0.001	
Inlet discharge ( $\text{L s}^{-1}$ )	-1.015		-1.299	
HRT (d)	-0.006		-0.001	-0.001***
Slope (%)	-9.325*	-8.990***	-0.155	
Constant	-22.342	-27.395	4.190**	3.866***
Observations	11	11	10	10
$R^2$	0.97	0.96	0.93	0.88
Adjusted $R^2$	0.91	0.93	0.70	0.81
p value	0.024	<0.001	0.212	0.004

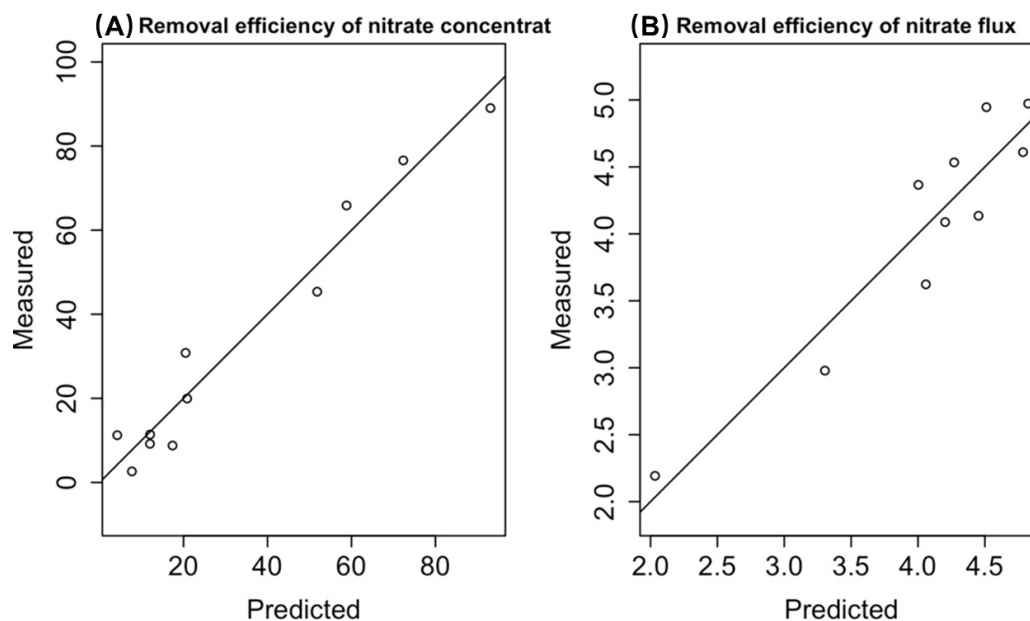


Fig. III-13. Measured vs. predicted PDR values according to the multiple linear regression model for removal efficiency of (A)  $\text{NO}_3^-$  concentration and of (B)  $\text{NO}_3^-$  flux.

## 2. Discussion

The studied agricultural catchments receive significant loadings of N-P-K fertilizers (Perrin et al., 2008; Ferrant et al., 2011), which could explain the high  $\text{NO}_3^-$  concentration measured in the stream waters, as a consequence of soil leaching and surface runoff. The rapid transfer of  $\text{NO}_3^-$  from soil to stream explained the high  $\text{NO}_3^-$  concentration in the very upstream part of the catchment and noticeably in the first upper ponds of the Mican/Montoussé catchments (MON2, NUG1 and MIC1, Fig. III-9). Only MON1 has low  $\text{NO}_3^-$  value since it is mainly a pluvial pond disconnected from the stream and surrounded by grass buffer strip. Even if sampling was done at a similar period, the hydrological conditions between the two years may be a little bit different as evidenced by the dual stable isotopes ( $^2\text{H}$  and  $^{18}\text{O}$ , Fig. III-10). The hydrological condition in 2018 sampling campaign was wetter than that in 2016 as the isotopic values in 2018 was much closer to the Local Meteoric Water Line, which was consistent with other studies in the same catchment. However, the similar  $\text{NO}_3^-$  patterns along the streams observed for the two sampling campaigns (Fig. III-9), indicated that the samples were representative for both the sampling period conditions and the whole area.

Despite entirely cultivated areas, the overall significant  $\text{NO}_3^-$  concentration decrease

observed downstream in the Mican and Nuguet streams resulted mainly of a dilution process with increasing discharge (Paul et al., 2015) and the denitrification process. Indeed, the high denitrification rate in stream sediments could participate to the  $\text{NO}_3^-$  removal in stream water, but the high discharge also dilutes the  $\text{NO}_3^-$  concentration and could indirectly lower the denitrification activity. This could explain why  $\text{NO}_3^-$  removal is higher in Nuguet stream (low discharge) compared with Mican (high discharge).

However, in the Montoussé catchment, the  $\text{NO}_3^-$  concentration was still high ( $> 50 \text{ mg L}^{-1}$ ) downstream MON2, indicating a low removal efficiency of this pond. On the opposite, MIC1 has a significant positive  $\text{NO}_3^-$  removal (Fig. III-9), but the  $\text{NO}_3^-$  increase observed before the Mican village (980 m away from MIC1-OUT, station not sampled during the 2016 campaign), indicated a very important  $\text{NO}_3^-$  loading from surrounding soil into the stream and makes the stream  $\text{NO}_3^-$  concentration high again, towards the very upstream value. In term of  $\text{NO}_3^-$  removal along the stream, it is like if there was no pond upstream. Indeed, during the water course, the discharge increased was low (Fig. III-9B), indicating no significant groundwater or runoff water input with potential dilution process compared to downstream. The soil water drainage of this important agricultural area (up to 21% of the catchment area) thus contributed mainly without efficient denitrification process. A potential influence of the village on  $\text{NO}_3^-$  in the Mican stream was excluded by the second sampling period. The similar removal efficiency of  $\text{NO}_3^-$  concentration ( $\text{RE}_{\text{conc}}$ , Table III-8) in each pond for the two sampling campaigns indicates that these ponds perform stable function of mitigation and the relationships between  $\text{RE}_{\text{conc}}$  and environmental factors could be reasonable.

The  $\text{NO}_3^-$  removal in the ponds (Table III-8) could be attributed to a joint effect of various environmental factors, including inlet  $\text{NO}_3^-$  concentration, HRT, and the pond management along the stream. In MON, though MON2 had a high PDR in sediments, the removal efficiency of  $\text{NO}_3^-$  in MON2 (2.6% in 2016) was the lowest positive value among all ponds. This may attribute to the lower HRT in MON2 compared with the ponds with high  $\text{RE}_{\text{conc}}$ , since it was shown that a long HRT is preferable to obtain a high  $\text{NO}_3^-$  removal (Jordan et al., 2003; Vymazal, 2017). Indeed, in low HRT ponds, the  $\text{NO}_3^-$  has less time and opportunity to be denitrified in the water-sediment interface. Meanwhile, MON2 is a small single pond in its stream with low HRT, receiving a high  $\text{NO}_3^-$  load from soil drainage, without any help of nitrate



removal by upstream ponds. This also indicates that the stream with a single small pond in these conditions may not be efficient in  $\text{NO}_3^-$  removal compared to the stream with a chain of ponds (Carluer et al., 2017). Meanwhile, in a similar position and with a similar input of  $\text{NO}_3^-$ , a pond with higher HRT like MIC1 can be efficient. A high  $\text{NO}_3^-$  flux has an inverse effect on  $\text{RE}_{\text{conc}}$  (Table III-9). The high  $\text{NO}_3^-$  flux and low HRT contributed to the low  $\text{RE}_{\text{conc}}$  of MIC2 (timely disconnected) and MIC3 (shallow water depth). It signifies again the importance of a chain of multiple ponds and their position in a stream in order to reach an acceptable  $\text{NO}_3^-$  removal efficiency. In 2016, the  $\text{NO}_3^-$  concentration in MIC4 was far lower than in its adjacent stream due to the long water HRT, since it was disconnected, but this was not the case in 2018. Consequently, this large pond did not contribute to the  $\text{NO}_3^-$  removal in stream in 2016. In 2018, MIC4 was continuously refilled with upstream water by a pump. The water was overflowing from the pond when sampling, explaining its low HRT. As a result, its  $\text{RE}_{\text{conc}}$  was slightly negative. Generally, the NUG ponds showed a stronger ability of  $\text{NO}_3^-$  removal than the MIC ponds. The higher PDR value could be one explanation. Besides, NUG ponds distributed more equally along the stream than MIC ponds, which relieved the stress to receive upstream  $\text{NO}_3^-$  flux and because of MIC ponds temporary disconnection. However,  $\text{RE}_{\text{conc}}$  in NUG2 was always negative. This may be an unexpected result partially due to its inner floating macrophytes without being harvested (Dhir et al., 2009). Though certain macrophytes have been approved to be effective in reducing water  $\text{NO}_3^-$  concentration (Sehar et al., 2015), since macrophytes in MIC2 were not harvested, most of sequestered nitrogen could be released again into water after macrophyte decay and decomposition (Kumwimba et al., 2016).

Meanwhile, according to multiple linear regression models (Eq. III-7 and Eq. III-8), some important factors were identified. Though a pond with large volume and high HRT may remove  $\text{NO}_3^-$  significantly, the mitigation function could be restricted by ratio of its area to the upstream catchment area. Studies have shown that there is a threshold (varying from 1 to 7%) for the ratio of pond area to entire catchment area in order to reach an acceptable removal efficiency (Vymazal, 2017). However, few studies considered the ratio of pond area to its upstream catchment area. For an experimental pond (located SW of Paris in the Brie region), Tournebize et al. (2017) indicated a 50% of  $\text{NO}_3^-$  removal with 1% of the above ratio approximately of this ratio and a 0.8 m pond depth. However, the pond area ratio needs to be determined according

to local features. The predictive model in this study could shed light on the pond design with long enough HRT and moderate area ratio to its upstream catchment. In this study, a pond with 1-2% of the pond area of upstream catchment could remove nearly 50% of water  $\text{NO}_3^-$ . The catchment and pond slope could also affect the  $\text{NO}_3^-$  removal. A steep terrain tends to promote the discharge. The higher water discharge in the Mican catchment than in the Nuguet catchment reflected this tendency. Indeed, a steep pond is not preferable for  $\text{NO}_3^-$  removal since the pond HRT is shorten and then cannot contribute to a considerable denitrification process (Clow and Sueker, 2000; Harms et al., 2016; Tournebize et al., 2017).

## Summary

The denitrification investigation in three adjacent agricultural catchments (southwestern France) highlighted a spatial variation of the denitrification process in stream and pond sediments at a given period, and the key driving factors considering a variety of ponds in similar cultivated catchments.

The water/sediment bio-physicochemical characteristics and environmental factors could affect the denitrification interactively. The potential denitrification (at the period of the year even considered not optimum), was one order of magnitude higher than groundwater sediment in the Garonne river and had a great variation on the spatial dimension. Regardless the sediment type, the denitrification was controlled by the sediment organic carbon content in common. The stream sediment was additionally controlled by the nitrate concentration in overlying water while the pond sediment not. Hence, the denitrification was more active in the stream sediments than in the pond sediments due to the sustainable supply of water nitrate and organic carbon brought by the stream water compared to the continuously consumed nitrate and organic carbon in pond sediments. Indeed, higher denitrification rate in stream sediments could participate to the nitrate mitigation in stream water, but the high discharge dilutes the nitrate concentration, and could indirectly lower the denitrification activity downstream. In pond sediments, the pond hydraulic retention time (HRT) and slope could also influence the denitrification indirectly. The longer HRT and flat pond slope inhibit the nitrate supply and contribute to the consumption of nitrate and organic carbon. Moreover, the denitrifiers were found to be much lower in a long-HRT pond. These all together contributed to a low denitrification rate. In terms of pond sediments in different depths, the surface sediment showed a more active denitrification rate than the deeper sediment due to the availability of nitrate, organic carbon, and the denitrifier abundance. Dredging activity should be well considered regarding the pond volume, the water depth, and surrounding soil erosion rate. The predictive empirical models proposed a combination of water/sediment properties as well as originally put forward the importance of environmental factors. The study highlighted the importance of some variables and allow to successfully predict PDR in a robust way with few key physicochemical and environmental factors rather easy to be measured.

Consequently, they could be used to estimate the denitrification process, offering help to a suitable pond construction and management. However, large N<sub>2</sub>O emissions were observed in some upstream ponds due to incomplete denitrification process. Since denitrification process is only a part of the nitrogen cycle, the consequence of N<sub>2</sub>O emissions as greenhouse gas from ponds, should be estimated in a complementary way to evaluate the benefit on a global nitrogen removal by ponds, as well as a complete annual hydrological survey on selected ponds. These management tools must also be combined with upstream measures such as limitation of fertilizers application and landscaping, which were shown to reduce nitrogen input to surface water in the agricultural area.

A graphical summary is presented in Fig. III-14 to highlight this conclusion.

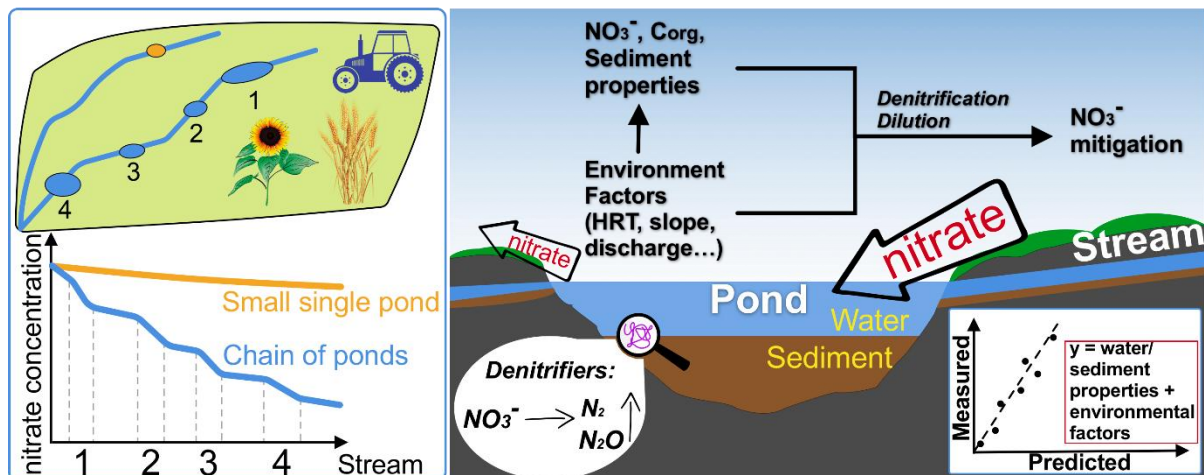


Fig. III-14. Graphical summary of the Chapter III.

## **Chapter IV**

# **Influence of ponds on hazardous metal distribution in sediments at a catchment scale (agricultural critical zone, S-W France)<sup>3</sup>**

---

<sup>3</sup> The content of this chapter has been accepted by *Journal of Hazardous Materials*. X. WU and A. PROBST (2021). Influence of ponds on hazardous metal distribution in sediments at a catchment scale (agricultural critical zone, S- W France). *Journal of Hazardous Materials*, 411, 125077, DOI: 10.1016/j.jhazmat.2021.125077

## Chapter IV

### **Influence of ponds on hazardous metal distribution in sediments at a catchment scale (agricultural critical zone, S-W France)**

#### **Introduction**

Trace elements are increasingly released into the environment due to various human activities, which include -but are not limited to- industrial emissions (Viana et al., 2008), agricultural input (Jiao et al., 2012), and urbanization (Wei and Yang, 2010). Although essential trace elements (Cu, Zn, *etc.*) are indispensable for life (Mertz, 1981; Hostetler et al., 2003), some trace elements, also known as potential toxic elements (PTE, such as Cd, Pb, Hg, and Ni), can be hazardous when their concentration exceeds an acceptable level (Goldhaber, 2003). Trace elements in agricultural areas have drawn much attention because of their potential risks to the ecosystem, food, and human health (Senesil et al., 1999). The anthropogenic sources of trace elements in these areas are mainly commercial fertilizers (N'guessan et al., 2009), wastewater effluent and irrigation (Xu et al., 2010), manures (Leclerc and Laurent, 2017), and pesticides (Gimeno-García et al., 1996). For instance, commercial mineral fertilizers are responsible for up to 85% of anthropogenic Cd in French cultivated soils (Sterckeman et al., 2018). Spreading Cu-fungicides (e.g., Bordeaux mixtures) contributed to the enrichment of Cu and Zn in the soils of French vineyards (Duplay et al., 2014). Physical erosion leads to the removal of soil particles, which are then transported downstream as suspended matter. PTEs are mainly adsorbed onto those particles in carbonated systems with high pH conditions (N'guessan et al., 2009; Redon et al., 2013). Stream and river waters contribute to most of their transfer downstream from soils to oceans. Generally, intensively cultivated catchments undergoing traditional practices such as tillage are affected by a high soil erosion rate due to their frequent exposure to various erosive powers (such as runoff), particularly when slopes are significant (Oost et al., 2009). In addition to physical erosion, fertilizers can increase soil chemical weathering by increasing the release of base cations due to excessive protons produced during the nitrification process under intensive N-P-K fertilizer spreading (Perrin et

al., 2008; Gandois et al., 2011). All the above processes enhance the transfer and deposition of suspended particulate matter along the main water channels and constitute the bottom sediments. The transfer of such sediments may be delayed by other anthropogenic objects such as reservoirs and dams, which are known to be important traps for both particles and PTEs in large basins (Audry et al., 2004; Benabdelkader et al., 2018). Such transfer of sediments and their anthropogenic content from upstream to downstream in the presence of ponds has rarely been evaluated in agricultural areas.

Bottom sediments are usually recognized as a sink for most PTEs (Singh et al., 2002; Çevik et al., 2009; Duan et al., 2010), and thus can be a reservoir for both anthropogenic and geogenic PTEs (Jiao et al., 2015). The accumulation of PTEs in sediments is controlled by several processes depending on the properties of both the sediments and the PTEs themselves: adsorption, absorption, and/or complexation to fine particles containing clay minerals, iron and/or manganese oxides, organic matter, and co-precipitation with other elements (Ghrefat and Yusuf, 2006; Çevik et al., 2009). Sediment physicochemical properties, including pH, carbonate and organic matter contents, and redox condition, and so on, can affect these processes (Du Laing et al., 2007). The different combining processes and the sources mean that PTEs in sediments are associated with residual and/or labile phases. Anthropogenic PTEs are normally prone to bond to non-residual rather than to residual phases (Leleyter et al., 2012), which makes them more or less easily released from the sediments by water disturbance and changes in water/sediment physicochemical conditions (Duan et al., 2010). Sediments can then be a secondary source of the downstream contamination (Jiao et al., 2015). Meanwhile, metal distribution between sediments and plants may be a concern in places where vegetation is abundant, as some plants can absorb the metals through the rhizosphere (Nagajyoti et al., 2010). Evaluating the available fraction of PTEs in sediment is thus a necessary step in investigating their potential risks to the environment, and especially to living organisms. In cultivated areas of southwestern France, numerous ponds have been constructed by local farmers for water storage, irrigation, and/or private landscaping, and a chain of several ponds can sometimes be seen along the main water channel in a given upstream agricultural catchment. The constructed ponds can store water and sediments transported by surface runoff and stormwaters and provide a favorable environment for sedimentation (Casey et al., 2007; Frost et al., 2015) and the

unintentional storage of PTEs. Few studies have examined the different distributions of PTEs in stream and pond sediments from upstream agricultural catchments, as these kinds of sediments and catchments can have different physicochemical characteristics. The position and the characteristics of the ponds that contribute to the PTE transfer downstream remain poorly understood, particularly in channels with a chain of multiple constructed ponds. Such ponds can be alternatively dredged by the owners, which question the effect of the pond management on the transfer.

To fill some of these mentioned gaps of knowledge, the stream and pond sediments from three adjacent agricultural catchments in southwestern France were collected and analyzed for their physicochemical characteristics, especially for the concentrations of eight PTEs (As, Pb, Co, Cr, Zn, Cu, Ni, and Cd). The objectives of this study were to:

- (1) Investigate the various sources of PTEs based on the effect of the anthropogenic activities, and to assess the contamination magnitude.
- (2) Identify the key physicochemical and environmental factors that regulate the contribution and distribution of PTEs, especially in stream and pond sediments.
- (3) Assess the availability of PTEs in the different kinds of sediments.
- (4) And, finally, evaluate the effect of ponds on PTE transfer in catchments.

The main hypothesis was that some metals in sediments originated from anthropogenic activities and were transferred downstream, and that the presence of ponds would affect this transfer through their storage capacity according to their physicochemical and environmental characteristics.



## 1. Materials and methods

Main materials and methods used in this chapter has been introduced in Chapter II. In this section, some contamination indices and methods for the multivariate analysis were supplemented.

### 1.1 Geoaccumulation index ( $I_{geo}$ )

The geoaccumulation index ( $I_{geo}$ ) was introduced to assess the degree of contamination by a given element in sediment (Müller, 1969):

$$I_{geo} = \log_2 \frac{C_n}{1.5B_n} \quad (\text{Eq. IV-1})$$

Where  $C_n$  is the concentration of an element,  $B_n$  is the background concentration of the corresponding element. A correction factor of 1.5 is used to correct the fluctuation of background value due to the lithogenic effect. Seven classes of  $I_{geo}$  are defined ranging from Class 0 ( $I_{geo} \leq 0$ , unpolluted) to Class 6 ( $I_{geo} \geq 5$ , extremely polluted), where Class 1 ( $0 < I_{geo} < 1$ ) reflects an uncontaminated to moderately contaminated situation and Class 2 ( $1 < I_{geo} < 2$ ) indicates moderate contamination. The local molasse bedrock was used as the background material.

### 1.2 Enrichment factor (EF)

The enrichment factor (EF) has been widely applied to evaluate the anthropogenic contribution of metal to the total concentration in a river sediment (Chester and Stoner, 1973):

$$EF = \frac{\left(\frac{C_i}{RE}\right)_{sample}}{\left(\frac{C_i}{RE}\right)_{background}} \quad (\text{Eq. IV-2})$$

Where  $C_i$  is the concentration of a given element, and RE is the concentration of the reference element.

The choice of a reference element, also called the normalizer, and of the background reference material are the two key points since EF is sensitive to both the reference material and the reference element according to the Eq. IV-2. Though it could be still subjective, an appropriate reference element should fulfill the following requirements (Roussiez et al., 2005; Hissler and Probst, 2006; Bur et al., 2009):

- (1) To covary in proportion with the natural concentration of a given element.
- (2) To be inertial to the anthropogenic contributions.
- (3) To be mainly distributed in the residual fraction of the sediment.

Studies have adopted local background materials as the reference material rather than global values such as PAAS or UCC if the element concentrations in local background materials are available (Singh et al., 2002; N’guessan et al., 2009; Jiao et al., 2015). This is particularly beneficial in calcareous areas (N’guessan et al., 2009; Benabdelkader et al., 2018), where the local bedrock composition has, for example, a higher arsenic content than UCC (Table IV-1 in Section 2.1). It was also evidenced in this study that using UCC instead of the local molasse bedrock led to an overestimation of EF (Fig. IV-1).

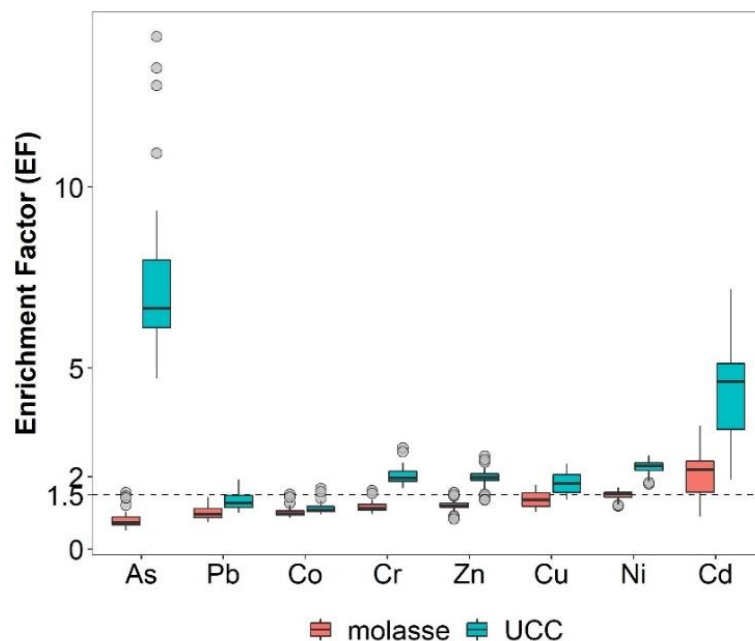


Fig. IV-1. Enrichment factor (EF) using different background materials. The color indicated different background materials: the local molasse bedrock (in light red) and the upper continent crust (UCC, in indigo-blue).

Concerning the normalizer element, several elements such as Al and Fe have been used in previous studies based on their significant relationships with the clay content and the conservative property (Zhang and Liu, 2002; Ghrefat and Yusuf, 2006; Jiao et al., 2015). In this study, Al, Fe, Cs, and Sc were four best proxies because of their much strong relationships with the clay content (Fig. IV-2). Fig. IV-3 illustrated the EF values based on molasse as the

reference material and of four candidate reference elements. The EF patterns are similar whatever the reference element. However, EF values based on Al and Sc showed two extremes, and no significant differences were observed between EF using Cs and Fe ( $p < 0.01$ ), which was also reported by Roussiez et al (2005), since these elements have the best relationships with most of PTEs (Cd having the least one). Meanwhile, in stream sediments from this Gascogne region, 98% of Cs was found in the residual fraction, whereas it was only 53, 75, and 88% for Fe, Sc, and Al, respectively (N'guessan et al., 2009).

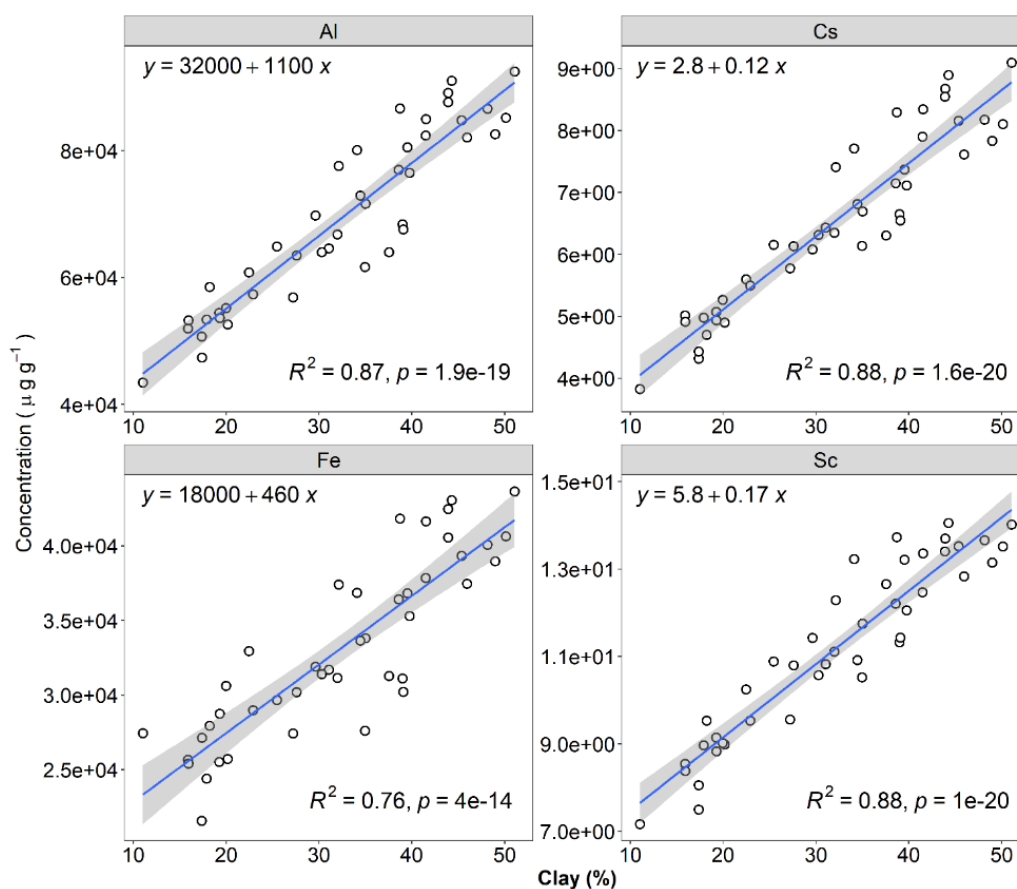


Fig. IV-2. Concentration of candidate reference elements (Al, Fe, Cs, and Sc) vs. the clay content. The linear regression line is shown with its confidence interval in grey.

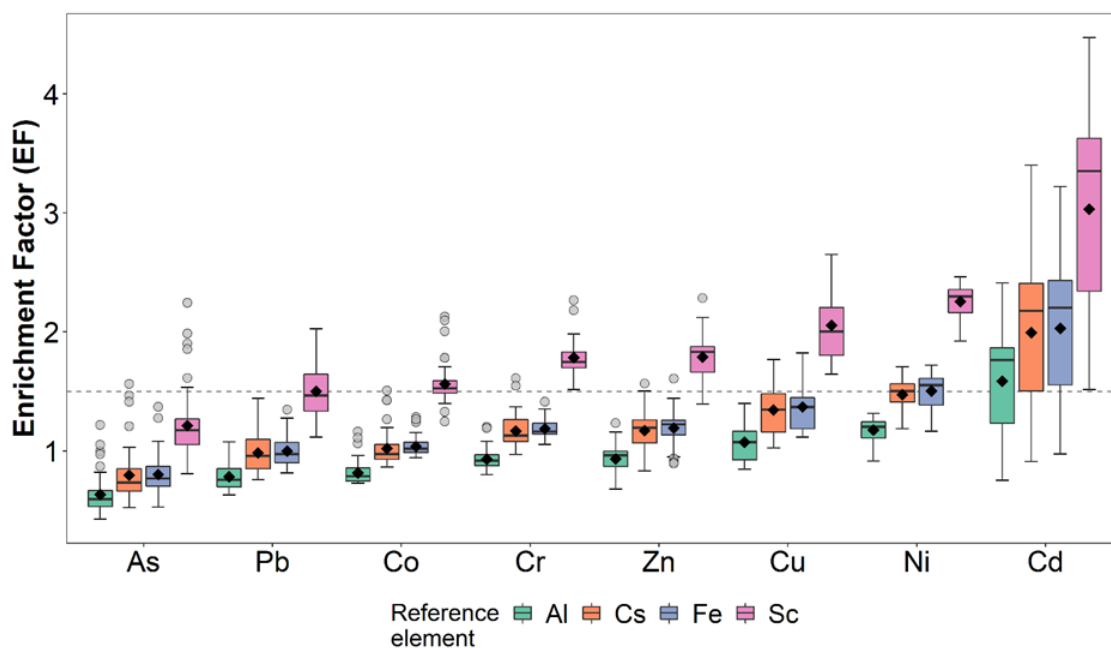


Fig. IV-3. Enrichment factor (EF) based on 4 different reference elements (Al, Cs, Fe, and Sc). The dashed line indicated the EF value of 1.5.

Finally, Cesium was selected as the normalizer element in agreement with previous studies on the same area, with the similar physicochemical characteristics of sediments. The local molasse bedrock composition was chosen as the reference material (Bur et al., 2009; N’guessan et al., 2009).

### 1.3 Anthropogenic contribution (AC, %)

The total concentration of a given element in the sediment could be considered the consequence of both lithogenic and anthropogenic activity. Assuming that the lithogenic ratio of a given element to the reference element remains the same between the molasse and the sediment sample, the lithogenic element concentration could be calculated as follows:

$$C_{lithogenic} = RE_{sample} \times \left( \frac{C_i}{RE} \right)_{molasse} \quad (\text{Eq. IV-3})$$

Where  $C_{lithogenic}$  is the lithogenic concentration of a certain trace element,  $RE_{sample}$  is the concentration of reference element in the sediment, and  $C_i$  is the concentration of a certain trace element in the background bedrock.

The anthropogenic concentration, then, can be obtained as the difference between the total and the lithogenic contribution. The anthropogenic contribution (%) is calculated as follows:

$$\text{Anthropogenic contribution (\%)} = \frac{(C_i)_{\text{sample}} - RE_{\text{sample}} \times (C_i / RE)_{\text{molasse}}}{(C_i)_{\text{sample}}} \times 100\% \quad (\text{Eq. IV-4})$$

#### 1.4 Statistical analysis

The statistical analysis was conducted in R (version 3.4). The Shapiro-Wilk test, accompanied by the quantile-comparison plot, was used to test the normality of a parameter. The permutation t-test was applied to compare the differences of given values between groups. The Spearman correlation coefficient was applied to calculate correlations among various parameters. Principle component analysis (PCA) was carried out based on z-scored data to investigate the factors that could affect the behavior of major and trace elements in stream and pond sediments, respectively. The Kaiser-Meyer-Olkin measure of sampling adequacy and Bartlett's test of sphericity were conducted before PCA to test the feasibility of performing PCA with the data.

## 2. Results

### 2.1 Concentrations of major elements and eight potential toxic elements (PTE) in sediments

The descriptive statistics of the concentrations of concerned elements in all sediments are shown in Table IV-1. The average concentrations of major elements were in the increasing order of Mn < Mg < Fe < Al < Ca. Iron, Al, and Mn were in the range of concentrations measured in various stream sediments from the Gascogne region, while Mg and Ca were a little bit higher (N'guessan et al., 2009). The concentrations exceeded the molasse content in the same region (N'guessan et al., 2009). In terms of the chemical composition for major elements (Fig. IV-4A), Ca + Mg (%) varied from 21.4% (NUG1-CP-D, near the non-carbonate endmember [Ca < 15%]) to 59.3% (MIC2-CP-D, near the carbonate end-member [Ca > 60%]), with a mean of 44.3±7.9%. There was a significant difference between the MON/MIC and NUG catchments (p < 0.01). The relative percentage of Ca was lower in the NUG sediment than in the MON/MIC sediments although few NUG sediments fell into the cluster of the MON/MIC group.

Table IV-1. Concentration of major elements and eight potential toxic elements (PTE) in sediments and other materials

	This study			Gascogne <sup>(a)</sup>			Molasse <sup>(b)</sup>	UCC <sup>(c)</sup>	PAAS <sup>(d)</sup>
	Min	Max	Mean (SD)	Min	Max	Mean			
<i>Major element (mg g<sup>-1</sup>)</i>									
Al	43.44	92.48	68.91(13.79)	31.87	98.17	52.99	46.53	77.44	189.00
Ca	26.36	129.56	71.10(22.64)	2.01	104.50	29.18	48.85	29.45	13.00
Mg	4.96	13.36	9.73(2.18)	1.64	8.76	4.36	3.60	13.50	22.00
Fe	21.57	43.65	33.01(5.94)	17.63	60.09	28.59	28.43	30.89	72.00
Mn	0.41	4.52	1.01(0.76)	0.36	2.41	1.05	0.55	0.53	1.10
<i>Potential toxic element (PTE) (µg g<sup>-1</sup>)</i>									
As	8.17	27.32	16.27(3.97)	8.77	27.48	17.19	17.19	2.00	NA
Pb	18.19	28.52	24.58(2.56)	16.52	41.94	21.45	21.45	17.00	20.00
Co	9.65	17.88	14.58(2.03)	8.15	33.16	12.19	12.19	11.60	23.00
Cr	52.08	97.09	78.36(11.4)	33.49	84.98	52.98	57.56	35.00	110.00
Zn	66.63	147.52	111.55(19.69)	55.46	140.59	80.96	80.96	52.00	85.00
Cu	16.86	42.62	29.16(6.64)	11.25	29.62	18.04	18.04	14.30	50.00
Ni	26.62	60.75	46.49(9.03)	17.01	43.92	26.73	26.73	18.60	55.00
Cd	0.23	0.67	0.48(0.15)	0.11	0.79	0.20	0.20	0.10	NA
Cs	3.83	9.09	6.54(1.41)	2.24	5.97	5.50	5.50	5.80	15.00
Sc	7.17	14.06	11.17(2.00)	6.30	21.88	12.97	14.48	7.00	16.00

(a) Gascogne stream sediments (N'guessan et al., 2009)

(b) Molasse is the local background bedrock of Gascogne (N'guessan et al., 2009)

(c) Upper Continental Crust (Wedepohl, 1995)

(d) Post Archean Australia Shale (McLennan, 2001). NA: data not available

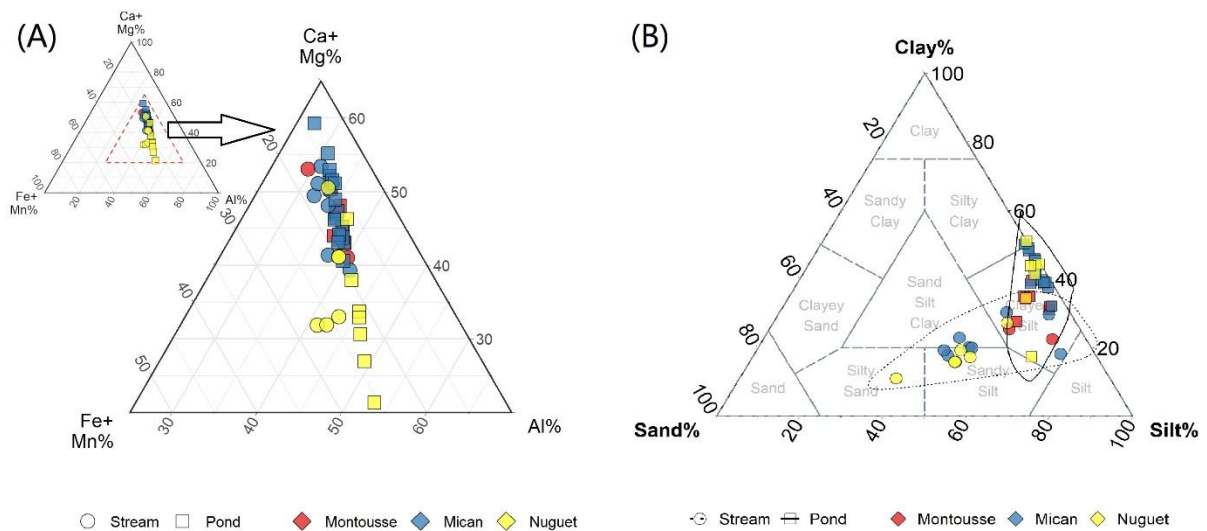


Fig. IV-4. Ternary diagrams for (A) major elements composition, and (B) sediment texture. Stream and pond sediments are indicated by round and square points, respectively. The red, blue, and yellow colors correspond to the Montoussé (MON), Mican (MIC), and Nuguet (NUG) catchments, respectively.

This study focused on eight PTEs as regards their potential hazard to the environment and the living organisms. The order of PTEs was  $Cd < Co < As < Pb < Cu < Ni < Cr < Zn$  according to the average concentration (Table IV-1 and Fig. IV-5A). Arsenic, Pb, Co, and Cd fell in the range of concentrations of stream sediments in the Gascogne region (N’guessan et al., 2009) with less value dispersion around the mean, while Cr, Zn, Cu, and Ni were slightly greater, particularly with higher maximum and minimum values (Table IV-1). As with major elements, the mean concentrations of PTEs were greater than the molasse background value, except for As. The ratios of mean concentration in sediments to the local background value were: 0.95 (As), 1.15 (Pb), 1.20 (Co), 1.36 (Cr), 1.38 (Zn), 1.62 (Cu), 1.75 (Ni), and 2.40 (Cd). The concentrations of PTEs were always higher in MON and MIC than in NUG, particularly for Cd, Cu, Ni, and Zn (Fig. IV-5B). The pond sediments exhibited higher PTE concentrations than the stream sediments (Fig. IV-5C), however, no significant differences were found between the surface and deeper layers of the pond sediments (Fig. IV-5D).

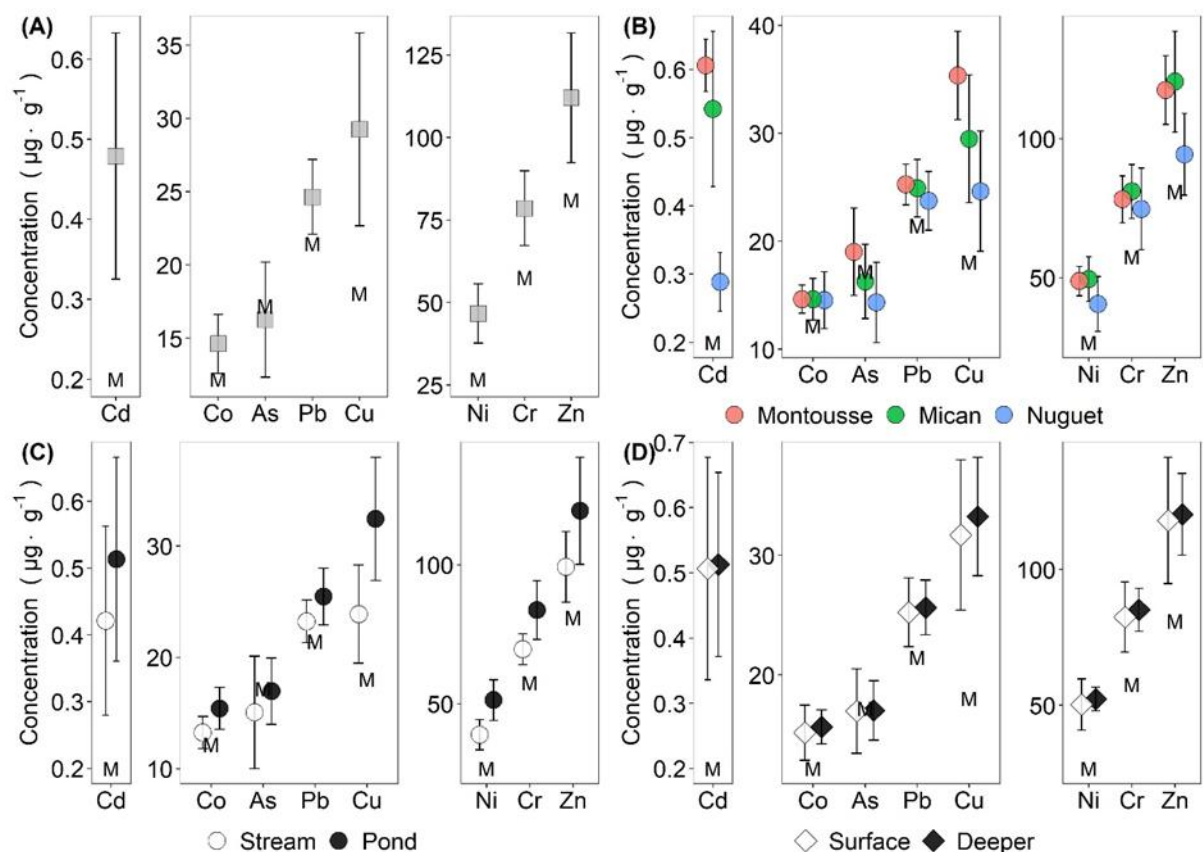


Fig. IV-5. Mean concentrations and standard variation of eight potential toxic elements (PTE): (A) all sediments; (B) by different catchments (Montoussé/Mican/Nuguet); (C) by different sediment types (stream/pond sediments); (D) by different layers of pond sediments (surface/deeper layers). “M” indicates the concentration of a given element in the background molasse (data from N<sup>o</sup>guessan et al., 2009).

## 2.2 Sediment texture

The sediment texture (Shepard’s classification) was shown in Fig. IV-4B. There was no difference in sediment textures between the three catchments. Although most of sediments fall in the clayey-silt domain, the texture differed significantly between stream and pond sediments ( $p < 0.01$ ). Stream sediments are located between sandy-silt and silty-sand domains, with most in the clayey-silt and sandy-silt domains, whereas pond sediments were in the clayey-silt domain, except for two (MIC1-LP-D and NUG3-LP-D) near the border of the silty-clay domain. The lowest clay content (17.4%) was found in NUG3-CP-S and the highest sand content (51.4%) was in NUG1-IN in the very upstream of NUG. As a whole, the pond sediments normally contained more fine particles than the stream sediments, especially for the fine fractions ( $< 63 \mu\text{m}$ ). This observation was also supported by the granulometry of particle size



distribution (Fig. IV-6).

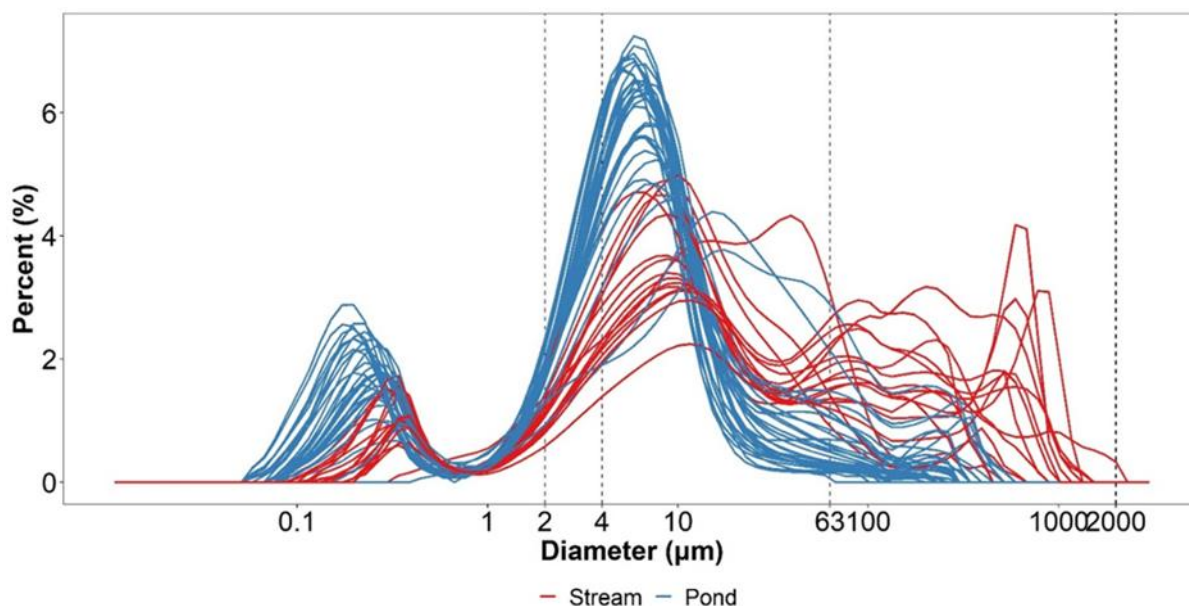


Fig. IV-6. Granulometry of particle size distribution of sediments. The colors of lines indicated the stream sediments (in red) and the pond sediments (in blue), respectively.

## 2.3 Contamination indices

### 2.3.1 Geoaccumulation index ( $I_{geo}$ )

Table IV-2 showed the descriptive statistics of  $I_{geo}$  for eight PTEs in all sediments. The values of  $I_{geo}$  were in the order of  $As < Pb < Co < Cr < Zn < Cu < Ni < Cd$ , and were either negative or between 0 and 1, which indicated unpolluted to moderately polluted sediments for the PTEs considered. The values of three PTEs (As, Pb, and Co) were always negative, except that As in MON2-OUT was the only sample with  $I_{geo}$  greater than 0. The average values of  $I_{geo}$  for Cr and Zn were  $-0.16 \pm 0.21$  and  $-0.15 \pm 0.26$ , respectively. Copper, Ni, and Cd presented the highest  $I_{geo}$  in the average between 0.07 and 0.58, with a maximum value for Cd of 1.6 (MON2-IN).

Table IV-2. Geoaccumulation index ( $I_{geo}$ ) of eight potential toxic elements (PTE) in all sediments.

Element	Min	Max	Mean	SD
As	-1.66	0.08	-0.71	0.38
Pb	-0.82	-0.17	-0.40	0.15
Co	-0.92	-0.03	-0.34	0.21
Cr	-0.73	0.17	-0.16	0.21
Zn	-0.87	0.28	-0.15	0.26
Cu	-0.68	0.66	0.07	0.34
Ni	-0.59	0.60	0.18	0.30
Cd	-0.40	1.16	0.58	0.52

### 2.3.2 Enrichment factor (EF)

The order of EF was  $As < Pb < Co < Cr < Zn < Cu < Ni < Cd$ , for all sediments (Fig. IV-7A), which is the same as that of  $I_{geo}$ . A threshold of 2 was accepted to discriminate whether a certain element was enriched in sediment. This threshold could be decreased to 1.5 if a local reference material is used to calculate EF (Hernandez et al., 2003; Roussiez et al., 2005; N'guessan et al., 2009; Benabdelkader et al., 2018). The EF of the first five elements, particularly for As, were lower than the threshold of 1.5, although a few outliers were higher than 1.5. Although the average value of EF(Cu) did not exceed 1.5, 25% of sediments (sediments mainly from upstream ponds in three catchments, respectively) exhibited an EF(Cu) value exceeding 1.5. The average EF (Ni) was not different from the threshold of 1.5 ( $p = 0.14$ ). Cadmium had an average EF value greater than 1.5 ( $p < 0.001$ ). It was the most enriched element with a mean EF value of  $1.99 \pm 0.60$ , but also had the most dispersed values and a maximum value reaching 3.40 in MIC1-OUT (the upstream MIC catchment).

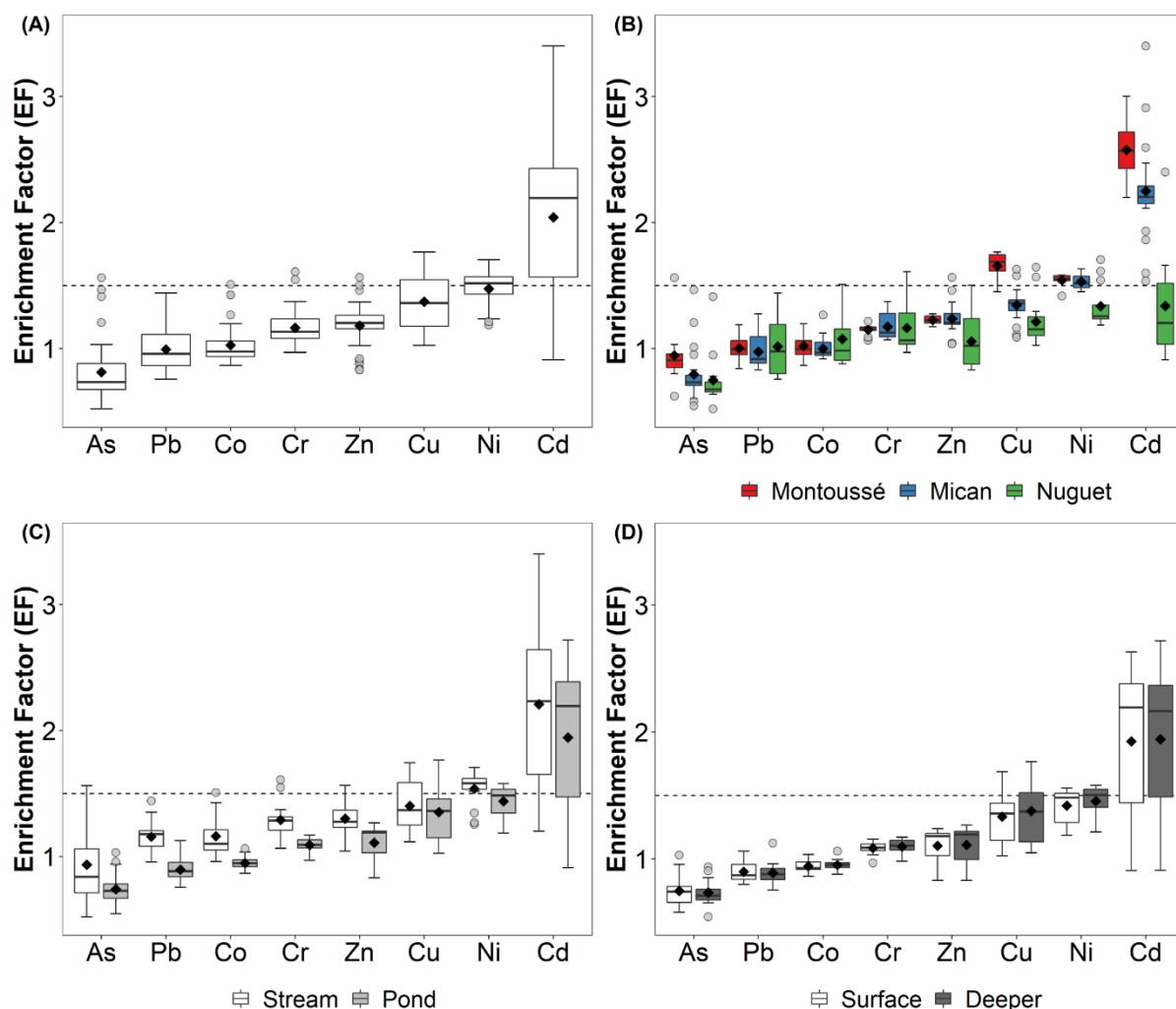


Fig. IV-7. Enrichment factors (EF) of trace elements: (A) all samples; (B) by different catchments (Montoussé/Mican/Nuguet); (C) by different sediment types (stream/pond sediments); (D) by different layers of pond sediments (surface/deeper layers).

The same EF pattern was observed for the three adjacent catchments (Fig. IV-7B), particularly from As to Cr, even if NUG had more dispersed values. Only the differences in the mean values of EF between MIC and NUG catchments were tested statistically, because the sediment samples in MON were from only two ponds, of which one is isolated from the drainage stream. The mean value of three elements showed a significant difference between MIC and NUG, e.g., Zn (MIC > NUG,  $p = 0.013$ ), Ni (MIC > NUG,  $p < 0.001$ ), and Cd (MIC > NUG,  $p < 0.001$ ). It should be noted that the upstream sediments usually had relatively high EF values, which were particularly observed in the ponds in the MON and MIC catchments, for Cd and Cu.

The EF of six elements (As, Pb, Co, Cr, Zn, and Ni) of stream sediments were also significantly greater than those of pond sediments ( $p < 0.05$  for Ni,  $p < 0.001$  for the others) (Fig. IV-7C). Interestingly, although Cu and Cd had relatively high EF values, they were not significantly different between stream and pond sediments. No significant differences in EF were observed between surface and deeper pond sediments for each element (Fig. IV-7D), and a very consistent dispersion of the EF values was observed for all the trace elements in pond sediments.

#### **2.4 Principal component analysis (PCA) and correlation matrix (CM)**

Three principal component analyses (Fig. IV-8) were performed, based on (A) all sediments, (B) stream sediments, and (C) pond sediments in order to inspect the potentially different factors, which can control the PTE concentrations in stream and/or pond sediments, and in different conditions (e.g., catchments, sediment types, sediment depths). The general input variables included the concentrations of five major elements and eight PTEs, the sediment texture (clay, silt, and sand), the pH, and the organic carbon content ( $C_{org}$ ) of the sediments. Additionally, to assess the catchment-scale environmental effect, the stream discharge (Q) was introduced into the PCA for stream sediments, and the hydraulic retention time (HRT) and the surface area of the sub-catchment of a given pond (UC.Area) were added to the PCA for pond sediments. The main results are shown in Fig. IV-8 and Table IV-4. The eigenvalues of the components are shown Table IV-3. The spearman correlation matrix between PTE concentrations, EFs, and the main factors are presented in Annex VII.

Table IV-3. Eigenvalues and variances of components for (A) all sediments, (B) stream sediments, and (C) pond sediments. The first six components were listed.

	(A) All sediments			(B) Stream sediments			(C) Pond sediments		
	Eigenvalue	Variance (%)	Cumulative variance (%)	Eigenvalue	Variance (%)	Cumulative variance (%)	Eigenvalue	Variance (%)	Cumulative variance (%)
PC1	8.55	65.78	65.78	7.31	45.71	45.71	8.47	49.82	49.82
PC2	1.65	12.69	78.46	2.93	18.34	64.04	3.04	17.87	67.68
PC3	1.38	10.64	89.1	2.46	15.36	79.4	2.49	14.65	82.34
PC4	0.67	5.15	94.25	1.11	6.92	86.32	1.3	7.66	90
PC5	0.28	2.12	96.37	0.74	4.61	90.93	0.8	4.69	94.69
PC6	0.15	1.16	97.53	0.43	2.72	93.65	0.46	2.73	97.42

Table IV-4. Relationships and contributions of variables to principal components of principal component analyses for (A) all sediments; (B) stream sediments; and (C) pond sediments. The % symbol stands for the contribution (%) of a given variable to a dimension. Bold fonts indicate significant factors in the component. Corg = organic carbon content, Q = discharge, HRT = hydraulic retention time, and UC.Area = upstream sub-catchment area.

Variable	(A) All sediments						(B) Stream sediments						(C) Pond sediments					
	PC1		PC2		PC3		PC1		PC2		PC3		PC1		PC2		PC3	
	r	%	r	%	r	%	r	%	r	%	r	%	r	%	r	%	r	%
Al	<b>0.91</b>	<b>9.76</b>	-0.28	4.73	0.01	0.01	<b>0.91</b>	<b>11.38</b>	-0.04	0.06	-0.06	0.13	<b>0.82</b>	<b>7.86</b>	<b>-0.55</b>	<b>10.14</b>	-0.08	0.24
Ca	0.27	0.85	<b>0.71</b>	<b>30.39</b>	<b>-0.51</b>	<b>19.00</b>	0.51	3.49	-0.22	1.61	<b>0.66</b>	<b>17.80</b>	-0.04	0.02	<b>0.57</b>	<b>10.62</b>	<b>0.73</b>	<b>21.60</b>
Mg	<b>0.94</b>	<b>10.31</b>	0.08	0.44	-0.22	3.61	<b>0.85</b>	<b>9.90</b>	-0.31	3.25	0.23	2.13	<b>0.88</b>	<b>9.22</b>	-0.03	0.03	0.39	6.21
Fe	<b>0.91</b>	<b>9.71</b>	-0.28	4.89	0.16	1.81	<b>0.73</b>	<b>7.37</b>	0.42	5.91	0.10	0.44	<b>0.86</b>	<b>8.73</b>	-0.47	7.15	-0.11	0.51
Mn	-0.31	1.13	0.50	14.88	<b>0.74</b>	<b>39.62</b>	0.12	0.18	<b>0.79</b>	<b>21.36</b>	0.36	5.41	0.08	0.07	0.50	8.13	-0.48	9.15
As	0.62	4.56	0.32	6.32	<b>0.63</b>	<b>28.41</b>	0.52	3.77	<b>0.68</b>	<b>15.91</b>	0.30	3.65	<b>0.85</b>	<b>8.49</b>	0.23	1.68	-0.41	6.84
Pb	<b>0.84</b>	<b>8.34</b>	-0.21	2.62	0.05	0.16	0.60	4.85	-0.36	4.34	<b>-0.64</b>	<b>16.67</b>	<b>0.90</b>	<b>9.49</b>	-0.10	0.34	-0.10	0.42
Co	<b>0.87</b>	<b>8.90</b>	-0.30	5.49	0.24	4.22	0.57	4.42	0.39	5.13	-0.49	9.84	<b>0.88</b>	<b>9.22</b>	-0.41	5.48	-0.08	0.28
Cr	<b>0.95</b>	<b>10.58</b>	-0.19	2.29	0.02	0.03	<b>0.84</b>	<b>9.75</b>	-0.16	0.84	0.08	0.25	<b>0.93</b>	<b>10.18</b>	-0.28	2.64	-0.01	0.00
Zn	<b>0.91</b>	<b>9.65</b>	0.22	2.98	-0.18	2.40	<b>0.79</b>	<b>8.50</b>	-0.35	4.18	0.23	2.07	<b>0.91</b>	<b>9.83</b>	0.28	2.53	0.23	2.18
Cu	<b>0.91</b>	<b>9.66</b>	0.18	2.05	0.04	0.11	<b>0.90</b>	<b>11.06</b>	0.22	1.71	-0.26	2.72	<b>0.85</b>	<b>8.61</b>	0.43	6.05	-0.15	0.85
Ni	<b>0.99</b>	<b>11.38</b>	0.04	0.11	-0.09	0.57	<b>0.97</b>	<b>12.79</b>	-0.12	0.51	0.10	0.40	<b>0.97</b>	<b>11.09</b>	0.02	0.02	0.16	1.03
Cd	0.67	5.18	<b>0.61</b>	<b>22.82</b>	-0.03	0.05	<b>0.90</b>	<b>10.97</b>	0.15	0.73	-0.05	0.09	0.62	4.59	<b>0.66</b>	<b>14.37</b>	0.27	2.91
Corg	-	-	-	-	-	-	-0.05	0.04	<b>0.81</b>	<b>22.20</b>	0.08	0.25	-0.04	0.02	<b>0.55</b>	<b>10.11</b>	<b>-0.68</b>	<b>18.63</b>
pH	-	-	-	-	-	-	0.33	1.47	-0.24	2.01	<b>-0.62</b>	<b>15.62</b>	0.41	2.02	<b>0.61</b>	<b>12.20</b>	0.14	0.81
Q	-	-	-	-	-	-	0.06	0.06	<b>-0.55</b>	<b>10.25</b>	<b>0.74</b>	<b>22.53</b>	-	-	-	-	-	-
UC.Area	-	-	-	-	-	-	-	-	-	-	-	-	0.11	0.13	0.36	4.23	0.42	7.23
HRT	-	-	-	-	-	-	-	-	-	-	-	-	-0.19	0.43	-0.36	4.28	<b>0.72</b>	<b>21.09</b>

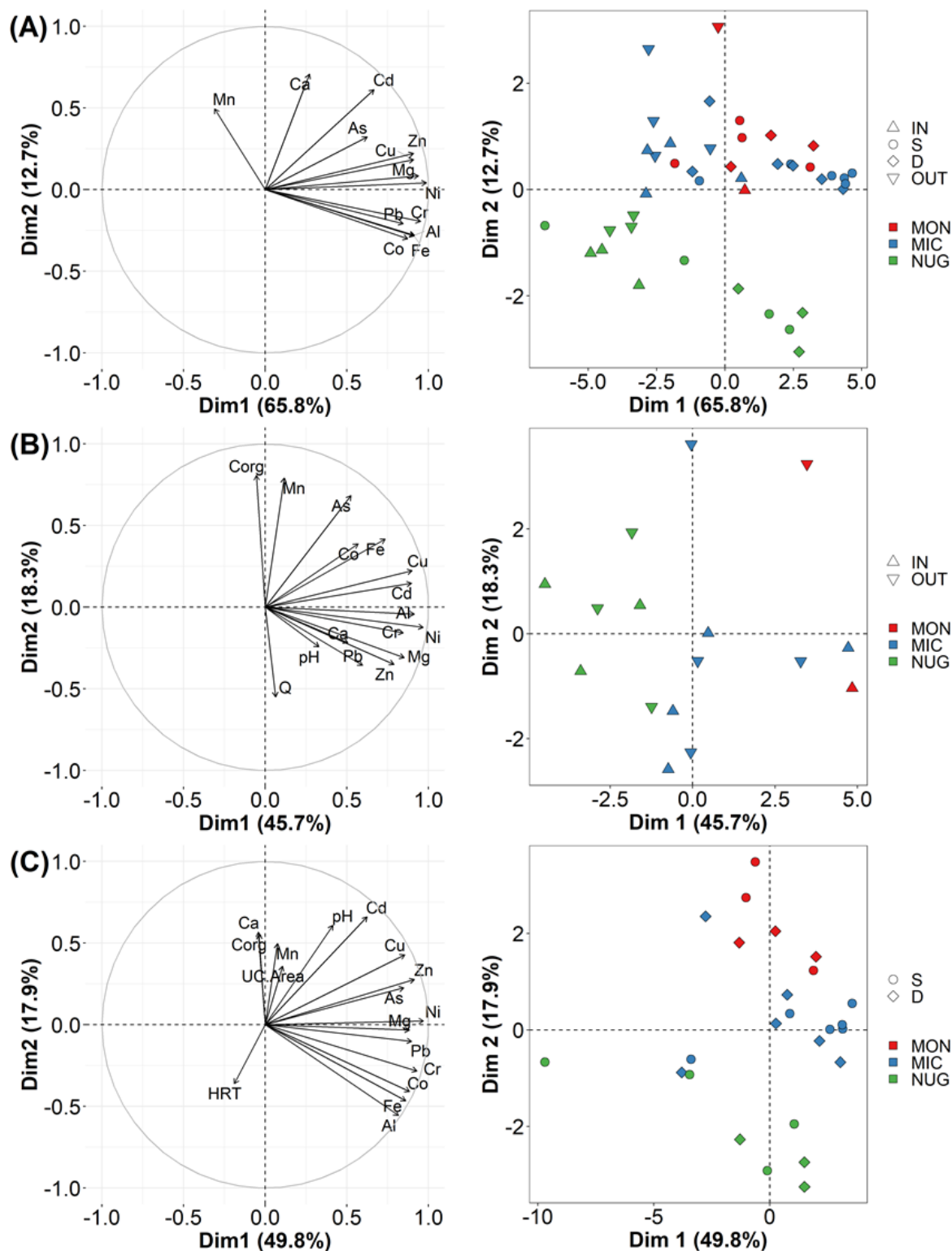


Fig. IV-8. First two dimensions (also known as ‘axes’ or ‘components’) of principal component analysis (PCA) for: (A) all sediments; (B) stream sediments; (C) pond sediments. The left column represents the variable loadings of PCA, while the right shows the individual scores. The PCA was calculated based on the concentrations of major and trace elements. Other physicochemical variables were abbreviated as follows: Corg = organic carbon content, Q = discharge, HRT = hydraulic retention time, and UC.Area = upstream sub-catchment area.

Catchments were differentiated by colors (MON = Montoussé, MIC = Mican, NUG = Nuguet in the legend). Sediments were classified into different symbols (IN = Inlet (stream sediment), S = Surface layer (pond sediment), D = Deeper layer (pond sediment), OUT = Outlet (stream sediment) in the legend).

#### **2.4.1 All sediments**

The first three principal components (PC) accounted for 89.1% of the total variance, 65.8% for PC1, 12.7% for PC2, and 10.6% for PC3 respectively (Table IV-3). Major elements (Al, Ca, Mg, Fe, and Mn) and most PTEs (except As and Cd) were positively linked to PC1 due to their high loadings ( $> 0.80$ ) and contributions (Table IV-4 and Fig. IV-8A). PC2 was mainly positively associated with Ca and Cd (loading  $> 0.6$ ). Arsenic and Mn were positively related to PC3 (loading  $> 0.60$ ), and Ca was negative (loading =  $-0.51$ ). In the individual scores of all sediments (Fig. IV-8A right), stream or pond sediments were mainly characterized by PC1, as stream sediments usually had negative scores and pond sediments were positive. The pond sediments from the upstream pond in each catchment (e.g., MON2, MIC1, and NUG1) normally scored higher in PC1. Sediments from different catchments were distinguished by PC2 as sediments from MON and MIC scored positive and were higher than those from NUG.

The considered PTEs for all sediments were closely positively interrelated (Annex VII-A,  $p < 0.01$ ). These PTEs were positively linked to Al, Mg, and Fe ( $p < 0.01$ ). Zinc, Ni, and Cd were also positively related to Ca ( $p < 0.01$ ). All the elements (except for Ca, Mn, As, and Cd) were positively associated with the clay content and negatively linked to the sand content. Aluminum, Mg, Cr and Ni were negatively linked to Corg, and Mn showed a positive relationship ( $p < 0.01$ ). The pH value positively affected Pb, Zn, Cu, and Cd.

#### **2.4.2 Stream sediments**

79.4% of the total variance was explained by PC1 (45.7%), PC2 (18.3%), and PC3 (15.4%) (Table IV-3). In PC1 (Table IV-4 and Fig. IV-8B left), high positive loadings ( $> 0.70$ ) were observed for Al, Mg, Fe, Cr, Zn, Cu, Ni, and Cd. In PC2, high positive loadings ( $> 0.65$ ) were observed for Mn, As, and Corg, and a negative high loading ( $-0.55$ ) for Q. PC3 was positively contributed by Ca and Q, and negatively contributed by Pb and pH. Stream sediments from the different catchments were separated by PC1 (Fig. IV-8B right), and the most positive scores

were for stream sediments in MON and MIC, particularly those located in the very upstream part (e.g., MON2-IN and MIC1-IN), whereas the negative scores were for those in NUG (Fig. IV-8B right). No obvious differences were observed for the inlet and outlet sediments of the ponds.

### 2.4.3 Pond sediments

82.3% of the total variance was explained by the first three PCs (49.8% by PC1, 17.9% by PC2, 14.7% by PC3, respectively) (Table IV-3). The positive high loadings ( $> 0.80$ ) of most major and trace elements (except for Ca, Mn, and Cd) were observed in PC1 (Table IV-4 and Fig. IV-8C left). PC2 was mainly positively contributed by Cd, pH, Ca, and Corg (loading  $> 0.55$ ), and negatively contributed by Al (loading =  $-0.55$ ). Calcium and HRT showed high positive loadings ( $> 0.70$ ) in PC3, while Corg possessed a high negative loading (=  $-0.68$ ). Most pond sediments in MIC and MON showed positive scores in PC2 (Fig. IV-8C right), while those in NUG scored negatively. The highest score in PC2 was for MON2. No differences were observed between the pond sediments of the surface layer and the deeper layer.

Finally, the complementary data of the correlation coefficients presented in Annex VII-B and Annex VII-C indicated that in both stream and pond sediments, Co, Cr, Zn, and Ni were positively related to Al, Mg, and Fe. In stream sediments, most major element and PTEs (except for Mn, As, and Pb) were positively linked to the clay content and also to silt (for Cu and Cd as ex.), while in pond sediments (Annex VII-B), such relationships with clays were only observed for Al, Mg, Fe, Pb, Co, Cr, and Ni (Annex VII-C). Most elements were linked to silt content. Arsenic was only positively associated with Mn and Corg in stream sediments (Annex VII-B). Cadmium was positively related to Al, Fe, and clay in stream sediments, and it was positively linked to Ca, pH, and the surface area of the sub-catchment of a given pond (UC.Area). Additionally, in pond sediments, As, Zn, Cu, and Cd was positively related to pH. The UC.Area, Ca, and pH exhibited positive correlations.



## 2.5 EDTA extraction

A single EDTA extraction was performed to assess the available fraction, where anthropogenic metal can be fixed and consequently be easily accessed by living organisms (Sahuquillo et al., 2003; Leleyter et al., 2012). Table IV-5 presents the concentrations of the available fractions and the proportions of the total concentrations in all sediments. The order of the available fraction was  $Cr < As < Ni < Zn < Co < Cu < Pb < Cd$  (Fig. IV-9A). This pattern was commonly observed in sediments from the considered catchments/types/layers, although the sequences of Zn and Co may sometimes be reversed in MON sediments, or in surface pond sediments.

Considering all sediments, the available fraction of five PTEs (Cr, As, Ni, Zn, and Co) was very low (less than 5%, ranging from  $0.09 \pm 0.03$  to  $4.91 \pm 3.17\%$ , although some outliers did reach 10% for Zn and Co), whereas it was relatively high for Cu, Pb, and Cd ( $20.50 \pm 5.78$ ,  $30.6 \pm 7.97$ , and  $47.86 \pm 12.19\%$ , respectively). The highest available fractions of Cu, Pb, and Cd were normally observed in MON2, MIC1, MIC4, and NUG1. Although the proportion of the available fraction in MIC appeared to be higher than in NUG, the differences were only significant ( $p < 0.05$ ) for As, Pb, Co, and Ni, while two elements (Cu and Cd) with large available fractions were not statistically different between MIC and NUG (Fig. IV-9B). No significant differences were observed between surface and deeper layers of pond sediments (particularly for Cu, Pb, or Cd), nor between stream and pond sediments, despite a higher extraction for stream compared with pond, particularly for the less extracted elements (Fig. IV-9 C and D).

Table IV-5. Concentration ( $\mu\text{g g}^{-1}$ ) of metal in the available fraction and its proportion (%) of the total concentration in all sediments using EDTA extraction.

Element	Min		Max		Mean		SD	
	$\mu\text{g g}^{-1}$	%	$\mu\text{g g}^{-1}$	%	$\mu\text{g g}^{-1}$	%	$\mu\text{g g}^{-1}$	%
As	0.12	0.80	0.8	6.64	0.28	1.89	0.16	1.30
Pb	4.41	20.27	13.38	49.40	7.40	30.63	2.14	7.97
Co	0.32	1.95	2.33	16.12	0.70	4.91	0.44	3.17
Cr	0.03	0.04	0.11	0.18	0.07	0.09	0.02	0.03
Zn	2.77	2.44	12.71	10.88	4.72	4.38	2.04	1.97
Cu	3.12	12.22	10.94	43.47	5.66	20.50	1.57	5.78
Ni	0.83	1.45	1.84	4.97	1.19	2.69	0.25	0.93
Cd	0.10	33.89	0.48	92.17	0.22	47.86	0.09	12.19

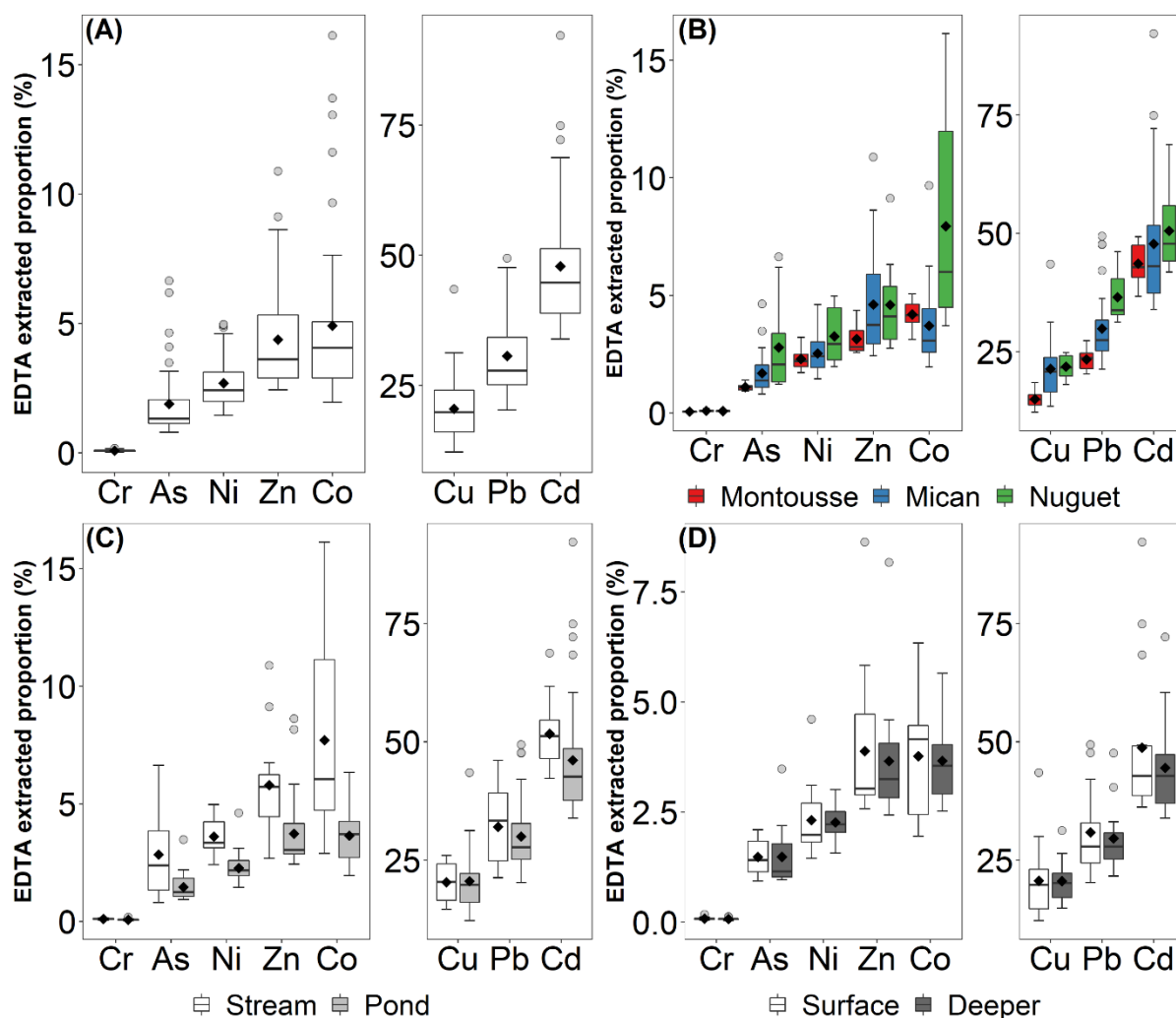


Fig. IV-9. Available fractions (%) of eight potential toxic elements (PTE) extracted by EDTA: (A) all samples; (B) by different catchments (Montoussé/Mican/Nuguet); (C) by different sediment types (stream/pond sediments); (D) by different layers of pond sediments (surface/deeper layers).

### 3. Discussion

#### 3.1 Natural vs. anthropogenic origins of PTEs in sediments, and their distributions

The concentrations of eight PTEs fell into the range of those determined in other streams from the same Gascogne region (Bur et al., 2009; N'guessan et al., 2009), although slightly higher values were observed for Cu, Ni, Cr, and Zn, which may indicate the similar origins and distributions of eight PTEs in the three catchments compared to those in Gascogne region. Copper, Ni, and Cd showed the greatest accumulation in the sediments as their average concentrations were 1.62 to 2.40 times higher than the background concentrations of molasse, while other five PTEs were barely accumulated (Table IV-1), suggesting a natural origin of the molasse through the mineral weathering processes (N'guessan et al., 2009). The same ascending order observed between  $I_{geo}$  and EF indicated a convincing result that Cd was the most enriched PTE in most sediments. Cadmium contamination was, however, far lower than that originated from mining exploitation where concentrations can reach 100 to 200 times the background value, such as in the dam from the Cajarc reservoir on the Lot river (Audry et al., 2004) or in the Milluni reservoir in Bolivia (Salvarredy-Aranguren et al., 2008).

EF could also indicate whether a PTE in the sediment is of anthropogenic origin (Ghrefat et al., 2011). As confirmed by low EF values ( $< 1.5$ ), five PTEs (As, Pb, Co, Cr, and Zn) mainly originated from the weathering process of the molasse (Zhang and Liu, 2002; N'guessan et al., 2009; Tang et al., 2010), which is a mainly carbonated event also containing some silicate minerals (Bur et al., 2009). Although Cu and Ni were not considered enriched in most sediments due to  $EF < 1.5$ , they showed greater EF values ( $> 1.5$ ) in some very upstream sediments, meaning that the anthropogenic contribution of Cu and Ni to these places cannot be neglected.

The quantitative anthropogenic contribution (AC, %) indicated no obvious anthropogenic contribution for As, Pb, and Co. Chromium and Zn exhibited an AC of 13%, but with a very variable range of values, confirming if anything a relatively low contamination of these elements (in accordance with the interpretation of  $I_{geo}$  values). Conversely, Cu, Ni, and Cd

reached an average AC of 25, 32, and 45%, respectively, which is consistent with previous observations on soils and suspended particulate matters transported during flood events (Roussiez et al., 2013). The supply of Cu, Ni, and Cd mainly resulted from spreading fertilizer and fungicide in the surrounding soils, as revealed by the analysis of fertilizers used in the area (Roussiez et al., 2013). Farmers use mainly synthetic fertilizers (from phosphate exploitation) for wheat and sunflowers cultivation, and Bordeaux mixtures for ancient vineyards. Similar contaminations were observed in an agricultural catchment cultivated for several decades (Jiao et al., 2015), and Cd proved to be the highest enriched trace element due to fertilizer spreading in other agricultural catchments (Ghrefat et al., 2011; Bing et al., 2016; Liao et al., 2019; Mao et al., 2020).

The absence of differences between both concentrations and EFs for As, Pb, Co, and Cr among the three catchments also argued for their natural origin. The higher anthropogenic impact of Zn, Ni, and Cd in MON and MIC compared with NUG, shown by the concentrations and EFs, might result from the effect of environmental catchment characteristics and/or the physicochemical settings of sediments (see Section 3.2), since these catchments involve similar agricultural practices and land cover. Indeed, the MON and MIC catchments have steeper slopes and higher carbonate content than NUG, and the anthropogenic PTEs were particularly associated with Ca (Annex VII-A). Redon et al. (2013) also reported a higher trace element content in calcareous agricultural soils from the Midi-Pyrénées region compared with non-calcareous soils. We thus propose that the arable soil erosion was responsible for the accumulation of anthropogenic Ni and Cd due to the presence of carbonated soil in these catchments (Bur et al., 2012; Benabdelkader et al., 2018). The highest contamination for Ni and Cd was always observed in the upstream ponds (MON2, MIC1, and NUG1) of the three catchments. These ponds were the first repository of sediments that originated from the soil erosion of upstream catchments without the effect of discharge dilution (N'guessan et al., 2009). The effect of soil erosion regulating anthropogenically originating elements, especially Cd, were also reported by other studies (Bing et al., 2016; Benabdelkader et al., 2018; Liao et al., 2019). The greater anthropogenic contribution of Cu in sediments from MON compared to MIC and NUG could be related to Bordeaux mixture application in two parcels of vineyards that were pulled up in the recent decades (in sub-catchment of MON2, see the land use map in

Ponnou-Delaffon et al., 2020). The average PTE concentrations in sediments from ponds were always higher than in streams in relation to higher clay content in pond sediments (Fig. IV-5C and Fig. IV-6) since these elements were strongly positively related to the clay content (Fig. IV-8A and Annex VII). The mostly naturally originating PTEs (As, Pb, Co, Cr, and Zn), however were lower in ponds than in stream sediments, even if EFs were low, which was the opposite of the pattern of concentrations, while the EFs of Cu and Cd showed no difference. One explanation could be the higher content of fine particles in pond sediments. Indeed, the concentration of the reference element (Cs), used as the normalizer in the EF calculation, was higher in the pond sediments. Meanwhile, Al, Cs, and Fe showed the same high correlations ( $r = 0.93$ ,  $p < 0.001$ ) to the clay content (Annex VII-A) as other metals. The higher accumulation of the reference element may unintentionally restrain the EF. It can also be confirmed by EF values based on Fe showing less affinity to fine particles, as the EF difference between stream and pond sediments was minimized (Fig. IV-10). In the pond sediments, the absence of a statistical difference between PTE enrichment in surface and deeper sediments (Fig. IV-7D) indicated the probable similar natural or anthropogenic origin of PTEs in these sediments.

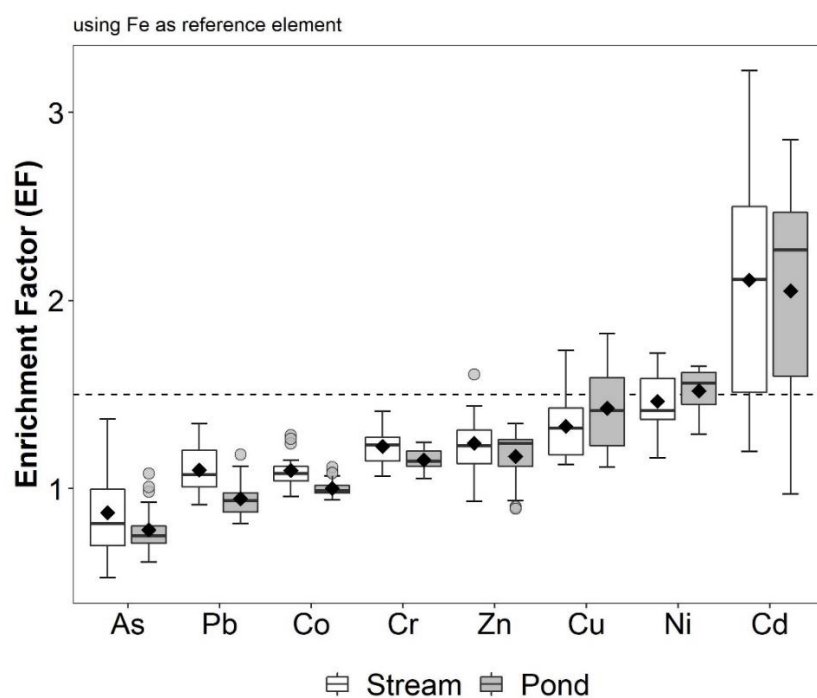


Fig. IV-10. Enrichment factor (EF) using Fe as the reference element. Different colors indicated the stream sediments (in white) and the pond sediments (in grey), respectively.

### 3.2 Distribution of PTE concentration and its controlling factors

The PCA (Fig. IV-8 and Table IV-4) and the correlation matrix (Annex VII) allowed the controlling factors for the PTEs to be investigated. Three preliminary tests (Bartlett's test of sphericity, the KMO test, and the determinant test) showed that the following PCA results were reliable.

For all sediments, the significant positive interrelations among PTEs and their low EF values (Annex VII-A and Section 2.4) confirmed the main origin as from the natural weathering process, as discussed above in Section 3.1. Most PTEs (except As and Cd) were controlled by clay minerals and/or iron oxides due to their high loadings and high associations with Al and Fe in PC1 (Fig. IV-8). The same phenomenon has been observed in other stream sediments in the Gascogne region (N'guessan et al., 2009). The positive relationship between As, Mn, and Corg in stream sediments indicated that As was associated with manganese oxides and/or complicated by sediment organic matters, which were also found in various stream conditions (Salvarredy-Aranguren et al., 2008). The fine sediments in the ponds can provide a higher specific surface area that favors the adsorption process of metals (Leleyter and Probst, 1999; Duan et al., 2010) and explains why PTE concentrations in pond sediments were higher than in stream sediments (Fig. IV-8). As explained above, Cd, and to a less extent Ni and Cu, originated from anthropogenic agricultural inputs, were eroded from soil during storm events (Ponnou-Delaffon et al., 2020) and transported to accumulate in sediments downstream. Since carbonate minerals contain low Cd, the strong link between Ca and Cd in intensively agricultural areas suggest that Cd was controlled by calcite co-precipitation under the  $\text{pH} > 8$  condition (Benabdelkader et al., 2018; Ponnou-Delaffon et al., 2020) (Table IV-4C and Annex VII). Considering the higher temperatures in ponds and the higher hydraulic retention time (HRT), this co-precipitation process might be particularly enhanced (Fig. IV-8C and Annex VII), however, in stream sediments, Cd was more controlled by silicates (clay and iron oxides).

Since the three catchments were closely adjacent and the geomorphological characteristics were similar except on the slope, the hydrodynamic condition which affects the soil erosion (Duan et al., 2010) might be a main controlling factor. The steeper slopes of the catchments

(MON and MIC) favored a greater soil erosion and transport of Cd from the fertilizers into the downstream river systems. The NUG sediments were also less carbonated (Fig. IV-8A), which resulted in less Cd control. Compared to other ponds in the Mican catchment, the lowest Cd concentration found in MIC4 pond could be explained by its position downstream, which undergoes a strong dilution.

### 3.3 Availability of PTE in sediments

Both low EF (Fig. IV-7) and available fraction (Fig. IV-9) for As, Co, Cr, and Zn indicated their limited potential environmental risk to the aquatic system, which was consistent with the natural origin of these PTEs (Benabdelkader et al., 2018). Although the anthropogenic contribution of Ni was significant (Section 3.1), Ni showed a low extractability (Fig. IV-9). This may be a result of binding strength, since Ni formed a strong binding to clay minerals in sediments (Yoo et al., 2013). The similar low extractability of Ni was observed in other studies (Hamdoun et al., 2015; Kouassi et al., 2019). Copper, Pb, and Cd exhibited high available fractions in increasing order, which was observed in other catchments with agricultural practices (Roussiez et al., 2013; Guo et al., 2018). A complexation process could have mobilized these three PTEs. Previous studies have shown that the availability of Cu and Pb with EDTA was attributed to their high complexation constants with EDTA, and due to the high affinity of Cu and Pb to Fe oxides (Annex VII). These PTEs can be remobilized with the complexation of Fe oxides (Sahuquillo et al., 2003). Copper and Cd both had high EF and a high available fraction that evidenced their potential environmental risk to the aquatic system if physicochemical conditions changes allowed desorption processes. Although Pb was mostly of natural origin in the agricultural catchments, its mobility can be significant (Bur et al., 2009; Benabdelkader et al., 2018). Similar observations were also made by Leleyter and Baraud (2005) relative to EDTA extraction in the Vire river sediments.

Interestingly, the average available fraction was always lower in the Mican catchment than in the Nuguet catchment, in opposition to the higher degree of anthropogenic contribution. This could result from the higher calcium carbonate content in MON and MIC, which is consistent with the significant ( $p < 0.01$ ) negative relationship between available fractions of most PTEs and available Ca concentrations (Fig. IV-11). The dissolution of calcite by excessive EDTA

during the extraction process increased at high pH values (Papassiopi et al., 1999), contributing to the precipitation of released PTEs and their re-adsorption onto fine particles (Manouchehri et al., 2006). Contrary to expected results, the higher proportion of available fraction of PTEs in stream sediments (Fig. IV-9C) was associated with coarse particles (as attested by the positive correlation to sand negative to clays, Fig. IV-11). The probable higher oxides content in pond sediments may provide a more specific surface for the metal binding.

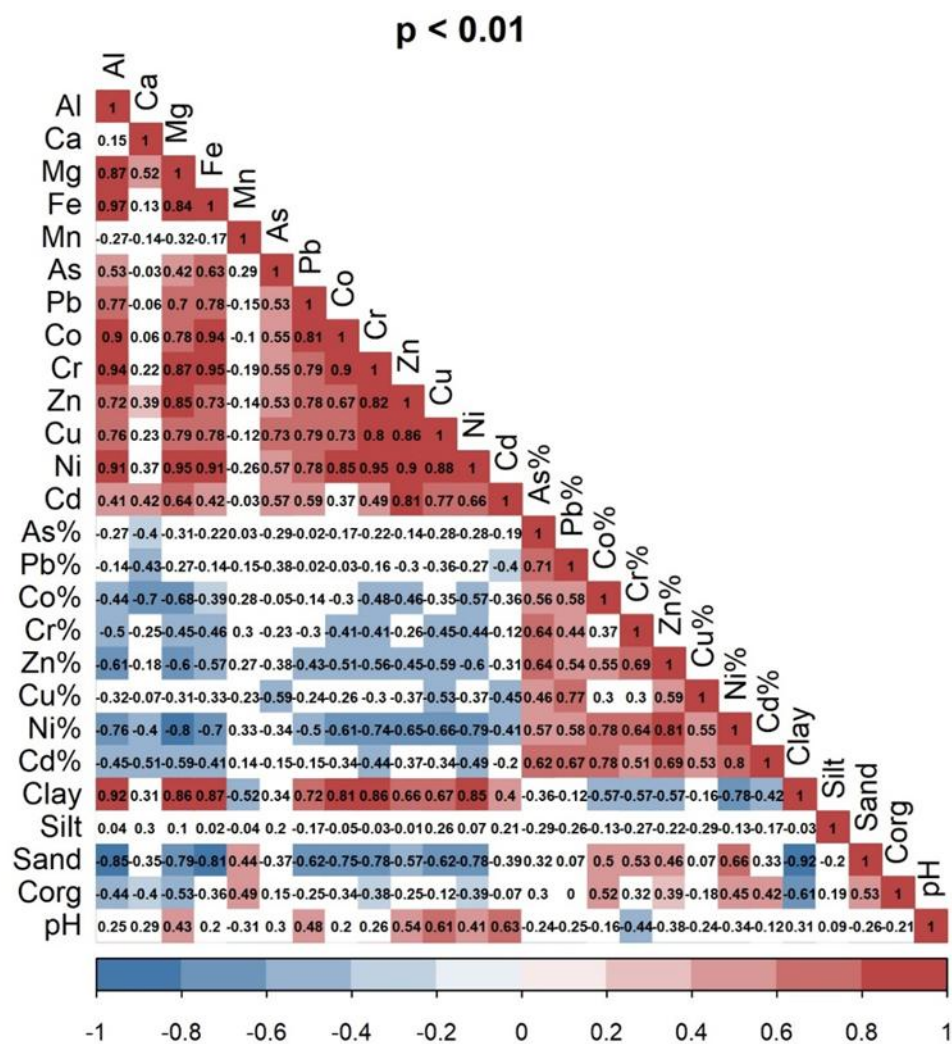


Fig. IV-11. Correlation matrix of concentrations, available fractions (%), and sediment properties in all sediments. The color bar indicated the r value from -1 (blue) to 1 (red). The significance level ( $p < 0.01$ ) was highlighted by colored blocks in the figures.

### 3.4 Effect of ponds on PTE transfer in catchments

The distribution of PTE needs to be specifically regulated since the spatial variation of



PTE concentrations observed in close adjacent catchments was non negligible. This is specifically important for the anthropogenically originated elements, so as to reduce the potential environmental risk to the ecosystem in a limited geographic area. In agricultural catchments, constructed ponds have proved to be an effective way to control this risk (Frost et al., 2015; Jiao et al., 2015). In this study, the constructed ponds can be a sink for PTEs as the pond sediments concentrated more PTEs than the stream sediments.

As discussed before, the large surface area and the steeper slopes led to the higher input of PTEs due to the more intensive fertilizer application, the greater soil erosion, and surface runoff. The streams located in the upstream catchments were thus normally confronted with higher PTE concentrations than downstream, which may be reflected in the higher PTE enrichment in MON and MIC than in NUG. However, the discharge dilution was an important factor in minimizing the PTE loads exported to a tributary of the next order, as revealed by the Mican stream, where a greater decrease of Cu, Ni and Cd was observed in its downstream section compared to NUG. The storage function of the pond was evidenced in this study, since in general, the PTE concentration was higher in the inlet of a given pond than in the outlet. MIC3 and NUG1 were two exceptions, however MIC3 was never dredged, the long-term (several decades) accumulation of sediments led to the lowest pond water depth of all the studied ponds. Although the pond sediments in MIC3 accumulated PTEs in the same way as other pond sediments, the low water depth and water volume limited the effective accumulation of fresh suspended matter from its upstream inlet. Meanwhile, the low water depth made MIC3 much vulnerable to the turbulence process by upstream discharge. Sediment re-suspension could occur in pond sediments during high discharge periods. This contributed to particulate transfer downstream with adsorbed/complexed PTEs, and contributed to PTE desorption, which make this pond only temporary sinks for PTEs (Acevedo-Figueroa et al., 2006). Although no statistical difference was observed in PTE concentration between the surface and relative deeper sediment in ponds as a whole, the concentration was higher in surface sediments than in deeper sediments in the Mican catchment, except in the Nuguet catchment. Due to the larger pond volume and longer HRT in the MIC pond than in NUG pond, the MIC pond exhibited a better retention capacity for fine particles, and thus the MIC ponds demonstrated a better PTE storage function than the NUG ponds. In the MON2 pond, the surface pond

sediment was supposed to accumulate more anthropogenically originating PTEs, however, recent sediment dredging activity (one year before the sampling campaign), meant that the PTE concentration in its surface sediment was lower than in the deeper sediments. The dredging activity enabled the accumulated PTEs in pond sediments to be removed, however, the treatment of the contaminated sediments after excavation needs to be managed.

## Summary

This study, firstly, assessed the contamination of potential toxic elements (PTE) in both stream and pond sediments in the three adjacent agricultural catchments in southwestern France. According to the geoaccumulation index ( $I_{geo}$ ) and the enrichment factor (EF), As, Pb, Co, Cr, and Zn were not enriched in sediments, indicating their natural origin from the molasse bedrock weathering process. Cadmium was the most enriched element ( $EF > 1.5$ ), and the average EFs of Cu and Ni were close to 1.5. The use of local molasse bedrock and Cs as the reference element in calculating EF assured the accuracy of interpretation regarding the potential natural/anthropogenic sources for PTEs. The anthropogenic contribution (AC, %) quantifies a significant anthropogenic impact on Cu, Ni, and Cd, in increasing order. The spread of agricultural mineral fertilizer and pesticides in upstream soils was the main anthropogenic source for Cu, Ni, and Cd, and the Bordeaux mixtures used in the ancient vineyards also contributed to Cu. In general, a higher EF was observed in sediments from upstream catchments and in MIC compared to NUG, and there was no difference between surface and depth of ponds.

The highest finer particle content contributed to the highest concentration observed in ponds. Clay minerals and/or iron oxides were key factors in the distribution of most PTEs (except for As and Cd). Cadmium showed different controlling factors between stream and pond sediments. In stream sediments, Cd was more controlled by silicates (clay and iron oxides), while in pond sediments, longer hydraulic retention time and increased water temperature contributed to Cd co-precipitation with calcite due to higher pH conditions and Ca content. This explained the difference in the control of Cd observed between MIC and NUG catchments. Arsenic was bound to manganese oxides and/or complexed with organic matter in stream sediments.

In general, Cu, Pb, and Cd showed the highest EDTA extractability, suggesting a hazardous potential environmental risk, whereas the lower Ni extractability may be due to a lesser extraction efficiency of the extractant. Extractability was affected by the calcite content in sediments due to the dissolution of calcite and the consequent pH increase, since the highest anthropogenically affected sediments (MIC) exhibited the lower extractability. Surprisingly,

the coarse sediments from streams supported a higher proportion of extractable PTEs.

The geomorphological properties of the catchments and the management of constructed ponds can affect the spatial variation of PTE concentrations. The larger surface area of an upper sub-catchment and the steeper slope leads to higher PTE accumulation in stream and pond sediments, especially for anthropogenically originating elements, relative to intensive fertilizer spreading, the greater soil erosion and surface runoff. The increasing discharge along the channel contributes to the dilution of PTEs downstream. While the constructed pond having a considerable hydraulic retention time can be a sink for fine particles and PTEs, the non-dredged ponds were vulnerable to particle resuspension and the transfer of PTEs downstream. Ponds temporarily ensure a storage of sediments, and sediment dredging activity therefore contributes to regularly remove the PTEs associated with the accumulated sediments, but this involves planning for their downstream treatment.

The graphical summary has been presented in Fig. IV-12.

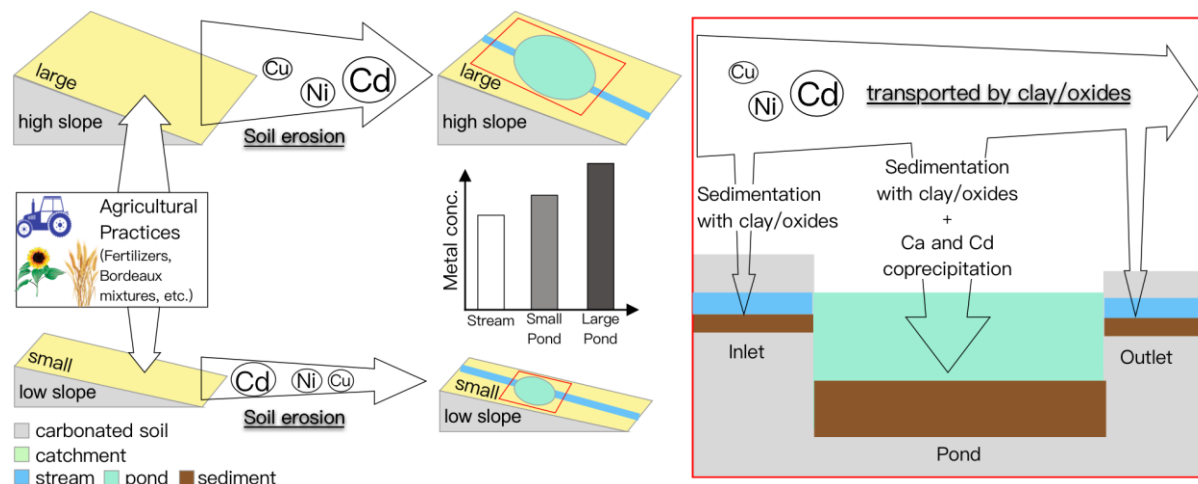


Fig. IV-12. Graphical summary of the Chapter IV.

**Chapter V**

**Role of ponds in mitigating contaminants (nitrate and trace metals): a synthetic study in agricultural critical zone (southwestern France)**

## Chapter V

### **Role of ponds in mitigating contaminants (nitrate and trace metals): a synthetical study in agricultural critical zone (southwestern France)**

#### **Introduction**

Previous chapters have investigated the nitrate concentration in waters and the accompanied denitrification process in sediments (Chapter III), and the potential hazardous metals in sediments (Chapter IV), respectively.

The sources, distributions are well discussed for nitrate and metals in independent chapters. Though two single-element indices are used to evaluate the contamination for each metal and to identify the origins of metals, the overall contamination intensities by a set of hazardous metals in sediments are not known since the absence of using some multi-element indices.

The study on the denitrification process shows that it is mainly controlled by the availability of nutrients (e.g., sediment organic carbon and water nitrate concentration). The concentrations of metals and their enrichment depends on the clay minerals and/or iron oxides. These physicochemical characteristics related waters and sediments themselves can directly influence the transfer and transformation of the nitrate and the hazardous metals.

Meanwhile, these two kinds of contaminants are also influenced by the environmental features according to the types and locations of sediments. For example, the rapid stream discharge can dilute the nitrate concentration and violate the favorable undynamic environment for progressing the denitrification process, thus this process is restrained. The upstream large pond stores more metals compare to the downstream small ponds because of soil erosion without the discharge dilution and a high hydraulic retention time for sedimentation. Considering geophysicochemical as a whole, the desirable managements for constructed ponds in agricultural catchments are proposed, which targets to alleviate the environmental stress from nitrate and hazardous metals, respectively.

However, previous chapters have never discussed about the two kinds of contaminations together. Will the metal contamination and the denitrification process affect each other? What would be the satisfying managements for ponds when considering different sorts of

contaminants simultaneously? Are they still identical to previous ones regarding merely nitrate or metals? Yet, these questions are not answered by previous discussion.

In such a condition, as a synthesis as well as a complement to previous chapters, the objectives of this chapter are to:

- (1) Assess the overall contamination magnitude by using various integrated multi-element indices and compare the effectiveness of different multi-element indices.
- (2) Evaluate the potential ecological risks of metals to the denitrification process.
- (3) Investigate the geophysicochemical characteristics that controls the metal contamination and the denitrification process simultaneously.
- (4) Propose a favorable management of the constructed ponds to regulate complex contaminant synchronously.

## **1. Materials and methods**

Main materials and methods used in this chapter have been introduced in Chapter II. In this section, Multi-element contamination indices, sediment quality guidelines, and data treatment were described additionally.

### **1.1 Multi-element contamination indices**

Various kinds of indices have been utilized to assess the metallic contamination intensity in the sediments. In Chapter IV, two single-element contamination indices (EF and  $I_{geo}$ ) were calculated to evaluate the contamination in three adjacent agricultural catchments in the Save basin (southwestern France). Though these two factors have already been applied by many other studies and are proved to be valid in this study, the overall metal contamination in sediments cannot be represented by such two single-element indices. As a synthetic chapter, several commonly used integrated multi-element indices were calculated to investigate the overall metal contamination in sediments. Their details were described below. According to the values obtained by these multi-element indices, the metal contamination in the sediments can be classified into various categories of contamination magnitude (Table V-1).



Table V-1. Classes of contamination intensities defined by the integrated multi-element indices, including concentration-based indices (PLI, CD, mCD, PI, and mPI) and ecological indices (Er<sup>i</sup> and PERI). PLI = pollution load index, CD = contamination degree, mCD = modified contamination degree, PI = Nemerow’s pollution index, mPI = modified Nemerow’s pollution index, Er<sup>i</sup> = potential ecological risk of a single element, PERI = potential ecological risk of all calculated metals (sum of Er<sup>i</sup>).

<b>Concentration based index</b>										
Score	PLI		CD		mCD		PI		mPI	
	Value	Class of contamination	Value	Class of contamination	Value	Class of contamination	Value	Class of contamination	Value	Class of contamination
0	< 1	Nil			< 1.5	Nil to very low	< 0.7	unpolluted	< 1	unpolluted
1	> 1	contaminated	<8	low	1.5 - 2	low	0.7 - 1	slight	1 - 2	slight
2			8 - 16	moderate	2 - 4	moderate	1 - 2	moderate	2 - 3	moderate
3			16 - 32	considerable	4 - 8	high	-	moderate-heavy	3 - 5	moderate-heavy
4			> 32	very high	8 - 16	very high	2 - 3	heavy	5 - 10	heavy
5					16 - 32	extremely high	> 3	severe	> 10	severe
6					> 32	ultra high				

<b>Ecological index</b>				
Score	Er <sup>i</sup>		PERI	
	Value	Class of contamination	Value	Class of contamination
0				
1	< 40	low	< 150	low
2	40 - 80	moderate	150 - 300	moderate
3	80 - 160	considerable	300 - 600	high
4	160 - 320	high	> 600	significantly high
5	> 320	serious		
6				

### 1.1.1 Contamination degree (CD)

Hakanson’s contamination degree (CD) is one of the most used integrated multi-element indices to assess the overall metal contaminants in sediments (Hakanson, 1980). It can be calculated as follows:

$$CD = \sum_{i=1}^n CF_i \quad (\text{Eq. V-1})$$

Where CF<sub>i</sub> is the contamination factor, which is the ratio of the concentration of a given *i* metal to its background concentration; *n* is the number of the considered contaminants. In this study, the local molasse bedrock (Cayeux, 1935; N’guessan et al., 2009) was used as the background reference. The benefit of using the local background material rather than the global background matters (UCC, PAAS, etc.) has been validated by previous studies in the same region (Bur et al., 2009; N’guessan et al., 2009; and also see the discussion in Chapter IV).

### 1.1.2 Modified contamination degree (mCD)

The modified contamination degree (mCD), proposed by Abraham and Parker (2008), is the mean value of the Hakanson's contamination degree according to the number of concerned contaminants. Its calculation is as follows:

$$mCD = \frac{\sum_i^n CF_i}{n} \quad (\text{Eq. V-2})$$

Where  $CF_i$  is the contamination factor, and  $n$  is the number of calculated elements.

### 1.1.3 Pollution load index (PLI)

The pollution load index (PLI) is the  $n^{\text{th}}$  root of the product of the contamination factors of studied PTEs (Tomlinson et al., 1980).

$$PLI = \sqrt[n]{CF_1 \times CF_2 \times \dots \times CF_n} \quad (\text{Eq. V-3})$$

Where  $CF_i$  is the contamination factor, and  $n$  is the number of calculated elements.

### 1.1.4 Nemerow's pollution index (PI)

The Nemerow's pollution index (PI) uses both the mean value and the maximum of the contamination factors of all the analyzed metals in a sediment (Nemerow, 1991).

$$PI = \sqrt{\frac{(CF_{\text{mean}})^2 + (CF_{\text{max}})^2}{2}} \quad (\text{Eq. V-4})$$

Where  $CF_{\text{mean}}$  refers to the mean value of CF of all analyzed metals in a sediment, and  $CF_{\text{max}}$  is the maximum of these CF.

### 1.1.5 Modified pollution index (mPI)

Brady et al. (2015) proposed a modified Nemerow's pollution index (mPI), which used the enrichment factor (EF) instead of CF, to assess the pollution intensity of metals in a sediment.

$$mPI = \sqrt{\frac{(EF_{mean})^2 + (EF_{max})^2}{2}} \quad (\text{Eq. V-5})$$

Where  $EF_{mean}$  refers to the mean value of EF of all analyzed metals in a sediment, and  $EF_{max}$  is their maximum.

### 1.1.6 Potential ecological risk index (PERI)

The potential ecological risk index (PERI) aims to assess the potential ecological risk (PER) of hazardous metals in sediments (Hakanson, 1980). Unlike the aforementioned integrated indices, which merely depends on the metal concentrations, PERI also takes into consideration the ecological responses of the analyzed metals. It can be calculated as follows:

$$PERI = \sum_{i=1}^n Er^i = \sum_{i=1}^n Tr^i \times CF_i \quad (\text{Eq. V-6})$$

where  $Tr^i$  is the toxic response factor for a given element,  $CF_i$  is its contamination factor. The value of  $Tr^i$  is 1 for Co and Zn, 2 for Cr, 5 for Pb, Cu, and Ni, 10 for As, and 30 for Cd (Hakanson, 1980; Tang et al., 2017). The  $Er^i$  is defined as the production of the contamination factor and the toxic response factor, which expresses the potential ecological risk of a single  $i$  element. The PERI is the sum of  $n$  terms of  $Er^i$  as an integrated PER. The value of  $Er^i$  and PERI (Table V-1) can assess the potential ecological risk for a single metal and the integrated multiple metals, respectively (Guo et al., 2010; Soliman et al., 2015).

## 1.2 Sediment quality guidelines (SQGs)

Sediment quality guidelines have been attested to be useful methods to assess the quality of freshwater sediments (MacDonald et al., 2000; Long, 2006). The SQGs are mainly derived

from two approaches: (1) the theoretical methods upon equilibrium partitioning models, and (2) the empirical methods based on analyses of field-collected chemistry and biological data (Long, 2006). In order to meet the agreement among previously published SQGs, the consensus-based SQGs are developed by MacDonald et al. (2002), which contain the threshold effect concentration (TEC) and the probable effect concentration (PEC) as two baselines. The TEC emphasizes the concentration of a contaminant below which the adverse effects on living organisms in sediments are not expected to occur, while the PEC reflects the concentration above which the adverse effects on organisms are likely to appear. These consensus-based SQGs have been proved to be effective in freshwater sediments to evaluate the sediment toxicity, especially concerning the concentrations of analyzed metals above the PEC. Table V-2 showed the values of TEC and PEC for 7 metals concerned in this study (MacDonald et al., 2000).

Table V-2. Consensus-based sediments quality guidelines (SQGs) for freshwater sediments (MacDonald et al., 2000). TEC: threshold effect concentration; PEC: probable effect concentration, unit = mg kg<sup>-1</sup> dry weight of sediment.

Element	TEC	PEC
As	9.79	33.0
Cd	0.99	4.98
Cr	43.4	111
Cu	31.6	149
Pb	35.8	128
Ni	22.7	48.6
Zn	121	459

### 1.3 Statistical analysis

The statistical analyses were performed using the R language version 3.6.2 (R Core Team, 2017). Spearman correlation was applied to determine the relationships among various variables. The Kruskal-Wallis rank sum test was used to investigate the statistical difference between different groups of data. Principle component analysis (PCA) was performed based on z-scored data. The implementation of PCA was finished by the FactoMineR package in R

(Lê et al., 2008). The Bartlett's test of sphericity and the determinant of a matrix were conducted to test the data reliability to perform PCA. The statistical figures in this article were mainly generated via the ggplot2 package in R (Wickham, 2009).

## **2. Results and discussion**

### **2.1 Overall metal contamination in sediments**

#### **2.1.1 Integrated contamination magnitude**

Studies have shown that the use of various multi-element indices is credible to assess the contamination intensity in freshwater sediments, offsetting the possible deficiency brought by merely relying on one index (Varol, 2011; Ferati et al., 2015; Duodu et al., 2016; Mao et al., 2020). In general, although minor differences of terminology occur regarding various indices, the contamination can be classified into six ranks: (1) nil to very low, (2) low/slight, (3) moderate/considerable/high, (4) heavy/very high, (5) extremely high/severe/serious, and (6) ultra-high (Table V-1). Scores are labelled according to their corresponding ranks (Table V-1), ranging from 0 (nil to very low) to 6 (ultra-high). The values and scores of the sediments according to the indices were listed in detail (Table V-3).

Table V-3. Values and scores calculated by integrated multi-element indices and the ecological index. CD = contamination degree, mCD = modified contamination degree, PLI = pollution load index, PI = Nemerow’s pollution index, mPI = modified Nemerow’s pollution index, PERI = potential ecological risk index, Sum.1 = sum of scores for indices except PERI, Sum.2 = sum of scores for all studied indices. The level of scores for each index is listed in Table V-1.

Sample	Concentration based indices										Ecological index		Sum of scores	
	CD		mCD		PLI		PI		mPI		PERI		Sum.1	Sum.2
	Value	Score	Value	Score	Value	Score	Value	Score	Value	Score	Value	Score		
MON1-CP-S	11.12	2	1.39	0	1.29	1	2.57	4	2.56	2	114.2	1	9	10
MON2-IN	13.23	2	1.65	1	1.55	1	2.65	4	2.62	2	140.2	1	10	11
MON2-UP-S	13.14	2	1.64	1	1.56	1	2.65	4	2.60	2	134.4	1	10	11
MON2-UP-D	12.77	2	1.60	1	1.51	1	2.63	4	2.61	2	130.8	1	10	11
MON2-CP-S	12.80	2	1.60	1	1.52	1	2.63	4	2.60	2	127.8	1	10	11
MON2-CP-D	13.61	2	1.70	1	1.60	1	2.66	4	2.60	2	136.6	1	10	11
MON2-LP-S	14.24	2	1.78	1	1.68	1	2.69	4	2.57	2	137.2	1	10	11
MON2-LP-D	14.46	2	1.81	1	1.70	1	2.70	4	2.59	2	140.0	1	10	11
MON2-OUT	12.60	2	1.58	1	1.51	1	2.63	4	2.64	2	128.0	1	10	11
MIC1-IN	12.99	2	1.62	1	1.53	1	2.64	4	2.62	2	136.1	1	10	11
MIC1-UP-S	13.64	2	1.70	1	1.61	1	2.67	4	2.58	2	137.7	1	10	11
MIC1-UP-D	13.23	2	1.65	1	1.55	1	2.65	4	2.57	2	133.9	1	10	11
MIC1-CP-S	14.71	2	1.84	1	1.74	1	2.71	4	2.56	2	143.5	1	10	11
MIC1-CP-D	14.25	2	1.78	1	1.68	1	2.69	4	2.56	2	141.2	1	10	11
MIC1-LP-S	14.49	2	1.81	1	1.71	1	2.70	4	2.55	2	143.7	1	10	11
MIC1-LP-D	14.54	2	1.82	1	1.73	1	2.70	4	2.56	2	138.1	1	10	11
MIC1-OUT	11.24	2	1.40	0	1.32	1	2.58	4	2.67	2	123.1	1	9	10
MIC2-IN	9.87	2	1.23	0	1.16	1	2.53	4	2.59	2	91.3	1	9	10
MIC2-CP-S	14.99	2	1.87	1	1.78	1	2.72	4	2.56	2	144.5	1	10	11
MIC2-CP-D	11.29	2	1.41	0	1.34	1	2.58	4	2.56	2	101.9	1	9	10
MIC2-OUT	10.42	2	1.30	0	1.22	1	2.55	4	2.60	2	101.8	1	9	10
MIC3-IN	10.02	2	1.25	0	1.20	1	2.54	4	2.60	2	92.0	1	9	10
MIC3-CP-S	14.80	2	1.85	1	1.75	1	2.71	4	2.56	2	144.4	1	10	11
MIC3-CP-D	13.52	2	1.69	1	1.60	1	2.66	4	2.56	2	131.0	1	10	11
MIC3-OUT	11.60	2	1.45	0	1.39	1	2.59	4	2.57	2	110.1	1	9	10
MIC4-IN	10.62	2	1.33	0	1.29	1	2.56	4	2.60	2	98.2	1	9	10
MIC4-CP-S	10.46	2	1.31	0	1.26	1	2.55	4	2.52	2	88.6	1	9	10
MIC4-CP-D	10.31	2	1.29	0	1.23	1	2.55	4	2.52	2	88.9	1	9	10
MIC4-OUT	10.05	2	1.26	0	1.23	1	2.54	4	2.56	2	89.0	1	9	10
NUG1-IN	8.37	2	1.05	0	1.04	1	2.49	4	2.63	2	64.7	1	9	10
NUG1-CP-S	12.05	2	1.51	1	1.48	1	2.60	4	2.50	2	86.5	1	10	11
NUG1-CP-D	12.27	2	1.53	1	1.51	1	2.61	4	2.50	2	87.2	1	10	11
NUG1-OUT	9.90	2	1.24	0	1.20	1	2.53	4	2.65	2	87.2	1	9	10
NUG2-IN	9.30	2	1.16	0	1.13	1	2.51	4	2.57	2	72.9	1	9	10
NUG2-CP-S	9.86	2	1.23	0	1.22	1	2.53	4	2.51	2	76.4	1	9	10
NUG2-CP-D	11.05	2	1.38	0	1.35	1	2.57	4	2.50	2	87.3	1	9	10
NUG2-OUT	8.71	2	1.09	0	1.07	1	2.50	4	2.51	2	66.6	1	9	10
NUG3-CP-S	6.97	1	0.87	0	0.85	0	2.46	4	2.52	2	56.8	1	7	8
NUG3-LP-S	11.32	2	1.41	0	1.39	1	2.58	4	2.49	2	81.4	1	9	10
NUG3-LP-D	12.28	2	1.53	1	1.51	1	2.61	4	2.49	2	93.5	1	10	11
NUG4-IN	8.37	2	1.05	0	1.01	1	2.49	4	2.54	2	67.3	1	9	10
NUG4-OUT	8.57	2	1.07	0	1.06	1	2.49	4	2.55	2	67.1	1	9	10
CV (%)	17.86		17.86		16.85		2.81		1.75		25.84			

All the analyzed sediments exhibited PLI ranging from 1.01 to 1.78, except NUG3-CP-S (PLI < 0.9) (Table V-3), indicating that these sediments apart from NUG3-CP-S were more or less contaminated by the concerned potential hazardous metals. However, unlike other indices, PLI only provided one baseline (PLI = 1) below which the sediment was not contaminated. It did not present any other specified levels of contamination. Therefore, additional integrated

multi-element indices should be considered to assess the contamination more precisely instead of applying PLI solely.

NUG3-CP-S always showed the least value whatever the index except for mPI. Apart from NUG3-CP-S, the range of CD was between 8.37 and 14.99, while mCD varied from 1.05 to 1.87 (Table V-3). The sediments fell into the range of moderate contamination in accordance with CD, whereas mCD indicated very low to low contamination in sediments (Fig. V-1 and Table V-3). It was not surprising that the judgements of the contamination intensity by these two indices were different, although they were derived from the sum of concentration factors for 8 potential hazardous metals (Eq. V-1 and Eq. V-2). Two single-element indices previously shown that the sediments in these three agricultural catchments was slightly to moderately contaminated by Cu, Ni, and Cd. Hence, the overall contamination intensity was underestimated by mCD due to its high trigger value. The underestimation by mCD was also reported by other studies (Duodu et al., 2016).

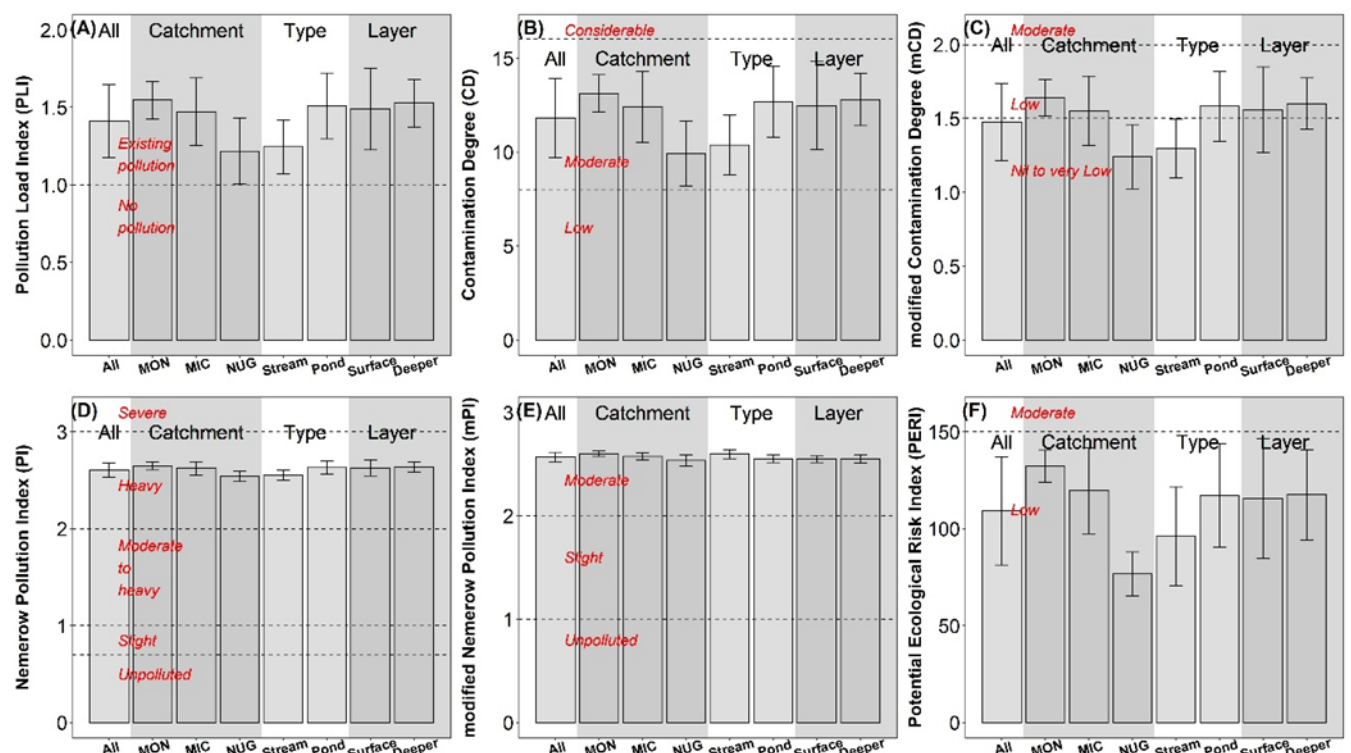


Fig. V-1. Various indices for sediments regarding different types of sediments. Red italic texts indicate the range of contamination levels highlighted by dashed lines.

The PI, ranging from 2.46 to 2.72, indicated that all sediments were heavily contaminated

even for NUG3-CP-S, which was very contrary to CD/mCD. Meanwhile, sediments were inferred to be moderately contaminated by mPI, which varied from 2.49 to 2.67. As a weighted average rather than the arithmetic average (Eq. V-4), PLI was subject to generate a high value for the index. And the trigger thresholds of PLI were lower than those of other multi-element indices. Though these two aspects made PLI powerful to identify the contamination hotspot in the areas which suffered high metallic contamination, it would overestimate the contamination where the anthropogenic and industrial impact was not much significant, especially in the agricultural catchments. The same overestimation was observed by other studies (Brady et al., 2015; Duodu et al., 2016).

Table V-4 showed the correlations between the multi-element indices and the metal concentrations. Attributing to the significant association between indices and metal concentrations ( $p < 0.01$ ), the indices used in this study, except for mPI, could be good proxies for the metal concentrations taken as a whole.

Table V-4. Correlation matrix for metal concentrations and various indices. Bold:  $p < 0.01$ , Italic:  $0.01 < p < 0.05$ .

	CD	mCD	PLI	PI	mPI	PERI
As	<b>0.716</b>	<b>0.716</b>	<b>0.733</b>	<b>0.716</b>	0.222	<b>0.623</b>
Pb	<b>0.771</b>	<b>0.771</b>	<b>0.773</b>	<b>0.771</b>	-0.115	<b>0.628</b>
Co	<b>0.718</b>	<b>0.718</b>	<b>0.746</b>	<b>0.718</b>	<i>-0.305</i>	<b>0.470</b>
Cr	<b>0.807</b>	<b>0.807</b>	<b>0.834</b>	<b>0.807</b>	<i>-0.348</i>	<b>0.580</b>
Zn	<b>0.914</b>	<b>0.914</b>	<b>0.904</b>	<b>0.914</b>	0.021	<b>0.848</b>
Cu	<b>0.944</b>	<b>0.944</b>	<b>0.946</b>	<b>0.944</b>	0.061	<b>0.835</b>
Ni	<b>0.913</b>	<b>0.913</b>	<b>0.932</b>	<b>0.913</b>	-0.255	<b>0.745</b>
Cd	<b>0.880</b>	<b>0.880</b>	<b>0.852</b>	<b>0.880</b>	<b>0.401</b>	<b>0.983</b>
Sum=	6.664	6.664	6.720	6.664	-0.318	5.713
	CD	mCD	PLI	PI	mPI	PERI
CD						
mCD	<b>1.000</b>					
PLI	<b>0.995</b>	<b>0.995</b>				
PI	<b>1.000</b>	<b>1.000</b>	<b>0.995</b>			
mPI	0.091	0.091	0.041	0.091		
PERI	<b>0.925</b>	<b>0.925</b>	<b>0.903</b>	<b>0.925</b>	<i>0.323</i>	

Besides, the sensitivity is an important factor to assess the effectiveness of a contamination index (Hakanson, 1980; Brady et al., 2015). The coefficients of variation (CV, %) were, in the increasing order, 1.75 for mPI, 2.81 for PI, 16.85 for PLI, and 17.86 % for both CD and mCD. The least CV of PI and mPI showed that the sensitivity of these two indices was far weaker



than other indices, which indicated that it may be not suitable to use them in adjacent catchments at a small scale. The high sensitivity also made it possible to easily compare the significant differences. The non-weighted indices (PLI, CD, mCD) demonstrated the greater contamination in MON and MIC than in NUG, as well as the higher contamination in pond sediments compared to the stream sediments (Fig. V-1ABC), while the weighted ones (PI and mPI) was not able to show the distinctions apparently (Fig. V-1DE).

### **2.1.2 Potential ecological risk in sediments and the effect of metal contamination on denitrification**

The overall potential ecological risk in the sediment can be represented by PERI, which is the sum of single potential ecological risks ( $E_r$ ) for the 8 concerned toxic elements. The strongly positive relationship between PERI and other sensitive indices ( $p < 0.01$ , Table V-4) indicated that the potential ecological risk was accompanied by the increasing contamination in sediments. As a whole, all the sediments showed low potential ecological risk, indicated by the PERI values lower than 150 (Table V-3 and Fig. V-1F). The similar differences of the potential ecological risk between catchments and between sediment types observed by PERI as other sensitive indices (Fig. V-1ABCF) showed that more attention should be paid to the sediments in MON and MIC as well as to those in ponds since these sediments showed higher contamination than others.

Since PERI is the sum of single potential ecological risks ( $E_r$ ), the  $E_r$  itself can be used to assess the potential ecological risk for a given element (Eq. V-6). Fig. V-2A showed the potential ecological risk of each analyzed toxic elements for all sediments. Four metals (Cu, Ni, As, and Cd) showed the highest  $E_r$  in sediments. It is consistent with the highest anthropogenic contribution for Cu, Ni, and Cd, which was identified in the previous study in the same area (N'guessan et al., 2009; also see the discussion in Chapter 4). It was also not surprising by the high  $E_r$  for As since As was much abundant in the background molasse (N'guessan et al., 2009) and other similar carbonated sediments (Benabdelkader et al., 2018). Cadmium was the only element showing the moderate to considerable potential ecological risk in most sediments, while other elements were much below the trigger threshold for a moderate risk (Fig. V-2AB). In accordance with the contamination, the sediments in MON and MIC

presented the moderate to considerable Er, particularly for the upstream sediments, whereas the sediments in NUG showed the low to moderate Er.

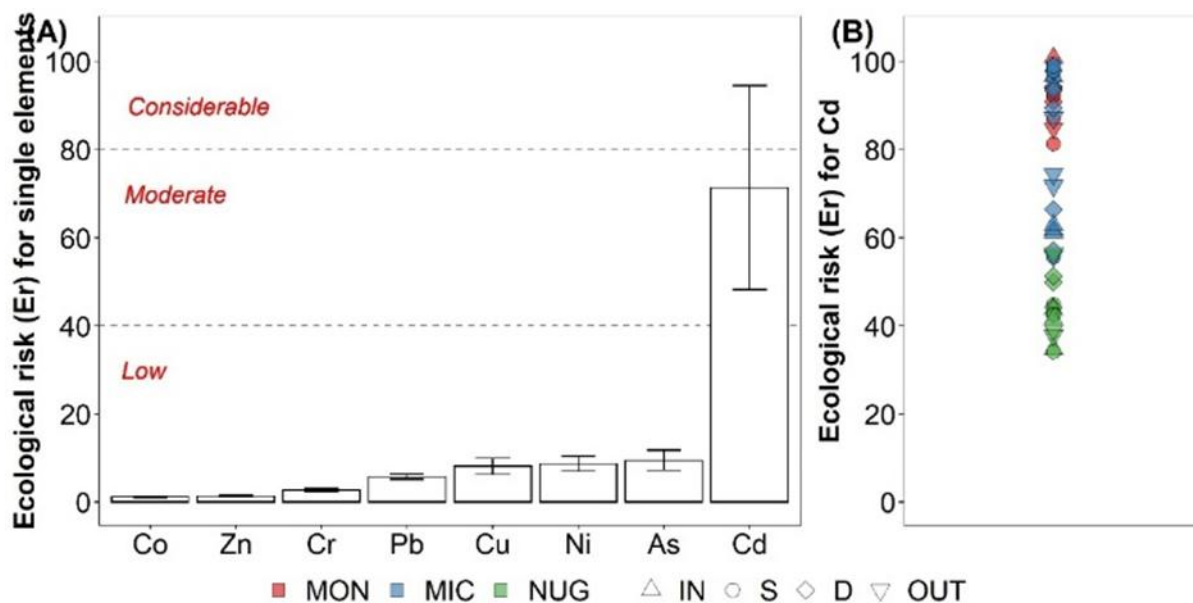


Fig. V-2. (A) The potential ecological risk (Er) of each element for all sediments; (B) Er for Cd in detail. The dashed lines indicate the levels of the potential ecological risk highlighted by the red italic texts.

The relationship between the denitrification, metal concentrations, and the indices were presented in Table V-5. Only  $\log N_2O$  was found to be significantly positively related to the Cu concentration ( $p < 0.05$ ), while other relationships were not significant ( $p > 0.05$ ). However, this relationship was not strong enough to reflect the positive effect of Cu on boosting the  $N_2O$  emission rate, which was evidenced by the unclear linear pattern in Fig. V-3. In general, in the three adjacent agricultural catchments, the denitrification process was not much influenced by neither the metal concentrations nor the overall contamination magnitude.

Table V-5. Relationship of the denitrification process to metal concentrations and their indices.  $\log N_2O = \log_{10}(N_2O \text{ emission rate})$ ,  $\log PDR = \log_{10}(\text{potential denitrification rate})$ .

	Concentration								Index					
	As	Pb	Zn	Co	Cr	Cu	Ni	Cd	CD	mCD	PLI	PI	mPI	PERI
$\log N_2O$	0.29	0.16	0.08	0.20	0.07	0.35	0.15	0.17	0.27	0.27	0.28	0.27	0.14	0.18
$\log PDR$	0.12	-0.08	-0.24	0.03	-0.14	0.02	-0.15	-0.20	-0.09	-0.09	-0.08	-0.09	0.04	-0.18

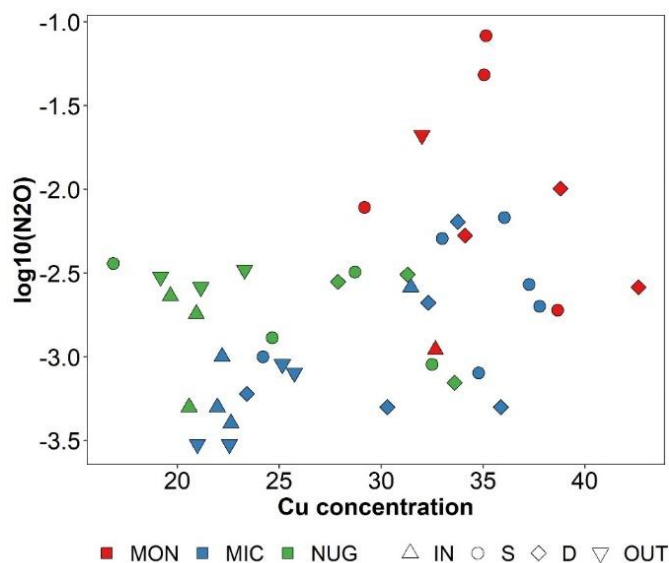


Fig. V-3.  $\log_{10}$ (potential denitrification rate) vs. the sediment clay content in pond sediments. Colors indicated the different catchment (MON = the Montoussé catchment; MIC = the Mican catchment; NUG = the Nuguet catchment), and symbols highlighted the sediment type (stream sediment: IN = inlet | OUT = outlet; pond sediment: S = surface layer | D = deeper layer).

Probable effect quotient (PEQ, %) is a ratio of the concentration of a given metal in the sediment to its PEC regarding to SQGs. Only Ni in some sediments (mainly from MON and MIC) exceeded 100% above which the adverse effect to the living organisms occurred. For other two metals with high anthropogenic inputs (Cd and Cu), their PEQs were far below the threshold, especially for Cd showing the least PEQ (Fig. V-4).

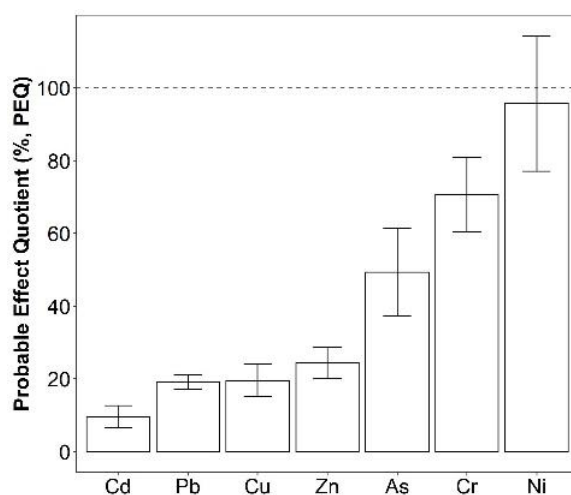


Fig. V-4. Probable effect quotient (PEQ, %) for the concerned metals according to the consensus-based sediment quality guidelines (SQGs). The dashed line indicates below above which the adverse effect on sediment-living organisms.

In summary, the denitrification process was not much inhibited by the metal contaminations in low or low-to-moderately contaminated sites, like the agricultural catchments which were not influenced by the industrial or residential activities. The same observation was also found in the muddy sediment (Magalhães et al., 2005). Labbé et al. (2003) also reported a stimulation for the denitrification process even after the addition of trace metals.

## **2.2 Role of ponds in types of contaminants simultaneously**

Multivariate analyses, including the correlation matrix and the principal analysis (PCA), were conducted to synthetically investigate the role of pond and surrounding environment in mitigating the complex contaminants (nitrate and the potential hazardous metals) simultaneously. The input variables were the denitrification rate (logPDR), the multi-element indices (PLI and PERI), sediment physicochemical characteristics (the organic carbon content (%), Corg; the clay content (%), Clay; Fe concentration; and pH), and the sum of concentration ratio extracted by EDTA (EDTA%). Additional environment factors were also added, e.g., the discharge (Q) for stream sediments, and the hydraulic retention time (HRT) for pond sediments. The PLI showed the highest association with the metal concentrations. In the agricultural catchments, the accumulation of Cd in sediments was mainly due to the fertilizer spreading (N'guessan et al., 2009; Benabdelkader et al., 2018). Therefore, PERI was also a good indicator for the potential ecological risk of Cd as the most remarkable link between PERI and Cd concentration (Table V-4). According to these facts, PLI and PERI were selected to be representative for the sediment contamination intensity, as well as to avoid the redundancy of too many well-related indices used in PCA. The preliminary test for the reliability showed that the datasets were suitable to perform PCA. Three datasets were used for the PCA: (A) all sediments (n = 38), (B) stream sediments (n = 14), and (C) pond sediments (n = 24).

### **2.2.1 All sediments**

The first 3 principal components (PC) explained 77.3% of the total variance, while the first two accounted for 48.0% and 16.3%, respectively (Table V-6A), which explained the majority of the total variance. All the variables can be mainly expressed by these two PCs. Positive variables (PLI, Clay, Fe, PERI, and pH) and one negative variable (EDTA%) were

well associated with PC1, whereas logPDR and Corg were positively related to PC2 (Table V-7A and Fig. V-5A). Though PC3 explained 13.0% of the total variance, only logPDR were found to be significant in this component (Table V-7A).

The PCA for all sediments discriminated the distinctions of the contamination intensity and the denitrification process in stream and pond sediments depending on the individual scores of PC1 and PC2. The individual scores along PC1 (Fig. V-5A right) showed that most of pond sediments were positive, while the negative scores were mainly stream sediments, which indicated that the contamination intensity and the potential ecological risk in pond sediments were normally greater than the conditions in stream sediments. Pond sediments normally possessed higher clay content than stream sediments, contributing to a higher affinity to metals. Thus, the contamination and the potential ecological risk should be more focused on the pond sediments.

Table V-6. Eigenvalues and variance (%) explained by the principal component analysis (PCA): (A) all sediments, (B) stream sediments, and (C) pond sediments.

	(A) All sediments			(B) Stream sediments			(C) Pond sediments		
	Eigenvalue	Total		Eigenvalue	Total		Eigenvalue	Total	
		Variance%	Variance%		Variance%	Variance%		Variance%	Variance%
Dim.1	3.8	48.0	48.0	3.6	39.6	39.6	3.1	34.2	34.2
Dim.2	1.3	16.3	64.3	2.3	25.2	64.8	2.4	26.7	60.9
Dim.3	1.0	13.0	77.3	1.4	15.4	80.2	1.4	15.5	76.3
Dim.4	0.8	10.0	87.3	0.9	9.9	90.0	1.0	11.3	87.6
Dim.5	0.7	8.8	96.1	0.4	4.3	94.4	0.6	6.8	94.4
Dim.6	0.2	2.9	99.0	0.3	3.1	97.5	0.3	3.2	97.6
Dim.7	0.1	1.0	99.9	0.2	1.8	99.3	0.2	1.9	99.5
Dim.8	0.0	0.1	100.0	0.1	0.7	100.0	0.0	0.5	100.0
Dim.9				0.0	0.0	100.0	0.0	0.0	100.0

Table V-7. Loadings and contributions (%) of variables to the first 3 principal components (PC) in PCA for (A) all sediments, (B) stream sediments, and (C) pond sediments. The significant variables to a given PC were highlighted by bold texts. logPDR = log10(potential denitrification rate); PERI = potential ecological risk index; PLI = pollution load index; Clay = sediment clay content; Fe = sediment Fe concentration; EDTA% = the sum of concentration ratios of EDTA-extractable for 8 concerned metals; Corg = sediment organic content; Q = stream discharge; HRT = hydraulic retention time.

Variable	(A) All sediments						(B) Stream sediments						(C) Pond sediments					
	PC1		PC2		PC3		PC1		PC2		PC3		PC1		PC2		PC3	
	r	contrib%	r	contrib%	r	contrib%	r	contrib%	r	contrib%	r	contrib%	r	contrib%	r	contrib%	r	contrib%
PLI	<b>0.94</b>	<b>22.83</b>	0.24	4.31	0.01	0.02	<b>0.95</b>	<b>25.43</b>	0.15	0.93	-0.13	1.14	<b>0.98</b>	<b>30.99</b>	0.17	1.16	0.03	0.06
Clay	<b>0.85</b>	<b>18.92</b>	-0.32	7.80	0.24	5.64	<b>0.75</b>	<b>15.67</b>	-0.15	1.00	0.53	<b>20.31</b>	<b>0.64</b>	<b>13.36</b>	<b>-0.61</b>	<b>15.42</b>	0.38	10.20
Fe	<b>0.82</b>	<b>17.48</b>	-0.16	1.98	0.40	15.50	<b>0.84</b>	<b>19.63</b>	0.31	4.15	-0.05	0.20	<b>0.73</b>	<b>17.20</b>	-0.22	1.96	<b>0.63</b>	<b>28.78</b>
PERI	<b>0.80</b>	<b>16.49</b>	0.46	16.19	-0.28	7.42	<b>0.88</b>	<b>21.53</b>	0.07	0.23	-0.14	1.50	<b>0.84</b>	<b>22.86</b>	0.31	4.03	-0.37	9.78
pH	<b>0.60</b>	<b>9.26</b>	0.42	13.36	-0.40	15.20	-0.08	0.17	0.04	0.07	0.93	<b>61.97</b>	<b>0.61</b>	<b>12.13</b>	0.26	2.72	<b>-0.64</b>	<b>29.01</b>
logPDR	-0.16	0.65	<b>0.50</b>	<b>19.33</b>	<b>0.75</b>	<b>54.06</b>	-0.07	0.13	<b>0.78</b>	<b>27.14</b>	0.16	1.90	-0.23	1.66	<b>0.62</b>	<b>16.01</b>	0.27	5.12
Corg	-0.48	5.97	<b>0.69</b>	<b>36.94</b>	0.09	0.72	0.13	0.46	<b>0.74</b>	<b>24.01</b>	-0.33	8.08	-0.06	0.13	<b>0.88</b>	<b>31.91</b>	0.23	3.86
EDTA%	<b>-0.57</b>	<b>8.39</b>	0.04	0.11	-0.12	1.44	<b>-0.77</b>	<b>16.82</b>	0.41	7.37	-0.05	0.18	-0.16	0.82	-0.25	2.66	0.15	1.51
Q	-	-	-	-	-	-	0.08	0.16	<b>-0.89</b>	<b>35.10</b>	-0.26	4.71	-	-	-	-	-	-
HRT	-	-	-	-	-	-	-	-	-	-	-	-	-0.16	0.84	<b>-0.76</b>	<b>24.12</b>	-0.40	11.68

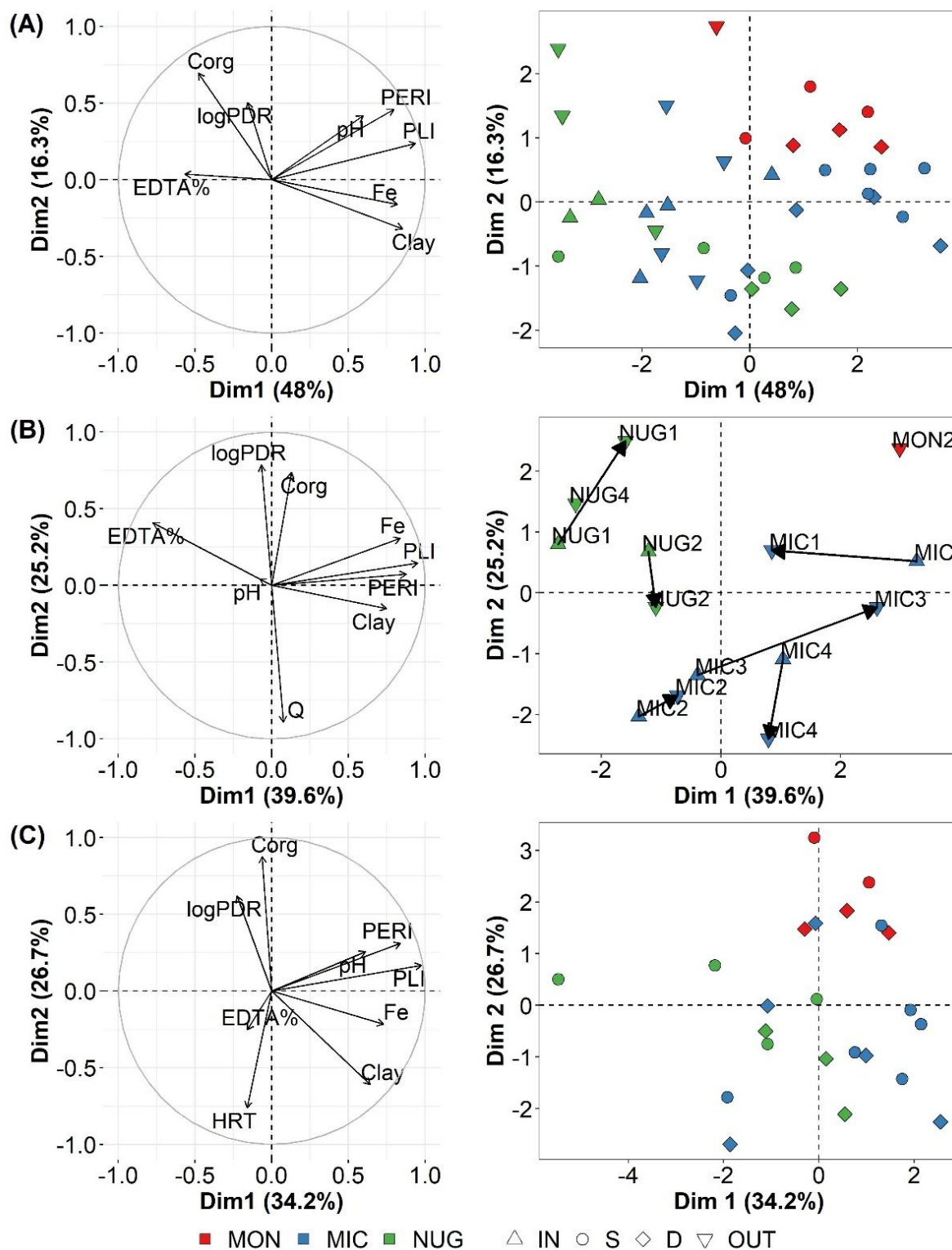


Fig. V-5. Principal component analysis (PCA) for (A) all sediments, (B) stream sediments, and (C) pond sediments. The variable loadings were presented in the left column, while the individual scores for sediments were shown in the right column. Colors indicated the different catchment (MON = the Montoussé catchment; MIC = the Mican catchment; NUG = the Nuguet catchment), and symbols highlighted the sediment type (stream sediment: IN = inlet | OUT = outlet; pond sediment: S = surface layer | D = deeper layer). logPDR =  $\log_{10}$ (potential denitrification rate); PERI = potential ecological risk index; CLI = pollution load index; Clay

= sediment clay content; Fe = sediment Fe concentration; EDTA% = the sum of concentration ratios of EDTA-extractable for 8 concerned metals; Corg = sediment organic content; Q = stream discharge; HRT = hydraulic retention time.

### 2.2.2 Stream and pond sediments

For PCA based on the stream sediments, 80.2% of the total variance was explained by the first 3 PCs, 39.6% for PC1, 25.2% for PC2, and 15.4% for PC3, respectively (Table V-6B). Whereas for PCA based on the pond sediments, the first three PCs explained 76.3% of the total variance (34.2% by PC1, 26.7% by PC2, and 15.5% by PC3, respectively, Table V-6C). In general, the first two components explained more than 60% of the total variance for both stream and pond sediments. Meanwhile, whatever the stream type, PLI, Clay, Fe, and PERI were always well positively associated with PC1 according to their high loadings and contributions to this component, whereas logPDR and Corg were positively linked to PC2. Moreover, some different variables were found to be related to PC1 and PC2 for stream and pond sediments, respectively. The EDTA% was highly associated with PC1 for stream sediments, while for pond sediments, no significant links were found to any first 3 components. In terms of PC2, the stream discharge (Q) was also contributed regarding stream sediments, whereas for pond sediments, Clay and HRT were another two major variables.

The identical major variables expressed by PC1 (e.g., PLI, PERI, Clay, and Fe) for both stream sediments and pond sediments (Fig. V-5BC and Fig. V-7BC) showed the importance of the sediment clay minerals and iron oxides, regardless of the sediment type, in the transfer of metals and the following metallic contamination and potential ecological risk as Clay, Fe, metal concentrations, and integrated indices were well positively related (Table V-4 and Table V-7). Studies have already shown the function of the clay minerals and the iron oxides in regulating the metal concentrations in sediments (Duan et al., 2010). This was also highlighted by the individual scores of sediments along PC1. For stream sediments (Fig. V-5B), the sediments in MON and MIC normally scored higher than those in NUG. The higher slope and larger surface of upstream catchment of MON and MIC could contribute to a great amount of soil erosion and thus bring higher concentrations of metals into the stream, especially for the very upstream sediments (e.g., MON2-OUT and MIC1-IN as they exhibited the highest scores) (see the discussion in Chapter IV). It should be noticed that MIC3-OUT also presented the third highest



score though MIC3 was not located upstream. As a small pond that was never dredged, the accumulation of the sediment in pond was more significant than other dredged ponds, which contributed to the shallow pond water in MIC3. Therefore, the pond sediment could be resuspended and transferred downstream to the outlet by the turbulence of the incoming discharge. As a result, the MIC3-OUT was more contaminated compared to its inlet sediment. The same phenomenon was observed in the outlet sediments from other small or moderate ponds (e.g., MIC2, NUG1, and NUG2) since their scores of outlet sediments in PC1 was higher than those of inlet sediments. The highest difference of PC1 scores between inlet and outlet sediments in MIC3 also indicated the unexpected consequence resulted from the long-term sediment accumulation. The opposite PC1 score trend of stream sediments from two representative very large ponds (e.g., MIC1 and MIC4) also confirmed the function of a large pond to alleviate the downstream metallic contamination in sediments (Casey et al., 2007; Vymazal et al., 2010).

As for all sediments, the EDTA% was highly associated with PC1. Though the metal contamination (the proxy of the metal concentrations) in stream sediments was less than in pond sediments, higher metal concentrations was extracted by EDTA in stream sediments since their affinity to the solid was weaker compared to the pond sediments due to the less existence of clay minerals/iron oxides in stream sediments. The EDTA% was well related to PC1 for stream sediments, while for pond sediments, the EDTA% showed no links to the first 3 PCs. One explanation could be the larger range of clay minerals/iron oxides in stream sediments compared to pond sediments. The variation of clay minerals/iron oxides in pond sediments may not be enough to demonstrate their control over the extractable concentration of metals. The discrepancy of EDTA% between stream and pond sediments also highlighted the excessive potential availability of toxic metals in stream sediments and the function of a constructed pond to alleviate such a risk for surrounding living organics.

In this study, the denitrification process was another considered aspect. However, whatever the sediment type, the denitrification process showed neither straight association with the metal concentration nor with the contamination intensity (Fig. V-5 and Table V-4). The denitrification was always highly related to Corg in sediments (Table V-7, Table V-8, and Fig. V-5), which is consistent with the results from Chapter 3 even the set of the input variables was

different. This supported the power of sediment organic carbon over the denitrification process (Arango et al., 2007). In stream sediments, the denitrification and Corg were also highly negatively related to the discharge (Table V-7B, Table V-8B, and Fig. V-5B). Higher discharge could wash out the Corg in sediments and violate the favorable stagnant condition for the denitrification process, thus contributing to the less denitrification activity (Hernandez and Mitsch, 2007). It can be observed that the NUG stream sediments presented higher denitrification than the MIC since the lower discharge in NUG due to its gentle slope compared to MIC (Fig. V-5B right). Indicated by PCA based on pond sediments, the denitrification was also linked with the sediment clay content (Clay) and the hydraulic retention time (HRT). It was worth noting that, in pond sediments, Clay was a key factor that was both involved in the metal contamination and the denitrification. Though no direct adverse effect of metal contamination on the denitrification, Clay built an indirect connection between these two aspects. The negative relationship between denitrification and Clay was evidenced by the decreasing trend of *log* PDR with the increasing Clay, especially in MON and MIC (Fig. V-6). Studies have shown that a proper clay content may be a beneficial environment for the denitrification process, however, the growth of denitrifiers could be inhibited by the limited sediment pore space with the increasing clay content (Rivett et al., 2008). Thus, it turned out to be that the increasing high clay content in pond sediments could be warning to both the metallic contamination and the deficiency of the denitrification process.

Table V-8. Correlation matrix between the denitrification process, contamination intensity, sediment physicochemical characteristics, and environmental factors for (A) all sediments, (B) stream sediments, and (C) pond sediments. Bold:  $p < 0.01$ , Italic:  $0.01 < p < 0.05$ . logPDR =  $\log_{10}$ (potential denitrification rate); PERI = potential ecological risk index; PLI = pollution load index; Clay = sediment clay content; Fe = sediment Fe concentration; EDTA% = the sum of concentration ratios of EDTA-extractable for 8 concerned metals; Corg = sediment organic content; Q = stream discharge; HRT = hydraulic retention time.

(A) All sediments									
	PLI	PERI	EDTA%	logPDR	Corg	Clay	pH		
PERI	<b>0.88</b>								
EDTA%	<b>-0.56</b>	<b>-0.53</b>							
logPDR	-0.13	-0.24	-0.01						
Corg	-0.19	-0.06	0.20	<i>0.38</i>					
Clay	<b>0.71</b>	<b>0.42</b>	<b>-0.45</b>	-0.20	<b>-0.55</b>				
pH	<b>0.52</b>	<b>0.62</b>	-0.29	-0.08	-0.12	0.24			
Fe	<b>0.81</b>	<b>0.47</b>	<i>-0.41</i>	-0.03	-0.31	<b>0.87</b>	0.16		
(B) Stream sediments									
	PLI	PERI	EDTA%	logPDR	Corg	Clay	pH	Fe	
PERI	<b>0.95</b>								
EDTA%	<b>-0.72</b>	<i>-0.59</i>							
logPDR	-0.27	-0.33	0.30						
Corg	0.27	0.31	0.10	0.32					
Clay	<i>0.64</i>	0.49	<b>-0.77</b>	-0.11	-0.23				
pH	-0.03	0.09	0.08	-0.08	-0.02	0.02			
Fe	<b>0.71</b>	0.52	<i>-0.60</i>	0.16	0.16	<i>0.64</i>	-0.36		
Q	-0.05	-0.13	-0.32	<i>-0.56</i>	<i>-0.56</i>	0.25	-0.35	-0.18	
(C) Pond sediments									
	PLI	PERI	EDTA%	logPDR	Corg	Clay	pH	Fe	
PERI	<b>0.92</b>								
EDTA%	<i>-0.46</i>	<i>-0.51</i>							
logPDR	-0.12	-0.19	-0.10						
Corg	-0.01	0.01	-0.04	<i>0.51</i>					
Clay	0.33	0.16	-0.03	-0.40	<b>-0.59</b>				
pH	<b>0.53</b>	<b>0.61</b>	-0.39	-0.09	0.03	-0.07			
Fe	<b>0.55</b>	0.24	-0.03	-0.10	-0.19	<b>0.75</b>	-0.10		
HRT	-0.03	0.13	-0.13	-0.39	<b>-0.72</b>	0.29	0.18	-0.28	

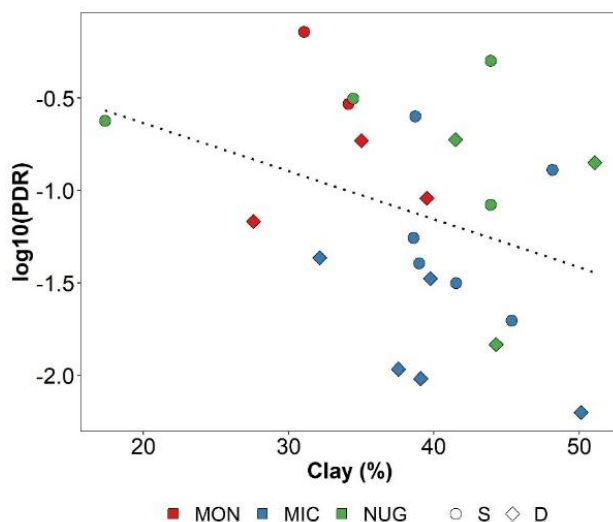


Fig. V-6.  $\log_{10}$ (potential denitrification rate) vs. the sediment clay content in pond sediments. Colors indicated the different catchment (MON = the Montoussé catchment; MIC = the Mican catchment; NUG = the Nuguet catchment), and symbols highlighted the layer of pond sediments (S = surface layer | D = deeper layer).

Finally, a schematic diagram showed the geophysicochemical controlling factors of the denitrification and the metal contamination simultaneously for different categories of sediments (Fig. V-7).

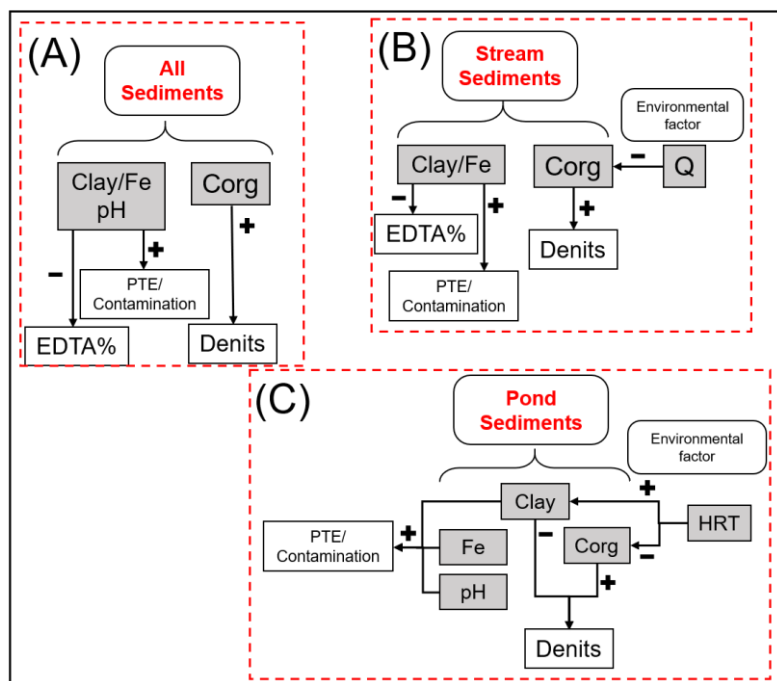


Fig. V-7. Schematic diagrams that depicted the geophysicochemical controlling factors for the denitrification and the metal contamination simultaneously regarding different categories of sediments: (A) all sediments, (B) stream sediments, and (C) pond sediments.

## Summary

This study applied several mostly used integrated multi-element indices (PLI, CD, mCD, PI, mPI, and PERI) to assess the overall metallic contamination in both stream and pond sediments from the three adjacent agricultural catchments in southwestern France. Considering the ways of calculating the indices and their trigger threshold for classifying the levels of contamination, it was evidenced that PLI, CD, and PERI could be reliable to assess the contamination intensity in the sediments from the catchments, at a small scale, where the industrial and residential pollutants were not severe. Low-to-moderate contamination were observed in the sediments from these three cultivated catchments, especially for the sediments located upstream. Low potential ecological risk in these sediments, as well as mostly below the probable effect concentrations regarding the sediment quality guidelines, showed that the toxicity was not considerable and may not much influence the denitrification process. This was also confirmed by the fact that the potential denitrification rates and the N<sub>2</sub>O emission rate were independent of the metal concentrations or the contamination intensities in sediments.

The high clay content resulted in the high contamination in sediments. Therefore, more attention should be paid to the pond sediments as they contained more finer particles than the stream sediments, particularly for the large ponds and the pond never dredged. However, the proportion of extractable metal concentration was higher in stream sediments due to the less affinity to metals resulted from the deficiency of fine particles. This would also alarm the potential extractability by surrounding living organisms in stream sediments. In terms of small ponds, the outlet sediment was exposed to a secondary metallic contamination resulting from the pond sediment resuspension and transfer downstream by inlet discharge. Though, whatever the sediment type, the denitrification process was not influenced by the metal contamination, clay was an indirect factor that affect this microbial activity since the excessively high content of clay may inhibit the growth of microbiomes due to the reduced pore space.

## **Conclusion and perspectives**

## Conclusions and perspectives

### Conclusion

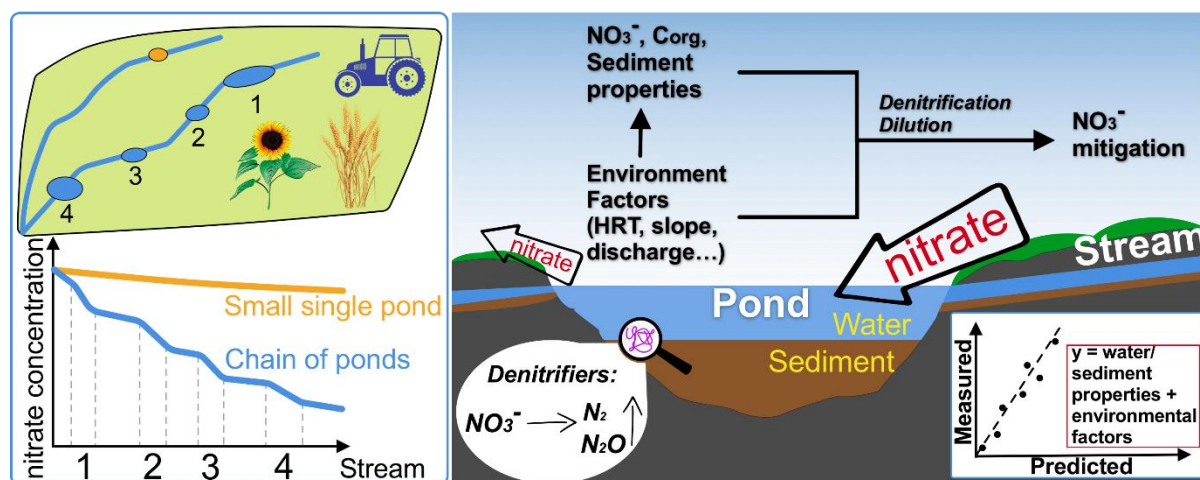
Intensively agricultural activities in southwestern France can lead to serious environmental issues, such as high-level of nitrate ( $\text{NO}_3^-$ ) concentration in drinking water and accumulation of potential hazardous element (PTE) in sediments. Nitrate concentration in waters denitrification rate in sediments, PTE concentrations in sediments, bio-physicochemical characteristics of waters and sediments, environmental properties of catchments and constructed ponds were investigated in this thesis in three adjacent agricultural catchments (the Montoussé catchment, MON; the Mican catchment, MIC; the Nuguet catchment, NUG) in the Save basin, southwestern France to mainly fill the gap of knowledge of the role of constructed ponds in the distribution of  $\text{NO}_3^-$  and PTEs in streams and ponds, respectively, which is rarely studied at a small catchment scale.

#### **Denitrification rate and nitrate ( $\text{NO}_3^-$ ) behavior**

A spatial variation of denitrification rate was observed even in three adjacent small catchments, ranging from 0.00126 to 2.19  $\mu\text{g N g}^{-1}$  dry sediment  $\text{h}^{-1}$ , which was however one order of magnitude higher than groundwater sediment in the Garonne river. Regardless the sediment type (stream or pond), potential denitrification rate (PDR) was controlled by sediment organic carbon ( $C_{\text{org}}$ ) in common. The stream sediment was additionally controlled by water  $\text{NO}_3^-$  in overlying water, while the pond sediment not. Hence, PDR was more active in the stream sediments than in the pond sediment due to the sustainable supply of water  $\text{NO}_3^-$  and  $C_{\text{org}}$  brought by the stream water compared to the continuously consumed nutrients in pond sediments. High PDR in stream sediments can boost the  $\text{NO}_3^-$  mitigation in stream water, but the high discharge diluted the  $\text{NO}_3^-$  concentration, which could indirectly lower downstream PDR. In pond sediments, HRT and pond slope can also affect the PDR indirectly. Longer HRT and flat pond slope inhibited the  $\text{NO}_3^-$  supply and contributed to the consumption of  $\text{NO}_3^-$  and  $C_{\text{org}}$ . Moreover, the abundance of denitrifiers were found to be much lower in a long-HRT

pond. These all together contributed to a low PDR. In terms of pond sediments in different benthic depths, the surface sediments showed a higher PDR than the deeper sediment due to the availability of nutrients and the abundance of denitrifiers. Predictive empirical models proposed a combination of easily measured characteristics of waters and sediments as well as originally considered the important role of environmental factors related to catchments and constructed sediments.

A high level of  $\text{NO}_3^-$  concentration ( $> 60 \text{ mg L}^{-1}$ ) was always observed in upstream waters, especially in steeper catchments (MON and MIC). Due to the denitrification process and the discharge dilution effect,  $\text{NO}_3^-$  generally decreased along the stream channel. It was also found that a chain of several constructed ponds in MIC and NUG generally performed a more efficient nitrate removal than a single pond in MON (though it is in upstream). A chain of ponds provided a long-HRT situation where  $\text{NO}_3^-$  can be mitigated by denitrification in a favorable stagnant environment even though a long HRT would negatively affect this process.



### Potential toxic element (PTE)

Two single element indicators (the geoaccumulation index,  $I_{\text{geo}}$ ; the enrichment factor, EF) were used to assess the contamination intensities of each PTE (e.g., As, Pb, Co, Cr, Zn, Cu, Ni, and Cd) in stream and pond sediments, respectively. Arsenic, Pb, Co, Cr, and Zn were not enriched in sediments, indicating their natural origin from the molasse bedrock weathering process. Cadmium was the most enriched element ( $\text{EF} > 1.5$ ), which was comparable to other



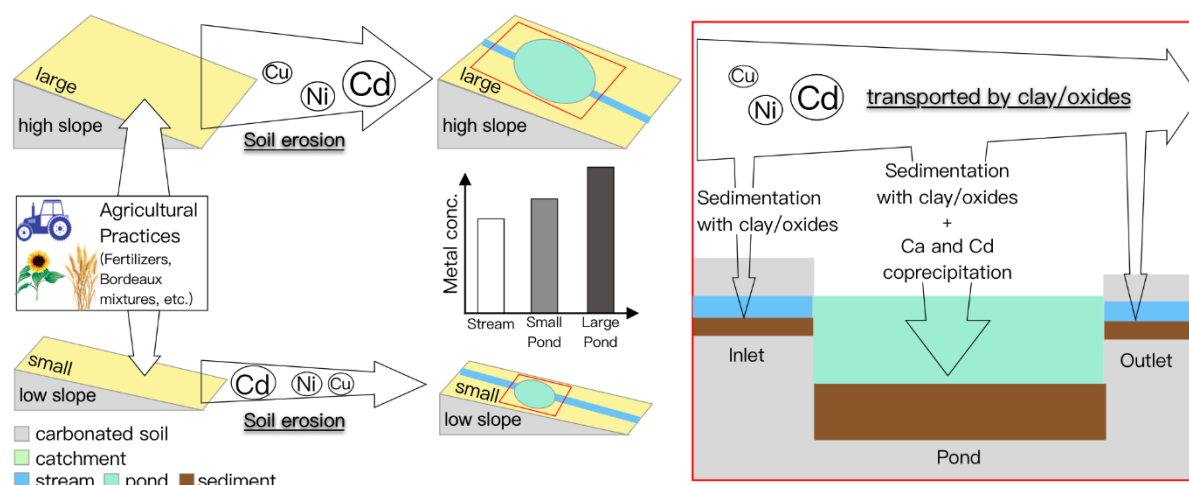
agricultural areas. The average EFs of Cu and Ni were close to 1.5. The use of local molasse bedrock and Cs as the reference element in calculating EF assured the accuracy of interpretation regarding the identification of natural/anthropogenic sources of PTEs. The anthropogenic contribution (AC, %) quantified a significant anthropogenic impact on Cu, Ni, and Cd, in increasing order. The spreading of N-P-K fertilizers and pesticides in upstream soils was the main anthropogenic source for Cu, Ni, and Cd, and the Bordeaux mixtures used in the ancient vineyards also contributed to Cu, especially in MON. In general, a higher EF was observed in sediments from upstream catchments and in MIC compared to in NUG, and there was no difference between surface and deeper sediments (though the “deeper” sediment in this study was actually not so deep, which was only 30 cm maximum beneath the water-sediment interface).

The highest finer particle content contributed to the highest concentration of PTEs observed in pond sediments. Clay minerals and/or iron oxides were key factors in the distribution of most PTEs (except for As and Cd). Cadmium showed different controlling factors between stream and pond sediments. In stream, sediments, Cd was more controlled by silicates (clay and iron oxides), while in pond sediments, longer HRT and increased water temperature contributed to Cd co-precipitation with calcite due to higher pH conditions and Ca content. This explained the difference in the control of Cd observed between the catchments MIC (with high carbonate content) and NUG (with more acid soil context). Arsenic was bound to manganese oxides and/or complexed with  $C_{org}$  in stream sediments.

In general, Cu, Pb, and Cd showed the highest EDTA extractability, suggesting a hazardous potential environmental risk, whereas the lower Ni extractability may be due to a lesser extraction efficiency of the extractant. Extractability was affected by the calcite content in sediments due to the dissolution of calcite and the consequent pH increase, since the highest anthropogenically affected sediments (MIC) exhibited the lower extractability. Surprisingly, the coarse sediments from streams supported a higher proportion of extractable PTEs.

The geomorphological properties of the catchments and the management of constructed ponds can affect the spatial variation of PTE concentrations. The larger surface area of an upper sub-catchment and the steeper slope leads to higher PTE accumulation in stream and pond sediments, especially for anthropogenically originating elements, relative to intensive fertilizer

spreading, the greater soil erosion and surface runoff. The increasing discharge along the channel contributes to the dilution of PTEs downstream. While the constructed pond having a considerable HRT can be a sink for fine particles and PTEs, the non-dredged ponds were vulnerable to particle resuspension and the transfer of PTEs downstream. Ponds temporarily ensure a storage of sediments, and sediment dredging activity therefore contributes to regularly remove the PTEs associated with the accumulated sediments, but this involves planning for their downstream treatment.

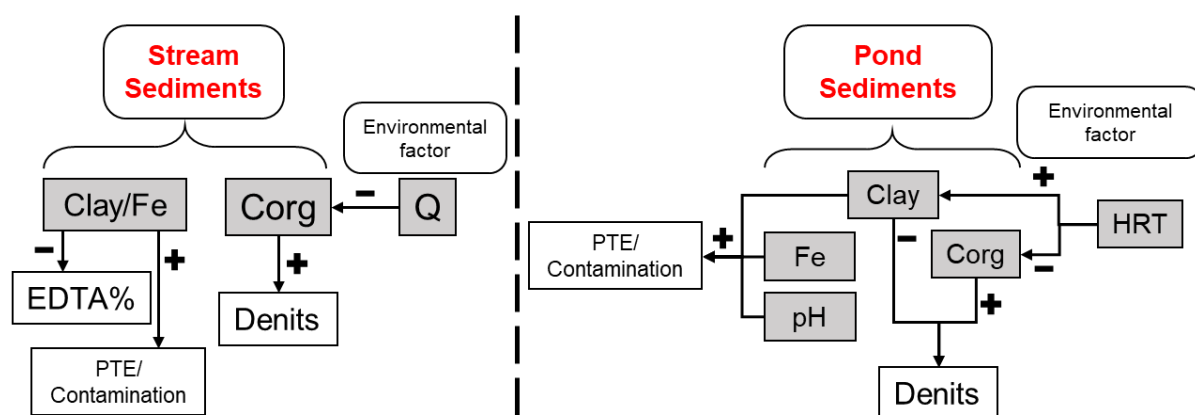


### **Links between denitrification and PTE and roles of ponds in two types of contaminants simultaneously**

Several mostly used integrated multi-element indices were calculated to assess the overall PTE contamination in both stream and pond sediments, which can overcome the deficiency of the single element indicators ( $I_{geo}$  and EF). Moreover, we can link the denitrification rate with the multi-element indices to have an overall view of the relationships between denitrification and PTE contamination. Considering the ways of calculating the indices and their trigger thresholds for classifying the levels of PTE contamination, it was evidenced that PLI, CD, and PERI could be reliable to assess the contamination intensity in the sediments from the agricultural catchments at a small scale, where the industrial and residential pollutants were not severe. Low-to-moderate contamination were observed in the sediments from these three cultivated catchments, especially for the sediments located upstream. Low potential ecological

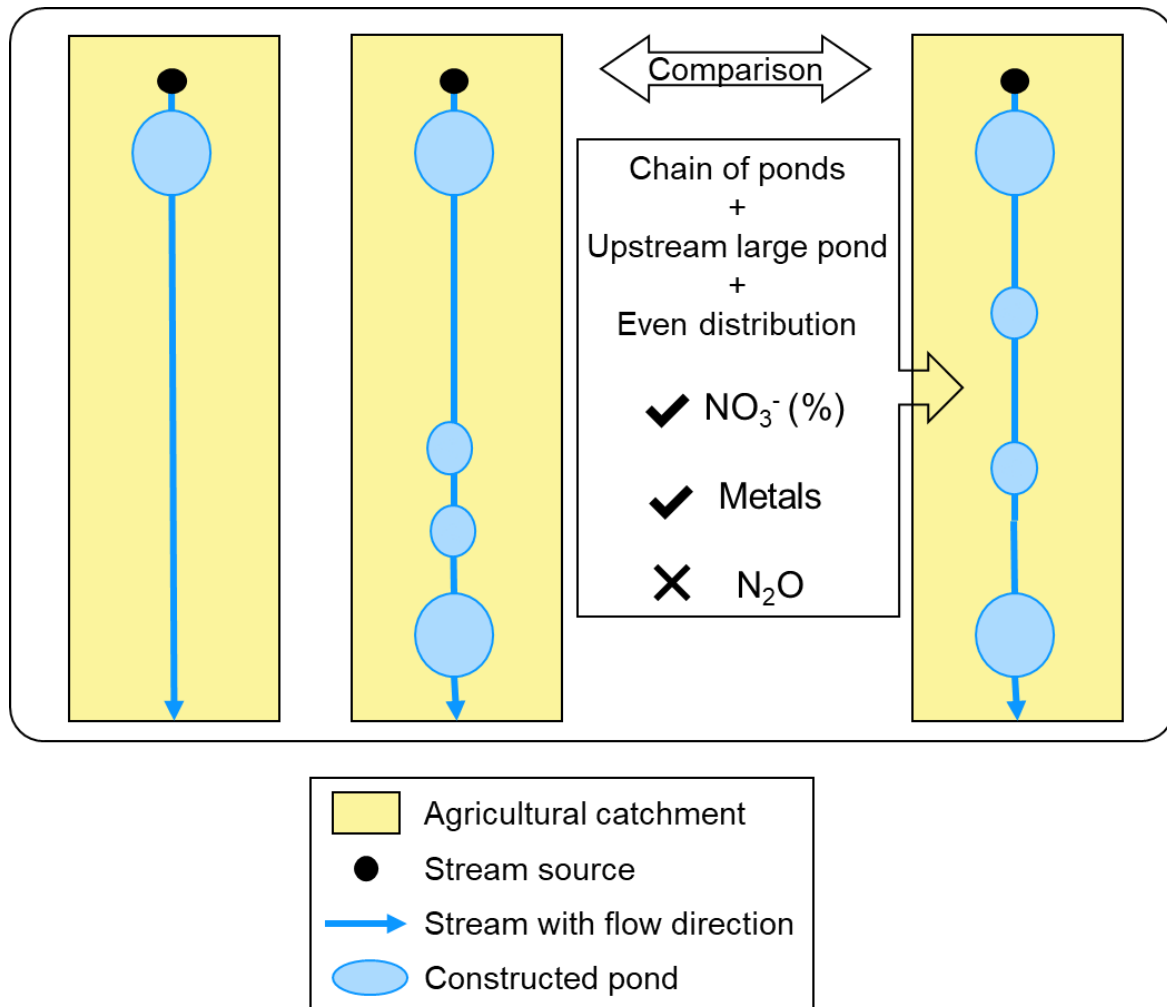
risk in these sediments, as well as mostly below the probable effect concentrations regarding the sediment quality guidelines (SQGs), showed that the toxicity was not considerable and may not much influence the denitrification process. This was also confirmed by the fact that the potential denitrification rates and the N<sub>2</sub>O emission rate were independent of the metal concentrations or the contamination intensities in sediments by multivariate analyses.

The high clay content resulted in the high contamination in sediments. Therefore, more attention should be paid to the pond sediments as they contained more finer particles than the stream sediments, particularly for the large ponds and the pond never dredged. However, the proportion of extractable metal concentration was higher in stream sediments due to the less affinity to metals resulted from the deficiency of fine particles. This would also alarm the potential extractability by surrounding living organisms in stream sediments. Though, whatever the sediment type, the denitrification process was not influenced by the metal contamination, clay was an indirect factor that affect this microbial activity since the excessively rather high content of clay may inhibit the growth of microbiomes due to the reduced pore space.



In general, pond management should pay attention to both denitrification and PTE accumulation. Upstream large pond with fine sediment and long HRT can store high proportion of PTEs, while it can also inhibit denitrification rate. However, nitrate level in large pond was greatly reduced due to long reaction time of denitrification, which is offset by long reaction time due to long HRT. A chain of several evenly distributed ponds in a given agricultural stream

is preferable to store PTEs and to mitigate excessive nitrate, especially with some large ponds located in upstream. Outlet stream sediment may become a secondary source of downstream PTEs due to the turbulence of discharge removing particles charged with PTEs, especially in the shallow pond, which has never been dredged. The dredging activity for pond sediments should also be cautiously managed to prevent the dredged sediments from being a secondary source of PTEs.



## Perspectives

### Nitrate and denitrification

Unfortunately, the higher but incomplete denitrification process observed in upstream ponds can contribute to unexpected large  $N_2O$  emissions. Other studies have already observed the incomplete denitrification under the high nitrate condition. The consequence of  $N_2O$  emission as greenhouse gas from stream and pond sediments should be investigated in further studies to assess the benefits and/or drawbacks on a global nitrogen removal and the climate change by constructed ponds. Several studies also carried out various methods to alter the  $N_2O:N_2$  production ratio, such as the regulation of nitrate and organic carbon availability, control stream pH, and addition of engineered substance, etc. This is also of great interest to make constructed ponds more environmentally friendly.

Temporal (seasonal and annual) survey of both hydrology and denitrification should also be investigated. These management tools must also be combined with upstream measurements, such as limitation of N-P-K fertilizers and landscaping, which is shown to reduce  $NO_3^-$  input to stream waters in the agricultural areas.

The respective contribution of denitrification,  $NO_3^-$ , pond/catchment environmental factors should be investigated in depth in order to optimize the management of a chain of constructed ponds.

### PTE

It has to be admitted that the so called “deeper” sediments in this study was actually not deep enough. Further study can collect the sediments much deeper to investigate the horizontal gradient of PTE distribution.

Like nitrate and denitrification, temporal distribution of PTEs in sediments is lacking in current study, which can become one focus to trace the continuous function of constructed ponds in mitigating contaminants.

### **Internal links between denitrification, PTEs, and pesticides**

In traditional agricultural areas, one has to be cautious that pesticides represent very significant contaminants to the ecosystem. This is the case for the studied catchments. Consequently, they have to be considered in further studies that is currently the case with the ANR PESTIPOND project (<https://pestipond.cnrs.fr/>). Indeed, as an example, if the inhibition of denitrification was not observed regarding PTEs, it may be the case with pesticides contamination. If PTEs are conservative in the system, it is not the case for pesticides, and this may lead to adapt the conclusions in terms of pond management process. Some new results related to the pesticides and ponds in the area can be found in Chaumet et al. (2021).

### **Pilot test**

Field experiments are time and monetary consuming. Moreover, the monitoring programs in the CZO is a passive process. An ordinary way of CZO study is usually “Sample collection → Sample analysis → Data treatment → Result interpretation”. However, it cannot evaluate the feasibility, duration, cost, and other aspects regarding the new ideas or proposals based on the interpretation of the long-term monitored data. A pilot test platform may be much preferable for advances in investigating the optimization of a constructed wetlands.

## Conclusions et perspectives

### Conclusions

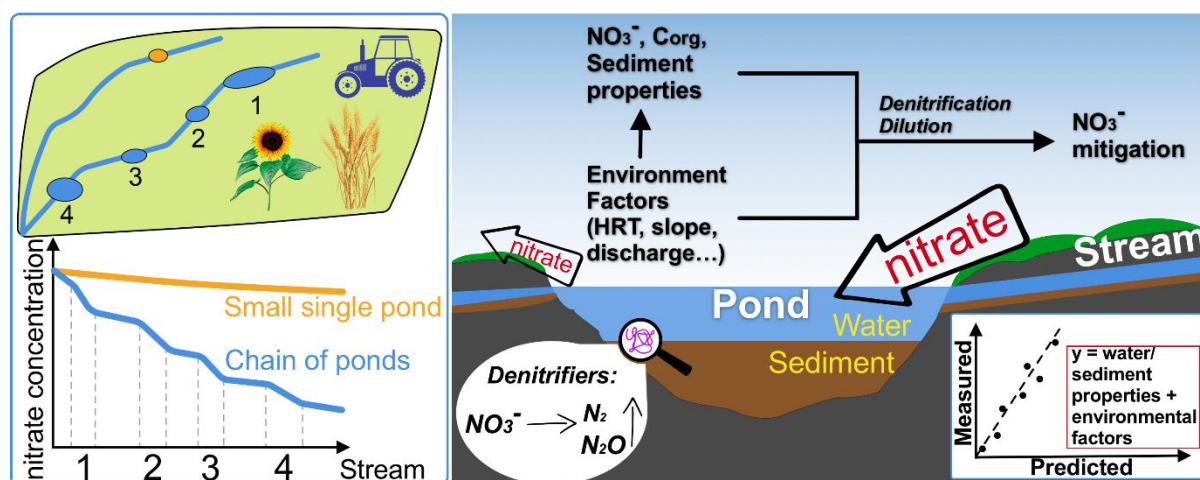
Les activités agricoles intensives dans le sud-ouest de la France peuvent entraîner de graves problèmes environnementaux, tels qu'une concentration élevée de nitrates ( $\text{NO}_3^-$ ) dans l'eau potable et une accumulation des ETPs dans les sédiments. La concentration de nitrate dans les eaux, le taux de dénitrification dans les sédiments, les concentrations de ETP dans les sédiments, les caractéristiques bio-physicochimiques des eaux et des sédiments, les propriétés environnementales des bassins versants et des étangs construits ont été étudiés dans cette thèse dans trois bassins versants agricoles adjacents (le bassin versant de Montoussé, MON; le bassin versant du Mican, MIC; le bassin versant du Nuguet, NUG) dans le bassin de Save, dans le sud-ouest de la France pour combler principalement le manque de connaissances sur le rôle des étangs construits dans la distribution du  $\text{NO}_3^-$  et des ETPs dans les cours d'eau et les étangs, petite échelle de captage.

#### Taux de dénitrification et $\text{NO}_3^-$

Une variation spatiale du taux de dénitrification a été observée même dans trois petits bassins versants adjacents, allant de 0,00126 à 2,19  $\mu\text{g N g}^{-1}$  de sédiment  $\text{sec h}^{-1}$ , qui était cependant d'un ordre de grandeur plus élevé que les sédiments souterrains de la Garonne. Quel que soit le type de sédiment (cours d'eau ou étang), le taux de dénitrification potentiel (TDP) était contrôlé par le carbone organique des sédiments (Corg) en commun. Les sédiments fluviaux étaient en outre contrôlés par l'eau  $\text{NO}_3^-$  dans l'eau sus-jacente, contrairement aux sédiments de l'étang. Par conséquent, le PDR était plus actif dans les sédiments des cours d'eau que dans les sédiments de l'étang en raison de l'approvisionnement durable en eau  $\text{NO}_3^-$  et Corg apportés par l'eau du cours d'eau par rapport aux nutriments consommés en continu dans les sédiments de l'étang. Un TDP élevé dans les sédiments des cours d'eau peut augmenter l'atténuation du  $\text{NO}_3^-$  dans l'eau des cours d'eau, mais le débit élevé a dilué la concentration de

$\text{NO}_3^-$ , ce qui pourrait indirectement abaisser le TDP en aval. Dans les sédiments des étangs, la TRH et la pente de l'étang peuvent également affecter indirectement le PDR. Un TRH plus long et une pente plate de l'étang ont inhibé l'apport de  $\text{NO}_3^-$  et contribué à la consommation de  $\text{NO}_3^-$  et de Corg. De plus, l'abondance des dénitrificateurs s'est avérée beaucoup plus faible dans un étang à longue TRH. Tous ces éléments ont contribué à un TDP faible. En termes de sédiments d'étang à différentes profondeurs benthiques, les sédiments de surface ont montré un TDP plus élevé que les sédiments plus profonds en raison de la disponibilité des nutriments et de l'abondance des dénitrifiants. Les modèles empiriques prédictifs ont proposé une combinaison de caractéristiques facilement mesurables des eaux et des sédiments et ont initialement considéré le rôle important des facteurs environnementaux liés aux bassins versants et aux sédiments construits.

Un niveau élevé de concentration de  $\text{NO}_3^-$  ( $> 60 \text{ mg L}^{-1}$ ) a toujours été observé dans les eaux en amont, en particulier dans les bassins versants plus raides (MON et MIC). En raison du processus de dénitrification et de l'effet de dilution des rejets, le  $\text{NO}_3^-$  a généralement diminué le long du canal du cours d'eau. Il a également été constaté qu'une chaîne de plusieurs étangs construits dans MIC et NUG effectuait généralement une élimination des nitrates plus efficace qu'un seul étang dans MON (bien qu'il soit en amont). Une chaîne d'étangs a fourni une situation de TRH longue où le  $\text{NO}_3^-$  peut être atténué par la dénitrification dans un environnement stagnant favorable même si un TRH long aurait un effet négatif sur ce processus.





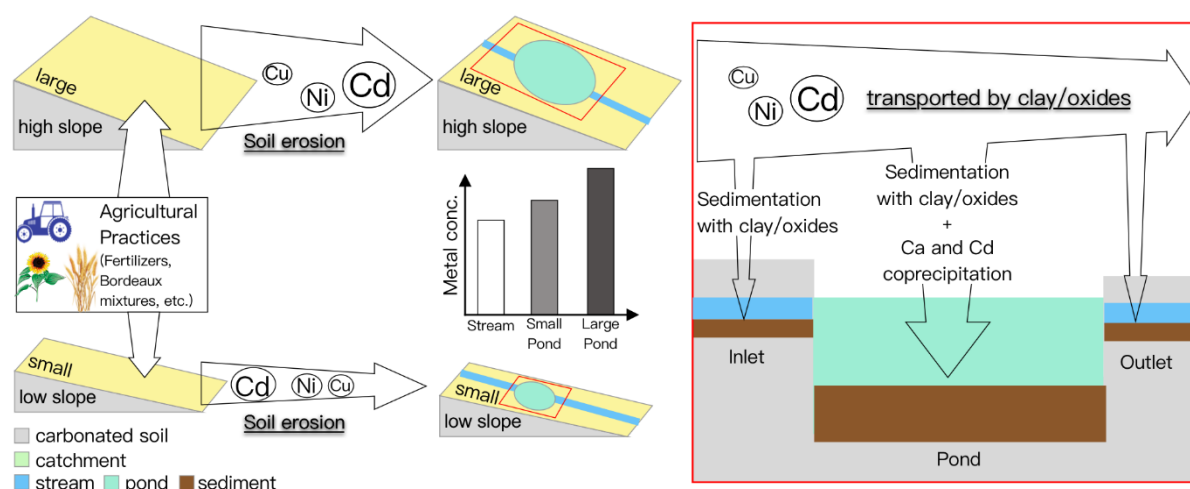
### **Élément toxique potentiel (ETP)**

Deux indicateurs à un seul élément (l'indice de géoaccumulation,  $I_{geo}$  ; le facteur d'enrichissement, FE) ont été utilisés pour évaluer les intensités de contamination de chaque ETP (par exemple, As, Pb, Co, Cr, Zn, Cu, Ni et Cd) dans les cours d'eau et sédiments de l'étang, respectivement. L'arsenic, le Pb, le Co, le Cr et le Zn n'étaient pas enrichis en sédiments, ce qui indique leur origine naturelle à partir du processus d'altération du substrat rocheux de la molasse. Le cadmium était l'élément le plus enrichi ( $FE > 1,5$ ), ce qui était comparable à d'autres zones agricoles. Les FE moyens de Cu et Ni étaient proches de 1,5. L'utilisation du substratum de molasse locale et du C comme élément de référence dans le calcul de l'FE a assuré l'exactitude de l'interprétation concernant l'identification des sources naturelles / anthropiques de ETP. La contribution anthropique (CA, %) a quantifié un impact anthropique significatif sur Cu, Ni et Cd, par ordre croissant. L'épandage d'engrais et de pesticides dans les sols en amont était la principale source anthropique de Cu, Ni et Cd, et les bouillies bordelaises utilisés dans les anciens vignobles contribuaient également au Cu, en particulier dans le MON. En général, une FE plus élevée a été observée dans les sédiments des bassins versants en amont et dans la MIC par rapport à la NUG, et il n'y avait pas de différence entre les sédiments de surface et les sédiments plus profonds (bien que le sédiment « plus profond » dans cette étude n'était en fait pas si 30 cm maximum sous l'interface eau-sédiment).

La teneur la plus élevée en particules fines a contribué à la plus forte concentration de ETP observée dans les sédiments des étangs. Les minéraux argileux et / ou les oxydes de fer étaient des facteurs clés dans la distribution de la plupart des ETP (à l'exception de l'As et du Cd). Le cadmium a montré différents facteurs de contrôle entre les sédiments des cours d'eau et des étangs. Dans les ruisseaux, les sédiments, le Cd était plus contrôlé par les silicates (argile et oxydes de fer), tandis que dans les sédiments des étangs, un TRH plus long et une température de l'eau plus élevée ont contribué à la coprécipitation du Cd avec la calcite en raison des conditions de pH et de la teneur en Ca plus élevées. Ceci explique la différence de contrôle du Cd observée entre les bassins versants MIC (à forte teneur en carbonate) et NUG (avec un contexte de sol plus acide). L'arsenic était lié aux oxydes de manganèse et / ou complexé avec le Corg dans les sédiments fluviaux.

En général, Cu, Pb et Cd ont montré la plus grande capacité d'extraction de l'EDTA, ce qui suggère un risque environnemental potentiel dangereux, tandis que l'extraction plus faible du Ni peut être due à une efficacité d'extraction moindre de l'agent d'extraction. L'extractibilité a été affectée par la teneur en calcite dans les sédiments en raison de la dissolution de la calcite et de l'augmentation conséquente du pH, puisque les sédiments anthropogéniquement affectés (MIC) les plus élevés présentaient une extractibilité plus faible. Étonnamment, les sédiments grossiers des ruisseaux supportaient une proportion plus élevée de ETP extractibles.

Les propriétés géomorphologiques des bassins versants et la gestion des étangs construits peuvent affecter la variation spatiale des concentrations de ETP. La plus grande superficie d'un sous-bassin supérieur et la pente plus raide entraînent une accumulation plus élevée de ETP dans les sédiments des cours d'eau et des étangs, en particulier pour les éléments d'origine anthropique, par rapport à l'épandage intensif d'engrais, à une plus grande érosion du sol et au ruissellement de surface. Le rejet croissant le long du chenal contribue à la dilution des ETP en aval. Alors que l'étang construit ayant une TRH considérable peut être un puits pour les particules fines et les ETP, les étangs non dragués étaient vulnérables à la remise en suspension des particules et au transfert de ETP en aval. Les étangs assurent temporairement un stockage des sédiments, et l'activité de dragage des sédiments contribue donc à éliminer régulièrement les ETP associés aux sédiments accumulés, mais cela implique de planifier leur traitement en aval.

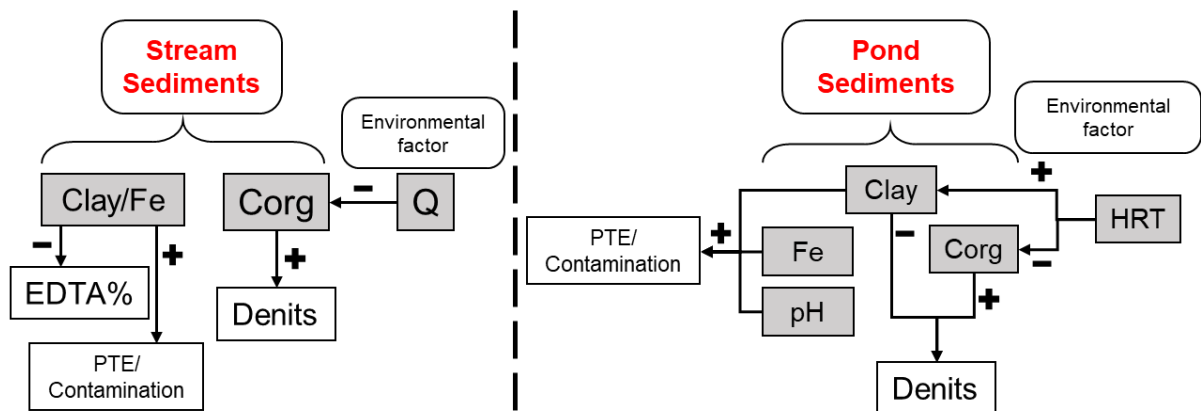


## **Liens entre dénitrification et ETP et rôle des étangs dans deux types de contaminants simultanément**

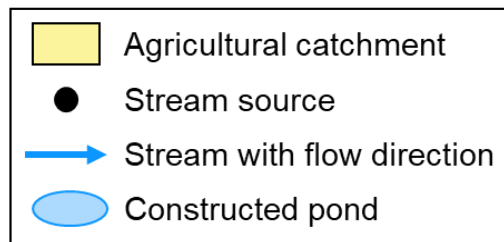
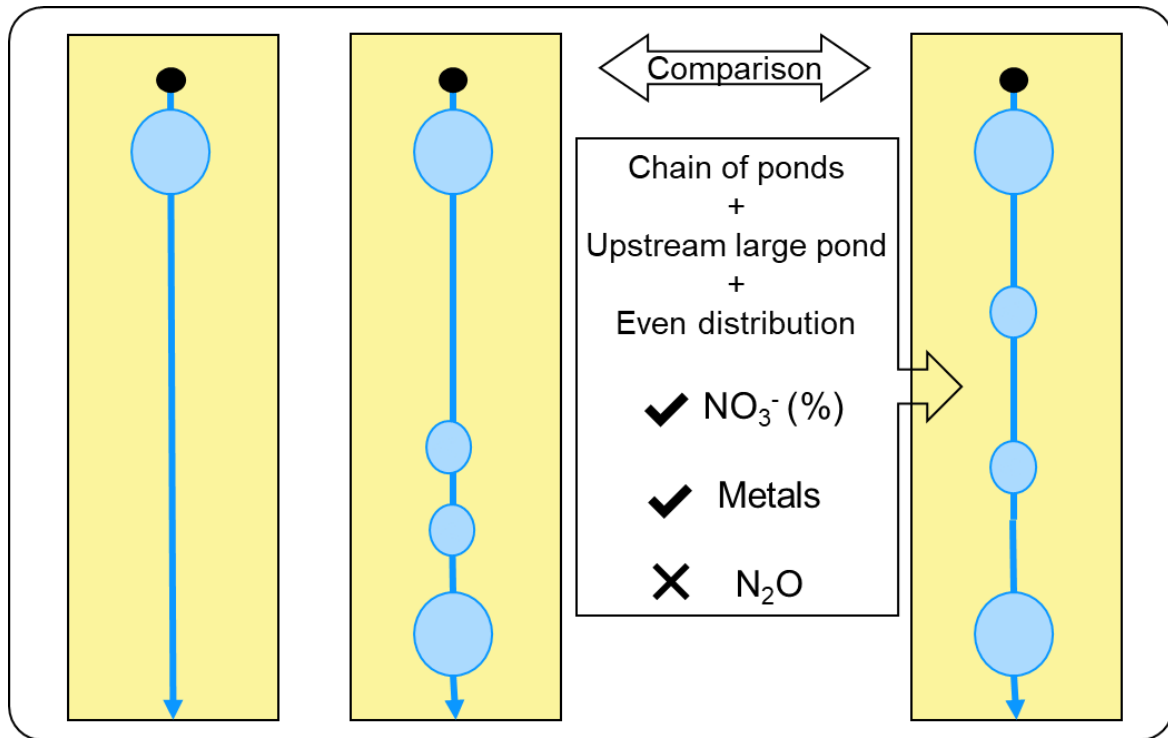
Plusieurs indices multi-éléments intégrés principalement utilisés ont été calculés pour évaluer la contamination globale au ETP dans les sédiments des cours d'eau et des étangs, ce qui peut pallier la carence des indicateurs à élément unique (Igeo et FE). De plus, nous pouvons relier le taux de dénitrification aux indices multi-éléments pour avoir une vision globale des relations entre dénitrification et contamination par ETP. Compte tenu des méthodes de calcul des indices et de leurs seuils de déclenchement pour classer les niveaux de contamination ETP, il a été démontré que PLI, CD et PERI pouvaient être fiables pour évaluer l'intensité de la contamination dans les sédiments des bassins versants agricoles à petite échelle, où les polluants industriels et résidentiels n'étaient pas graves. Une contamination faible à modérée a été observée dans les sédiments de ces trois bassins cultivés, notamment pour les sédiments situés en amont. Le faible risque écologique potentiel dans ces sédiments, ainsi que la plupart du temps en deçà des concentrations avec effet probable selon les recommandations pour la qualité des sédiments (SQG), a montré que la toxicité n'était pas considérable et pourrait peu influencer le processus de dénitrification. Cela a également été confirmé par le fait que les taux potentiels de dénitrification et le taux d'émission de N<sub>2</sub>O étaient indépendants des concentrations métalliques ou des intensités de contamination dans les sédiments par des analyses multivariées.

La teneur élevée en argile a entraîné une forte contamination des sédiments. Par conséquent, une plus grande attention devrait être accordée aux sédiments de l'étang car ils contenaient plus de particules plus fines que les sédiments du cours d'eau, en particulier pour les grands étangs et l'étang jamais dragué. Cependant, la proportion de concentration de métaux extractibles était plus élevée dans les sédiments fluviaux en raison de la moindre affinité pour les métaux résultant de la carence en particules fines. Cela alerterait également sur l'extraction potentielle des organismes vivants environnants dans les sédiments des cours d'eau. Bien que, quel que soit le type de sédiment, le processus de dénitrification n'ait pas été influencé par la contamination métallique, l'argile était un facteur indirect qui affectait cette activité microbienne car la teneur excessivement assez élevée en argile peut inhiber la croissance des

microbiomes en raison de l'espace poreux réduit.



En général, la gestion des étangs doit prêter attention à la fois à la dénitrification et à l'accumulation de ETP. Un grand étang en amont avec des sédiments fins et un TRH long peut stocker une forte proportion de ETP, alors qu'il peut également inhiber le taux de dénitrification. Cependant, le niveau de nitrate dans les grands étangs a été considérablement réduit en raison du long temps de réaction de dénitrification, qui est compensé par un long temps de réaction dû à un TRH long. Une chaîne de plusieurs étangs construits dans un courant agricole donné est préférable pour stocker les ETP et pour atténuer l'excès de nitrate, en particulier avec certains grands étangs situés en amont. Les sédiments du courant de sortie peuvent devenir une source secondaire de ETP en aval en raison de la turbulence des rejets éliminant les particules chargées de ETP, en particulier dans l'étang peu profond, qui n'a jamais été dragué. L'activité de dragage des sédiments des étangs doit également être gérée avec prudence pour éviter que les sédiments dragués ne soient une source secondaire de ETP.



## **Perspectives**

### **Nitrate et dénitrification**

Malheureusement, le processus de dénitrification plus élevé mais incomplet observé dans les étangs en amont peut contribuer à d'importantes émissions de  $N_2O$  inattendues. D'autres études ont déjà observé la dénitrification incomplète dans des conditions de nitrate élevé. Les conséquences de l'émission de  $N_2O$  sous forme de gaz à effet de serre provenant des sédiments des cours d'eau et des étangs devraient être étudiées dans des études complémentaires pour évaluer les avantages et / ou les inconvénients d'une élimination globale de l'azote et du changement climatique par les étangs construits. Plusieurs études ont également mené à bien diverses méthodes pour modifier le rapport de production de  $N_2O$  :  $N_2$ , telles que la régulation de la disponibilité des nitrates et du carbone organique, le contrôle du pH du courant et l'ajout de substances artificielles, etc. écologique.

Une étude temporelle (saisonnière et annuelle) de l'hydrologie et de la dénitrification devrait également être étudiée. Ces outils de gestion doivent également être combinés avec des mesures en amont, comme la limitation des engrais N-P-K et l'aménagement paysager, qui réduisent l'apport de  $NO_3^-$  dans les eaux des cours d'eau dans les zones agricoles.

La contribution respective des facteurs environnementaux de dénitrification, de  $NO_3^-$ , bassin / bassin versant doit être étudiée en profondeur afin d'optimiser la gestion d'une chaîne d'étangs construits.

### **ETP**

Il faut admettre que les sédiments dits « plus profonds » dans cette étude n'étaient en fait pas assez profonds. Une étude plus approfondie peut collecter les sédiments beaucoup plus profondément pour étudier le gradient horizontal de la distribution du ETP.

Comme le nitrate et la dénitrification, la distribution temporelle des PTE dans les sédiments fait défaut dans l'étude actuelle, qui peut devenir un objectif pour retracer la fonction

continue des étangs construits dans l'atténuation des contaminants.

### **Liens internes entre dénitrification, ETP et pesticides**

Dans les zones agricoles traditionnelles, il faut être prudent que les pesticides représentent des contaminants très importants pour l'écosystème. C'est le cas des bassins versants étudiés. Par conséquent, ils doivent être pris en compte dans des études complémentaires comme c'est actuellement le cas avec le projet ANR PESTIPOND (<https://pestipond.cnrs.fr/>). En effet, à titre d'exemple, si l'inhibition de la dénitrification n'a pas été observée vis-à-vis des ETP, cela peut être le cas avec la contamination par les pesticides. Si les ETP sont conservateurs dans le système, ce n'est pas le cas pour les pesticides et cela peut conduire à adapter les conclusions en termes de processus de gestion des bassins.

### **Test pilote**

Les expériences sur le terrain demandent du temps et de l'argent. De plus, les programmes de surveillance dans le CZO sont un processus passif. Une méthode ordinaire d'étude CZO est généralement «Prélèvement d'échantillons → Analyse d'échantillon → Traitement des données → Interprétation des résultats». Cependant, il ne peut pas évaluer la faisabilité, la durée, le coût et d'autres aspects concernant les nouvelles idées ou propositions sur la base de l'interprétation des données suivies à long terme. Une plate-forme d'essai pilote peut être de loin préférable pour les progrès dans l'étude de l'optimisation d'une zone humide construite.

## References

### A

- Abraham, G. M. S., & Parker, R. J. (2008). Assessment of heavy metal enrichment factors and the degree of contamination in marine sediments from Tamaki Estuary, Auckland, New Zealand. *Environmental Monitoring and Assessment*, *136*(1), 227–238. <https://doi.org/10.1007/s10661-007-9678-2>
- Acevedo-Figueroa, D., Jiménez, B. D., & Rodríguez-Sierra, C. J. (2006). Trace metals in sediments of two estuarine lagoons from Puerto Rico. *Environmental Pollution*, *141*(2), 336–342. <https://doi.org/10.1016/j.envpol.2005.08.037>
- Ackrill, R. (2000). *Common Agricultural Policy*. A&C Black.
- Ali, H., Khan, E., & Ilahi, I. (2019, March 5). *Environmental Chemistry and Ecotoxicology of Hazardous Heavy Metals: Environmental Persistence, Toxicity, and Bioaccumulation* [Review Article]. *Journal of Chemistry*; Hindawi. <https://doi.org/10.1155/2019/6730305>
- Almaraz, M., Wong, M. Y., & Yang, W. H. (2020). Looking back to look ahead: A vision for soil denitrification research. *Ecology*, *101*(1). <https://doi.org/10.1002/ecy.2917>
- Alvarez-Cobelas, M., Angeler, D. G., & Sánchez-Carrillo, S. (2008). Export of nitrogen from catchments: A worldwide analysis. *Environmental Pollution*, *156*(2), 261–269. <https://doi.org/10.1016/j.envpol.2008.02.016>
- Arango, C. P., Tank, J. L., Schaller, J. L., Royer, T. V., Bernot, M. J., & David, M. B. (2007). Benthic organic carbon influences denitrification in streams with high nitrate concentration. *Freshwater Biology*, *52*(7), 1210–1222. <https://doi.org/10.1111/j.1365-2427.2007.01758.x>
- Attard, E., Recous, S., Chabbi, A., Berranger, C. D., Guillaumaud, N., Labreuche, J., Philippot, L., Schmid, B., & Roux, X. L. (2011). Soil environmental conditions rather than denitrifier abundance and diversity drive potential denitrification after changes in land uses. *Global Change Biology*, *17*(5), 1975–1989. <https://doi.org/10.1111/j.1365-2486.2010.02340.x>
- Audry, S., Schäfer, J., Blanc, G., & Jouanneau, J.-M. (2004). Fifty-year sedimentary record of heavy metal pollution (Cd, Zn, Cu, Pb) in the Lot River reservoirs (France). *Environmental Pollution*, *132*(3), 413–426. <https://doi.org/10.1016/j.envpol.2004.05.025>

### B

- Baeseman, J. L., Smith, R. L., & Silverstein, J. (2006). Denitrification Potential in Stream Sediments Impacted by Acid Mine Drainage: Effects of pH, Various Electron Donors, and Iron. *Microbial Ecology*, *51*(2), 232–241. <https://doi.org/10.1007/s00248-005-5155-z>
- Barraclough, D., & Puri, G. (1995). The use of <sup>15</sup>N pool dilution and enrichment to separate the heterotrophic and autotrophic pathways of nitrification. *Soil Biology and Biochemistry*, *27*(1), 17–22. [https://doi.org/10.1016/0038-0717\(94\)00141-M](https://doi.org/10.1016/0038-0717(94)00141-M)
- Basic Research Opportunities in Earth Science* (p. 9981). (2001). National Academies Press. <https://doi.org/10.17226/9981>
- Bates, R. L., & Jackson, J. A. (1987). *Glossary of geology*. <https://www.osti.gov/biblio/5128638>
- Beaulieu, J. J., Tank, J. L., Hamilton, S. K., Wollheim, W. M., Hall, R. O., Mulholland, P. J., Peterson, B. J., Ashkenas, L. R., Cooper, L. W., Dahm, C. N., Dodds, W. K., Grimm, N.



- B., Johnson, S. L., McDowell, W. H., Poole, G. C., Valett, H. M., Arango, C. P., Bernot, M. J., Burgin, A. J., ... Thomas, S. M. (2011). Nitrous oxide emission from denitrification in stream and river networks. *Proceedings of the National Academy of Sciences*, *108*(1), 214–219. <https://doi.org/10.1073/pnas.1011464108>
- Benabdelkader, A., Taleb, A., Probst, J. L., Belaidi, N., & Probst, A. (2018). Anthropogenic contribution and influencing factors on metal features in fluvial sediments from a semi-arid Mediterranean river basin (Tafna River, Algeria): A multi-indices approach. *Science of The Total Environment*, *626*, 899–914. <https://doi.org/10.1016/j.scitotenv.2018.01.107>
- Bernard-Jannin, L., Sun, X., Teissier, S., Sauvage, S., & Sánchez-Pérez, J.-M. (2017). Spatio-temporal analysis of factors controlling nitrate dynamics and potential denitrification hot spots and hot moments in groundwater of an alluvial floodplain. *Ecological Engineering*, *103*(Part B), 372–384. <https://doi.org/10.1016/j.ecoleng.2015.12.031>
- Białowiec, A., Janczukowicz, W., & Randerson, P. F. (2011). Nitrogen removal from wastewater in vertical flow constructed wetlands containing LWA/gravel layers and reed vegetation. *Ecological Engineering*, *37*(6), 897–902. <https://doi.org/10.1016/j.ecoleng.2011.01.013>
- Bijay-singh, Ryden, J. C., & Whithead, D. C. (1988). Some relationships between denitrification potential and fractions of organic carbon in air-dried and field-moist soils. *Soil Biology and Biochemistry*, *20*(5), 737–741. [https://doi.org/10.1016/0038-0717\(88\)90160-5](https://doi.org/10.1016/0038-0717(88)90160-5)
- Bing, H., Zhou, J., Wu, Y., Wang, X., Sun, H., & Li, R. (2016). Current state, sources, and potential risk of heavy metals in sediments of Three Gorges Reservoir, China. *Environmental Pollution*, *214*, 485–496. <https://doi.org/10.1016/j.envpol.2016.04.062>
- Birgand, F., Skaggs, R. W., Chescheir, G. M., & Gilliam, J. W. (2007). Nitrogen Removal in Streams of Agricultural Catchments—A Literature Review. *Critical Reviews in Environmental Science and Technology*, *37*(5), 381–487. <https://doi.org/10.1080/10643380600966426>
- Blackmer, A. M., & Bremner, J. M. (1977). Nitrogen isotope discrimination in denitrification of nitrate in soils. *Soil Biology and Biochemistry*, *9*(2), 73–77. [https://doi.org/10.1016/0038-0717\(77\)90040-2](https://doi.org/10.1016/0038-0717(77)90040-2)
- Blaszczak, J. R., Steele, M. K., Badgley, B. D., Heffernan, J. B., Hobbie, S. E., Morse, J. L., Rivers, E. N., Hall, S. J., Neill, C., Pataki, D. E., Groffman, P. M., & Bernhardt, E. S. (2018). Sediment chemistry of urban stormwater ponds and controls on denitrification. *Ecosphere*, *9*(6), e02318. <https://doi.org/10.1002/ecs2.2318>
- Boggs Jr, S. (2014). Principles of sedimentology and stratigraphy. Pearson Education.
- Boithias, L., Sauvage, S., Taghavi, L., Merlina, G., Probst, J.-L., & Sánchez Pérez, J. M. (2011). Occurrence of metolachlor and trifluralin losses in the Save river agricultural catchment during floods. *Journal of Hazardous Materials*, *196*, 210–219. <https://doi.org/10.1016/j.jhazmat.2011.09.012>
- Boithias, L., Srinivasan, R., Sauvage, S., Macary, F., & Sánchez-Pérez, J. M. (2014). Daily Nitrate Losses: Implication on Long-Term River Quality in an Intensive Agricultural Catchment of Southwestern France. *Journal of Environment Quality*, *43*(1), 46. <https://doi.org/10.2134/jeq2011.0367>
- Brady, J. P., Ayoko, G. A., Martens, W. N., & Goonetilleke, A. (2015). Development of a hybrid

- pollution index for heavy metals in marine and estuarine sediments. *Environmental Monitoring and Assessment*, 187(5), 306. <https://doi.org/10.1007/s10661-015-4563-x>
- Braker, G., Zhou, J., Wu, L., Devol, A. H., & Tiedje, J. M. (2000). Nitrite Reductase Genes (nirK and nirS) as Functional Markers To Investigate Diversity of Denitrifying Bacteria in Pacific Northwest Marine Sediment Communities. *Applied and Environmental Microbiology*, 66(5), 2096–2104. <https://doi.org/10.1128/AEM.66.5.2096-2104.2000>
- Brantley, S. L., Goldhaber, M. B., & Ragnarsdottir, K. V. (2007). Crossing Disciplines and Scales to Understand the Critical Zone. *Elements*, 3(5), 307–314. <https://doi.org/10.2113/gselements.3.5.307>
- Brunet, R. C., & Garcia-Gil, L. J. (1996). Sulfide-induced dissimilatory nitrate reduction to ammonia in anaerobic freshwater sediments. *FEMS Microbiology Ecology*, 21(2), 131–138. <https://doi.org/10.1111/j.1574-6941.1996.tb00340.x>
- Bur, T., Crouau, Y., Bianco, A., Gandois, L., & Probst, A. (2012). Toxicity of Pb and of Pb/Cd combination on the springtail *Folsomia candida* in natural soils: Reproduction, growth and bioaccumulation as indicators. *Science of The Total Environment*, 414, 187–197. <https://doi.org/10.1016/j.scitotenv.2011.10.029>
- Bur, T., Probst, A., Bianco, A., Gandois, L., & Crouau, Y. (2010). Determining cadmium critical concentrations in natural soils by assessing Collembola mortality, reproduction and growth. *Ecotoxicology and Environmental Safety*, 73(3), 415–422. <https://doi.org/10.1016/j.ecoenv.2009.10.010>
- Bur, T., Probst, J. L., N'guessan, M., & Probst, A. (2009). Distribution and origin of lead in stream sediments from small agricultural catchments draining Miocene molassic deposits (SW France). *Applied Geochemistry*, 24(7), 1324–1338. <https://doi.org/10.1016/j.apgeochem.2009.04.004>
- Burgin, A. J., & Hamilton, S. K. (2007). Have we overemphasized the role of denitrification in aquatic ecosystems? A review of nitrate removal pathways. *Frontiers in Ecology and the Environment*, 5(2), 89–96. [https://doi.org/10.1890/1540-9295\(2007\)5\[89:HWOTRO\]2.0.CO;2](https://doi.org/10.1890/1540-9295(2007)5[89:HWOTRO]2.0.CO;2)
- Bushaw, K. L., Zepp, R. G., Tarr, M. A., Schulz-Jander, D., Bourbonniere, R. A., Hodson, R. E., Miller, W. L., Bronk, D. A., & Moran, M. A. (1996). Photochemical release of biologically available nitrogen from aquatic dissolved organic matter. *Nature*, 381(6581), 404–407. <https://doi.org/10.1038/381404a0>
- Butterbach-Bahl, K., & Dannenmann, M. (2011). Denitrification and associated soil N<sub>2</sub>O emissions due to agricultural activities in a changing climate. *Current Opinion in Environmental Sustainability*, 3(5), 389–395. <https://doi.org/10.1016/j.cosust.2011.08.004>

## C

- Camargo Valero, M. A., Read, L. F., Mara, D. D., Newton, R. J., Curtis, T. P., & Davenport, R. J. (2010). Nitrification–denitrification in waste stabilisation ponds: A mechanism for permanent nitrogen removal in maturation ponds. *Water Science and Technology*, 61(5), 1137–1146. <https://doi.org/10.2166/wst.2010.963>
- Cameron, E. N. (1980). Evolution of the Lower Critical Zone, central sector, eastern Bushveld Complex, and its chromite deposits. *Economic Geology*, 75(6), 845–871. <https://doi.org/10.2113/gsecongeo.75.6.845>

- Carluer, N., Babut, M., Belliard, J., Bernez, I., Leblanc, B., Burger-Leenhardt, D., Dorioz, J. M., Douez, O., Dufour, S., Grimaldi, S., Habets, F., Le Bissonnais, Y., Molenat, J., Rollet, A. J., Rosset, V., Sauvage, S., & Usseglio-Polatera, P. (2017). *Impact cumulé des retenues d'eau sur le milieu aquatique*. Expertise scientifique collective (Irstea).
- Casal, L., Durand, P., Akkal-Corfini, N., Benhamou, C., Laurent, F., Salmon-Monviola, J., Ferrant, S., Probst, A., Probst, J.-L., & Vertès, F. (2019). Reduction of stream nitrate concentrations by land management in contrasted landscapes. *Nutrient Cycling in Agroecosystems*, 114(1), 1–17. <https://doi.org/10.1007/s10705-019-09985-0>
- Casey, R. E., Simon, J. A., Atueyi, S., Snodgrass, J. W., Karouna-Renier, N., & Sparling, D. W. (2007). Temporal Trends of Trace Metals in Sediment and Invertebrates from Stormwater Management Ponds. *Water, Air, and Soil Pollution*, 178(1), 69–77. <https://doi.org/10.1007/s11270-006-9132-z>
- Cayeux, L. (1935). *Les Roches sédimentaires de France. Roches carbonatées calcaires et dolomies*. - Paris: Masson 1935. IV, 463 S., XXVI Taf. 4°. Masson et Cie.
- Çevik, F., Göksu, M. Z. L., Dericci, O. B., & Findik, Ö. (2009). An assessment of metal pollution in surface sediments of Seyhan dam by using enrichment factor, geoaccumulation index and statistical analyses. *Environmental Monitoring and Assessment*, 152(1–4), 309–317. <https://doi.org/10.1007/s10661-008-0317-3>
- Chaumet, B.; Probst, J.-L.; Eon, P.; Camboulive, T.; Riboul, D.; Payré-Suc, V.; Granouillac, F.; Probst, A. Role of Pond Sediments for Trapping Pesticides in an Agricultural Catchment (Auradé, SW France): Distribution and Controlling Factors. *Water* 2021, 13, 1734. <https://doi.org/10.3390/w13131734>
- Chen, N., Wu, J., Chen, Z., Lu, T., & Wang, L. (2014). Spatial-temporal variation of dissolved N<sub>2</sub> and denitrification in an agricultural river network, southeast China. *Agriculture, Ecosystems & Environment*, 189, 1–10. <https://doi.org/10.1016/j.agee.2014.03.004>
- Chester, R., & Stoner, J. H. (1973). Pb in Particulates from the Lower Atmosphere of the Eastern Atlantic. *Nature*, 245(5419), 27–28. <https://doi.org/10.1038/245027b0>
- Chorover, J., Troch, P. A., Rasmussen, C., Brooks, P. D., Pelletier, J. D., Breshears, D. D., Huxman, T. E., Kurc, S. A., Lohse, K. A., McIntosh, J. C., Meixner, T., Schaap, M. G., Litvak, M. E., Perdrial, J., Harpold, A., & Durcik, M. (2011). How Water, Carbon, and Energy Drive Critical Zone Evolution: The Jemez-Santa Catalina Critical Zone Observatory. *Vadose Zone Journal*, 10(3), 884–899. <https://doi.org/10.2136/vzj2010.0132>
- Clow, D. W., & Sueker, J. K. (2000). Relations between basin characteristics and stream water chemistry in alpine/subalpine basins in Rocky Mountain National Park, Colorado. *Water Resources Research*, 36(1), 49–61. <https://doi.org/10.1029/1999WR900294>

## D

- Davidson, E. A., Chorover, J., & Dail, D. B. (2003). A mechanism of abiotic immobilization of nitrate in forest ecosystems: The ferrous wheel hypothesis. *Global Change Biology*, 9(2), 228–236. <https://doi.org/10.1046/j.1365-2486.2003.00592.x>
- Dhir, B., Sharmila, P., & Saradhi, P. P. (2009). Potential of Aquatic Macrophytes for Removing Contaminants from the Environment. *Critical Reviews in Environmental Science and Technology*, 39(9), 754–781. <https://doi.org/10.1080/10643380801977776>
- Dong, L. F., Smith, C. J., Papaspyrou, S., Stott, A., Osborn, A. M., & Nedwell, D. B. (2009).

- Changes in Benthic Denitrification, Nitrate Ammonification, and Anammox Process Rates and Nitrate and Nitrite Reductase Gene Abundances along an Estuarine Nutrient Gradient (the Colne Estuary, United Kingdom). *Applied and Environmental Microbiology*, 75(10), 3171–3179. <https://doi.org/10.1128/AEM.02511-08>
- Du Laing, G., Vandecasteele, B., De Grauwe, P., Moors, W., Lesage, E., Meers, E., Tack, F. M. G., & Verloo, M. G. (2007). Factors affecting metal concentrations in the upper sediment layer of intertidal reedbeds along the river Scheldt. *Journal of Environmental Monitoring*, 9(5), 449. <https://doi.org/10.1039/b618772b>
- Duan, L., Song, J., Xu, Y., Li, X., & Zhang, Y. (2010). The distribution, enrichment and source of potential harmful elements in surface sediments of Bohai Bay, North China. *Journal of Hazardous Materials*, 183(1), 155–164. <https://doi.org/10.1016/j.jhazmat.2010.07.005>
- Duodu, G. O., Goonetilleke, A., & Ayoko, G. A. (2016). Comparison of pollution indices for the assessment of heavy metal in Brisbane River sediment. *Environmental Pollution*, 219, 1077–1091. <https://doi.org/10.1016/j.envpol.2016.09.008>
- Duplay, J., Semhi, K., Errais, E., Imfeld, G., Babcsanyi, I., & Perrone, T. (2014). Copper, zinc, lead and cadmium bioavailability and retention in vineyard soils (Rouffach, France): The impact of cultural practices. *Geoderma*, 230–231, 318–328. <https://doi.org/10.1016/j.geoderma.2014.04.022>

## E

- Earth's critical zone. (2019). In *Wikipedia*. [https://en.wikipedia.org/w/index.php?title=Earth%27s\\_critical\\_zone&oldid=913440367](https://en.wikipedia.org/w/index.php?title=Earth%27s_critical_zone&oldid=913440367)
- El Azzi, D., Laurent, F., Roussiez, V., Chou, L., Guisresse, M., & Probst, J.-L. (2018). Adsorption of Aclonifen, Alachlor, Cd and Cu onto Natural River Suspended Matter in the Context of Multi-Pollutions: Influence of Contaminant Co-Presence and Order of Input into the Aqueous Solution. *Water*, 10(9), 1222. <https://doi.org/10.3390/w10091222>
- EPA. (2002). *Nitrification*. [https://www.epa.gov/sites/production/files/2015-09/documents/nitrification\\_1.pdf](https://www.epa.gov/sites/production/files/2015-09/documents/nitrification_1.pdf)
- Erisman, J. W., Sutton, M. A., Galloway, J., Klimont, Z., & Winiwarter, W. (2008). How a century of ammonia synthesis changed the world. *Nature Geoscience*, 1(10), 636–639. <https://doi.org/10.1038/ngeo325>

## F

- FAO. (2014). *World reference base for soil resources 2014: International soil classification system for naming soils and creating legends for soil maps*. FAO.
- FAO. (2020). *The State of Food and Agriculture 2020*. FAO. <https://doi.org/10.4060/cb1447en>
- Ferati, F., Kerolli-Mustafa, M., & Kraja-Ylli, A. (2015). Assessment of heavy metal contamination in water and sediments of Trepça and Sitnica rivers, Kosovo, using pollution indicators and multivariate cluster analysis. *Environmental Monitoring and Assessment*, 187(6), 338. <https://doi.org/10.1007/s10661-015-4524-4>
- Ferrant, S., Oehler, F., Durand, P., Ruiz, L., Salmon-Monviola, J., Justes, E., Dugast, P., Probst, A., Probst, J.-L., & Sanchez-Perez, J.-M. (2011). Understanding nitrogen transfer dynamics in a small agricultural catchment: Comparison of a distributed (TNT2) and a semi distributed (SWAT) modeling approaches. *Journal of Hydrology*, 406(1–2), 1–15.

- <https://doi.org/10.1016/j.jhydrol.2011.05.026>
- Fisher, J., & Acreman, M. C. (2004). Wetland nutrient removal: A review of the evidence. *Hydrology and Earth System Sciences*, 8(4), 673–685. <https://doi.org/10.5194/hess-8-673-2004>
- Friedl, J., De Rosa, D., Rowlings, D. W., Grace, P. R., Müller, C., & Scheer, C. (2018). Dissimilatory nitrate reduction to ammonium (DNRA), not denitrification dominates nitrate reduction in subtropical pasture soils upon rewetting. *Soil Biology and Biochemistry*, 125, 340–349. <https://doi.org/10.1016/j.soilbio.2018.07.024>
- Frink, C. R., Waggoner, P. E., & Ausubel, J. H. (1999). Nitrogen fertilizer: Retrospect and prospect. *Proceedings of the National Academy of Sciences*, 96(4), 1175–1180. <https://doi.org/10.1073/pnas.96.4.1175>
- Frost, P. C., Song, K., Buttle, J. M., Marsalek, J., McDonald, A., & Xenopoulos, M. A. (2015). Urban biogeochemistry of trace elements: What can the sediments of stormwater ponds tell us? *Urban Ecosystems*, 18(3), 763–775. <https://doi.org/10.1007/s11252-014-0428-2>

## G

- Gail, M. (1998). *Where are we headed? Soft rock research into the new millenium*.
- Gaillardet, J., Braud, I., Hankard, F., Anquetin, S., Bour, O., Dorfliger, N., Dreuzy, J. R. de, Galle, S., Galy, C., Gogo, S., Gourcy, L., Habets, F., Laggoun, F., Longuevergne, L., Borgne, T. L., Naaim-Bouvet, F., Nord, G., Simonneaux, V., Six, D., ... Zitouna, R. (2018). OZCAR: The French Network of Critical Zone Observatories. *Vadose Zone Journal*, 17(1), 1–24. <https://doi.org/10.2136/vzj2018.04.0067>
- Galloway, J. N., Dentener, F. J., Capone, D. G., Boyer, E. W., Howarth, R. W., Seitzinger, S. P., Asner, G. P., Cleveland, C. C., Green, P. A., Holland, E. A., Karl, D. M., Michaels, A. F., Porter, J. H., Townsend, A. R., & Vöosmarty, C. J. (2004). Nitrogen Cycles: Past, Present, and Future. *Biogeochemistry*, 70(2), 153–226. <https://doi.org/10.1007/s10533-004-0370-0>
- Gandois, L., Perrin, A.-S., & Probst, A. (2011). Impact of nitrogenous fertiliser-induced proton release on cultivated soils with contrasting carbonate contents: A column experiment. *Geochimica et Cosmochimica Acta*, 75(5), 1185–1198. <https://doi.org/10.1016/j.gca.2010.11.025>
- Gao, H., Schreiber, F., Collins, G., Jensen, M. M., Kostka, J. E., Lavik, G., de Beer, D., Zhou, H., & Kuypers, M. M. M. (2010). Aerobic denitrification in permeable Wadden Sea sediments. *The ISME Journal*, 4(3), 417–426. <https://doi.org/10.1038/ismej.2009.127>
- García-ruiz, Pattinson, & Whitton. (1998). Denitrification in river sediments: Relationship between process rate and properties of water and sediment. *Freshwater Biology*, 39(3), 467–476. <https://doi.org/10.1046/j.1365-2427.1998.00295.x>
- Garnier, J. A., Mounier, E. M., Laverman, A. M., & Billen, G. F. (2010). Potential Denitrification and Nitrous Oxide Production in the Sediments of the Seine River Drainage Network (France). *Journal of Environment Quality*, 39(2), 449. <https://doi.org/10.2134/jeq2009.0299>
- Ghestem, J. P., & Bermond, A. (2010). EDTA Extractability of Trace Metals in Polluted Soils: A Chemical-Physical Study. *Environmental Technology*. <https://doi.org/10.1080/09593331908616696>
- Ghrefat, H. A., Abu-Rukah, Y., & Rosen, M. A. (2011). Application of geoaccumulation index

- and enrichment factor for assessing metal contamination in the sediments of Kafraïn Dam, Jordan. *Environmental Monitoring and Assessment*, 178(1), 95–109. <https://doi.org/10.1007/s10661-010-1675-1>
- Ghrefat, H., & Yusuf, N. (2006). Assessing Mn, Fe, Cu, Zn, and Cd pollution in bottom sediments of Wadi Al-Arab Dam, Jordan. *Chemosphere*, 65(11), 2114–2121. <https://doi.org/10.1016/j.chemosphere.2006.06.043>
- Gimeno-García, E., Andreu, V., & Boluda, R. (1996). Heavy metals incidence in the application of inorganic fertilizers and pesticides to rice farming soils. *Environmental Pollution*, 92(1), 19–25. [https://doi.org/10.1016/0269-7491\(95\)00090-9](https://doi.org/10.1016/0269-7491(95)00090-9)
- Goldhaber, S. B. (2003). Trace element risk assessment: Essentiality vs. toxicity. *Regulatory Toxicology and Pharmacology*, 38(2), 232–242. [https://doi.org/10.1016/S0273-2300\(02\)00020-X](https://doi.org/10.1016/S0273-2300(02)00020-X)
- Grebliunas, B. D., & Perry, W. L. (2016). The role of C:N:P stoichiometry in affecting denitrification in sediments from agricultural surface and tile-water wetlands. *SpringerPlus*, 5(1), 359. <https://doi.org/10.1186/s40064-016-1820-6>
- Groffman, P. M., Altabet, M. A., Böhlke, J. K., Butterbach-Bahl, K., David, M. B., Firestone, M. K., Giblin, A. E., Kana, T. M., Nielsen, L. P., & Voytek, M. A. (2006). METHODS FOR MEASURING DENITRIFICATION: DIVERSE APPROACHES TO A DIFFICULT PROBLEM. *Ecological Applications*, 16(6), 2091–2122. [https://doi.org/10.1890/1051-0761\(2006\)016\[2091:MFMDDA\]2.0.CO;2](https://doi.org/10.1890/1051-0761(2006)016[2091:MFMDDA]2.0.CO;2)
- Grusson, Y. (2016). *Modélisation de l'évolution hydroclimatique des flux et stocks d'eau verte et d'eau bleue du bassin versant de la Garonne—Modelling the hydroclimatic evolution of flow and stocks of green and blue water over the Garonne river watershed.*
- Guo, L., & Lin, H. (2016). Critical Zone Research and Observatories: Current Status and Future Perspectives. *Vadose Zone Journal*, 15(vzj2016.06.0050). <https://doi.org/10.2136/vzj2016.06.0050>
- Guo, W., Liu, X., Liu, Z., & Li, G. (2010). Pollution and Potential Ecological Risk Evaluation of Heavy Metals in the Sediments around Dongjiang Harbor, Tianjin. *Procedia Environmental Sciences*, 2, 729–736. <https://doi.org/10.1016/j.proenv.2010.10.084>
- Guo, X., Zhang, G., Wei, Z., Zhang, L., He, Q., Wu, Q., & Qian, T. (2018). Mixed chelators of EDTA, GLDA, and citric acid as washing agent effectively remove Cd, Zn, Pb, and Cu from soils. *Journal of Soils and Sediments*, 18(3), 835–844. <https://doi.org/10.1007/s11368-017-1781-6>

## H

- Haag, D., & Kaupenjohann, M. (2001). Landscape fate of nitrate fluxes and emissions in Central Europe: A critical review of concepts, data, and models for transport and retention. *Agriculture, Ecosystems & Environment*, 86(1), 1–21. [https://doi.org/10.1016/S0167-8809\(00\)00266-8](https://doi.org/10.1016/S0167-8809(00)00266-8)
- Hakanson, L. (1980). An ecological risk index for aquatic pollution control. a sedimentological approach. *Water Research*, 14(8), 975–1001. [https://doi.org/10.1016/0043-1354\(80\)90143-8](https://doi.org/10.1016/0043-1354(80)90143-8)
- Hamdoun, H., Van-Veen, E., Basset, B., Lemoine, M., Coggan, J., Leleyter, L., & Baraud, F. (2015). Characterization of harbor sediments from the English Channel: Assessment of

- heavy metal enrichment, biological effect and mobility. *Marine Pollution Bulletin*, 90(1), 273–280. <https://doi.org/10.1016/j.marpolbul.2014.10.030>
- Hammer, D. A. (2020). *Constructed Wetlands for Wastewater Treatment: Municipal, Industrial and Agricultural*. CRC Press.
- Hang, Q., Wang, H., Chu, Z., Ye, B., Li, C., & Hou, Z. (2016). Application of plant carbon source for denitrification by constructed wetland and bioreactor: Review of recent development. *Environmental Science and Pollution Research*, 23(9), 8260–8274. <https://doi.org/10.1007/s11356-016-6324-y>
- Hans Wedepohl, K. (1995). The composition of the continental crust. *Geochimica et Cosmochimica Acta*, 59(7), 1217–1232. [https://doi.org/10.1016/0016-7037\(95\)00038-2](https://doi.org/10.1016/0016-7037(95)00038-2)
- Harms, T. K., Edmonds, J. W., Genet, H., Creed, I. F., Aldred, D., Balsler, A., & Jones, J. B. (2016). Catchment influence on nitrate and dissolved organic matter in Alaskan streams across a latitudinal gradient. *Journal of Geophysical Research: Biogeosciences*, 121(2), 350–369. <https://doi.org/10.1002/2015JG003201>
- Harper, D. (1992). What is eutrophication? In D. Harper (Ed.), *Eutrophication of Freshwaters: Principles, problems and restoration* (pp. 1–28). Springer Netherlands. [https://doi.org/10.1007/978-94-011-3082-0\\_1](https://doi.org/10.1007/978-94-011-3082-0_1)
- Hefting, M. M., Bobbink, R., & de Caluwe, H. (2003). Nitrous Oxide Emission and Denitrification in Chronically Nitrate-Loaded Riparian Buffer Zones. *Journal of Environment Quality*, 32(4), 1194. <https://doi.org/10.2134/jeq2003.1194>
- Hernandez, L., Probst, A., Probst, J. L., & Ulrich, E. (2003). Heavy metal distribution in some French forest soils: Evidence for atmospheric contamination. *Science of The Total Environment*, 312(1–3), 195–219. [https://doi.org/10.1016/S0048-9697\(03\)00223-7](https://doi.org/10.1016/S0048-9697(03)00223-7)
- Hernandez, M. E., & Mitsch, W. J. (2007). Denitrification in created riverine wetlands: Influence of hydrology and season. *Ecological Engineering*, 30(1), 78–88. <https://doi.org/10.1016/j.ecoleng.2007.01.015>
- Hissler, C., & Probst, J.-L. (2006). Impact of mercury atmospheric deposition on soils and streams in a mountainous catchment (Vosges, France) polluted by chlor-alkali industrial activity: The important trapping role of the organic matter. *The Science of the Total Environment*, 361(1–3), 163–178. <https://doi.org/10.1016/j.scitotenv.2005.05.023>
- Holland, J. F., Martin, J. F., Granata, T., Bouchard, V., Quigley, M., & Brown, L. (2004). Effects of wetland depth and flow rate on residence time distribution characteristics. *Ecological Engineering*, 23(3), 189–203. <https://doi.org/10.1016/j.ecoleng.2004.09.003>
- Hostetler, C. E., Kincaid, R. L., & Mirando, M. A. (2003). The role of essential trace elements in embryonic and fetal development in livestock. *The Veterinary Journal*, 166(2), 125–139. [https://doi.org/10.1016/S1090-0233\(02\)00310-6](https://doi.org/10.1016/S1090-0233(02)00310-6)
- Huber, B., Bernasconi, S. M., Pannatier, E. G., & Luster, J. (2012). A simple method for the removal of dissolved organic matter and  $\delta^{15}\text{N}$  analysis of  $\text{NO}_3^-$  from freshwater. *Rapid Communications in Mass Spectrometry*, 26(12), 1475–1480. <https://doi.org/10.1002/rcm.6243>
- Humbert, S., Zopfi, J., & Tarnawski, S.-E. (2012). Abundance of anammox bacteria in different wetland soils. *Environmental Microbiology Reports*, 4(5), 484–490. <https://doi.org/10.1111/j.1758-2229.2012.00347.x>
- Hynes, R. K., & Knowles, R. (1978). Inhibition by acetylene of ammonia oxidation in

Nitrosomonas europaea. *FEMS Microbiology Letters*, 4(6), 319–321. <https://doi.org/10.1111/j.1574-6968.1978.tb02889.x>

## I

Inwood, S. E., Tank, J. L., & Bernot, M. J. (2007). Factors Controlling Sediment Denitrification in Midwestern Streams of Varying Land Use. *Microbial Ecology*, 53(2), 247–258. <https://doi.org/10.1007/s00248-006-9104-2>

IPCC. (2006). *2006 IPCC Guidelines for National Greenhouse Gas Inventories*.

IPCC. (2019). *2019 Refinement to the 2006 IPCC Guidelines for National Greenhouse Gas Inventories—IPCC*. <https://www.ipcc.ch/report/2019-refinement-to-the-2006-ipcc-guidelines-for-national-greenhouse-gas-inventories/>

Iribar, A., Hallin, S., Pérez, J. M. S., Enwall, K., Poulet, N., & Garabétian, F. (2015). Potential denitrification rates are spatially linked to colonization patterns of nosZ genotypes in an alluvial wetland. *Ecological Engineering*, 80, 191–197. <https://doi.org/10.1016/j.ecoleng.2015.02.002>

Iribar, A., Sánchez-Pérez, J. M., Lyautey, E., & Garabétian, F. (2008). Differentiated free-living and sediment-attached bacterial community structure inside and outside denitrification hotspots in the river–groundwater interface. *Hydrobiologia*, 598(1), 109–121. <https://doi.org/10.1007/s10750-007-9143-9>

Islam, A., Chen, D., & White, R. E. (2007). Heterotrophic and autotrophic nitrification in two acid pasture soils. *Soil Biology and Biochemistry*, 39(4), 972–975. <https://doi.org/10.1016/j.soilbio.2006.11.003>

ISO. (2005). *ISO 11732:2005*. ISO. <https://www.iso.org/cms/render/live/en/sites/isoorg/contents/data/standard/03/89/38924.html>

## J

Jiao, Wei, Ouyang, W., Hao, F., & Lin, C. (2015). Anthropogenic impact on diffuse trace metal accumulation in river sediments from agricultural reclamation areas with geochemical and isotopic approaches. *Science of The Total Environment*, 536, 609–615. <https://doi.org/10.1016/j.scitotenv.2015.07.118>

Jiao, Wentao, Chen, W., Chang, A. C., & Page, A. L. (2012). Environmental risks of trace elements associated with long-term phosphate fertilizers applications: A review. *Environmental Pollution*, 168, 44–53. <https://doi.org/10.1016/j.envpol.2012.03.052>

Jordan, T. E., Whigham, D. F., Hofmockel, K. H., & Pittek, M. A. (2003). Nutrient and Sediment Removal by a Restored Wetland Receiving Agricultural Runoff. *Journal of Environment Quality*, 32(4), 1534. <https://doi.org/10.2134/jeq2003.1534>

Jung, M.-Y., Gwak, J.-H., Rohe, L., Giesemann, A., Kim, J.-G., Well, R., Madsen, E. L., Herbold, C. W., Wagner, M., & Rhee, S.-K. (2019). Indications for enzymatic denitrification to N<sub>2</sub>O at low pH in an ammonia-oxidizing archaeon. *The ISME Journal*, 13(10), 2633–2638. <https://doi.org/10.1038/s41396-019-0460-6>

## K

Kabata-Pendias, A. (2010). *Trace Elements in Soils and Plants*. CRC Press.



- Kadlec, R. H., & Knight, R. L. (1996). *Treatment wetlands*. Lewis Publishers.  
<https://agris.fao.org/agris-search/search.do?recordID=US9620810>
- Kadlec, R., & Wallace, S. (2008). *Treatment Wetlands, Second Edition*.
- Kapoor, A., & Viraraghavan, T. (1997). Nitrate Removal From Drinking Water—Review. *Journal of Environmental Engineering*, 123(4), 371–380.  
[https://doi.org/10.1061/\(ASCE\)0733-9372\(1997\)123:4\(371\)](https://doi.org/10.1061/(ASCE)0733-9372(1997)123:4(371))
- Kizito, S., Lv, T., Wu, S., Ajmal, Z., Luo, H., & Dong, R. (2017). Treatment of anaerobic digested effluent in biochar-packed vertical flow constructed wetland columns: Role of media and tidal operation. *Science of The Total Environment*, 592, 197–205.  
<https://doi.org/10.1016/j.scitotenv.2017.03.125>
- Klomjek, P., & Nitorisavut, S. (2005). Constructed treatment wetland: A study of eight plant species under saline conditions. *Chemosphere*, 58(5), 585–593.  
<https://doi.org/10.1016/j.chemosphere.2004.08.073>
- Knowles, R. (1982). Denitrification. *Microbiological Reviews*, 46(1), 43–70.
- Komada, T., Anderson, M. R., & Dorfmeier, C. L. (2008). Carbonate removal from coastal sediments for the determination of organic carbon and its isotopic signatures,  $\delta^{13}\text{C}$  and  $\Delta^{14}\text{C}$ : Comparison of fumigation and direct acidification by hydrochloric acid. *Limnology and Oceanography: Methods*, 6(6), 254–262. <https://doi.org/10.4319/lom.2008.6.254>
- Korbie, D. J., & Mattick, J. S. (2008). Touchdown PCR for increased specificity and sensitivity in PCR amplification. *Nature Protocols*, 3(9), 1452–1456.  
<https://doi.org/10.1038/nprot.2008.133>
- Kouassi, N. L. B., Yao, K. M., Sangare, N., Trokourey, A., & Metongo, B. S. (2019). The mobility of the trace metals copper, zinc, lead, cobalt, and nickel in tropical estuarine sediments, Ebrie Lagoon, Côte d’Ivoire. *Journal of Soils and Sediments*, 19(2), 929–944.  
<https://doi.org/10.1007/s11368-018-2062-8>
- Kumwimba, M. N., Dzakpasu, M., Zhu, B., & Muyembe, D. K. (2016). Uptake and Release of Sequestered Nutrient in Subtropical Monsoon Ecological Ditch Plant Species. *Water, Air, & Soil Pollution*, 227(11), 405. <https://doi.org/10.1007/s11270-016-3105-7>

## L

- Labbé, N., Parent, S., & Villemur, R. (2003). Addition of trace metals increases denitrification rate in closed marine systems. *Water Research*, 37(4), 914–920.  
[https://doi.org/10.1016/S0043-1354\(02\)00383-4](https://doi.org/10.1016/S0043-1354(02)00383-4)
- Lê, S., Josse, J., & Husson, F. (2008). FactoMineR: An R Package for Multivariate Analysis. *Journal of Statistical Software*, 25(1), 1–18. <https://doi.org/10.18637/jss.v025.i01>
- Leclerc, A., & Laurent, A. (2017). Framework for estimating toxic releases from the application of manure on agricultural soil: National release inventories for heavy metals in 2000–2014. *Science of The Total Environment*, 590–591, 452–460.  
<https://doi.org/10.1016/j.scitotenv.2017.01.117>
- Leleyter, L., & Baraud, F. (2005). Évaluation de la mobilité des métaux dans les sédiments fluviaux du bassin de la Vire (Normandie, France) par extractions simples ou séquentielles. *Comptes Rendus Geoscience*, 337(6), 571–579. <https://doi.org/10.1016/j.crte.2005.01.001>
- Leleyter, L., & Probst, J.-L. (1999). A New Sequential Extraction Procedure for the Speciation of Particulate Trace Elements in River Sediments. *International Journal of Environmental*

- Analytical Chemistry*, 73(2), 109–128. <https://doi.org/10.1080/03067319908032656>
- Leleyter, L., Rousseau, C., Biree, L., & Baraud, F. (2012). Comparison of EDTA, HCl and sequential extraction procedures, for selected metals (Cu, Mn, Pb, Zn), in soils, riverine and marine sediments. *Journal of Geochemical Exploration*, 116–117, 51–59. <https://doi.org/10.1016/j.gexplo.2012.03.006>
- Lewin, P. K., Hancock, R. G. V., & Voynovich, P. (1982). Napoleon Bonaparte—No evidence of chronic arsenic poisoning. *Nature*, 299(5884), 627–628. <https://doi.org/10.1038/299627a0>
- Li, B., & Irvin, S. (2007). The comparison of alkalinity and ORP as indicators for nitrification and denitrification in a sequencing batch reactor (SBR). *Biochemical Engineering Journal*, 34(3), 248–255. <https://doi.org/10.1016/j.bej.2006.12.020>
- Li, F., Yang, R., Ti, C., Lang, M., Kimura, S. D., & Yan, X. (2010). Denitrification characteristics of pond sediments in a Chinese agricultural watershed. *Soil Science & Plant Nutrition*, 56(1), 66–71. <https://doi.org/10.1111/j.1747-0765.2010.00450.x>
- Liao, Z., Chen, Y., Ma, J., Islam, Md. S., Weng, L., & Li, Y. (2019). Cd, Cu, and Zn Accumulations Caused by Long-Term Fertilization in Greenhouse Soils and Their Potential Risk Assessment. *International Journal of Environmental Research and Public Health*, 16(15). <https://doi.org/10.3390/ijerph16152805>
- Lin, H. (2010). Earth's Critical Zone and hydrogeology: Concepts, characteristics, and advances. *Hydrol. Earth Syst. Sci.*, 21.
- Lin, J.-G., & Chen, S.-Y. (1998). The relationship between adsorption of heavy metal and organic matter in river sediments. *Environment International*, 24(3), 345–352. [https://doi.org/10.1016/S0160-4120\(98\)00012-9](https://doi.org/10.1016/S0160-4120(98)00012-9)
- Liu, B., Mørkved, P. T., Frostegård, Å., & Bakken, L. R. (2010). Denitrification gene pools, transcription and kinetics of NO, N<sub>2</sub>O and N<sub>2</sub> production as affected by soil pH. *FEMS Microbiology Ecology*, 72(3), 407–417. <https://doi.org/10.1111/j.1574-6941.2010.00856.x>
- Liu, T., Xia, X., Liu, S., Mou, X., & Qiu, Y. (2013). Acceleration of Denitrification in Turbid Rivers Due to Denitrification Occurring on Suspended Sediment in Oxidic Waters. *Environmental Science & Technology*, 47(9), 4053–4061. <https://doi.org/10.1021/es304504m>
- Long, E. R. (2006). Calculation and Uses of Mean Sediment Quality Guideline Quotients: A Critical Review. *Environmental Science & Technology*, 40(6), 1726–1736. <https://doi.org/10.1021/es058012d>
- Lu, S., Zhang, P., Jin, X., Xiang, C., Gui, M., Zhang, J., & Li, F. (2009). Nitrogen removal from agricultural runoff by full-scale constructed wetland in China. *Hydrobiologia*, 621(1), 115–126. <https://doi.org/10.1007/s10750-008-9636-1>
- Luo, X. X., Yang, S. L., & Zhang, J. (2012). The impact of the Three Gorges Dam on the downstream distribution and texture of sediments along the middle and lower Yangtze River (Changjiang) and its estuary, and subsequent sediment dispersal in the East China Sea. *Geomorphology*, 179, 126–140. <https://doi.org/10.1016/j.geomorph.2012.05.034>
- Lyu, T., He, K., Dong, R., & Wu, S. (2018). The intensified constructed wetlands are promising for treatment of ammonia stripped effluent: Nitrogen transformations and removal pathways. *Environmental Pollution*, 236, 273–282. <https://doi.org/10.1016/j.envpol.2018.01.056>

## M

- Macary, F., Dias, J. A., Figueira, J. R., & Roy, B. (2014). A Multiple Criteria Decision Analysis Model Based on ELECTRE TRI-C for Erosion Risk Assessment in Agricultural Areas. *Environmental Modeling & Assessment*, *19*(3), 221–242. <https://doi.org/10.1007/s10666-013-9387-x>
- Macary, Francis, Leccia, O., Almeida Dias, J., Morin, S., & Sanchez-Pérez, J.-M. (2013). Agro-environmental risk evaluation by a spatialised multi-criteria modelling combined with the PIXAL method. *Revue Internationale de Géomatique*, *23*(1), 39–70. <https://doi.org/10.3166/rig.23.39-70>
- MacDonald, D. D., Ingersoll, C. G., & Berger, T. A. (2000). Development and Evaluation of Consensus-Based Sediment Quality Guidelines for Freshwater Ecosystems. *Archives of Environmental Contamination and Toxicology*, *39*(1), 20–31. <https://doi.org/10.1007/s002440010075>
- Magalhães, C. M., Joye, S. B., Moreira, R. M., Wiebe, W. J., & Bordalo, A. A. (2005). Effect of salinity and inorganic nitrogen concentrations on nitrification and denitrification rates in intertidal sediments and rocky biofilms of the Douro River estuary, Portugal. *Water Research*, *39*(9), 1783–1794. <https://doi.org/10.1016/j.watres.2005.03.008>
- Manouchehri, N., Besancon, S., & Bermond, A. (2006). Major and trace metal extraction from soil by EDTA: Equilibrium and kinetic studies. *Analytica Chimica Acta*, *559*(1), 105–112. <https://doi.org/10.1016/j.aca.2005.11.050>
- Mao, L., Liu, L., Yan, N., Li, F., Tao, H., Ye, H., & Wen, H. (2020). Factors controlling the accumulation and ecological risk of trace metal(loid)s in river sediments in agricultural field. *Chemosphere*, *243*, 125359. <https://doi.org/10.1016/j.chemosphere.2019.125359>
- Marchetti, D., Cittadini, F., & Giovanni, N. D. (2020). Did poisoning play a role in Napoleon's death? A systematic review. *Clinical Toxicology*, *0*(0), 1–15. <https://doi.org/10.1080/15563650.2020.1843658>
- McLennan, S. M. (2001). Relationships between the trace element composition of sedimentary rocks and upper continental crust: TRACE ELEMENT COMPOSITION AND UPPER CONTINENTAL CRUST. *Geochemistry, Geophysics, Geosystems*, *2*(4), n/a-n/a. <https://doi.org/10.1029/2000GC000109>
- Mekonnen, M. M., & Hoekstra, A. Y. (2015). Global Gray Water Footprint and Water Pollution Levels Related to Anthropogenic Nitrogen Loads to Fresh Water. *Environmental Science & Technology*, *49*(21), 12860–12868. <https://doi.org/10.1021/acs.est.5b03191>
- Mertz, W. (1981). The essential trace elements. *Science*, *213*(4514), 1332–1338. <https://doi.org/10.1126/science.7022654>
- Miller, A. J. (1984). Selection of Subsets of Regression Variables. *Journal of the Royal Statistical Society: Series A (General)*, *147*(3), 389–410. <https://doi.org/10.2307/2981576>
- Montgomery, D. R. (2007). Soil erosion and agricultural sustainability. *Proceedings of the National Academy of Sciences*, *104*(33), 13268–13272. <https://doi.org/10.1073/pnas.0611508104>
- Mulder, A., van de Graaf, A. A., Robertson, L. A., & Kuenen, J. G. (1995). Anaerobic ammonium oxidation discovered in a denitrifying fluidized bed reactor. *FEMS Microbiology Ecology*, *16*(3), 177–183. <https://doi.org/10.1111/j.1574->

6941.1995.tb00281.x

Müller, G. (1969). Index of geoaccumulation in sediments of the Rhine river. *GeoJournal*, 2, 108–118.

## N

Nagajyoti, P. C., Lee, K. D., & Sreekanth, T. V. M. (2010). Heavy metals, occurrence and toxicity for plants: A review. *Environmental Chemistry Letters*, 8(3), 199–216. <https://doi.org/10.1007/s10311-010-0297-8>

Nemerow, N. L. (1991). *Stream, lake, estuary, and ocean pollution, 2nd edition*. <https://www.osti.gov/biblio/7030475>

N'guessan, Y. M., Probst, J. L., Bur, T., & Probst, A. (2009). Trace elements in stream bed sediments from agricultural catchments (Gascogne region, S-W France): Where do they come from? *Science of The Total Environment*, 407(8), 2939–2952. <https://doi.org/10.1016/j.scitotenv.2008.12.047>

Novara, A., Gristina, L., Saladino, S. S., Santoro, A., & Cerdà, A. (2011). Soil erosion assessment on tillage and alternative soil managements in a Sicilian vineyard. *Soil and Tillage Research*, 117, 140–147. <https://doi.org/10.1016/j.still.2011.09.007>

## O

Oehler, F., Bordenave, P., & Durand, P. (2007). Variations of denitrification in a farming catchment area. *Agriculture, Ecosystems & Environment*, 120(2–4), 313–324. <https://doi.org/10.1016/j.agee.2006.10.007>

Oost, K. V., Cerdan, O., & Quine, T. A. (2009). Accelerated sediment fluxes by water and tillage erosion on European agricultural land. *Earth Surface Processes and Landforms*, 34(12), 1625–1634. <https://doi.org/10.1002/esp.1852>

## P

Papassiopi, N., Tambouris, S., & Kontopoulos, A. (1999). Removal of Heavy Metals from Calcareous Contaminated Soils by EDTA Leaching. *Water, Air, and Soil Pollution*, 109(1), 1–15. <https://doi.org/10.1023/A:1005089515217>

Park, J.-H., Kim, S.-H., Delaune, R. D., Cho, J.-S., Heo, J.-S., Ok, Y. S., & Seo, D.-C. (2015). Enhancement of nitrate removal in constructed wetlands utilizing a combined autotrophic and heterotrophic denitrification technology for treating hydroponic wastewater containing high nitrate and low organic carbon concentrations. *Agricultural Water Management*, 162, 1–14. <https://doi.org/10.1016/j.agwat.2015.08.001>

Pattinson, S. N., García-Ruiz, R., & Whitton, B. A. (1998). Spatial and seasonal variation in denitrification in the Swale–Ouse system, a river continuum. *Science of The Total Environment*, 210–211, 289–305. [https://doi.org/10.1016/S0048-9697\(98\)00019-9](https://doi.org/10.1016/S0048-9697(98)00019-9)

Paul, A., Moussa, I., Payre, V., Probst, A., & Probst, J.-L. (2015). Flood survey of nitrate behaviour using nitrogen isotope tracing in the critical zone of a French agricultural catchment. *Comptes Rendus Geoscience*, 347(7), 328–337. <https://doi.org/10.1016/j.crte.2015.06.002>

Peoples, M. B., Herridge, D. F., & Ladha, J. K. (1995). Biological nitrogen fixation: An efficient source of nitrogen for sustainable agricultural production? In J. K. Ladha & M.

- B. Peoples (Eds.), *Management of Biological Nitrogen Fixation for the Development of More Productive and Sustainable Agricultural Systems: Extended versions of papers presented at the Symposium on Biological Nitrogen Fixation for Sustainable Agriculture at the 15th Congress of Soil Science, Acapulco, Mexico, 1994* (pp. 3–28). Springer Netherlands. [https://doi.org/10.1007/978-94-011-0055-7\\_1](https://doi.org/10.1007/978-94-011-0055-7_1)
- Pérez, C. A., Carmona, M. R., Fariña, J. M., & Armesto, J. J. (2010). *Effects of nitrate and labile carbon on denitrification of southern temperate forest soils*. <https://tspace.library.utoronto.ca/handle/1807/45813>
- Perrin, A.-S., Probst, A., & Probst, J.-L. (2008). Impact of nitrogenous fertilizers on carbonate dissolution in small agricultural catchments: Implications for weathering CO<sub>2</sub> uptake at regional and global scales. *Geochimica et Cosmochimica Acta*, 72(13), 3105–3123. <https://doi.org/10.1016/j.gca.2008.04.011>
- Piña-Ochoa, E., & Álvarez-Cobelas, M. (2006). Denitrification in Aquatic Environments: A Cross-system Analysis. *Biogeochemistry*, 81(1), 111–130. <https://doi.org/10.1007/s10533-006-9033-7>
- Piper, A. M. (1944). A graphic procedure in the geochemical interpretation of water-analyses. *Eos, Transactions American Geophysical Union*, 25(6), 914–928. <https://doi.org/10.1029/TR025i006p00914>
- Ponnou-Delaffon, V., Probst, A., Payre-Suc, V., Granouillac, F., Ferrant, S., Perrin, A.-S., & Probst, J.-L. (2020). Long and short-term trends of stream hydrochemistry and high frequency surveys as indicators of the influence of climate change, agricultural practices and internal processes (Aurade agricultural catchment, SW France). *Ecological Indicators*, 110, 105894. <https://doi.org/10.1016/j.ecolind.2019.105894>
- Powlson, D. S., Addiscott, T. M., Benjamin, N., Cassman, K. G., Kok, T. M. de, Grinsven, H. van, L'hirondel, J.-L., Avery, A. A., & Kessel, C. van. (2008). When Does Nitrate Become a Risk for Humans? *Journal of Environmental Quality*, 37(2), 291–295. <https://doi.org/10.2134/jeq2007.0177>
- Probst, A., Party, J. P., Fevrier, C., Dambrine, E., Thomas, A. L., & Stussi, J. M. (1999). Evidence of Springwater Acidification in the Vosges Mountains (North-East of France): Influence of Bedrock Buffering Capacity. *Water, Air, and Soil Pollution*, 114(3), 395–411. <https://doi.org/10.1023/A:1005156615921>

## Q

- Quevauviller, Ph., Lachica, M., Barahona, E., Rauret, G., Ure, A., Gomez, A., & Muntau, H. (1996). Interlaboratory comparison of EDTA and DTPA procedures prior to certification of extractable trace elements in calcareous soil. *Science of The Total Environment*, 178(1), 127–132. [https://doi.org/10.1016/0048-9697\(95\)04804-9](https://doi.org/10.1016/0048-9697(95)04804-9)

## R

- R Core Team. (2017). *R: A Language and Environment for Statistical Computing*. R Foundation for Statistical Computing. <https://www.R-project.org/>
- Ramsar Convention. (2016). *An introduction to the Ramsar Convention on wetlands*.
- Ramsar Convention. (2018). *Global Wetland Outlook—Status and trends*. <https://www.global-wetland-outlook.ramsar.org>

- Rassamee, V., Sattayatewa, C., Pagilla, K., & Chandran, K. (2011). Effect of oxic and anoxic conditions on nitrous oxide emissions from nitrification and denitrification processes. *Biotechnology and Bioengineering*, *108*(9), 2036–2045. <https://doi.org/10.1002/bit.23147>
- Raymond, J., Siefert, J. L., Staples, C. R., & Blankenship, R. E. (2004). The Natural History of Nitrogen Fixation. *Molecular Biology and Evolution*, *21*(3), 541–554. <https://doi.org/10.1093/molbev/msh047>
- Reddy, K. R., Patrick, W. H., & Broadbent, F. E. (2009). Nitrogen transformations and loss in flooded soils and sediments. *Critical Reviews in Environmental Science and Technology*. <https://doi.org/10.1080/10643388409381709>
- Reddy, K. R., Patrick, W. H., & Lindau, C. W. (1989). Nitrification-denitrification at the plant root-sediment interface in wetlands. *Limnology and Oceanography*, *34*(6), 1004–1013. <https://doi.org/10.4319/lo.1989.34.6.1004>
- Redon, P.-O., Bur, T., Guisresse, M., Probst, J.-L., Toiser, A., Revel, J.-C., Jolivet, C., & Probst, A. (2013). Modelling trace metal background to evaluate anthropogenic contamination in arable soils of south-western France. *Geoderma*, *206*(Supplement C), 112–122. <https://doi.org/10.1016/j.geoderma.2013.04.023>
- Revel, J. C., & Guisresse, M. (1995). Erosion due to cultivation of calcareous clay soils on the hillsides of south west France. I. Effect of former farming practices. *Soil and Tillage Research*, *35*(3), 147–155. [https://doi.org/10.1016/0167-1987\(95\)00482-3](https://doi.org/10.1016/0167-1987(95)00482-3)
- Rivett, M. O., Buss, S. R., Morgan, P., Smith, J. W. N., & Bement, C. D. (2008). Nitrate attenuation in groundwater: A review of biogeochemical controlling processes. *Water Research*, *42*(16), 4215–4232. <https://doi.org/10.1016/j.watres.2008.07.020>
- Roussiez, V., Ludwig, W., Probst, J.-L., & Monaco, A. (2005). Background levels of heavy metals in surficial sediments of the Gulf of Lions (NW Mediterranean): An approach based on <sup>133</sup>Cs normalization and lead isotope measurements. *Environmental Pollution (Barking, Essex: 1987)*, *138*(1), 167–177. <https://doi.org/10.1016/j.envpol.2005.02.004>
- Roussiez, V., Probst, A., & Probst, J.-L. (2013). Significance of floods in metal dynamics and export in a small agricultural catchment. *Journal of Hydrology*, *499*, 71–81. <https://doi.org/10.1016/j.jhydrol.2013.06.013>
- Royer, T. V., Tank, J. L., & David, M. B. (2004). Transport and fate of nitrate in headwater agricultural streams in Illinois. *Journal of Environmental Quality*, *33*(4), 1296–1304.

## S

- Saeed, T., & Sun, G. (2012). A review on nitrogen and organics removal mechanisms in subsurface flow constructed wetlands: Dependency on environmental parameters, operating conditions and supporting media. *Journal of Environmental Management*, *112*, 429–448. <https://doi.org/10.1016/j.jenvman.2012.08.011>
- Saggar, S., Jha, N., Deslippe, J., Bolan, N. S., Luo, J., Giltrap, D. L., Kim, D.-G., Zaman, M., & Tillman, R. W. (2013). Denitrification and N<sub>2</sub>O:N<sub>2</sub> production in temperate grasslands: Processes, measurements, modelling and mitigating negative impacts. *Science of The Total Environment*, *465*, 173–195. <https://doi.org/10.1016/j.scitotenv.2012.11.050>
- Sahrawat, K. L. (2008). Factors Affecting Nitrification in Soils. *Communications in Soil Science and Plant Analysis*, *39*(9–10), 1436–1446. <https://doi.org/10.1080/00103620802004235>

- Sahuquillo, A., Rigol, A., & Rauret, G. (2003). Overview of the use of leaching/extraction tests for risk assessment of trace metals in contaminated soils and sediments. *TrAC Trends in Analytical Chemistry*, 22(3), 152–159. [https://doi.org/10.1016/S0165-9936\(03\)00303-0](https://doi.org/10.1016/S0165-9936(03)00303-0)
- Saleh-Lakha, S., Shannon, K. E., Henderson, S. L., Zebarth, B. J., Burton, D. L., Goyer, C., & Trevors, J. T. (2009). Effect of Nitrate and Acetylene on nirS, cnorB, and nosZ Expression and Denitrification Activity in *Pseudomonas mandelii*. *Applied and Environmental Microbiology*, 75(15), 5082–5087. <https://doi.org/10.1128/AEM.00777-09>
- Salvarredy-Aranguren, M. M., Probst, A., Roulet, M., & Isaure, M.-P. (2008). Contamination of surface waters by mining wastes in the Milluni Valley (Cordillera Real, Bolivia): Mineralogical and hydrological influences. *Applied Geochemistry*, 23(5), 1299–1324. <https://doi.org/10.1016/j.apgeochem.2007.11.019>
- Scaroni, A. E., Lindau, C. W., & Nyman, J. A. (2010). Spatial Variability of Sediment Denitrification Across the Atchafalaya River Basin, Louisiana, USA. *Wetlands*, 30(5), 949–955. <https://doi.org/10.1007/s13157-010-0091-1>
- Schaetzl, R. J., & Thompson, M. L. (2015). *Soils*. Cambridge University Press.
- Schindler, D. W. (2006). Recent advances in the understanding and management of eutrophication. *Limnology and Oceanography*, 51(1part2), 356–363. [https://doi.org/10.4319/lo.2006.51.1\\_part\\_2.0356](https://doi.org/10.4319/lo.2006.51.1_part_2.0356)
- Sehar, S., Sumera, Naeem, S., Perveen, I., Ali, N., & Ahmed, S. (2015). A comparative study of macrophytes influence on wastewater treatment through subsurface flow hybrid constructed wetland. *Ecological Engineering*, 81, 62–69. <https://doi.org/10.1016/j.ecoleng.2015.04.009>
- Seitzinger, S. P., Nielsen, L. P., Caffrey, J., & Christensen, P. B. (1993). Denitrification measurements in aquatic sediments: A comparison of three methods. *Biogeochemistry*, 23(3), 147–167. <https://doi.org/10.1007/BF00023750>
- Senesil, G. S., Baldassarre, G., Senesi, N., & Radina, B. (1999). Trace element inputs into soils by anthropogenic activities and implications for human health. *Chemosphere*, 39(2), 343–377. [https://doi.org/10.1016/S0045-6535\(99\)00115-0](https://doi.org/10.1016/S0045-6535(99)00115-0)
- ShaoYong, L., ZhengFen, W., FengMin, L., & XueQing, Z. (2016). Ammonia nitrogen adsorption and desorption characteristics of twenty-nine kinds of constructed wetland substrates. *Research of Environmental Sciences*, 29(8), 1187–1194.
- Shen, Q., Ji, F., Wei, J., Fang, D., Zhang, Q., Jiang, L., Cai, A., & Kuang, L. (2020). The influence mechanism of temperature on solid phase denitrification based on denitrification performance, carbon balance, and microbial analysis. *Science of The Total Environment*, 732, 139333. <https://doi.org/10.1016/j.scitotenv.2020.139333>
- Shi, H., & Shao, M. (2000). Soil and water loss from the Loess Plateau in China. *Journal of Arid Environments*, 45(1), 9–20. <https://doi.org/10.1006/jare.1999.0618>
- Shrewsbury, L. H., Smith, J. L., Huggins, D. R., Carpenter-Boggs, L., & Reardon, C. L. (2016). Denitrifier abundance has a greater influence on denitrification rates at larger landscape scales but is a lesser driver than environmental variables. *Soil Biology and Biochemistry*, 103, 221–231. <https://doi.org/10.1016/j.soilbio.2016.08.016>
- Šimek, M., & Cooper, J. E. (2002). The influence of soil pH on denitrification: Progress towards the understanding of this interaction over the last 50 years. *European Journal of Soil Science*, 53(3), 345–354. <https://doi.org/10.1046/j.1365-2389.2002.00461.x>

- Singh, M., Müller, G., & Singh, I. B. (2002). *Heavy Metals in Freshly Deposited Stream Sediments of Rivers Associated with Urbanisation of the Ganga Plain, India*. 20.
- Singh, P. (2009). Major, trace and REE geochemistry of the Ganga River sediments: Influence of provenance and sedimentary processes. *Chemical Geology*, 266(3), 242–255. <https://doi.org/10.1016/j.chemgeo.2009.06.013>
- Sinha, E., Michalak, A. M., & Balaji, V. (2017). Eutrophication will increase during the 21st century as a result of precipitation changes. *Science*, 357(6349), 405–408. <https://doi.org/10.1126/science.aan2409>
- Smith, D. R., & Pappas, E. A. (2007). Effect of ditch dredging on the fate of nutrients in deep drainage ditches of the Midwestern United States. *Journal of Soil and Water Conservation*, 62(4), 252–261.
- Smith, R. L., Kent, D. B., Repert, D. A., & Böhlke, J. K. (2017). Anoxic nitrate reduction coupled with iron oxidation and attenuation of dissolved arsenic and phosphate in a sand and gravel aquifer. *Geochimica et Cosmochimica Acta*, 196, 102–120. <https://doi.org/10.1016/j.gca.2016.09.025>
- Soliman, N. F., Nasr, S. M., & Okbah, M. A. (2015). Potential ecological risk of heavy metals in sediments from the Mediterranean coast, Egypt. *Journal of Environmental Health Science and Engineering*, 13(1), 70. <https://doi.org/10.1186/s40201-015-0223-x>
- Song, K., Kang, H., Zhang, L., & Mitsch, W. J. (2012). Seasonal and spatial variations of denitrification and denitrifying bacterial community structure in created riverine wetlands. *Ecological Engineering*, 38(1), 130–134. <https://doi.org/10.1016/j.ecoleng.2011.09.008>
- Song, X.-P., Hansen, M. C., Stehman, S. V., Potapov, P. V., Tyukavina, A., Vermote, E. F., & Townshend, J. R. (2018). Global land change from 1982 to 2016. *Nature*, 560(7720), 639–643. <https://doi.org/10.1038/s41586-018-0411-9>
- Sterckeman, T., Gossiaux, L., Guimont, S., Sirguey, C., & Lin, Z. (2018). Cadmium mass balance in French soils under annual crops: Scenarios for the next century. *Science of The Total Environment*, 639, 1440–1452. <https://doi.org/10.1016/j.scitotenv.2018.05.225>
- Subbarao, G. V., Ito, O., Sahrawat, K. L., Berry, W. L., Nakahara, K., Ishikawa, T., Watanabe, T., Suenaga, K., Rondon, M., & Rao, I. M. (2006). Scope and Strategies for Regulation of Nitrification in Agricultural Systems—Challenges and Opportunities. *Critical Reviews in Plant Sciences*, 25(4), 303–335. <https://doi.org/10.1080/07352680600794232>
- Syvitski, J. P. M., Vörösmarty, C. J., Kettner, A. J., & Green, P. (2005). Impact of Humans on the Flux of Terrestrial Sediment to the Global Coastal Ocean. *Science*, 308(5720), 376–380. <https://doi.org/10.1126/science.1109454>

## T

- Taghavi, L., Merlina, G., & Probst, J.-L. (2011). The role of storm flows in concentration of pesticides associated with particulate and dissolved fractions as a threat to aquatic ecosystems - Case study: The agricultural watershed of Save river (Southwest of France). *Knowledge and Management of Aquatic Ecosystems*, 400, 06. <https://doi.org/10.1051/kmae/2011002>
- Taghavi, Lobat, Probst, J.-L., Merlina, G., Marchand, A.-L., Durbe, G., & Probst, A. (2010). Flood event impact on pesticide transfer in a small agricultural catchment (Montoussé at Auradé, south west France). *International Journal of Environmental Analytical Chemistry*,



- 90(3–6), 390–405. <https://doi.org/10.1080/03067310903195045>
- Tang, W., Shan, B., Zhang, H., & Mao, Z. (2010). Heavy metal sources and associated risk in response to agricultural intensification in the estuarine sediments of Chaohu Lake Valley, East China. *Journal of Hazardous Materials*, 176(1), 945–951. <https://doi.org/10.1016/j.jhazmat.2009.11.131>
- Tang, Z., Chai, M., Cheng, J., Jin, J., Yang, Y., Nie, Z., Huang, Q., & Li, Y. (2017). Contamination and health risks of heavy metals in street dust from a coal-mining city in eastern China. *Ecotoxicology and Environmental Safety*, 138, 83–91. <https://doi.org/10.1016/j.ecoenv.2016.11.003>
- Targulian, V. O., Arnold, R. W., Miller, B. A., & Brevik, E. C. (2019). Pedosphere. In B. Fath (Ed.), *Encyclopedia of Ecology (Second Edition)* (pp. 162–168). Elsevier. <https://doi.org/10.1016/B978-0-12-409548-9.11153-4>
- Thostenson, A. (2014). *National Pesticide Applicator Certification Core Manual* (2nd edition). [https://s3.amazonaws.com/nasda2/media/Reports/Core-Chpt-1\\_Pest-Management.pdf?mtime=20171025135710](https://s3.amazonaws.com/nasda2/media/Reports/Core-Chpt-1_Pest-Management.pdf?mtime=20171025135710)
- Tiedje, J. M. (1994). Denitrifiers. *Methods of Soil Analysis: Part 2—Microbiological and Biochemical Properties*, *sssabookseries(methodsofsoilan2)*, 245–267. <https://doi.org/10.2136/sssabookser5.2.c14>
- Tomlinson, D. L., Wilson, J. G., Harris, C. R., & Jeffrey, D. W. (1980). Problems in the assessment of heavy-metal levels in estuaries and the formation of a pollution index. *Helgoländer Meeresuntersuchungen*, 33(1), 566–575. <https://doi.org/10.1007/BF02414780>
- Tournebize, J., Chaumont, C., & Mander, Ü. (2017). Implications for constructed wetlands to mitigate nitrate and pesticide pollution in agricultural drained watersheds. *Ecological Engineering*, 103, 415–425. <https://doi.org/10.1016/j.ecoleng.2016.02.014>
- Tuttle, A. K., McMillan, S. K., Gardner, A., & Jennings, G. D. (2014). Channel complexity and nitrate concentrations drive denitrification rates in urban restored and unrestored streams. *Ecological Engineering*, 73, 770–777. <https://doi.org/10.1016/j.ecoleng.2014.09.066>

## U

- UNFCCC. (1992). *UNITED NATIONS FRAMEWORK CONVENTION ON CLIMATE CHANGE*. <https://unfccc.int/resource/docs/convkp/conveng.pdf>

## V

- Van Iperen, J., & Helder, W. (1985). A method for the determination of organic carbon in calcareous marine sediments. *Marine Geology*, 64(1), 179–187. [https://doi.org/10.1016/0025-3227\(85\)90167-7](https://doi.org/10.1016/0025-3227(85)90167-7)
- Varol, M. (2011). Assessment of heavy metal contamination in sediments of the Tigris River (Turkey) using pollution indices and multivariate statistical techniques. *Journal of Hazardous Materials*, 195, 355–364. <https://doi.org/10.1016/j.jhazmat.2011.08.051>
- Verhoeven, J. T. A., Arheimer, B., Yin, C., & Hefting, M. M. (2006). Regional and global concerns over wetlands and water quality. *Trends in Ecology & Evolution*, 21(2), 96–103. <https://doi.org/10.1016/j.tree.2005.11.015>
- Viana, M., Kuhlbusch, T. A. J., Querol, X., Alastuey, A., Harrison, R. M., Hopke, P. K.,

- Winiwarter, W., Vallius, M., Szidat, S., Prévôt, A. S. H., Hueglin, C., Bloemen, H., Wählin, P., Vecchi, R., Miranda, A. I., Kasper-Giebl, A., Maenhaut, W., & Hitzenberger, R. (2008). Source apportionment of particulate matter in Europe: A review of methods and results. *Journal of Aerosol Science*, 39(10), 827–849. <https://doi.org/10.1016/j.jaerosci.2008.05.007>
- Vymazal, J. (1995). Algae and element cycling in wetlands. *Algae and Element Cycling in Wetlands*. <https://www.cabdirect.org/cabdirect/abstract/19951906893>
- Vymazal, Jan. (2007). Removal of nutrients in various types of constructed wetlands. *Science of The Total Environment*, 380(1), 48–65. <https://doi.org/10.1016/j.scitotenv.2006.09.014>
- Vymazal, Jan. (2011). Constructed Wetlands for Wastewater Treatment: Five Decades of Experience. *Environmental Science & Technology*, 45(1), 61–69. <https://doi.org/10.1021/es101403q>
- Vymazal, Jan. (2017). The Use of Constructed Wetlands for Nitrogen Removal from Agricultural Drainage: A Review. *Scientia Agriculturae Bohemica*, 48(2), 82–91. <https://doi.org/10.1515/sab-2017-0009>
- Vymazal, Jan, Švehla, J., Kröpfelová, L., Němcová, J., & Suchý, V. (2010). Heavy metals in sediments from constructed wetlands treating municipal wastewater. *Biogeochemistry*, 101(1), 335–356. <https://doi.org/10.1007/s10533-010-9504-8>

## W

- Wagener, T., Sivapalan, M., Troch, P., & Woods, R. (2007). Catchment Classification and Hydrologic Similarity. *Geography Compass*, 1(4), 901–931. <https://doi.org/10.1111/j.1749-8198.2007.00039.x>
- Wallenstein, M. D., Myrold, D. D., Firestone, M., & Voytek, M. (2006). Environmental Controls on Denitrifying Communities and Denitrification Rates: Insights from Molecular Methods. *Ecological Applications*, 16(6), 2143–2152. [https://doi.org/10.1890/1051-0761\(2006\)016\[2143:ECODCA\]2.0.CO;2](https://doi.org/10.1890/1051-0761(2006)016[2143:ECODCA]2.0.CO;2)
- Wang, S., Fu, B., Piao, S., Lü, Y., Ciais, P., Feng, X., & Wang, Y. (2016). Reduced sediment transport in the Yellow River due to anthropogenic changes. *Nature Geoscience*, 9(1), 38–41. <https://doi.org/10.1038/ngeo2602>
- Wani, A. L., Ara, A., & Usmani, J. A. (2015). Lead toxicity: A review. *Interdisciplinary Toxicology*, 8(2), 55–64. <https://doi.org/10.1515/intox-2015-0009>
- Waxman, S., & Anderson, K. C. (2001). History of the Development of Arsenic Derivatives in Cancer Therapy. *The Oncologist*, 6(S2), 3–10. [https://doi.org/10.1634/theoncologist.6-suppl\\_2-3](https://doi.org/10.1634/theoncologist.6-suppl_2-3)
- Wei, B., & Yang, L. (2010). A review of heavy metal contaminations in urban soils, urban road dusts and agricultural soils from China. *Microchemical Journal*, 94(2), 99–107. <https://doi.org/10.1016/j.microc.2009.09.014>
- Weier, K. L., Doran, J. W., Power, J. F., & Walters, D. T. (1993). Denitrification and the Dinitrogen/Nitrous Oxide Ratio as Affected by Soil Water, Available Carbon, and Nitrate. *Soil Science Society of America Journal*, 57(1), 66–72. <https://doi.org/10.2136/sssaj1993.03615995005700010013x>
- Weinzettel, J., Hertwich, E. G., Peters, G. P., Steen-Olsen, K., & Galli, A. (2013). Affluence drives the global displacement of land use. *Global Environmental Change*, 23(2), 433–438.

<https://doi.org/10.1016/j.gloenvcha.2012.12.010>

- Well, R., Augustin, J., Meyer, K., & Myrold, D. D. (2003). Comparison of field and laboratory measurement of denitrification and N<sub>2</sub>O production in the saturated zone of hydromorphic soils. *Soil Biology and Biochemistry*, 35(6), 783–799. [https://doi.org/10.1016/S0038-0717\(03\)00106-8](https://doi.org/10.1016/S0038-0717(03)00106-8)
- White, T. (2012). *Special Focus on US Critical Zone Program*. <https://czo-archive.criticalzone.org/shale-hills/news/story/international-innovation-publishes-august-edition-with-special-focus-on-us/>
- Wickham, H. (2009). *ggplot2: Elegant Graphics for Data Analysis*. Springer-Verlag New York. <http://ggplot2.org>
- Wu, X. D., Guo, J. L., Han, M. Y., & Chen, G. Q. (2018). An overview of arable land use for the world economy: From source to sink via the global supply chain. *Land Use Policy*, 76, 201–214. <https://doi.org/10.1016/j.landusepol.2018.05.005>
- Wu, X., & Probst, A. (2021). Influence of ponds on hazardous metal distribution in sediments at a catchment scale (agricultural critical zone, S-W France). *Journal of Hazardous Materials*, 411, 125077. <https://doi.org/10.1016/j.jhazmat.2021.125077>

## X

- Xu, H., Paerl, H. W., Qin, B., Zhu, G., & Gao, G. (2010). Nitrogen and phosphorus inputs control phytoplankton growth in eutrophic Lake Taihu, China. *Limnology and Oceanography*, 55(1), 420–432. <https://doi.org/10.4319/lo.2010.55.1.0420>
- Xu, J., Wu, L., Chang, A. C., & Zhang, Y. (2010). Impact of long-term reclaimed wastewater irrigation on agricultural soils: A preliminary assessment. *Journal of Hazardous Materials*, 183(1), 780–786. <https://doi.org/10.1016/j.jhazmat.2010.07.094>

## Y

- Yang, X., Wu, X., Hao, H., & He, Z. (2008). Mechanisms and assessment of water eutrophication. *Journal of Zhejiang University SCIENCE B*, 9(3), 197–209. <https://doi.org/10.1631/jzus.B0710626>
- Yang, Y., Sun, P., Padhye, L. P., & Zhang, R. (2020). Photo-ammonification in surface water samples: Mechanism and influencing factors. *Science of The Total Environment*, 143547. <https://doi.org/10.1016/j.scitotenv.2020.143547>
- Yoo, J.-C., Lee, C.-D., Yang, J.-S., & Baek, K. (2013). Extraction characteristics of heavy metals from marine sediments. *Chemical Engineering Journal*, 228, 688–699. <https://doi.org/10.1016/j.cej.2013.05.029>

## Z

- Zak, D., Kronvang, B., Carstensen, M. V., Hoffmann, C. C., Kjeldgaard, A., Larsen, S. E., Audet, J., Egemose, S., Jorgensen, C. A., Feuerbach, P., Gertz, F., & Jensen, H. S. (2018). Nitrogen and Phosphorus Removal from Agricultural Runoff in Integrated Buffer Zones. *Environmental Science & Technology*, 52(11), 6508–6517. <https://doi.org/10.1021/acs.est.8b01036>
- Zhang, J., & Liu, C. L. (2002). Riverine Composition and Estuarine Geochemistry of Particulate Metals in China—Weathering Features, Anthropogenic Impact and Chemical

Fluxes. *Estuarine, Coastal and Shelf Science*, 54(6), 1051–1070.  
<https://doi.org/10.1006/ecss.2001.0879>

## **Annex**

**Annex I** – A brief list of some Critical Zone Observatories (CZO) and CZ-like sites at the global scale.

No.	Project	Country/Region	CZO Name	Note
1	CZO (U.S.)	U.S.A	Boulder creek	
2	CZO (U.S.)	U.S.A	Calhoun	
3	CZO (U.S.)	U.S.A	Catalina-Jemez	
4	CZO (U.S.)	U.S.A	Eel river	
5	CZO (U.S.)	U.S.A	IML	
6	CZO (U.S.)	U.S.A	Reynolds creek	<a href="https://criticalzone.org/">https://criticalzone.org/</a>
7	CZO (U.S.)	U.S.A	Shale hills	
8	CZO (U.S.)	U.S.A	Southern Sierra	
9	CZO (U.S.)	U.S.A	Christina river basin	
10	CZO (U.S.)	Puerto Rico	Luquillo	
1	SoilTrEC	Austria	Fuchsenbigl	
2	SoilTrEC	Greece	Koiliaris river basin	<a href="https://esdac.jrc.ec.europa.eu/projects/soiltrec">https://esdac.jrc.ec.europa.eu/projects/soiltrec</a>
3	SoilTrEC	Switzerland	Damma glacier	
4	SoilTrEC	Czech Republic	Kladka lake	
1	TERENO	Germany	Eifel/Lower Rhine valley	
2	TERENO	Germany	Harz/Central German Lowland	
3	TERENO	Germany	Northeast German Lowland	<a href="https://www.tereno.net/">https://www.tereno.net/</a>
4	TERENO	Germany	Pre-Alpine	
1	OZCAR	France	AgrHys	
2	OZCAR	France	M-TROPICS	
3	OZCAR	Amazon	HYBAM	
4	OZCAR	France	BDOH	
5	OZCAR	west Africa	AMMA-CATCH	
6	OZCAR	France	OHMCV	<a href="https://www.ozcari.org/">https://www.ozcari.org/</a>
7	OZCAR	France	OHGE	
8	OZCAR	Guadeloupe	ObseRA	
9	OZCAR	France	OMERE	
10	OZCAR	France	Auradé	
11	OZCAR	France	SNO Karst	
1	TERN	Australia	Alice Mulga	
2	TERN	Australia	Tumbarumba	
3	TERN	Australia	Chowilla	
4	TERN	Australia	Credo	
5	TERN	Australia	Litchfield	<a href="https://www.tern.org.au">https://www.tern.org.au</a>
6	TERN	Australia	Robson creek	/
7	TERN	Australia	South East Queensland	
8	TERN	Australia	Warra	
9	TERN	Australia	Injune	
10	TERN	Australia	Fowler's Gap	

---

11	TERN	Australia	Rushworth Forest	
12	TERN	Australia	Watts creek	
13	TERN	Australia	Zig Zag creek	
1	UK-China CZO	China	Zhangxi	
2	UK-China CZO	China	Chenqi	
3	UK-China CZO	China	Sunjia red soil	<a href="http://www.czo.ac.cn/">http://www.czo.ac.cn/</a>
4	UK-China CZO	China	Loess plateau	

---

## Annex II

### Automatic online-data collection and thematic map plotting via R

*(technical document)*

#### AII 1. Libraries and prerequisites

The required packages were loaded as follows. Their purposes were described in comments.

```
# Set Locale
Sys.setlocale("LC_ALL", "English")

# map tools
library(rnaturalearth)      # maps from Natural Earth (NE)
library(rnaturalearthdata) # map data from NE
library(rnaturalearthhires) # high resolution maps from NE
library(maps)
library(maptools)
library(sf)                 # process shapefiles
library(raster)            # process raster and shapefiles
library(countrycode)       # convert country code

# data manipulation
library(tidyverse)         # data process tools
library(ggspatial)         # map toolkits
library(directlabels)      # add labels

# online databases
library(wbstats)           # tools for World Bank database
library(FAOSTAT)          # tools for FAO database
library(eurostat)         # tools for EUROSTAT database

# Color palette
library(viridis)           # color scales for pretty plots
```

Themes were configured for a better visualization.

```
# map theme ====
map_theme <- theme(
  panel.grid.major = element_line(color = gray(.5), linetype = 'dotted',
```



```

size = 0.2),
  panel.grid.minor = element_blank(),
  panel.background = element_rect(fill = 'aliceblue'),
  panel.border = element_rect(color = 'black', fill = 'transparent'),
  plot.background = element_rect(fill = 'aliceblue', color = NA),
  legend.position = 'bottom',
  legend.background = element_rect(fill = NA, color = NA),
)

# ggplot2 theme ====
gg_theme <- theme(
  plot.title = element_blank(),
  axis.text.x = element_text(size = 18, color = 'black'),
  axis.text.y = element_text(size = 18, color = 'black'),
  axis.title.x = element_text(size = 18, face = 'bold'),
  axis.title.y = element_text(size = 18, face = 'bold'),
  legend.text = element_text(size = 18, color = 'black'),
  legend.title = element_text(size = 18, face = 'bold'),
  strip.text = element_text(size = 18, color = 'black'),
  panel.grid.major = element_blank(),
  panel.grid.minor = element_blank()
)

```

## AII 2. Get map data online

The world map was downloaded from the Natural Earth database ([www.naturalearthdata.com](http://www.naturalearthdata.com)). It provides updated maps with country codes defined by various organizations, which can very easily match other databases from different statistical organizations. The package `rnaturalearth` offers some functions to obtain and facilitate interaction with Natural Earth map data.

- World map

```

# Get world map data
map_world <- ne_countries(scale = 'medium',
                          returnclass = 'sf')

```

- European map

The package `eurostat` also offers the European map data created by the Geographic Information System of the COMmission (GISCO).

```
map_eu_gisco <- get_eurostat_geospatial(
  output_class = 'sf',
  resolution = '60',
  nuts_level = 'all'
)
```

- French map

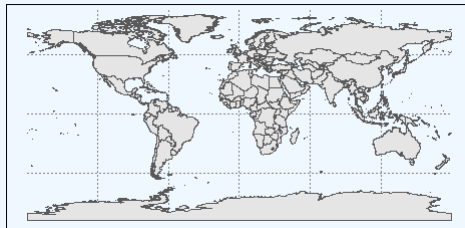
The metropolitan France map can also be acquired by `rnaturalearth`.

```
# France map without oversea departments
map_fr <- ne_states(
  country = 'france', returnclass = 'sf'
) %>%
  filter(type != 'Overseas département') # Remove oversea department
```

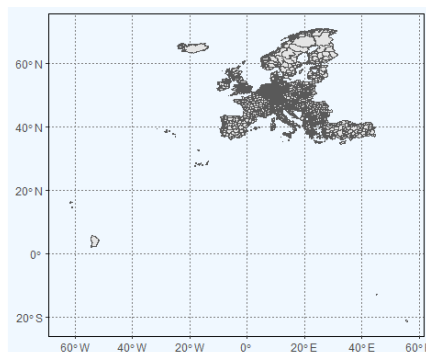
- Plot simple maps

The simple maps were plotted to check the validation of the map data.

```
map_world %>%
  ggplot()+
  geom_sf()+
  map_theme
```

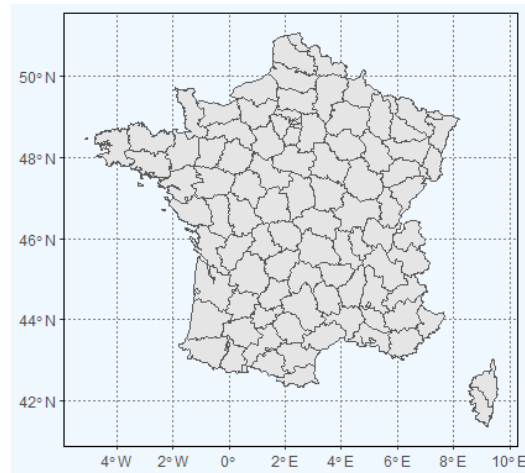


```
map_eu_gisco %>%
  ggplot()+
  geom_sf()+
  map_theme
```



```
map_fr %>%
  ggplot()+
```

```
geom_sf()+
map_theme
```



### AII 3. Get online census data

With the help of the Application Programming Interface (API) provided by online databases, the user can bulk download the target data easily.

In this study, three major online databases were concerned:

- The World Development Indicators (WDI) in the World Bank ([wdi.worldbank.org](http://wdi.worldbank.org))
- Food and Agricultural Organization (FAO, <http://www.fao.org/statistics/en/>)
- The statistical office of the European Union (EUROSTAT, <https://ec.europa.eu/eurostat/data/database>)

The data sets regarding fertilizers, gas emissions, land uses, water abstractions, and soil erosion were downloaded from these databases.

#### AII 3.1 WDI

The package `wbstats` contains several core functions to bulk download the data from the World Bank:

- `wb_cache()`: gets an updated list of information regarding countries, indicators, sources, regions, indicator topics, lending types, and income levels.
- `wb_search()`: searches the interested indicators.
- `wb_data()`: downloads the requested data from the World Bank.

```
# 0. Get metadata =====
df_wb_meta <- wb_cache(lang = 'en')
```

```
# 1. Fertilizer      =====
# 1.1 Search        -----
wb_search(pattern = 'fertilizer') %>% View()

# 1.2 Download      -----
# Fertilizer consumption
# Unit = kilograms per hectare of arable land
df_wb_fertuse_ha <- wb_data(
  indicator = 'AG.CON.FERT.ZS',
  country = 'countries_only',
  start_date = 2000, end_date = 2020,
  lang = 'en'
)

# 2. Emissions      =====
# 2.1 Search        -----
wb_search(pattern = 'emission') %>% View()

# 2.2 Download      -----
# Agricultural nitrous oxide emissions
# Unit = thousand metric tons of CO2 equivalent
df_wb_emi_n2o_agri <- wb_data(
  indicator = 'EN.ATM.NOXE.AG.KT.CE',
  country = 'countries_only',
  start_date = 2000, end_date = 2020,
  lang = 'en'
)

# Agricultural nitrous oxide emissions
# Unit = % of total
df_wb_emi_n2o_agri_ratio <- wb_data(
  indicator = 'EN.ATM.NOXE.AG.ZS',
  country = 'countries_only',
  start_date = 2000, end_date = 2020,
  lang = 'en'
)

# Nitrous oxide emissions
# Unit = thousand metric tons of CO2 equivalent
df_wb_emi_n2o_tot <- wb_data(
  indicator = 'EN.ATM.NOXE.KT.CE',
  country = 'countries_only',
```

```
    start_date = 2000, end_date = 2020,
    lang = 'en'
)

# Total greenhouse gas emissions
# Unit = kt of CO2 equivalent
df_wb_emi_ghg_tot <- wb_data(
  indicator = 'EN.ATM.GHGT.KT.CE',
  country = 'countries_only',
  start_date = 2000, end_date = 2020,
  lang = 'en'
)

# 3. Land cover      =====
# 3.1 Search        -----
wb_search(pattern = 'land', fields = 'indicator') %>% View()

# 3.2 Download      -----
# Agricultural Land
# Unit = % of Land area
df_wb_land_agri_ratio <- wb_data(
  indicator = 'AG.LND.AGRI.ZS',
  country = 'countries_only',
  start_date = 2000, end_date = 2020,
  lang = 'en'
)

# 4. Water          =====
wb_search(pattern = 'water', fields = 'indicator') %>% View()

# Annual freshwater withdrawals, agriculture
# Unit = % of total freshwater withdrawal
df_wb_watuse_agri_ratio <- wb_data(
  indicator = 'ER.H2O.FWAG.ZS',
  country = 'countries_only',
  start_date = 2000, end_date = 2020,
  lang = 'en'
)
```

### AII 3.2 FAO

The FAOSTAT provides several core functions to download the data from FAO:

- `FAOsearch()`: gets the full list of datasets from FAO, including the data code, name, and the description.
- `get_faostat_bulk`: bulk downloads the datasets from FAO.

**Note that** a folder must be created before starting the bulk download to store the downloaded datasets. Meanwhile, the user should pay attention to the countries to avoid double counting, especially for China, since FAO includes China, China (Mainland), China (Hong Kong), China (Macao), and China (Taiwan) simultaneously. Here only kept China for the plotting of a thematic map.

```
# 0. Get metadata =====
df_fao_meta <- FAOsearch()

# 1. Agri-environmental indicators =====
df_fao_ei <- get_faostat_bulk('EI', data_folder = './Data/df_get_fao/')
df_fao_em <- get_faostat_bulk('EM', data_folder = './Data/df_get_fao/')
df_fao_ef <- get_faostat_bulk('EF', data_folder = './Data/df_get_fao/')
df_fao_lc <- get_faostat_bulk('LC', data_folder = './Data/df_get_fao/')
df_fao_el <- get_faostat_bulk('EL', data_folder = './Data/df_get_fao/')
df_fao_ep <- get_faostat_bulk('EP', data_folder = './Data/df_get_fao/')
df_fao_et <- get_faostat_bulk('ET', data_folder = './Data/df_get_fao/')

# 2. Emissions =====
df_fao_gt <- get_faostat_bulk('GT', data_folder = './Data/df_get_fao/')
df_fao_gy <- get_faostat_bulk('GY', data_folder = './Data/df_get_fao/')
df_fao_gc <- get_faostat_bulk('GC', data_folder = './Data/df_get_fao/')
df_fao_gl <- get_faostat_bulk('GL', data_folder = './Data/df_get_fao/')

# 3. Input =====
df_fao_rfn <- get_faostat_bulk('RFN', data_folder = './Data/df_get_fao/')
df_fao_rfb <- get_faostat_bulk('RFB', data_folder = './Data/df_get_fao/')
df_fao_rl <- get_faostat_bulk('RL', data_folder = './Data/df_get_fao/')
df_fao_rp <- get_faostat_bulk('RP', data_folder = './Data/df_get_fao/')

# 4. Pre cleanup =====
# Only keep 'China' to avoid double counting
# Remove Region data (area code >= 5000)
# Set year from 2000 to 2020

func_fao_clean <- function(df) {
  df_edit <- df %>%
    filter(!area %in% c('China, Hong Kong SAR',
                       'China, Macao SAR',
```

```

        'China, mainland',
        'China, Taiwan Province of')) %>%
  filter(area_code < 1000) %>%
  filter(year >= 2000 & year <= 2020)

return(df_edit)
}

df_fao_ei_edit <- df_fao_ei %>% func_fao_clean()
df_fao_em_edit <- df_fao_em %>% func_fao_clean()
df_fao_ef_edit <- df_fao_ef %>% func_fao_clean()
df_fao_lc_edit <- df_fao_lc %>% func_fao_clean()
df_fao_el_edit <- df_fao_el %>% func_fao_clean()
df_fao_ep_edit <- df_fao_ep %>% func_fao_clean()
df_fao_et_edit <- df_fao_et %>% func_fao_clean()
df_fao_gt_edit <- df_fao_gt %>% func_fao_clean()
df_fao_gy_edit <- df_fao_gy %>% func_fao_clean()
df_fao_gc_edit <- df_fao_gc %>% func_fao_clean()
df_fao_gl_edit <- df_fao_gl %>% func_fao_clean()
df_fao_rfn_edit <- df_fao_rfn %>% func_fao_clean()
df_fao_rfb_edit <- df_fao_rfb %>% func_fao_clean()
df_fao_rl_edit <- df_fao_rl %>% func_fao_clean()
df_fao_rp_edit <- df_fao_rp %>% func_fao_clean()

```

### AII 3.3 EUROSTAT

The package `eurostat` offers some core functions to process the datasets in EUROSTAT:

- `get_eurostat_toc`: downloads the detailed list of eurostat datasets;
- `search_eurostat()`: searches the interested data in eurostat;
- `get_eurostat`: bulk downloads the datasets from eurostat.

```

# 0. Get metadata ====
df_eurostat_meta <- get_eurostat_toc()

# 1. Fertilizer ====

# 1.1 Search ----
search_eurostat(pattern = 'fertilizer') %>% View()

# 1.2 Get data ----
df_eurostat_fertuse <- get_eurostat('aei_fm_usefert', time_format = "num")
df_eurostat_fertuse$iso_3a <- countrycode(

```

```
df_eurostat_fertuse$geo,
  origin = 'eurostat', destination = 'iso3c'
)

# 2. Emissions =====

# 2.1 Search -----
search_eurostat(pattern = 'emission') %>% View()

# 2.2 Get data -----
df_eurostat_ghg <- get_eurostat('env_air_gge', time_format = 'num')
df_eurostat_ghg$iso_3a <- countrycode(
  df_eurostat_ghg$geo,
  origin = 'eurostat', destination = 'iso3c'
)

# 3. Land cover =====

# 3.1 Search -----
search_eurostat(pattern = 'land') %>% View()

# 3.2 Get data -----

# Estimated soil erosion by water, by erosion level, land cover and NUTS 3
regions
df_eurostat_soiler <- get_eurostat('aei_pr_soiler', time_format = 'num')
df_eurostat_soiler$iso_3a <- countrycode(
  df_eurostat_soiler$geo,
  origin = 'eurostat', destination = 'iso3c'
)

# Share of main land types in utilised agricultural area (UAA) by NUTS 2
regions
df_eurostat_lu_agri <- get_eurostat('aei_ef_lu', time_format = 'num')
df_eurostat_lu_agri$iso_3a <- countrycode(
  df_eurostat_lu_agri$geo,
  origin = 'eurostat', destination = 'iso3c'
)

# 4. Water =====

# 4.1 Search -----
search_eurostat(pattern = 'water') %>% View()
```



```
# 4.2 Get data ----

# Annual freshwater abstraction by source and sector ----
df_eurostat_watabs <- get_eurostat('env_wat_abs', time_format = 'num')
df_eurostat_watabs$iso_3a <- countrycode(
  df_eurostat_watabs$geo,
  origin = 'eurostat', destination = 'iso3c'
)
```

## AII 4. Thematic map plotting

Several examples of the thematic map plotting were shown in this section.

### AII 4.1 Fertilizer

The thematic map of the N fertilizers used by agricultural activities in 2018 was plotted. The data source was from FAO and combined with the maps from the Natural Earth.

```
# 1 Data clean and manipulation ----
df_fao_rfn_edit$iso_a3 <- countrycode( # convert country code
  df_fao_rfn_edit$area_code,
  origin = 'fao', destination = 'iso3c'
)

df_fao_rfn_n_agri_2018 <- df_fao_rfn_edit %>%
  filter(item == 'Nutrient nitrogen N (total)') %>%
  filter(element == 'Agricultural Use') %>%
  filter(year == 2018)

df_fao_rfn_n_agri_2018_map <- left_join(
  map_world,
  df_fao_rfn_n_agri_2018,
  by = 'iso_a3'
)

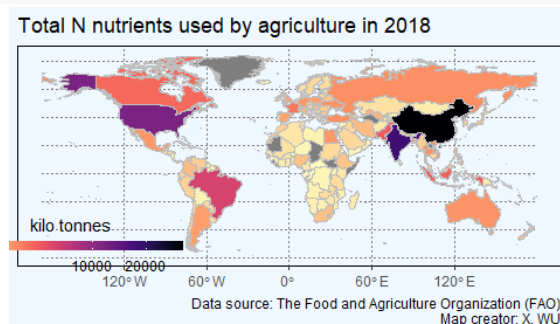
# 2 Plot thematic map ----

# 2.1 World map, N fert used by agri in 2018 ----
map_fao_rfn_n_agri_2018_world <- df_fao_rfn_n_agri_2018_map %>%
  filter(iso_a3 != 'ATA') %>%
  ggplot()+
  geom_sf(aes(fill = value / 1000),
          color = 'grey', size = 0.3)+
  labs(title = 'Total N nutrients used by agriculture in 2018',
```

```

# subtitle = 'Antarctica excluded; NA: grey',
caption = 'Data source: The Food and Agriculture Organization
(FAO)\nMap creator: X. WU')+
scale_fill_viridis(name = 'kilo tonnes',
                   option = "magma", direction = -1, trans = 'sqrt',
                   guide = guide_colorbar(
                     direction = "horizontal",
                     barheight = unit(2, units = "mm"),
                     barwidth = unit(50, units = "mm"),
                     draw.ulim = F,
                     title.position = 'top',
                     title.hjust = 0.5,
                     label.hjust = 0.5
                   ))+
map_theme+
theme(
  legend.position = c(0.1, 0.1)
)

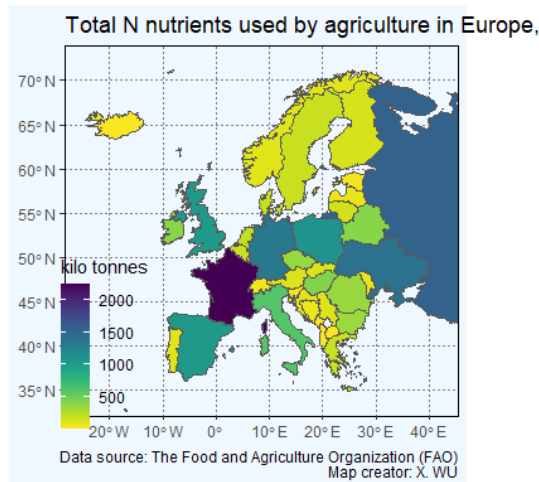
```



```

# 2.2 Europe map ----
map_fao_rfn_n_agri_2018_eu <- df_fao_rfn_n_agri_2018_map %>%
  filter(iso_a3 != 'ATA') %>%
  filter(region_un == 'Europe') %>%
  ggplot()+
  geom_sf(aes(fill = value / 1000))+
  labs(title = 'Total N nutrients used by agriculture in Europe, 2018',
       # subtitle = 'Antarctica excluded; NA: grey',
       caption = 'Data source: The Food and Agriculture Organization
(FAO)\nMap creator: X. WU')+
  scale_fill_viridis(name = 'kilo tonnes',
                    option = "viridis", direction = -1)+
  coord_sf(xlim=c(-25,42),
           ylim=c(34,72))+
  map_theme+
  theme(
    legend.position = c(0.1, 0.2)
  )

```



#### AII 4.2 Land share of agricultural lands

The share of agricultural land (%) in 2016 were plotted at both the global scale and the European scale.

The data sources were the World Bank and the Natural Earth.

```
# 1. World, thematic map, 2016 =====
```

```
# 1.1 Data manipulation -----
```

```
df_wb_land_agri_ratio_2016 <- df_wb_land_agri_ratio %>%  
  filter(date == '2016')
```

```
df_wb_land_agri_ratio_2016_map <- left_join(  
  map_world,  
  df_wb_land_agri_ratio_2016,  
  by = c('iso_a3' = 'iso3c')  
)
```

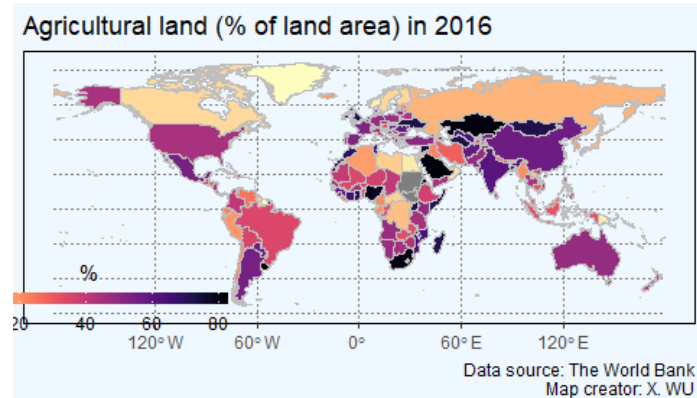
```
# 1.2 Plot thematic map -----
```

```
map_wb_land_agri_ratio_2016_world <- df_wb_land_agri_ratio_2016_map %>%  
  filter(iso_a3 != 'ATA') %>%  
  ggplot()+  
  geom_sf(aes(fill = AG.LND.AGRI.ZS),  
          color = 'grey', size = 0.3)+  
  labs(title = 'Agricultural land (% of land area) in 2016',  
        caption = 'Data source: The World Bank\nMap creator: X. WU')+  
  scale_fill_viridis(name = '%',  
                    option = "magma", direction = -1, # trans = 'sqrt',  
                    guide = guide_colorbar(  
                      direction = "horizontal",  
                      barheight = unit(2, units = "mm"),  
                      barwidth = unit(50, units = "mm"),  
                      draw.ulim = F,  
                      title.position = 'top',
```

```

        title.hjust = 0.5,
        label.hjust = 0.5
    ))+
map_theme+
theme(
  legend.position = c(0.1, 0.1)
)

```

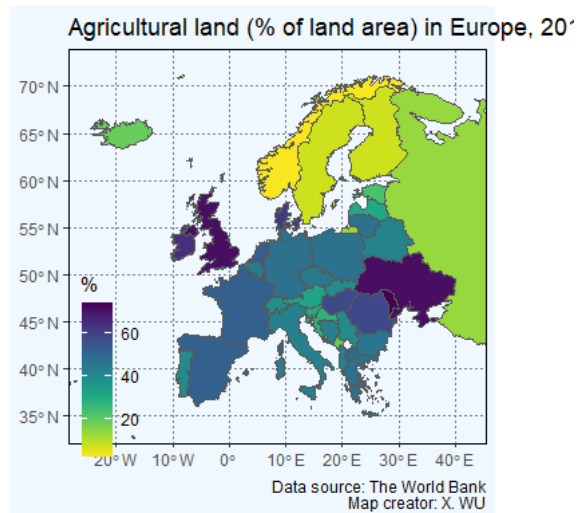


```
# 2. Europe, thematic map, 2016 =====
```

```

map_wb_land_agri_ratio_2016_eu <- df_wb_land_agri_ratio_2016_map %>%
  filter(iso_a3 != 'ATA') %>%
  filter(region_un == 'Europe') %>%
  ggplot()+
  geom_sf(aes(fill = AG.LND.AGRI.ZS))+
  labs(title = 'Agricultural land (% of land area) in Europe, 2016',
        caption = 'Data source: The World Bank\nMap creator: X. WU')+
  scale_fill_viridis(name = '%',
                     option = "viridis", direction = -1)+
  coord_sf(xlim=c(-25,42),
            ylim=c(34,72))+
  map_theme+
  theme(
    legend.position = c(0.1, 0.2)
  )

```



### AII 4.3 Fresh water abstraction by agricultural

The freshwater abstraction for agriculture in 2016 were plotted at the European scale. The data source was EUROSTAT and combined with the map from GISCO.

```
# 1. Europe, thematic map, 2016 =====
```

```
# 1.1 Data manipulation -----
```

```
df_eurostat_watabs_rdb <- label_eurostat(df_eurostat_watabs)
```

```
# Nomenclature:
```

```
# ABS_AGR = Water abstraction for agriculture
```

```
# ABS_AGR_IR = Water abstraction for agriculture - irrigation
```

```
# FSW = Fresh surface water
```

```
# MIO_M3 = Million cubic meters
```

```
df_eurostat_watabs_agri_2016 <- df_eurostat_watabs %>%
```

```
  filter(geo != 'TR') %>%
```

```
  filter(wat_proc == 'ABS_AGR') %>%
```

```
  filter(wat_src == 'FSW') %>%
```

```
  filter(unit == 'MIO_M3') %>%
```

```
  filter(time == '2016')
```

```
df_eurostat_watabs_agri_2016_map <- left_join(
```

```
  map_eu_gisco %>% filter(LEVL_CODE == 0),
```

```
  df_eurostat_watabs_agri_2016,
```

```
  by = c('geo')
```

```
)
```

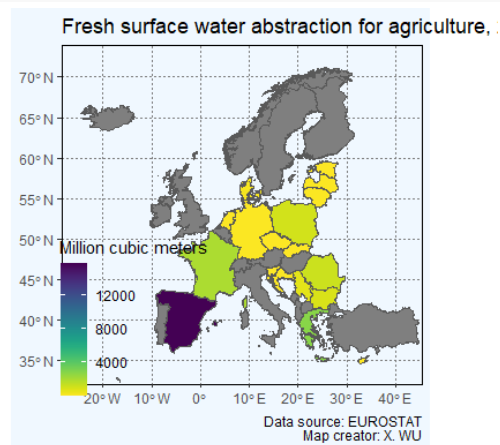
```
# 1.2 Map plot -----
```

```
map_eurostat_watabs_agri_2016_eu <- df_eurostat_watabs_agri_2016_map %>%
```

```

ggplot()+
geom_sf(aes(fill = values))+
labs(title = 'Fresh surface water abstraction for agriculture, 2016',
      caption = 'Data source: EUROSTAT\nMap creator: X. WU')+
scale_fill_viridis(name = 'Million cubic meters',
                   option = "viridis", direction = -1)+
coord_sf(xlim=c(-25,42),
          ylim=c(34,72))+
map_theme+
theme(
  legend.position = c(0.2, 0.2)
)

```



#### AII 4.4 Soil erosion

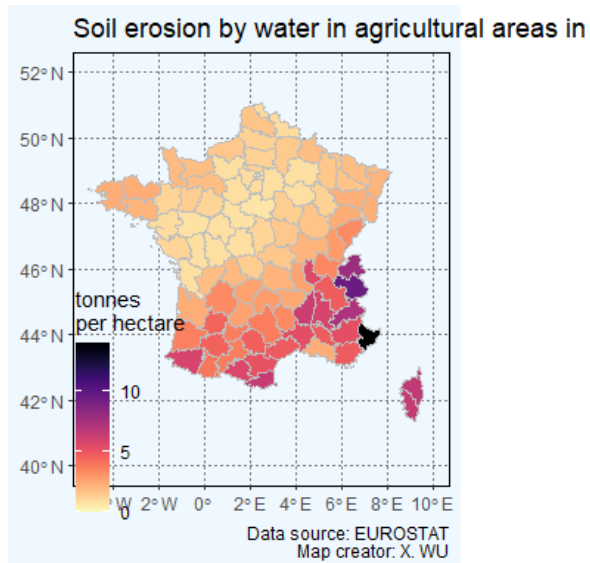
The soil erosion was plotted at the French scale. The data source was from EUROSTAT and combined with the map from the Natural Earth.

```

# 1. Data manipulation ====
df_eurostat_soiler_fr_2016 <- df_eurostat_soiler %>%
  filter(grepl('FR', geo)) %>%
  filter(levels == 'TOTAL') %>%
  filter(clc18 == 'CLC2X23') %>%
  filter(unit == 'T_HA') %>%
  filter(time == '2016')
df_eurostat_soiler_fr_2016_map <- left_join(
  map_eu_gisco %>% filter(grepl('FR', geo)),
  df_eurostat_soiler_fr_2016,
  by = c('geo')
)
# 2. Plot thematic map in 2016 ====
map_eurostat_soiler_fr_2016 <- df_eurostat_soiler_fr_2016_map %>%
  filter(!geo %in% c('FR', 'FRY1', 'FRY2', 'FRY3', 'FRY4', 'FRY5',
                    'FRY10', 'FRY20', 'FRY30', 'FRY40', 'FRY50')) %>%
  ggplot()+

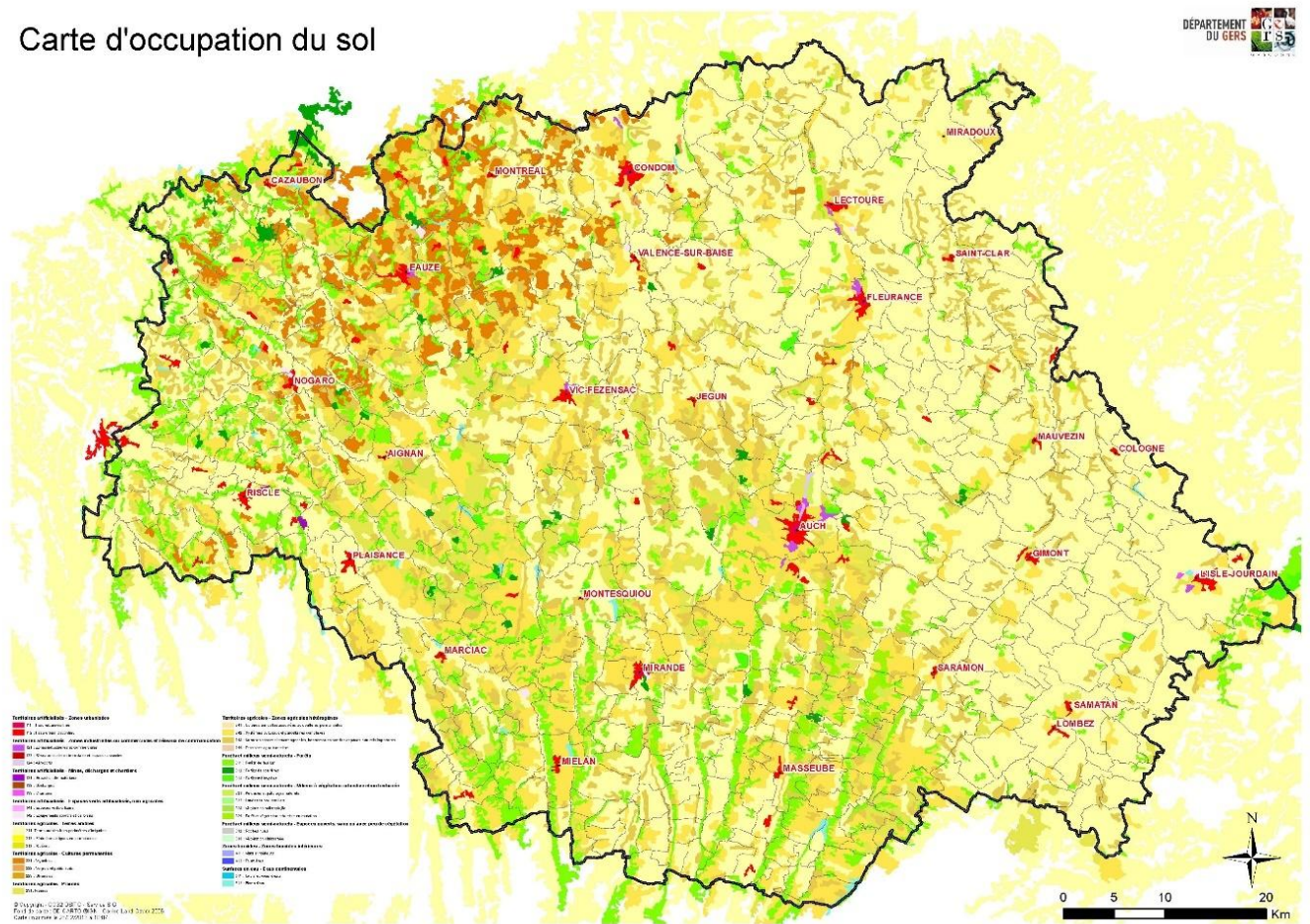
```

```
geom_sf(aes(fill = values),
        color = 'grey', size = 0.3)+
labs(title = 'Soil erosion by water in agricultural areas in 2016',
      caption = 'Data source: EUROSTAT\nMap creator: X. WU')+
scale_fill_viridis(name = 'tonnes\nper hectare',
                   option = "magma", direction = -1)+
coord_sf(xlim = c(-5,10),
          ylim = c(40, 52))+
map_theme+
theme(
  legend.position = c(0.15, 0.20)
)
```



**Annex III** – Map of land cover in Gers (source: Corine Land Cover, 2006). The agricultural and forest areas are indicated from light yellow to dark green. The original version of this map can be found from the website: <https://bdt.gers.fr/services/cartotheque/agriculture-et-environnement/36-carte-d-occupation-du-sol>.

Carte d'occupation du sol

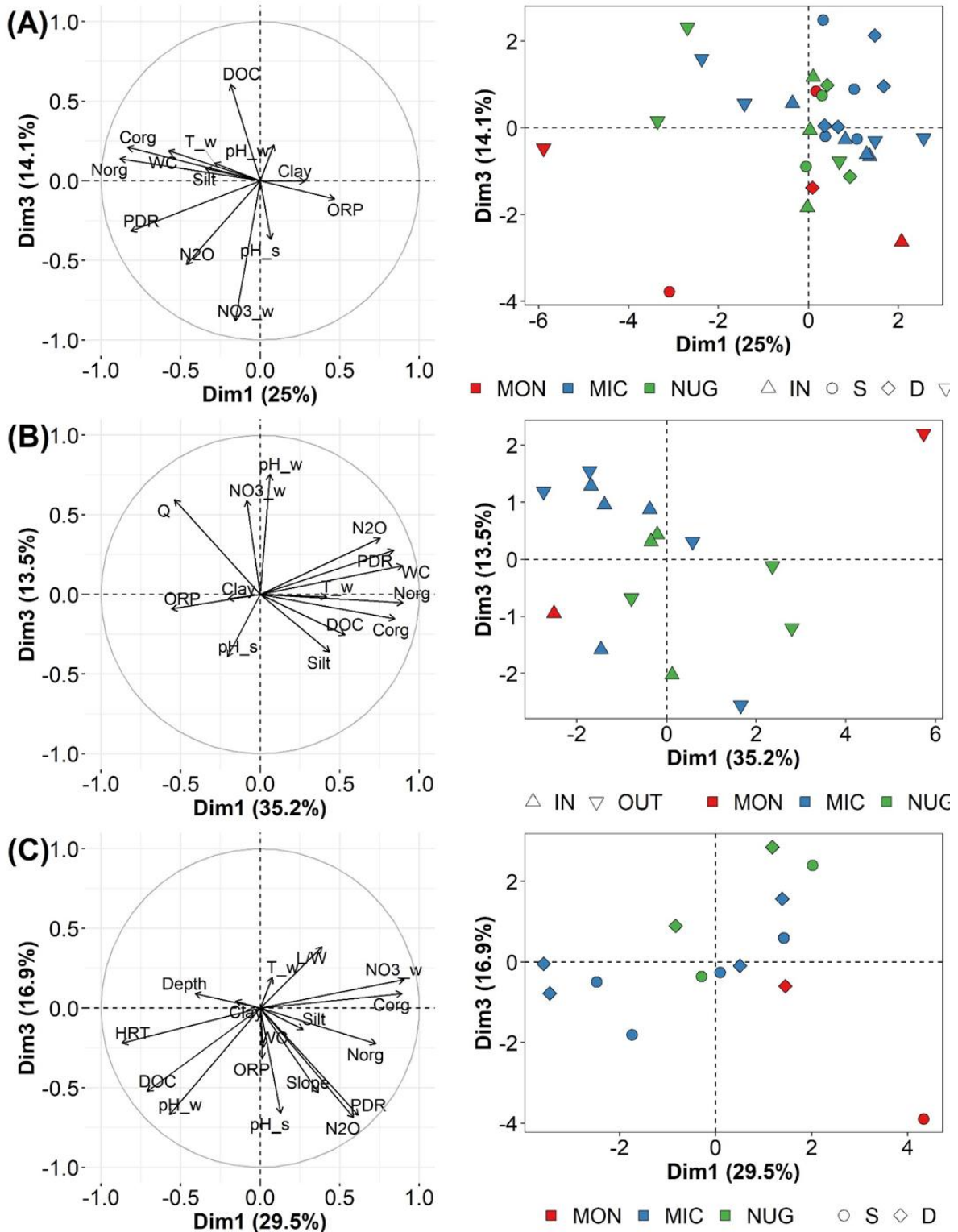




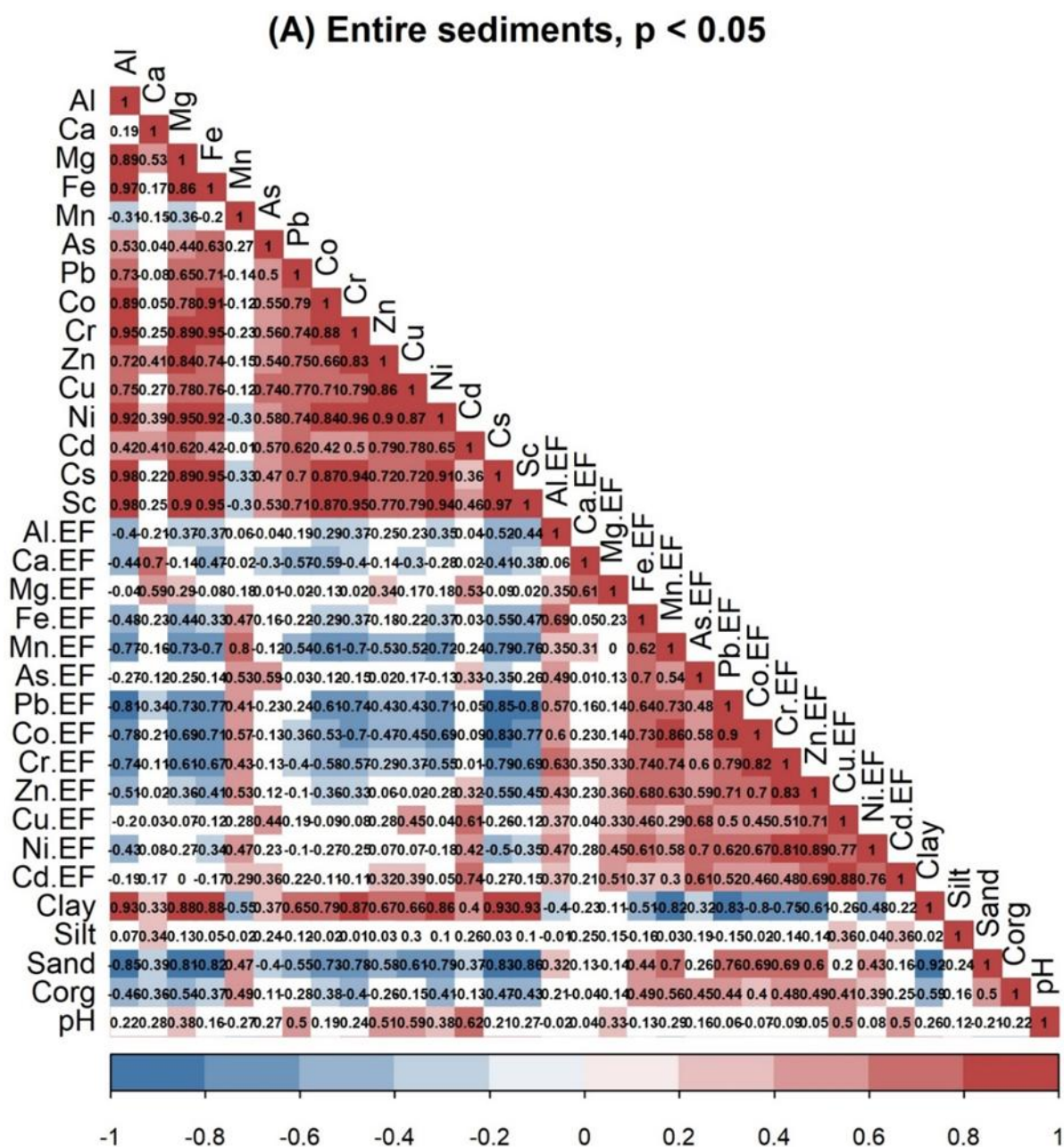
**Annex IV** – Land occupation in the Gers department in 2013 (source: Corine Land Cover, <https://www.annuaire-mairie.fr/occupation-des-sols-departement-gers.html>).

Type	Superficie (ha)	Pourcentage (%)
Terres arables hors périmètres d'irrigation	341457	54.17
Systèmes culturaux et parcellaires complexes	109681	17.40
Surfaces essentiellement agricoles, interrompues par des espaces naturels importants	52681	8.36
Forêts de feuillus	48366	7.67
Prairies et autres surfaces toujours en herbe à usage agricole	41581	6.60
Vignobles	18572	2.95
Tissu urbain discontinu	6062	0.96
Forêt et végétation arbustive en mutation	3539	0.56
Forêts mélangées	2258	0.36
Forêts de conifères	1873	0.30
Plans d'eau	1204	0.19
Vergers et petits fruits	828	0.13
Zones industrielles ou commerciales et installations publiques	718	0.11
Equipements sportifs et de loisirs	564	0.09
Pelouses et pâturages naturels	405	0.06
Extraction de matériaux	167	0.03
Tissu urbain continu	167	0.03
Aéroports	115	0.02
Chantiers	86.3	0.01
Espaces verts urbains	53.9	0.01

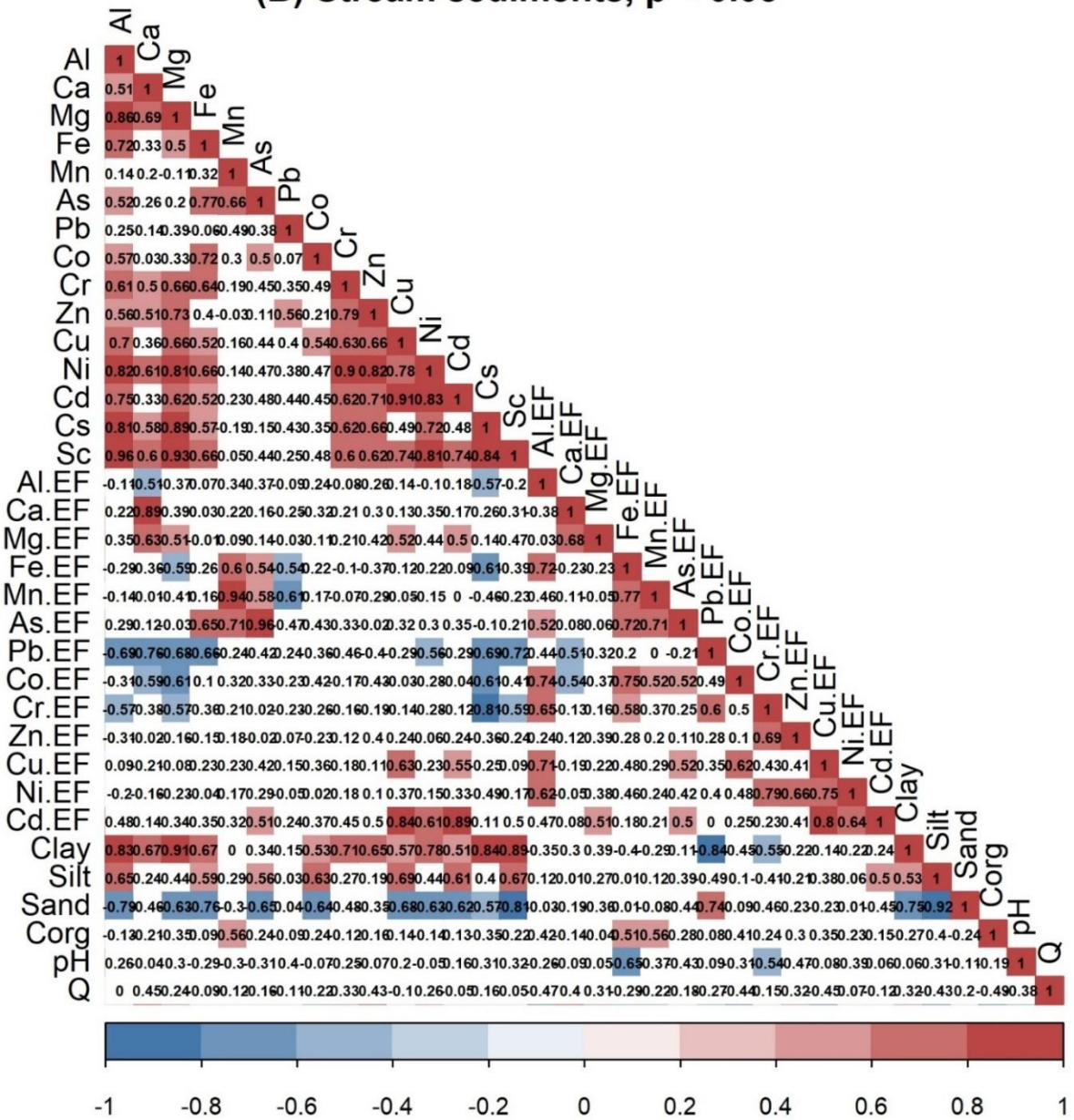
**Annex V** – Principal component analysis (PCA) combining the first component (PC1) and the third component (PC3); variable loadings (left) and individual scores (right)). (A) All sediments; (B) Stream sediments; (C) Pond sediments. In individual scores (right column), the color palette distinguishes the catchments, and the sediment types are highlighted by shapes. (Chapter III)



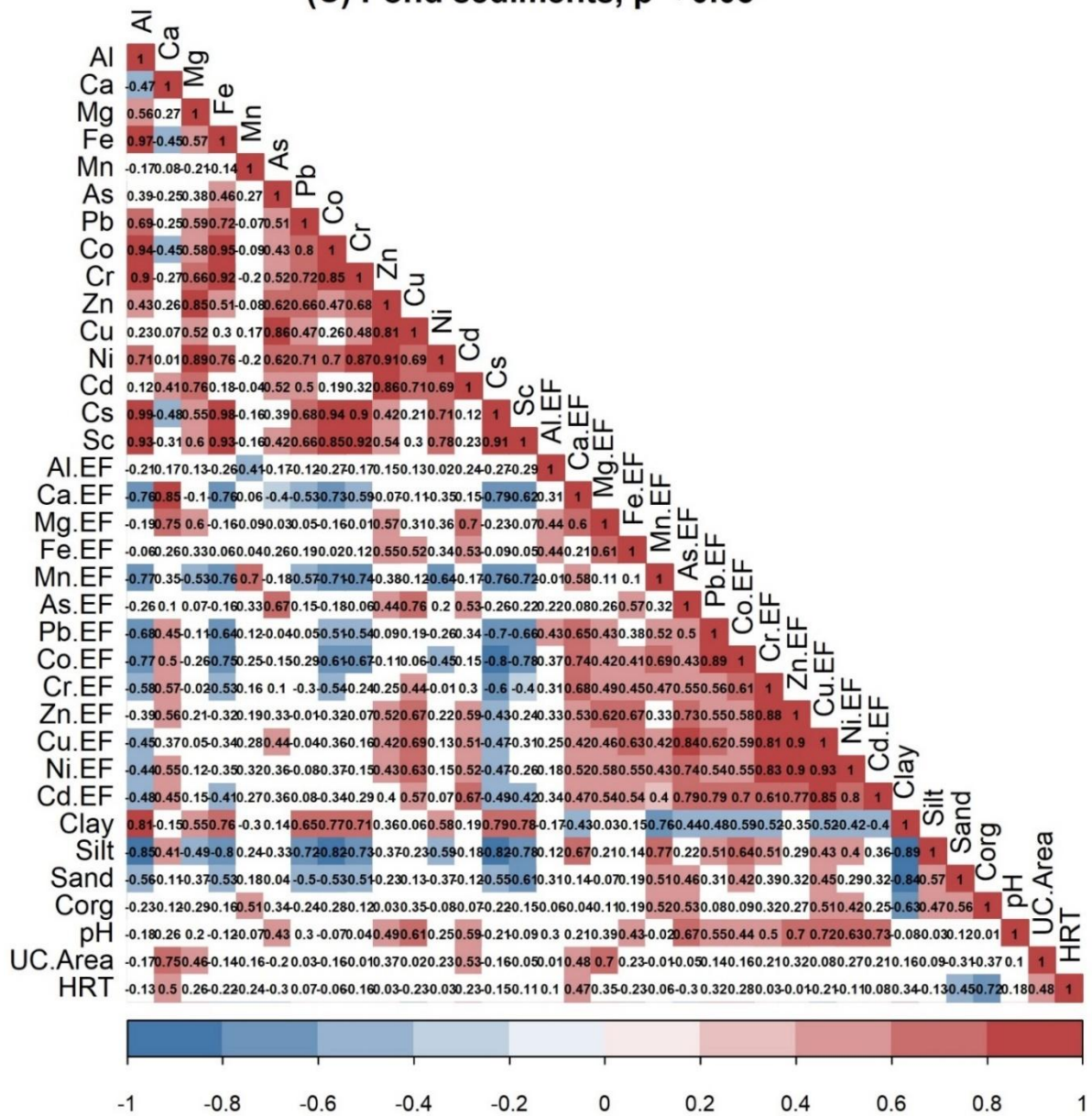
**Annex VI** – Correlations of concentrations, enrichment factors, and physicochemical/environmental parameters for (A) all sediments, (B) stream sediments and (C) pond sediments. The color bar indicated the r value from -1 (blue) to 1 (red). The significance level ( $p < 0.05$ ) was highlighted by colored blocks in the figures.



(B) Stream sediments, p < 0.05



(C) Pond sediments,  $p < 0.05$



**Annex VII** – X. WU, A. PROBST, 2021. Influence of ponds on hazardous metal distribution in sediments at a catchment scale (agricultural critical zone, S-W France). Accepted to *Journal of Hazardous Materials*. DOI: 10.1016/j.jhazmat.2021.125077

The copy of the article is not included in this thesis due to the concern of the copyright. Please visit <https://www.sciencedirect.com/science/article/pii/S0304389421000418> to get the full text.

**Annex VIII** - X. WU, A. PROBST, M. BARRET, V. PAYRE-SUC, T. CAMBOULIVE, F. GRANOUILAC, 2021. Spatial variation of denitrification and key controlling factors in streams and ponds sediments from a critical zone (southwestern France). *Applied Geochemistry*. 131, 105009. DOI: 10.1016/j.apgeochem.2021.105009

The copy of the article is not included in this thesis due to the concern of the copyright. Please visit <https://www.sciencedirect.com/science/article/pii/S0883292721001414> to get the full text.

**Annex IX - X. WU, V. PAYRE-SUC, T. CAMBOULIVE, A. PROBST, 2017. Role of very common artificial ponds on nitrogen behavior in the critical zone of agricultural areas (South-West of France).** *Goldschmidt*, Paris, France, 13-18 August. (poster)



**Role of very common artificial ponds on nitrogen behavior in the critical zone of agricultural areas (South-West of France)**

Xinda Wu, Virginie Payre-Suc, Thierry Camboulive, Anne Probst

EcoLab, Université de Toulouse, CNRS, INPT, UPS, France  
E-mail: xinda.wu@ensat.fr, wuxinda\_stark@163.com




**Backgrounds**

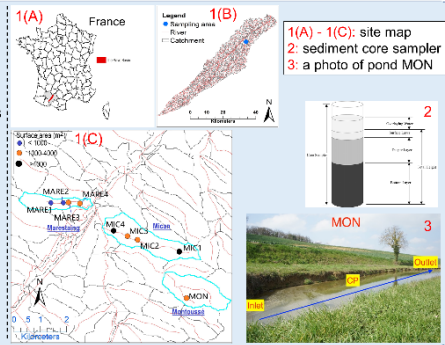
- Contamination of nitrogen and its transfer downstream is of concern in agricultural areas.
- Constructed ponds for water supply may mitigate nitrate contamination.
- However, their role in the transfer and transformation of nitrogen is not very well known at a catchment scale.
- Especially, the factors that influence the denitrification rates are not stated clearly.

**Objectives**

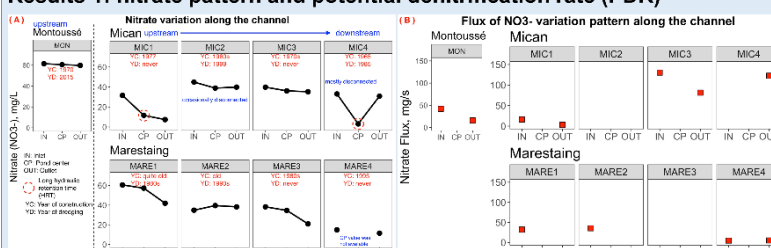
- Evaluate the nitrate pattern along the channel in agricultural catchments having a cumulative set of ponds,
- Determine the denitrification rate in ponds and stream sediments.
- Figure out factors influencing denitrification rates.

**Methods and Materials**

Water and benthic sediment were sampled inside constructed ponds by coring and in their inlets and outlets (March 2016, wet season, no flood event) along the channels (tributaries of the Save river, SW France) from three cultivated catchments with wheat and sunflower, similar carbonate bedrocks. Denitrification rates (by acetylene block technique) were determined. Water nitrate and other physicochemical parameters were analyzed.



**Results 1: nitrate pattern and potential denitrification rate (PDR)**



**Conclusion**

- PDR varied greatly in catchments and sediment types (0.003 - 1.941 µg-N g-sed<sup>-1</sup> h<sup>-1</sup>), consistent with literature data and with soil data in this region. Not only water temperature and the availability of nutrients could affect denitrification rate, but also HRT and pond size.
- High PDR in stream and pond can mitigate nitrate water channel. However, discharge pattern plays a major role as well.
- The presence of cumulative ponds could provide a favorable environment to nitrate mitigation. Environmental factors (HRT, pond surface, pond connection, etc.) should be considered when managing ponds in an agricultural channel.

(A): Mican and Marestaing showed a decreasing pattern of NO<sub>3</sub><sup>-</sup> concentration in the flow direction. The NO<sub>3</sub><sup>-</sup> removal efficiency (RE) was 50% and 80% in two catchments, respectively.

(B): The NO<sub>3</sub><sup>-</sup> mitigation in Mican may result from the dilution due to increasing discharge (Q<sub>i</sub>) downstream (Q<sub>i</sub> increased by 8 → nitrate flux increased by 4).

(C): Though the discharge decreased in Marestaing (Q<sub>i</sub> decreased by 1.2 → nitrate flux reduced by 7), resulting in less importance of the dilution effect, NO<sub>3</sub><sup>-</sup> RE was more substantial than that of Mican. It could attribute to the higher PDR in Marestaing.

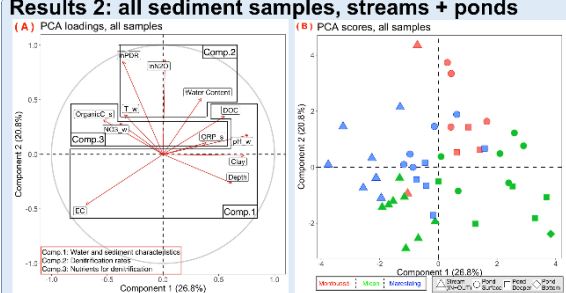
**References**

- Seitzinger (1988). *Limnol. Oceanogr.*, 33(4, part2), 702-724
- García-Ruiz et al. (1998). *STOTEN*, 210-211, 307-320
- Rivas et al. (2017). *J. Environ. Management*, 187, 476-489
- Teixeira et al. (2010). *Marine Environ. Research*, 70(5), 338-342
- Baron (2014). Master 2 report. UPS.
- Garnier et al. (2010). *J. Environ. Qual.*, 39(2):449-59

**Acknowledgement**

This study was supported by China Scholarship Council (CSC) and EcoLab. Our thanks go to those who helped in the field and analysis. From EcoLab analytic platform (PAPC). We are also grateful for the kind help from Groupement des Agriculteurs de la Gascogne Toulousaine (GAGT) and all the farmers in that region.

**Results 2: all sediment samples, streams + ponds**

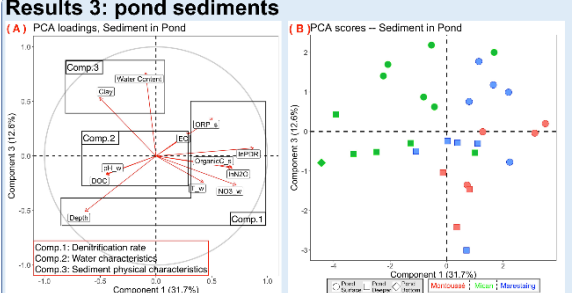


**(A):** Denitrification rates were related to sediment water content and water temperature.

**(B):** Denitrification rates varied greatly in the three catchments. Different sediment types (stream/pond) performed dissimilarly (Component 1).

**(C):** HRT played a negative role in denitrification from different sediment types as discriminated by Comp. 1. Large area and disconnection to stream (water stagnancy) may explain high HRT. Ponds with high HRT (MIC1 and MIC4) had lower PDRs.

**Results 3: pond sediments**



**(A):** Denitrification rates of pond sediments were related to water temperature, nutrients, sediment depth, and ORP.

**(B):** Denitrification rates decreased along the sediment depth due to the lower availability of nutrients.

**(C):** Pond surface area also have negative influence on denitrification rates (Comp. 1). Large ponds could not provide a favorable environment to denitrifiers as a result of the diluted concentration of nutrients in these ponds.